

**The Distribution of Caveolin-1 in Human Term Placenta and the
Derivation of the Endothelial Cells Lining its Basal Plate**

Thesis submitted for the degree of

Doctor of Philosophy

At the University of Leicester

By

Simon Byrne BSc

Department of Infection, Immunity and Inflammation

University of Leicester

January, 2010

**The Distribution of Caveolin-1 in Human Term Placenta and the Derivation of the
Endothelial Cells Lining its Basal Plate**

Thesis submitted for the degree of

Doctor of Philosophy

At the University of Leicester

By

Simon Byrne BSc

Department of Infection, Immunity and Inflammation

University of Leicester

January, 2010

Statement of originality

This accompanying thesis for the degree of PhD entitled “The distribution of caveolin-1 in human term placenta and the derivation of the endothelial cells lining its basal plate” is based on work conducted by the author at The University of Leicester mainly between the years 2000 to 2010.

All the work recorded in this thesis is original unless otherwise acknowledged in the text or by references.

None of the work has been submitted for another degree in this or any other university.

Signed:

Date:

The Distribution of Caveolin-1 in Human Term Placenta and the Derivation of the Endothelial Cells Lining its Basal Plate

Simon Byrne (2010)

Abstract

The initial aim of this research was to establish the distribution of the protein caveolin-1 in the human term placenta, using an indirect immunofluorescence technique. The findings of this survey showed that caveolin-1 was expressed in all the predicted places (vascular endothelium, smooth muscle and fibroblasts), but also by cells lining the basal plate. These cells were investigated further, firstly by transmission and scanning electron microscopy, then by immuno-gold electron microscopy. The findings of the immuno-gold study suggested a vectorial nature of caveolae trafficking in both foetal endothelial cells and in the endothelial-like cells lining the basal plate. This study also showed that some leucocytes express caveolin-1.

The cells lining the maternal blood space above the basal plate of the placenta had been thought to be trophoblastic (foetal) but the initial results obtained using immunofluorescence indicated that the lining consisted rather of a *mosaic* of two types of cells. Some of these were trophoblastic but others were seen to be more similar to endothelial cells.

To determine whether these latter cells were of maternal derivation, placentae from neonates of *known gender* were used in a cytogenetic analysis, to establish their provenance unequivocally. The probe used in these *in situ* hybridisation experiments was complementary to a portion of the human Y-chromosome (only found in males). Cells to which this probe hybridised must therefore be male; a failure to hybridise meant that they must be maternal. Some cells resident in the basal plate were shown to have more than one Y-chromosome in a single interphase nucleus and were taken to be polyploid trophoblast 'giant' cells.

Further collaborative experiments showed that the area fraction occupied by the lining endothelial cells was greater in pre-eclamptic placentae than in placentae from normotensive births; the significance of this in the aetiopathology of this disease is discussed.

Cells that play a key role at the maternal-foetal interface have been carefully characterised in this study and have been shown to form a continuous endothelial/epithelial layer of both maternal and foetal origin.

ACKNOWLEDGEMENTS

I would like to express my sincere thanks to those many people who have helped me, in different ways, during the years spent producing this piece of research.

Firstly to my wife, Susan, for her constant support and encouragement and to my daughter, Lucy, for her faith in me, I say “Thank you”.

I owe a great debt of gratitude to my friend and first supervisor, Professor Colin Ockleford, in whose laboratory this work was undertaken. His praise, as well as his great patience, was much appreciated.

To my former mentor and colleague Felix Beck, Professor of Anatomy at this University and presently Emeritus Professor in Biochemistry I owe a debt of gratitude; it was he who first acknowledged my capacity to achieve something in science.

The unpleasant task of supervising the final presentation of the manuscript itself fell to another friend and colleague Dr. Roger James. His careful proof reading and explanations concerning “what should go where” have been invaluable, especially as this task was assigned to him at the eleventh hour!

I thank also my other co-supervisors, Dr. Shaun Heaphy, whose healthy cynicism put me on my mettle and galvanised me into finishing this work and Dr. Revers Donga who helped me feel equal to the task of completing this thesis.

Dr. Howard Pringle kindly allowed me to visit his own laboratory to see how *in situ* hybridisation should be done. I thank him and his excellent technician, Ms. Angie Gillies, for this opportunity.

Mr. Stefan Hyman and Ms. Natalie Allcock, of the Electron Microscopy Suite, are thanked for their expertise and willing assistance.

My Ghanaian colleagues, Drs. John Ahenkorah and Bismarck Hottor, (the final PhD students in Professor Ockleford's laboratory in Leicester) are thanked for their cheerful presence, as is my old friend Mr Nick Court.

Mr Tim Smith is thanked for his expert advice concerning immunogold labelling techniques and image rendering.

To the other people, too numerous to mention individually, who have nevertheless been of assistance to me over the years, I salute you.

Last, but by no means least, I would like to express my gratitude to the staff at The Maternity Unit at The Leicester Royal Infirmary and to the mothers who kindly agreed to allow me to use the placentae from their newborn babies; without them, this research would obviously never have been possible.

Table of contents

Front part

Title page	(i)
Statement of originality	(ii)
Abstract	(iii)
Acknowledgements	(iv)
Table of contents	(vi)
List of figures and tables	(x)
Abbreviations	(xiii)
List of first-author papers	(xvii)
List of second-author papers	(xviii)

Chapter 1 Introduction 1

1.1	Development and structure of the placenta	1
1.2	Pre-eclampsia	15
1.3	Caveolae and the caveolins	19
1.4	Aims of the study	26

Chapter 2 Materials and methods 27

2.1	Tissues used, cryo-fixation and cryo-sectioning	27
2.2	Immuno-fluorescence cytochemistry	29
2.3	Polyacrylamide gel electrophoresis and blotting	30
2.4	Fluorescence microscopy	35
2.5	Semi-thin section light microscopy and transmission electron microscopy	35
2.6	Scanning electron microscopy	37
2.7	Tissue preparation and methacrylate resin embedding	38
2.8	Sectioning and immuno-gold labelling	39
2.9	Gold particles per unit area calculation	42

2.10	Cytogenetic study: tissue collection and preparation	42
2.11	Y-chromosome probe preparation and application	43
2.12	Visualisation of positive hybrids	44
2.13	Microscopy	45
2.14	Statistical analysis	46
 Chapter 3 Caveolae: immunofluorescence, transmission and scanning electron microscopy		48
3.1	Introduction	48
3.2	Results	50
3.2.1	Immuno-blotting	50
3.3	Immunofluorescence	55
3.4	Light and transmission electron microscopy	64
3.5	Scanning electron microscopy	70
3.6	Quantitation of fluorescence intensity across line-scans	74
3.7	Summary of results	77
3.8	Discussion	78
3.8.1	Distribution of caveolin-1	78
3.8.2	Morphology of basal plate lining cells	80
 Chapter 4 Immuno-electron microscopy using anti-caveolin-1 antibody		81
4.1	Introduction	81
4.2	Results	83
4.3	Statistical analysis of gold particles per unit area	91
4.4	Summary of results from immuno-gold study	100

4.5	Discussion	101
4.5.1	Specificity	101
4.5.2	Tissue distribution	102
4.5.3	Intracellular distribution	103
Chapter 5 Healthy and pre-eclamptic placental basal plate lining cells: quantitative comparisons based on confocal laser scanning microscopy		105
5.1.1	Introduction	105
5.1.2	Cytoskeletal and other markers	108
5.1.3	The intervillous space	109
5.1.4	Pre-eclampsia and maternal vascular remodelling	109
5.2	Results	110
5.2.1	Immunofluorescence results	110
5.3	Measurement of basal plate area fractions in healthy and pre-eclamptic placentae	115
5.4	Discussion	118
5.4.1	Basal plate composition changes in pre-eclampsia	118
5.4.2	Markers defining heterogeneity	119
5.4.3	Anchoring villi	119
5.4.4	Endothelial and trophoblast markers in pre-eclamptic tissue	119
5.4.5	Heterogeneity of cell types contributing to the basal plate lining	120
5.4.6	Basal plate composition changes in pre-eclampsia	121
5.4.7	Developmental aspects of pre-eclampsia	122

Chapter 6	A cytogenetic study to establish the derivation of cells lining the basal plate	124
6.1	Introduction	124
6.2	Results	129
6.3	Summary of results	141
6.4	Discussion	142
Chapter 7	Conclusions	146
7.1	General discussion	146
7.2	Future work	151
Bibliography		154
Appendices		170
1.	Patient information letter (pre-eclampsia)	170
2.	Permission to reproduce Figure 1.8	174
3.	Reprints of first-author papers used in this thesis	180
(i)	Byrne et al., 2001.	181
(ii)	Byrne et al., 2007.	194
(iii)	Byrne et al., 2010.	203
4.	Reprint of second-author paper used in this thesis	210
	Smith et al., 2004.	211

List of figures and tables

		Page
Figure 1.1	Invasion of endometrium by cytotrophoblast	4
Figure 1.2	Chorionic surface of term placenta	7
Figure 1.3	Basal surface of term placenta	9
Figure 1.4	Late first trimester pregnant uterus	12
Figure 1.5	Term placenta sectional diagram	13
Figure 1.6	Photomicrograph of term basal plate section	14
Figure 1.7	Destination of newly-synthesised caveolin-1	22
Figure 1.8	Caveolin, cavin and dynamin relationship	24
Figure 2.1	Basal plate sampling zones	28
Figure 2.2	Gradient acrylamide gel pouring apparatus	32
Figure 2.3	Apparatus for immunostaining EM grids	40
Figure 3.2.1a	Non-reducing anti-caveolin-1 western blot	52
Figure 3.2.1b	Reducing anti-caveolin-1 western blot	53
Figure 3.3.1	Anti-caveolin-1 immunofluorescence in term chorionic villi	56
Figure 3.3.2	Anti-caveolin-1 immunofluorescence in term amnio-chorion roll	58
Figure 3.3.3	Anti-caveolin-1 immunofluorescence in term basal plate	60
Figure 3.3.4	Anti-caveolin-1 immunofluorescence in term basal plate	61
Figure 3.3.5	Anti-caveolin-1 immunofluorescence in term chorionic plate and umbilical cord	63
Figure 3.4.1	Semi-thin plastic section light micrograph of term basal plate	65
Figure 3.4.2	Semi-thin plastic section light micrograph of term basal plate/epithelial junction zone	66

Figure 3.4.3	Transmission electron micrograph of basal plate junction zone	67
Figure 3.4.4	Transmission electron micrograph of villous capillary, basal plate trophoblast and endothelium	68
Figure 3.5.1	Scanning electron micrograph of anchoring villus, trophoblast microvilli and endothelium	71
Figure 3.5.2	Scanning electron micrograph of fibrin overlying Trophoblast microvilli	72
Figure 3.5.3	Scanning electron micrograph of endothelium, trophoblast and fibrin	73
Figure 3.6.1	Chorionic villus immunofluorescent line-scan using anti-caveolin-1 antibody	75
Figure 3.6.2	8 similar line-scans through chorionic villi to show the similarity of the pattern achieved	76
Figure 4.2.1	Immuno-electron micrograph of terminal chorionic villus using anti-caveolin-1 antibody	84
Figure 4.2.2	Immuno-electron micrograph of terminal chorionic villus using anti-caveolin-1 antibody	85
Figure 4.2.3	Immuno-electron micrograph of terminal chorionic villus using anti-caveolin-1 antibody	86
Figure 4.2.4	Immuno-electron micrograph of basal plate endothelium and underlying fibroblast	87
Figure 4.2.5	Immuno-electron micrograph of small foetal leucocyte (anti-caveolin-1 antibody)	88
Figure 4.2.6	Positive control using anti-pan-cytokeratin on extra-villous trophoblast	90
Figure 4.3.1	Gold particles/ μm^2 for villous tissues using anti-caveolin-1 antibody in immuno-EM	92
Figure 4.3.2	Zonal distribution in foetal capillary endothelium	94
Figure 4.3.3	Zonal distribution in basal plate endothelium	96
Figure 4.3.4	Comparison of labelling densities in different villous cell types using anti-caveolin-1 antibody	97

Figure 4.3.5	Zonal distribution in basal plate fibroblasts	98
Table 4.3.1	Labelling density in villous cells	99
Figure 5.1	Diagram: basal plate lining cells; anchoring villus	108
Figure 5.2.1	Normal chorionic villi labelled with anti-pancytokeratin and anti-von Willebrand factor	111
Figure 5.2.2	Anti-PECAM-1 and anti-pancytokeratin: normal basal plate	112
Figure 5.2.3	Anti-PECAM-1 and anti-pancytokeratin: normal basal plate	113
Figure 5.2.4	Anti-human chorionic gonadotrophin in normal basal plate	114
Figure 5.3.1a	Analysis of the length percentage of the basal plate occupied by trophoblast, endothelium and acellular material in normal and pre-eclamptic placentae	116
Figure 5.3.1b	Segregation of Figure 5.3.1 data by gestational age	117
Figure 6.1.1	c-DNA probe synthesis illustration	126
Figure 6.2.1	Negative control ISH female placenta	130
Figure 6.2.2	Absence of labelling in basal plate endothelium	131
Figure 6.2.3	Labelling of trophoblast and mesenchymal cells in chorionic villi	132
Figure 6.2.4	Extravillous trophoblast labelling within the basal plate	133
Figure 6.2.5	Absence of labelling in basal plate endothelium	134
Figure 6.2.6	Labelling of foetal endothelial cells in chorionic villous capillaries	135
Figure 6.2.7	Junction between lining trophoblast and endothelium	136
Figure 6.2.8	Polyploid cells in the basal plate	137
Figure 6.2.9	Immuno-fluorescent in situ hybridisation (FISH) using the same Y-chromosome probe	138

Figure 6.2.10	Bar chart showing % positive signal for different cell types examined	140
Figure 7.1	Possible links between caveolae and pre-eclampsia	150

ABBREVIATIONS

% v/v	volume in ml in 100 ml final solution
% w/v	weight (= mass) in g in 100 ml final solution
°C	degrees Celsius
µg	micrograms
µl	microlitres
µm	micrometres
ANOVA	analysis of variance
ASA	American Standards Association
Au	aurum (= gold)
BDH	British Drug Houses Company
BP <i>or</i> bp	basal plate
BSA	bovine serum albumin
CA	California
cDNA	complementary deoxyribonucleic acid
CLSM	confocal laser scanning microscope
cm	centimetres
CO ₂	carbon dioxide
DAB	diaminobenzidine (tetrahydrochloride)
DABCO	diazobicyclo[2,2,2]-octane
DIN	Deutsche Industrie Normen (= 'German Standards Organisation')
DNA	deoxyribonucleic acid

DNP	dinitrophenol
DPX	distyrene with plasticizer in xylene
dUTP	2'-deoxyuridine 5'-triphosphate
<i>E.coli</i>	<i>Escherichia coli</i>
EM	electron microscopy/micrograph
eNOS	endothelial nitric oxide synthase
<i>et seq.</i>	<i>et sequentia</i> (= 'and the following')
FISH	fluorescence <i>in situ</i> hybridisation
FITC	fluorescein isothiocyanate
FRSS	fellow of the Royal Statistical Society
GmbH	Gesellschaft mit beschränkter Haftung (= 'limited company')
GPI	glycophosphatidyl inositol
GTPase	guanosine triphosphatase
HCl	hydrochloric acid
hCG	human chorionic gonadotrophin
H ₂ O	water
H ₂ O ₂	hydrogen peroxide
HRP	horseradish peroxidase
HSD	honestly significant difference
IgG	immunoglobulin G
IL	Illinois
IMS	industrial methylated spirit
ISH	<i>in situ</i> hybridisation
ivs	inter-villus space
kB	kilobases

kV	kilovolts (10^3 volts)
KY	Kentucky
mA	milliAmpères
mbs	maternal blood space
MDCK	Madin Darby canine kidney (cells)
mg	milligrams
MgCl ₂	magnesium chloride
mm	millimetres
MMP	matrix metalloprotease
mM	millimolar
MSB	martius (yellow), (brilliant crystal) scarlet, (soluble) blue
Msp1	(restriction endonuclease from) <i>Moraxella spp.</i>
NaCl	sodium chloride
NaH ₂ PO ₄	sodium dihydrogen orthophosphate
Na ₂ H PO ₄	disodium hydrogen orthophosphate
NGS	normal goat serum
nm	nanometres
NOS	nitric oxide synthase
NOSIP	nitric oxide synthase interacting protein
NOSTRIN	nitric oxide synthase trafficker
OCT	optimum cutting temperature
PA	Pennsylvania
pBR328	<i>E.coli</i> plasmid
PECAM-1	platelet endothelial cell adhesion molecule-1
pHY2.1	2.1kB partial DNA sequence of human Y-chromosome

PBS	phosphate buffered saline
PBST	phosphate buffered saline + 0.1% v/v Tween-20
pH	hydrogen potential
PL	placental lactogen
PVDF	polyvinylidenedifluoride
RI	refractive index
rpm	revolutions per minute
RT	room temperature
SDS	sodium dodecyl (<i>or</i> lauryl) sulphate
SEM	standard error of the mean
SSC	standard saline citrate
tPA	tissue type plasminogen activator
Tris	tris-hydroxymethylmethyllamine
Tween-20	polyoxyethylenesorbitan monolaurate
Triton X-100	octylphenoxypolyethoxyethanol
UK	United Kingdom
uPA	urokinase plasminogen activator
USA	United States of America
<i>vid. inf.</i>	<i>vide infra</i> (= ‘see below’)
<i>vid. sup.</i>	<i>vide supra</i> (= ‘see above’)

List of first author papers arising from the thesis

Byrne S, Cheent A, Dimond J, Fisher G and Ockleford, CD (2001). Immunocytochemical Localisation of a Caveolin-1 isoform in Human Term Extra-embryonic Membranes using Confocal Laser Scanning Microscopy: Implications for the Complexity of the Materno-fetal Junction. *Placenta*, 22: 499-510.

Byrne S, Ahenkorah J, Hottor B, Lockwood C and Ockleford CD (2007) Immunoelectron microscopic localisation of Caveolin-1 in human placenta. *Immunobiology*, 212: 39-46.

Byrne S, Challis E, Williams JLR, Pringle JH, Hennessey JM and Ockleford CD (2010) A mosaic layer in human pregnancy. *Placenta*, 31: 373-379.

Byrne S, Barber H, Mercer N, D'Lacey C and Ockleford CD (2003) ACE in the basal plate. *Placenta*, 24: A43. (Abstract).

Second author papers referred to in this thesis

Ahenkorah J, Byrne S, Bosio P and Ockleford CD (2008) Immunofluorescence confocal laser scanning microscopy and immune-electron microscopic identification of keratins in human maternofetal interaction zone. *Journal of Cellular and Molecular Medicine* **13**: 735-748.

Feng Q, Liu K, Liu XY, Byrne S and Ockleford CD (2001) Plasminogen activators and inhibitors are transcribed during early macaque implantation. *Placenta*, **22**:186-199.

Hottor B, Bosio P, Waugh J, Diggle PJ, Byrne S, Ahenkorah J and Ockleford CD (2010) Variation in composition of the intervillous space lining in term placentas of mothers with pre-eclampsia. *Placenta* **31**: 409-417.

Ockleford C, Smith R, Byrne S, Sanders R and Bosio P (2003) Human placental basal plate lining cells: significant changes associated with pre-eclampsia. *Annals of Anatomy* (Supplement to) **185**: 166-167.

Ockleford CD, Smith RK, Byrne S, Sanders R and Bosio P (2004) A confocal laser scanning microscope study of cytokeratin dimming indicates a mechanism of trophoblast deportation and its upregulation in pre-eclampsia. *Microscopy Research and Technique* **64**: 43-53.

Ockleford CD, Cairns H, Rowe AJ, Byrne S, Scott JJA and Willingale R (2007)

The distribution of caveolin-3 immunofluorescence in skeletal muscle fibre membrane defined by dual channel confocal laser scanning microscopy, fast Fourier transform and image modelling. *Journal of Microscopy*, **206**: 139-151.

Smith RK, Ockleford CD, Byrne S, Bosio P and Sanders R. (2004) Healthy and pre-

eclamptic basal plate lining cells: Quantitative comparisons based on confocal laser scanning microscopy. *Microscopy Research and Technique*, **64**: 54-62.

Chapter One: Introduction

1.1 Development and structure of the placenta

The term placenta (*placenta uterina* or "uterine cake") was first used by the 16th century Italian anatomist Realdus Columbus. It is a temporary organ, which, in mammals, supplies the developing embryo and foetus with nutrients and oxygen and eliminates metabolic waste materials and carbon dioxide. It thus serves the function of gut, lungs and kidneys throughout gestation. In humans the embryonic stage lasts from 0 – 8 weeks; after this the developing infant is referred to as a foetus.

The fertilised ovum, or zygote, undergoes mitotic division to produce a solid sixteen-cell *morula* ("mulberry"), which is approximately the same size as the ovum (80-100µm). After this, the *zona pellucida*, its acellular surrounding matrix, is lost. Further cell division is now asymmetrical and gives rise to a distinct polarity in what is to become the *blastula* or blastocyst. The outermost cells of the *morula* divide and differentiate into trophoblast, whilst those on the inside become the inner cell mass. Because the trophoblasts divide as a *sheet* of cells (i.e. their growth is in two dimensions only), a hollow sac or blastocoel is formed within the blastocyst. By contrast, the inner cell mass, which will eventually become the embryo proper, continues to divide initially in three dimensions and is resident at one pole (the embryonic pole). The maturation of the zygote to form the blastocyst is thought to occur chiefly in the oviduct and to last about four or five days (Boyd and Hamilton, 1970).

Implantation, the process by which the blastocyst becomes attached to and establishes itself in the endometrial lining of the uterus, is crucial to the survival of the conceptus. The first phase of this event is attachment, when the embryonic pole makes contact with

and adheres to the endometrial lining of the uterus. Once the blastocyst has become attached, the endometrial cells in this vicinity respond to implantation in such a way that their phenotype and morphology are radically changed. These cells are now referred to as decidual cells, as they are all expelled at parturition. Those decidual cells at the *periphery* of the implantation site grow over and eventually completely cover the entire conceptus; at the same time, the trophoblasts in contact with the endometrium begin to proliferate and burrow into the cells underlying the implantation site. This is a carefully orchestrated process consisting of waves of proteolysis and apoptosis, where the catabolic activity of the trophoblasts is balanced by their ability to occupy the space created. If this invasive activity is too aggressive, the trophoblasts may penetrate as far as the myometrium (the muscular layer of the uterus) and beyond without making sufficient contacts with the uterine blood vessels, leading to placenta accrete. These contacts are essential to the establishment of the haemochorial placenta (where the trophoblasts are eventually in direct contact with maternal blood).

The method by which the endometrial epithelium is breached varies in different species. In rodents, attachment of the trophoblast induces apoptosis in the endometrium, whereas in ungulates, there is fusion of the maternal and foetal cells to produce a syncytium. In primates, however, the endometrial epithelium is penetrated interstitially (i.e. *between* the cells) by thin, flat projections of the outermost cells of the blastocyst (the trophoctoderm).

The proteases involved in implantation fall into three main classes: cysteine proteases, including cathepsins B and L, the serine proteases uPA and tPA (urokinase-type and tissue-type plasminogen activators, respectively) and the matrix metalloproteinases MMP-1, -2, -3, -7 and -9. Many of these proteases have “partner” inhibitors and it is the

differential expression of these pairs of molecules which effects the rapid remodelling of the decidua seen at this time (Salamonsen, 1999; Feng et al., 2001).

Besides forming stable anchorage points in the decidualised endometrial lining of the uterus, the trophoblast cells must also begin to penetrate the uterine spiral arteries as a prelude to the establishment of the maternal blood space. It is imperative that sufficient numbers of the maternal vessels are colonised in this way if there is to be enough maternal blood available to the foetus to support its continuing growth. (This type of placenta, in which the foetal syncytial cells are in direct contact with maternal blood, is referred to as a *haemochorial* placenta). This is illustrated overleaf in Figure 1.1.

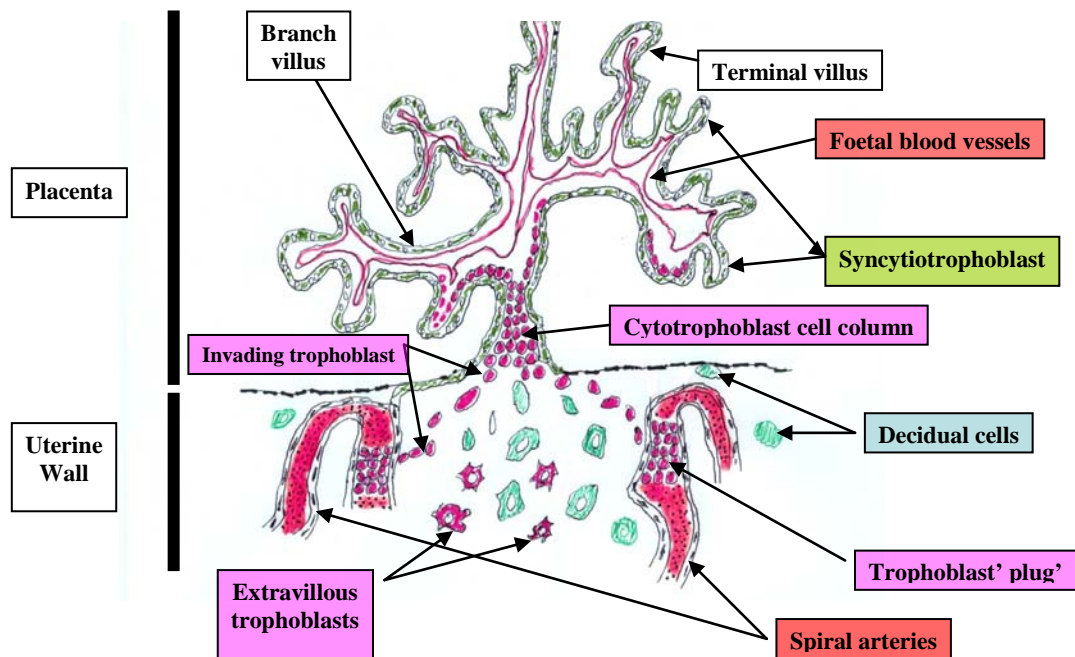


Figure 1.1 This diagram illustrates the way in which cytotrophoblast cells (pink) invade the underlying decidualised endometrium and migrate into the uterine spiral arteries. These (successful) invading cells continue to divide within the lumen and eventually occlude the spiral arteries, forming a temporary ‘plug’.

The uterine blood vessels - the spiral arterioles - are initially *plugged* by the migrating trophoblasts, which continue to divide within the lumina of these vessels and thus expand their diameter. This expansion is crucially important for the purpose of reducing the effective pressure of the incoming maternal blood once the trophoblast plugs have been 'removed' (presumably this is a time-dependent, programmed apoptotic process) and the vessels are once more patent. Poiseuille's Law states that the flow rate through a tubular vessel varies approximately as the *fourth* power of its radius, so this expansion of the vessel wall diameter is important in order to ensure that once the trophoblast plugs are no longer in place, an adequate blood flow to the placental bed does not require too great an elevation of maternal blood pressure.

The cytotrophoblast cells which now line the spiral arteries adopt a phenotype which is more typical of endothelium than epithelium (Goldman et al., 2000), whilst retaining their expression of cytokeratin. They are thus still foetal and epithelial.

Once the trophoblast plugs have been removed the blood emerging from the spiral arteries is now diverted into large sinuses in which the foetal villi are resident – the maternal blood space. These sinuses, initially quite small, are thought to be coincident with the ducts of the uterine glands within the endometrium in the vicinity of the implantation site.

During the first trimester (i.e. when the above changes are taking place) the respiratory processes of the embryo are essentially anaerobic. In the absence of a blood supply the embryo and developing placenta rely on diffusion for their metabolic needs.

Whilst the invading trophoblasts are establishing connections with the maternal blood supply, the embryo's own circulatory system is being elaborated. This consists of the heart and systemic blood vessels and equally importantly the villous circulation. This is

the part of the blood system outside the foetus where exchange will take place between the maternal and foetal compartments.

The umbilical vessels (normally two arteries and one vein) become subdivided at the chorionic surface of the placenta (the surface closest to the foetus). Because the blood entering here is at a relatively high pressure and for the requirements of mechanical stability, this surface is heavily invested with connective tissue fibres which ensheath these vessels, giving it its characteristic blue-white appearance (in the latter stages of pregnancy the unborn child will often kick with considerable force; without this protective reinforcement, these blood vessels could easily be breached). As these vessels ramify across the chorionic plate, they are seen to divert downwards into the body of the placenta. The chorionic aspect of a freshly-delivered placenta is illustrated below in Figure 1.2.

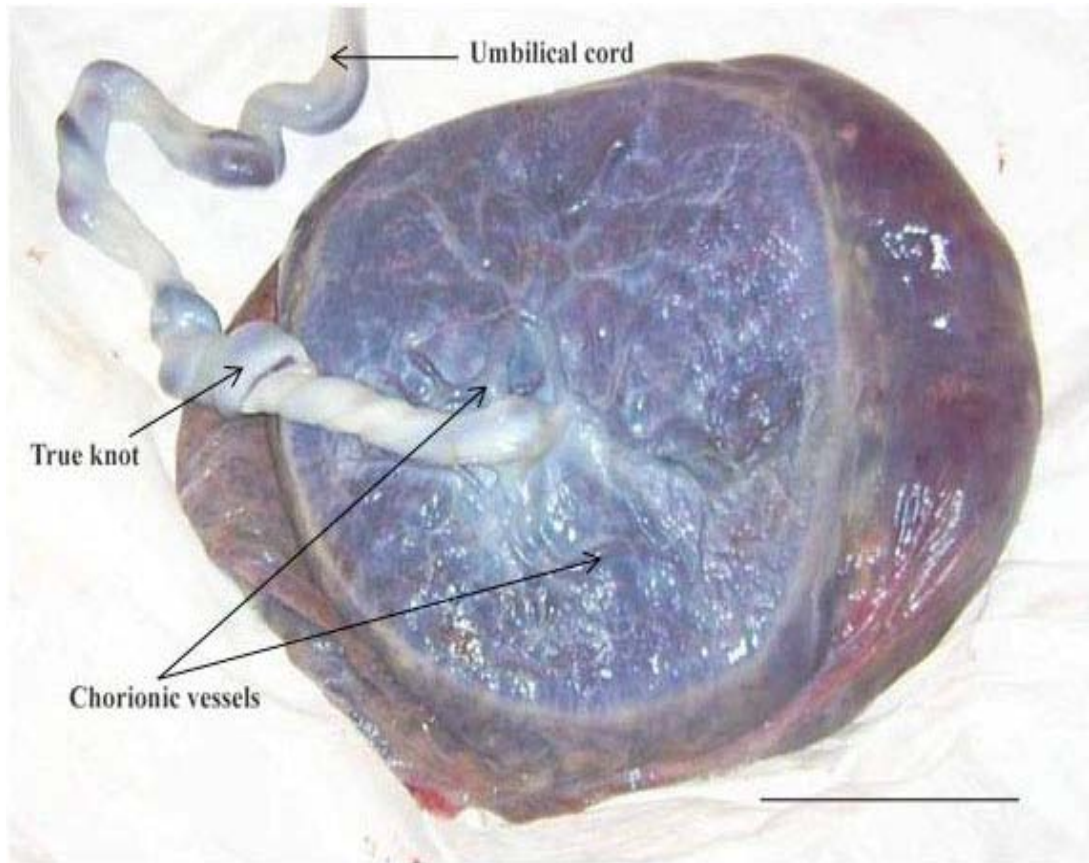


Figure 1.2 The chorionic surface of a freshly-delivered placenta, showing the manner in which the foetal vessels, which originate in the umbilical cord ramify outwards across the placental surface and divert downwards into separate cotyledons (arrows). The amniochorion, the membranous sac which surrounds the foetus and contains the amniotic fluid throughout gestation is visible as the semi-transparent material at the top left of this image. Scale bar = 5cm. (This image courtesy of Dr. John Ahenkorah)

These diversion points define the subdivisions of the placenta into separate functional units referred to as cotyledons. The cotyledonary nature of the placenta is best seen by examining the basal surface of a freshly delivered specimen. Each cotyledon is separated from its neighbours by partial septa. The maternal blood space is, in fact, continuous as these septa are incomplete. The basal surface of a freshly-delivered placenta is illustrated in Figure 1.3.

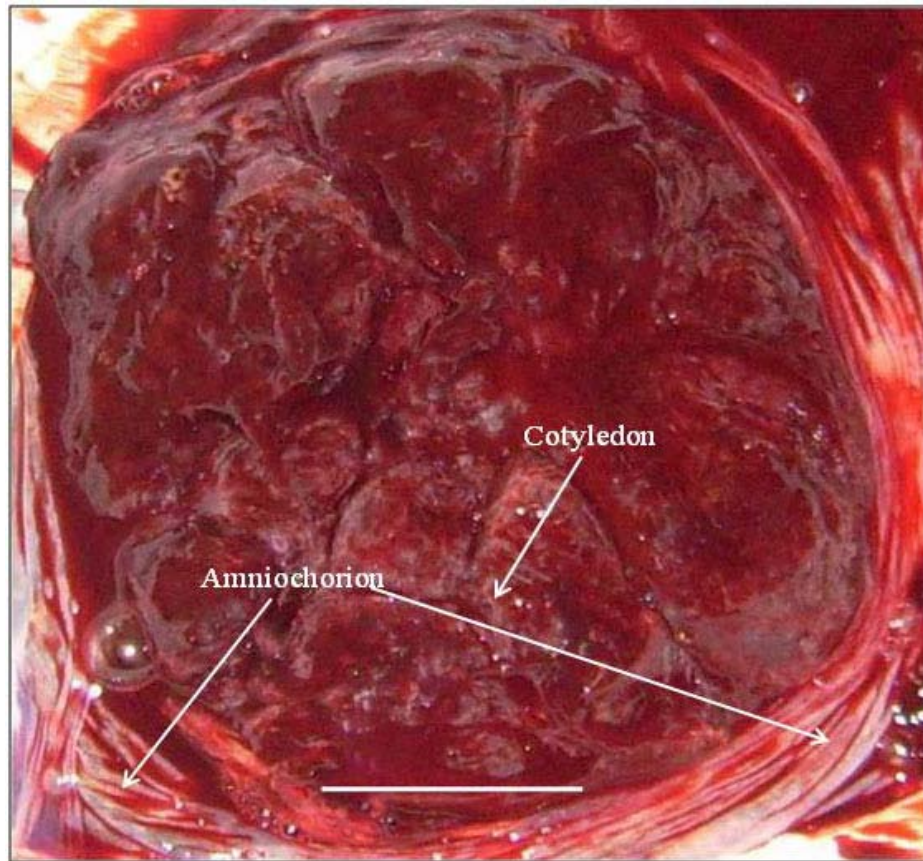


Figure 1.3 This image is of the basal surface of a freshly-delivered placenta. It shows the cotyledonary nature of this organ. The amniochorion (*vid.sup.*) is reflected forward, which is the opposite of how it would be *in vivo*. This basal surface is that part of the placenta which was formerly attached to the uterine wall and thus represents an *en face* view of the abscission layer. What may not be apparent in this image is the membranous nature of this surface, which, when palpated, is found to be continuous from one side of the placenta to the other; the septa between the cotyledons are often not palpable. Scale bar = 5cm. (This image courtesy of Dr. John Ahenkorah).

The foetal blood vessels develop initially in what is termed the *chorion frondosum*; this consists of an outer covering of trophoblast cells which become syncytialised (i.e. they lose their inter-cell membranes), an inner layer of cytotrophoblast cells and a mesenchymal core in which the blood vessels and capillaries themselves are elaborated. The structure of these units is, as its name suggests, reminiscent of a (fern) frond, having a more substantial central part, which will later become the stem and anchoring villi and numerous branched villi. (Stem villi are those villi in direct contact with chorionic plate, whilst anchoring villi are embedded in the basal plate). The final divisions of branch villi are the terminal villi, where most of the gas and metabolite exchange takes place.

It should be remembered that the placenta continues to grow, especially in a radial direction *throughout pregnancy*, so the processes described here continue to take place, particularly at the margin, at all times throughout gestation.

The embryo/foetus itself develops within a fluid-filled sac – the amniotic sac, which provides a physical barrier between mother and foetus. It acts as a shock absorber against any accidental trauma that may occur to the maternal abdomen. The foetus in its early stages of development is a very fragile organism. The innermost cells of this sac, i.e. those which are in direct contact with the amniotic fluid, constitute the amniotic epithelium. This is a simple (one cell thick) cuboidal epithelium which is continuous with, via the external covering of the umbilical cord, the skin of the foetus. This epithelium is responsible for the maintenance of the amniotic fluid within the sac and lies on a basement membrane. Beneath this simple epithelium is the amniotic mesoderm, a loose connective tissue sheet, also of foetal origin. Together these two layers are only some 50-60µm thick. Overlying the chorionic plate of the placenta, these

are the only foetal layers present, but elsewhere the foetal membranes have a more complex structure. To give an idea of the relationship between the various components of the decidual tissues, the following diagram is included. Here, there are several layers, of both foetal and maternal origin. As the amniotic sac expands, it pushes outwards and eventually contacts the decidual cells overlying the implantation site; the two layers fuse together to form the amnio-chorion.

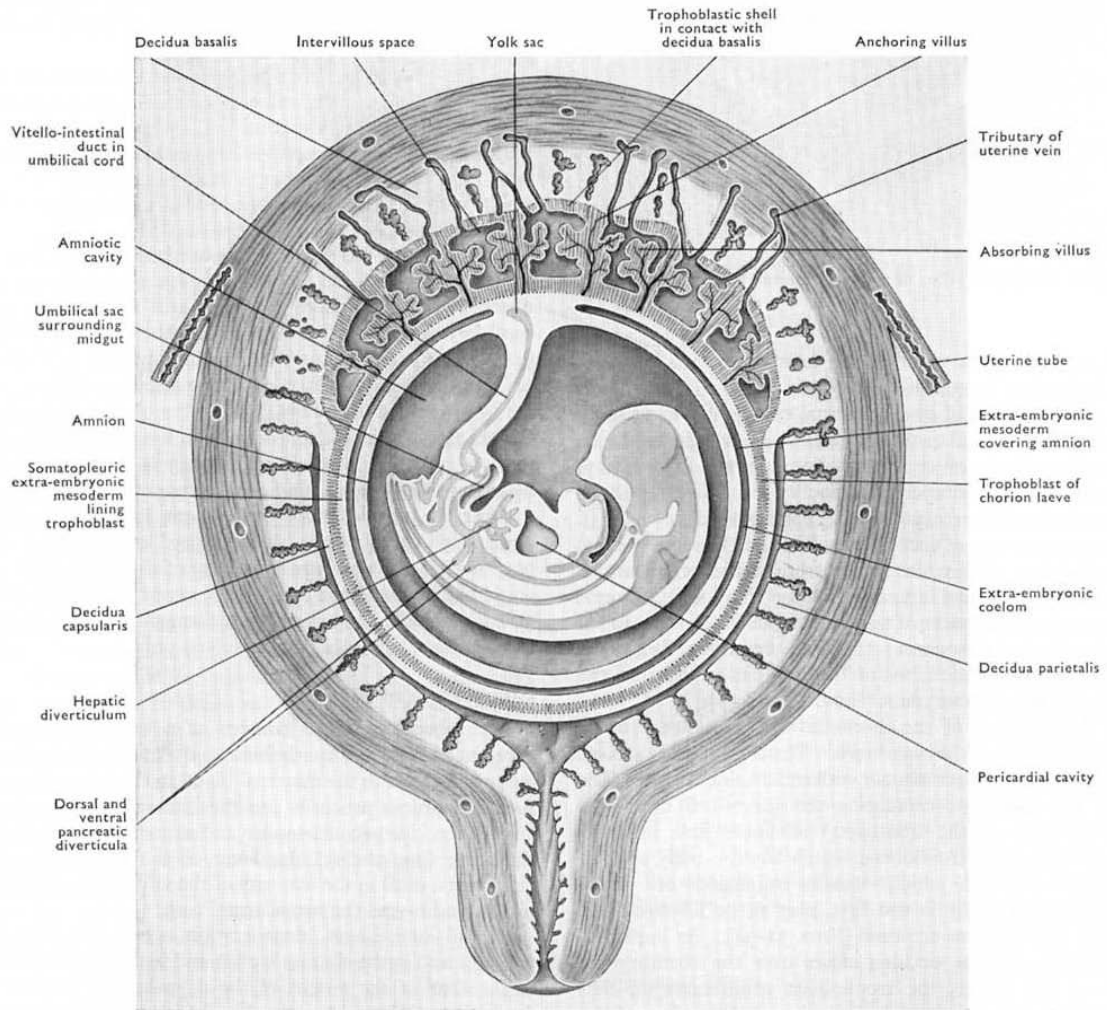


Figure 1.4 This illustration, a coronal section of a late first-trimester pregnant uterus, shows the constituent parts of the decidual and foetal tissues present at the stage immediately preceding the fusion of the *decidua capsularis* with the *decidua parietalis*. At this stage there are still villi within the *decidua capsularis*. After fusion of these two layers, these rudimentary villi rapidly regress. (This illustration is from *Cunningham's Textbook of Anatomy*, edited by GJ Romanes, Oxford University Press, 1972, page 37).

Figure 1.5 is a diagrammatic representation of a near-term placenta in cross-section.

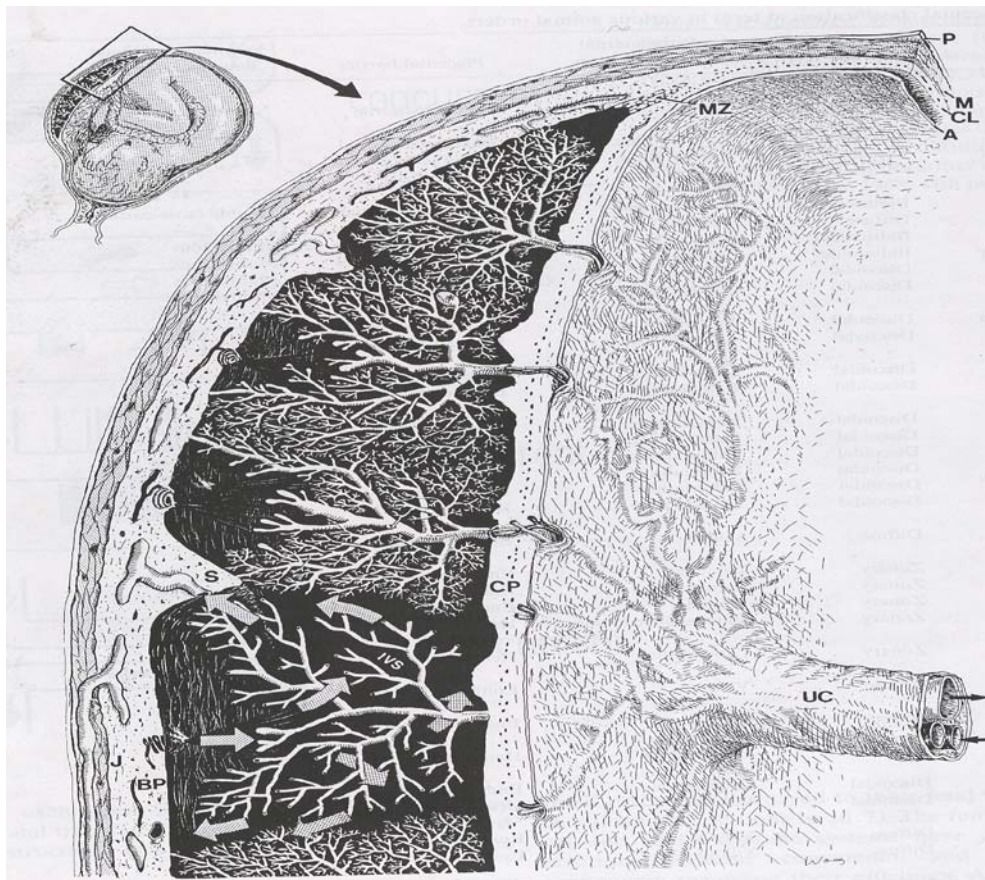


Figure 1.5 This diagram illustrates the arrangement of the essential constituent parts of the mature human placenta *in situ*. The umbilical cord (UC) contains the three major blood vessels from the foetus – two arteries and one vein. Branches from these vessels spread outwards from the cord's insertion across the chorionic plate (CP). The circulation of the maternal blood within the intervillous space (IVS) is suggested by the solid pale arrows. Maternal spiral arteries, arising in the myometrium and passing through the decidua of the basal plate (BP) supply the incoming blood. After percolating between the frond-like chorionic villi, the maternal blood is returned to the uterine veins via drainage vessels situated around the periphery of each cotyledon, adjacent to the septa (S). The marginal zone (MZ) is that part of the placenta where there cease to be any underlying chorionic villi; instead, there is a fusion of the maternally-derived cells of the *chorion laeve* (CL) and the foetally-derived amniotic epithelium and its basement membrane. (This figure is from Benirschke and Kaufmann, *Pathology of the Human Placenta*, 1999).

Figure 1.6 is a photomicrograph of a paraffin-embedded section of human term placental basal plate, stained with martius yellow, brilliant crystal scarlet and soluble blue (MSB). It is included to illustrate the various parts of the tissue which are described in the text.

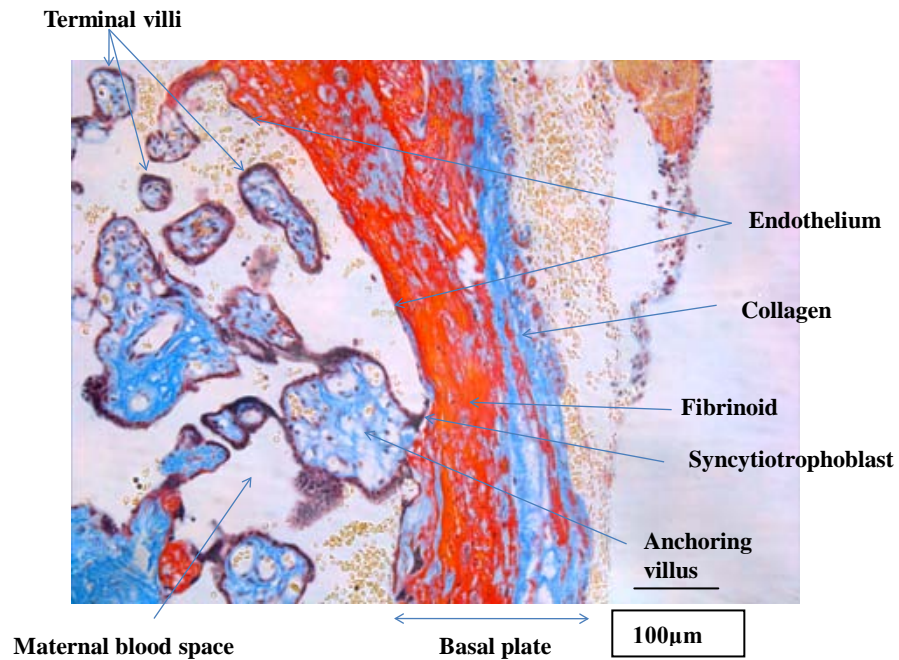


Figure 1.6 Martius yellow, brilliant crystal scarlet and aniline blue (MSB) stained paraffin- embedded section of human term placental basal plate.

The section shows that much of the basal plate consists of fibrin or fibrinoid, which stains orange-red in this technique. The anchoring villus is clearly invested in a different type of cellular covering (syncytiotrophoblast) from that of much of the rest of the basal plate lining. Several thin, tapering nuclei, more typical of squamous endothelial cells can be seen here. Adjacent to some of the branch and terminal villi are further red fibrin plaques, which are formed where foetal capillaries have leaked. Connective tissue (collagen) stains blue and is seen in the villous cores as well as in the basal plate. At the top right of the image is a fragment of myometrium which has become detached at parturition. Erythrocytes are stained a golden yellow. Scale bar= 100µm.

1.2 Pre-eclampsia

It has been suggested that the partial failure of this process of spiral arteriole invasion by cytotrophoblasts may contribute to the establishment of the disease pre-eclampsia, which is usually only manifest in the last trimester of pregnancy (Khong et al., 2005), though occasionally may present at a much earlier stage (Hazra et al., 2003). Pre-eclampsia is a disease of pregnancy characterised by elevated maternal blood pressure (>140/90 mmHg) and proteinuria (<300mg/day); normal non-pregnant values for these parameters are 120/80mmHg and 20-80 mg/day respectively. A slight increase in proteinuria is a normal feature of uncomplicated pregnancies and there are adaptive changes both in the structure and function of the kidneys to cope with the extra demands placed on this organ system at such times (Lindheimer and Katz, 1997). Hypertension in non-pregnant women is expected to raise the concentration of protein in their urine. In pre-eclampsia, however, the elevated maternal blood pressure and urinary protein levels are not simply explained by the hypertensive state which prevails in these patients; this must be uniquely related to the pregnancy itself and in particular to the placenta. Hydatidiform mole, where there is no viable foetus, often occurs with concomitant pre-eclampsia; this and the fact that there is a swift resolution of the symptoms of pre-eclampsia *post partum* both support this supposition (that the placenta, rather than the foetus, is responsible for this condition).

It seems likely that the manifestations of pre-eclampsia are principally caused by an endothelial response to factors which arise from an incompletely developed placenta. The maternal glomerular endothelium is particularly vulnerable to such trauma. Blood entering the kidneys is always at the maximum available systolic pressure, as the renal arteries form the very first major tributaries of the descending aorta. This is a requirement for normal, efficient filtration of the blood; however, where there are

factors which compromise the integrity of this barrier, the protein overload cannot be dealt with in the usual way by the renal tubular epithelial cells. An additional complication of this condition is oedema; this may be superficial, involving the face or the extremities, or it may present as the more serious pulmonary oedema. In all cases, this is caused by an endothelial response to factors arising in the diseased placenta, leading to leakage from capillaries at these various sites.

During normal placentation, when cytotrophoblasts invade the uterine spiral arteries, the division of these cells leads to the temporary occlusion of these vessels and also to the ablation of their medial smooth muscle layer. In pre-eclampsia, there seems to be a partial failure of this process, such that the calibre of the vessels remains relatively small and the smooth muscle layer virtually intact; also, the number of spiral arteries invaded seems to be reduced in pre-eclamptic placentae (Lockwood et al., 2007). These features taken together mean that the pre-eclamptic placenta requires a much greater maternal systemic blood pressure in order to maintain an adequate flow rate in the maternal blood space. This is especially true during the third trimester, when the symptoms of this disease often first present themselves, and are always most serious.

The fact that the symptoms of this disease can be controlled to a greater or lesser extent by the administration of anti-hypertensive drugs suggests that there is an *inappropriate* demand by the placenta for this elevated maternal blood pressure. However, it is almost always thought best to deliver the babies slightly prematurely by Caesarean section, because of the unpredictable course of the disease, especially during the last weeks of pregnancy.

If undiagnosed or left untreated, the disease may progress to eclampsia proper, where the mother suffers convulsions before or during labour which, in turn, may lead to the death of both the mother and her unborn child; this is why pre-eclamptic mothers are often prescribed magnesium sulphate as a prophylactic. The World Health Organization (WHO) in their “World Health Report” (2005) estimated that pre-eclampsia/eclampsia was responsible for some 63,000 maternal deaths worldwide in the year 2000. This represents 12% of the total maternal deaths. In the developing countries this percentage is as much as *four times* higher, as there is often little or no provision of prenatal monitoring. In such situations the condition often goes unrecognised until it is too late.

The failure to establish sufficient contacts with the underlying decidua and spiral arterioles means that the frequency of anchoring villi will often be reduced in pre-eclamptic placenta. In such placentae, the area fraction of the basal plate *not* occupied by anchoring villi is increased compared to normal placentae.

The results of the study by Byrne et al. (Byrne et al., 2001) drew attention to the fact that most of the basal surface lining of the maternal blood space comprised a mosaic of different cell types (trophoblast and endothelium); it was envisaged that the ratio of these may be disturbed in pre-eclamptic placentae. The investigation by Smith et al. (Smith et al., 2004) confirmed that the area ratio of the endothelial component of the lining of the basal plate was indeed increased, albeit by a small percentage, in pre-eclamptic placentae. The results from this paper are dealt with in Chapter 5.

The synthesis by endothelial cells of many vaso-active compounds such as nitric oxide (from nitric oxide synthase), carbon monoxide (from haemoxygenase), von Willebrand factor and thromboplastin suggest that any potentially pathological increase in the

proportion of endothelial cells at the expense of trophoblast at this site may contribute to the hypertensive abnormalities seen in pre-eclampsia.

It has been suggested elsewhere, however, that this disease may be related more accurately to an *inflammatory* response (in the mother) to the accumulation, in her systemic blood, of cells and other debris from the foetus (Matthiesen et al., 2005). It is well documented that the syncytiotrophoblast cells surrounding the chorionic villi gradually become less cohesive and form what are termed 'syncytial knots'. These are often composed of several syncytial nuclei and their associated cytoplasm, which become detached from the terminal villi and are released into the maternal circulation. The integrity of the syncytiotrophoblast, in terms of its cytoskeleton, is likely to define how much of this foetal material finds its way into the maternal circulation. This was examined by Ockleford et al. (Ockleford et al., 2004), who showed that the overall expression of cytokeratins by syncytiotrophoblast was down-regulated in pre-eclamptic placentae. This study used a pan-cytokeratin antibody to measure this parameter. Using a panel of specific antibodies raised against the many isoforms of cytokeratin, Ahenkorah et al. (Ahenkorah et al., 2008) have shown that many of these cytokeratins (which contribute to the integrity of the villous syncytiotrophoblast) are significantly down-regulated in placentae from pre-eclamptic mothers. This may, in part, explain the increased amount of foetal material found in the maternal blood of pre-eclamptic pregnancies.

As well as covering parts of the basal plate, the endothelial layer was seen to extend round the marginal zone of the placenta and onto the inner chorionic surface (Byrne, unpublished observation). Some recent (collaborative) research by Hottor et al. (Hottor et al., 2010) examined the area fractions (lining the entire maternal blood space)

occupied by trophoblast, endothelium and fibrin in placentae from mothers with pre-eclampsia of varying severity. This study showed that the acellular fibrin layer was significantly higher in pre-eclampsia and increased in proportion to the severity of the disease.

1.3 Caveolae and the caveolins

Caveolae are small (50 – 100nm), bulb-shaped or spherical invaginations in the cell membrane of many different cell types. First discovered in 1953, in the early days of electron microscopy, by Palade (Palade, 1953) when examining the fine structure of capillaries, these vesicles were soon shown to be present in a wide range of other cells. It was Yamada (Yamada, 1955) who proposed the name ‘caveolae’ for these structures.

Had these been static rather than dynamic features, their purpose might have been simply to increase the surface area of the cell membrane. Assuming that the neck, or porus, of a caveola has approximately the same surface area as the space which it creates in its own and the cell’s surface, knowing the (inner) area of a sphere to be $4\pi r^2$ (where r is the radius) and the area immediately overlying the caveola to be πr^2 , then by cancellation, the extra area created by the possession of a caveola is 4 times greater than if it was not present. This, of course, only applies to the area overlying the individual caveola and not to the total cell surface area. However, in squamous cells, where the plasmalemmal surface area is large compared to the cytoplasmic volume, the possession of large numbers of caveolae undoubtedly increases the total area by a significant amount. The same is true for mature adipocytes, where most of the cytoplasm is displaced outwards by the large, central lipid droplet; interestingly, these cells have a greater number of caveolae per unit area than any other cell type. Also in lymphocytes,

where the nucleus occupies the majority of the cell's total volume and the cytoplasm is reduced to a thin cortical shell, the possession of many caveolae would significantly increase the total absorptive area. However, the presence of similarly sized, membrane-bound cytoplasmic vesicles, both adjacent to and (less commonly) distant from the cell membrane suggested (to the electron microscopists) that these vesicles were probably derived from caveolae.

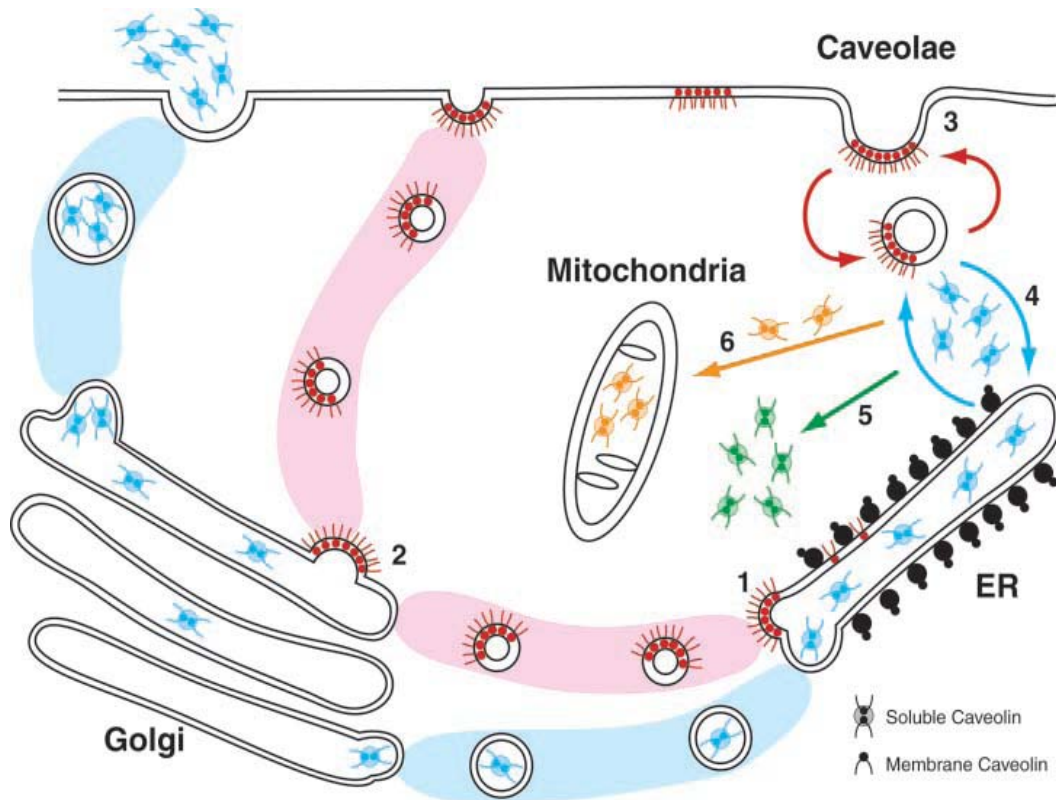
The discovery of dynamin, which forms an oligomeric collar around the necks of caveolae and has GTPase activity, implicated this protein in the pinching off or fission of caveolae and their release into the cytosol. Antibodies raised against dynamin and non-hydrolysable GTP analogues have both been shown to inhibit this fission process (Schnitzer et al., 1996). Caveolae thus represent a mechanism for trans-membrane transport for molecules whose size or other physical properties would otherwise preclude their entry into the cell. It has been suggested that multiple caveolae may form trans-endothelial channels which effectively fenestrate these cells (Stan, 2005).

Carbon-coated replicas from rapid-freeze, deep-etch cell membranes from caveolae-bearing cells (fibroblasts) revealed a fine, spiral pattern only on the *inner* surface of caveolae (Rothberg et al., 1992). It seemed likely that these threads were formed by a protein, or proteins, which were uniquely associated with caveolae. Caveolae were found to be selectively enriched in membrane preparations which had been treated with the detergents 3-[(3-cholamidopropyl)dimethylammonio]-1-propanesulfonate (CHAPS) or Triton X-114; two independent research groups showed that when the proteins derived from such preparations were subjected to electrophoresis, a major band of about 21kD was present. This was initially called VIP-21 (vesicle integral protein of molecular weight 21kD) but proved to be identical to caveolin-1 by sequence analysis

(Glenney, 1992). Once the nucleotide sequence for this protein had been established, it was soon discovered that two very similar proteins existed in caveolae. These were called caveolin-2 and caveolin-3 (Tang et al., 1996); all three members of this gene family share the amino acid motif FEDVIAEP. These three proteins differ in their tissue distribution, with caveolin-3 being restricted to muscle cells i.e. cardiac, skeletal and to a lesser extent smooth muscle (Song et al., 1996). Caveolin-1 and -3 are essential for the formation of caveolae, whereas caveolin-2 is not; yet each is able to form stable hetero-oligomers with the others. The most usual pattern of expression of the caveolins is as pairs of molecules in a single cell (Anderson, 1998).

Each has also been shown to bind cholesterol, which is essential to the formation of caveolae themselves. The presence of a cholesterol-binding domain in caveolin supports the notion that caveolae may represent specialised forms of membrane lipid rafts. These are microdomains of the cell membrane which are enriched in sphingolipids and cholesterol and have been shown to be important in signalling events. Although the caveolins are not trans-membrane proteins, being inserted only into the *inner* leaflet of the plasmalemma, they are associated intimately with whatever signalling or receptor molecules happen to be concentrated on the other side of the membrane (the *outer* leaflet). Thus, even if only by association, caveolins are involved in both signalling and endocytosis. Their capacity to bind cholesterol may also be responsible for intracellular cholesterol trafficking (Fielding and Fielding, 2001).

Beside the usual form of caveolin-1 (as filaments decorating caveolae) a soluble form of the protein has been shown to exist (Liu et al., 2002). These authors have proposed a schema for the pathways involved in the production of both the soluble and insoluble forms; this is represented in Figure 1.7



[This Figure courtesy of Liu et al. (2002) in “Multiple Functions of Caveolin-1” *Journal of Biological Chemistry* **277** (44): p 41297.]

Figure 1.7 A proposed scheme for the destination of newly-synthesised caveolin-1

Some newly formed caveolin-1 is incorporated into the endoplasmic reticulum (ER) membrane, with both its N- and C-termini on the cytoplasmic surface. Small vesicles are formed which bud from the ER surface and are transported to the Golgi apparatus. Here, the caveolin-1 oligomerises and becomes detergent insoluble; after being transported to the cell surface, this insoluble form becomes incorporated into functional caveolae (pink pathway). In a separate pathway, it was proposed that during the internalisation of caveolae some caveolin-1 becomes de-polymerised and is made soluble by attachment to minute lipid droplets. Some of this finds its way to mitochondria (orange arrow), some remains free in the cytoplasm (green arrow), whilst the remainder is thought to return to the ER and thence to the Golgi apparatus where it may be exported from the cell (blue pathway).

In addition to the caveolins and dynamin, other accessory proteins have also been found to associate with the cytosolic face of caveolae. Cavin, otherwise known as polymerase-1 transcript release factor (PTRF)-cavin (Hill et al., 2008) is a 60kD protein which binds both to caveolin and filamin; this latter protein binds to intracellular (cortical) f-actin. In this protein there might thus be a mechanistic candidate for translocation of detached caveolae. The structure of caveolae with respect to their constituent parts has been proposed in the following illustration, which is reproduced, with appended permission, from Hansen CG and Nichols BJ “Exploring the caves: cavins, caveolins and caveolae” in *Trends in Cell Biology* **24** (4): 177-186.

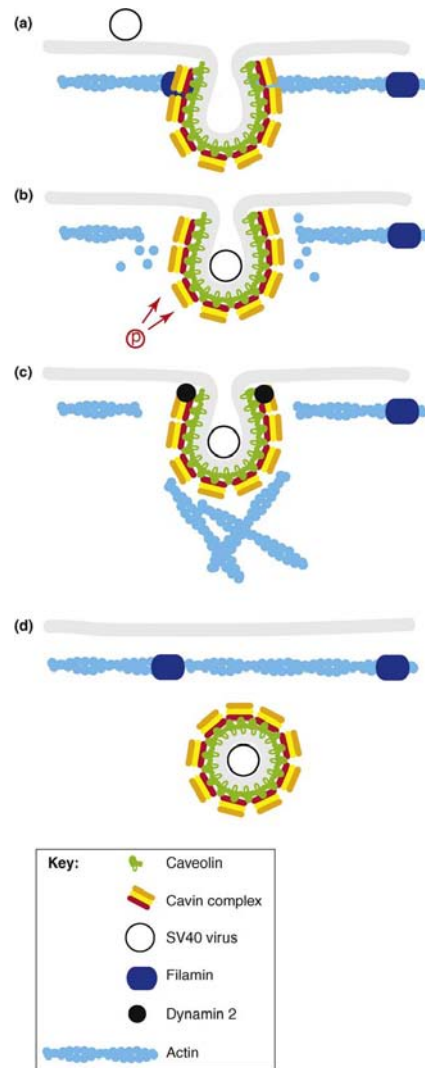


Figure 1.8 Proposed structure of caveolae in relation to caveolin, cavin and dynamin. How these proteins may interact with cytoplasmic proteins to effect fission and internalisation following binding of a caveolar ligand (SV40).

The cavin complex is thought to bind to caveolin-1 on the cytoplasmic surface of caveolae. It also binds filamin, which is associated with filamentous actin. When a ligand (in this case the simian virus SV40) attaches to the outer surface of the caveola, dynamin, which encircles the neck of the caveola, contracts and pinches off the vesicle which is then internalised and presumably transported to its intended destination via the actin cables.

It seemed likely that caveolae may have a significant role in trans-epithelial processes in the human placenta. Though the major transport vesicle in the syncytiotrophoblast is the clathrin-coated pit, the cytotrophoblast (from which it is derived) expresses caveolin-1. It appears that this expression is down-regulated upon syncytialisation (Linton et al., 2003). One hypothesis being tested is that antibodies to caveolin-1 may be used at a microscopic and ultra-structural level to identify cells that are involved in signalling and macromolecular trafficking across the placenta and to discriminate between these and other cells which use the 'coated pit' as a transport vesicle.

As is often the case in protracted pieces of research, there appeared to be further avenues to explore, based on the results of the initial studies. These included the investigation of the extent of the endothelial lining of the basal plate and whether this area ratio was significantly disturbed in placentae from pre-eclamptic pregnancies. It was also thought useful to establish the derivation of these endothelial cells – to determine unequivocally whether they were of foetal or maternal origin. The aims of the study are summarised in Section 1.3.

1.3 Aims of the study

The specific aims of this study were:

- (i) To determine the distribution of the protein caveolin- 1 in the human term placenta at both the cellular and sub-cellular level.
- (ii) To determine the extent of the caveolin-1 positive endothelial cells lining the basal plate.
- (iii) To establish whether there was any significant change in the *proportion* of the basal plate endothelial lining in pre-eclamptic placentae compared with those from normotensive pregnancies.
- (iv) To determine whether these caveolin-1-positive endothelial cells were of foetal or maternal origin.

Chapter Two: Materials and methods

Unless otherwise stated, all commonly-used chemicals and antibodies were obtained from Sigma Aldrich Ltd, St. Louis, MO, USA, or Sigma Aldrich Ltd, Poole, Dorset, UK.

2.1 Tissues used, cryo-fixation and cryo-sectioning.

For the anti-caveolin-1 immunocytochemical study human placentae, foetal membranes and umbilical cord specimens were obtained from The Leicester Royal Infirmary Maternity Unit following either natural (trans-vaginal) childbirth or elective Caesarean section. Ethical guidelines in place at the time were always adhered to; for the immunofluorescence study, verbal permission to use the material was obtained from the mothers via the duty midwife. For the later studies, when there was a legal requirement to do so, ethical approval was first granted and written consent obtained from the mothers. The tissue was obtained using procedures given approval by the Leicestershire Research Ethics Committee, Reference N^{os} 6336 and 7144 and the University Hospitals of Leicester NHS Trust, Project N^{os} 7180, 9161 (copies of patient information sheets and consent forms appear in the Appendix). Tissues for fluorescence immunocytochemical studies (from 13 births) were dissected and immersed in OCT (optimum cutting temperature) cryo-embedding medium (Miles, Elkhart, IL, USA) contained in aluminium foil moulds and frozen-fixed in a slush of solid CO₂ and hexane (-78°C), within minutes of delivery. For each placenta, 3 areas of the basal plate were chosen for sampling: one from the marginal zone, one from the central area and one from the intermediate zone. Other samples for this study (umbilical cord, chorionic plate and amnio-chorion roll) were prepared in a similar manner. For the pre-eclamptic

study, 15 healthy and 15 pre-eclamptic placentae were used and a more rigorous sampling procedure was adopted: for each placenta, 3 shallow, 2cm wide radial strips, separated by 120° were taken from the basal plate and rolled up ‘Swiss-roll style’ before being placed in the OCT-filled foil moulds. A schematic diagram (Figure 2.1) illustrates the sampling zones used in the experiments described herein.

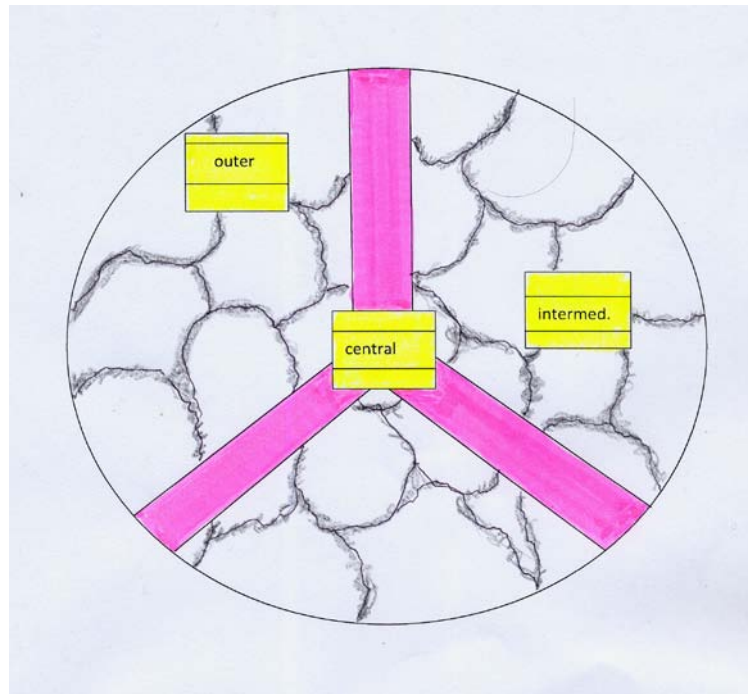


Figure 2.1 Schematic representation of basal plate sampling zones

The yellow areas (outer, intermed.[iate] and central) are those from which the basal plate samples were taken for the immunofluorescence, the immuno-electron microscopic and the cytogenetic studies. The pink areas are 2cm wide radial strips, separated by 120° which were used in the pre-eclampsia study.

Blocks for both sets of experiments were sectioned at 5-7 μ m using a Leitz cryomicrotome. Sections were thawed onto 3-aminopropyltriethoxy silane-coated glass slides, air-dried for 15 minutes and fixed for 10 minutes at ambient temperature in freshly prepared 50:50 acetone/methanol.

2.2 Immuno-fluorescence cytochemistry

Frozen sections were exposed for 18 hours at 4°C to a 1:100 dilution of the primary antibody in phosphate-buffered saline/Tween (PBST): 137mM NaCl, 10mM Na₂HPO₄ / NaH₂PO₄, 0.1% v/v Tween-20, pH 7.4, containing 20% non-immune goat serum. The primary antibody was a rabbit polyclonal anti-human caveolin-1 (Catalogue No. C13630, Transduction Laboratories, Lexington, KY, USA) supplied at a concentration of 1mg ml⁻¹. Following three 10-minute PBST washes, sections were exposed to the FITC-conjugated secondary antibody, a goat anti-rabbit IgG (Sigma # F-1262) with a starting concentration of 1.1 mg ml⁻¹, diluted 1:200 in PBST, again containing 20% non-immune goat serum, for up to 2 hours at ambient temperature (20-24°C). After three further 10-minute washes in PBST, sections were mounted under No.0 coverslips in a photo-bleach retardant, glycerol-based mountant (Citifluor, Canterbury, UK). A polyvinyl alcohol mountant Mowiol (Merck Chemicals, Nottingham, UK), with diazobicyclo[2,2,2]-octane (DABCO) as photobleach retardant was prepared in-house and used for all later cryo-sectioned applications.

For the pre-eclamptic study, a panel of trophoblast and endothelial cell markers was used: Trophoblast marker primary antibodies – Mouse monoclonal anti-Pan-cytokeratin (Sigma C2931), used at a concentration of 1:800; Rabbit polyclonal anti-human chorionic gonadotrophin, α - and β -chains (Sigma C8534) at 1:50; Mouse monoclonal

anti-human chorionic gonadotrophin, β -chain only (Sigma C7959) at 1:50 or 1:100 and Rabbit polyclonal anti-human placental lactogen (Novocastra NCL-PLp, Novocastra Laboratories, Newcastle, UK) at 1:800. Trophoblast secondary antibodies were (i) Cy3-conjugated sheep anti-mouse affinity-pure IgG Fab2 fragment-specific (Jackson ImmunoResearch, West Grove, PA, USA) and Cy3-conjugated sheep anti-rabbit IgG (Sigma C2306) at 1:200. Endothelial marker primary antibodies – Rabbit polyclonal anti-vimentin (Ab7783, Abcam, Cambridge, UK at 1:10-1:400; Rabbit polyclonal anti-human von Willebrand factor (Sigma F3520) at 1:400; Mouse monoclonal anti-thrombomodulin/CD141 (MS-1102-R7, Neomarkers, CA,USA) at 1:30-1:50; Mouse monoclonal anti PECAM-1/CD31 (MS-353-R7, Neomarkers) at 1:80 and the anti-caveolin-1 antibody used in the previous study (13630, Transduction Labs) at 1:100. The manner in which these antibodies were applied to the sections is the same as for the anti-caveolin-1 study.

2.3 Polyacrylamide gel electrophoresis (PAGE) and blotting

Samples of the following tissues: amnion, chorion, amniochorion, basal plate, chorionic plate, chorionic villi and umbilical cord were obtained following three deliveries of healthy babies from the above group. The tissues, which were taken without a specific sampling strategy, were rinsed in PBS, scissor-minced and frozen in liquid nitrogen then pulverised using a pre-cooled mortar and pestle. The powdered tissue samples were stored in small airtight containers at -80°C . An endothelial cell extract used as a positive control sample was supplied with the primary antibody. Samples were solubilised using Laemmli sample buffer (Laemmli, 1970), with or without 5% v/v β -mercaptoethanol (to reduce the proteins to single polypeptide chains). This buffer had the following

constituents: 180mM tris -hydroxymethylmethamine/hydrochloric acid (Tris/HCl), 5.7% w/v sodium dodecyl sulphate (SDS), 29% v/v glycerol, 0.003% w/v bromophenol blue, pH 6.8. The powdered tissue samples were solubilised directly in this buffer by vortexing and heating in a boiling-water bath for 3 minutes, then centrifuging at 13 000 rpm in a microcentrifuge for 3 minutes. The supernatants, which contain the solubilised proteins were retained for analysis, the insoluble proteins contained in the pellets (collagens, keratins etc., as well as nucleic acids) were discarded. Supernatants were stored at -80°C until use.

A modified version of Laemmli's original method was used for the electrophoresis. Samples were diluted to give a final protein concentration of 1 mg ml⁻¹; 25µl aliquots of these were loaded onto a 5–20 % polyacrylamide gradient gel, which was chosen for its superior resolution compared to that of gels with a single concentration of acrylamide. This was cast in the laboratory using a two-chamber gradient mixer illustrated in Figure 2.2. This contained (at the outset) solutions of 5% and 20 % acrylamide respectively. Both of these solutions were diluted from a 40% w/v stock solution containing 1.067% w/v *bis*-acrylamide (BDH, Loughborough, UK). The gel was cast between 2 glass plates 175mm wide and 140mm high (separated by 1.5mm thickness spacers) and carefully overlaid with 1-2ml distilled water. Once this resolving gel had polymerised, the water was poured off and a 4% acrylamide stacking gel was overlaid, which allowed the wells to be formed by placing a 'comb' between the top of the plates. The constituents of the gel mixtures are also shown in Figure 2.2.

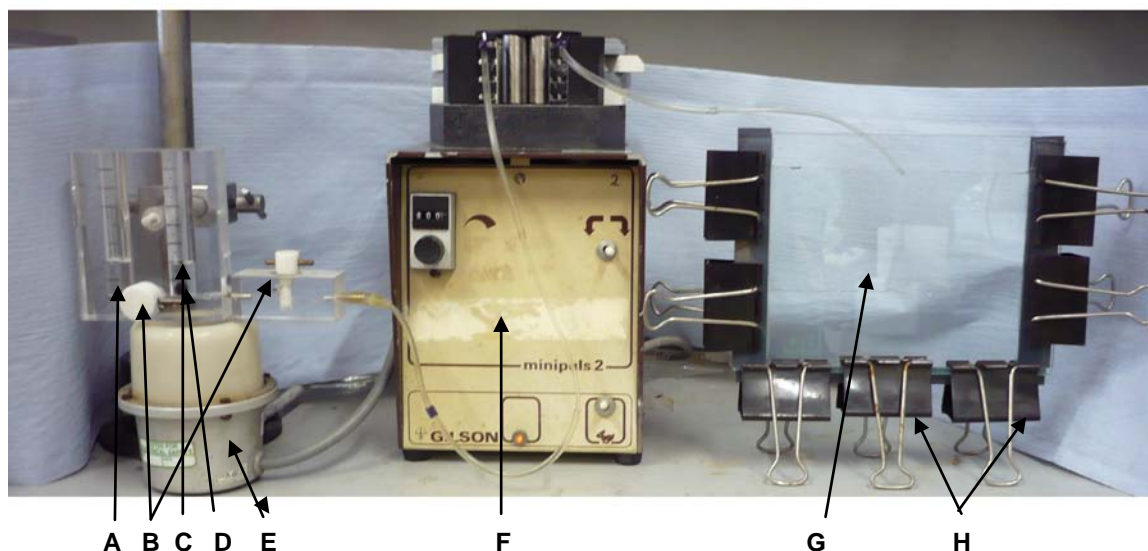


Figure 2.2 Gradient acrylamide gel pouring apparatus

- A. 5% acrylamide chamber.
- B. Valves (closed when filling, open when casting).
- C. 20% acrylamide chamber.
- D. Magnetic stirring bar ('flea').
- E. Magnetic stirrer.
- F. Peristaltic pump set to deliver 1.5ml minute⁻¹.
- G. Glass plates.
- H. Bulldog clips.

Constituents for casting 5-20% acrylamide gradient gels.

	5% acrylamide	20% acrylamide	4% (stacking gel)
40% acrylamide stock	1.25ml	5ml	1ml
Resolving gel buffer	2.5ml	2.5ml	-
Stacking gel buffer	-	2.5ml	-
Glycerol	-	-	0.25ml
Water	6.25ml	2.25ml	6.5ml
10% ammonium persulphate	32µl	32µl	40µl

The resolving gel buffer was 1.5M Tris/HCl pH 8.8 with 0.7% SDS and the stacking gel buffer was 0.5M Tris/HCl pH 6.8 with 0.7% SDS. The 10% w/v (aqueous) ammonium persulphate was freshly prepared and added just prior to pouring. Running buffer for both the upper and lower reservoirs was 25mM Tris base, 192mM glycine, 0.1% w/v SDS.

A fixed current of 40mA was used, with the maximum available voltage to maintain this current being set at a nominal 300V. Fractionation was continued until the bromophenol blue had migrated off the bottom of the gel (~2.5hours). A standard molecular weight reference track was used to estimate the molecular weights of the bands. Test gels were stained overnight in 0.1% w/v Coomassie brilliant blue R-250 in 10% v/v methanol, 10% v/v acetic acid. Destaining of these gels utilised several changes of 10% v/v acetic acid, 5% v/v industrial methylated spirit (IMS) over many hours. The inclusion of a small roll of paper towelling was found to facilitate the destaining, as the liberated dye is adsorbed onto the surface of the paper.

Proteins (from unstained gels) were transferred onto either a nitrocellulose or a polyvinylidenedifluoride (PVDF) membrane using a method derived initially from Towbin (Towbin *et al.*, 1979), only in this case, a semi-dry blotting system (LKB Multiphor II, LKB, Bromma, Sweden) was used. Transfer buffer was a modified version of that described by Bjerrum and Schafer-Nielson (Bjerrum and Schafer-Nielson, 1986). This consisted of 25 mM Tris/HCl, 192 mM glycine with 10% v/v methanol (but without SDS). Efficient transfer from the gel to the membrane was assured using Ponceau S staining (0.2% w/v Ponceau-S in 4% w/v trichloroacetic acid) for 30 seconds, followed by 3 distilled water rinses. This dye only stains the protein

bands at low pH, so when the membrane is returned to a neutral pH the staining is lost. For this reason, the positions of the bands in the marker track were marked permanently by pricking through the membrane using a sharp needle. Non-specific IgG binding sites were blocked by incubating the membrane in blocking buffer. This was 5% non-fat milk, 1% bovine serum albumin, 0.5 M glucose and 2.5% glycerol in Tris-buffered saline/ Tween (TBST; 20 mM Tris/HCl, 0.8% NaCl, 0.1% Tween-20, pH 7.6) for 30 minutes at room temperature (RT). Immunoreactivity was tested using a 1:10,000 dilution of the primary antibody (*vid. sup.*) in blocking buffer for 2 hours at room temperature. After 3 x 10-minute washes in TBST, the blot was incubated with a 1:50,000 dilution of a horseradish peroxidase-conjugated mouse monoclonal anti-rabbit IgG (A-2074, Sigma), in blocking buffer for a further 90 minutes at RT. After three further 10-minute washes in TBS/T, a chemiluminescent substrate (Pierce SuperSignal Rockford, IL, USA) was applied to the blot for 1 minute; the membrane was then quickly drained and wrapped in Saran Wrap™ (Dow Corning, GmbH, Wiesbaden, Germany). The membrane was then placed in a cassette under safelight conditions and a piece of Fuji medical X-ray film was placed on top and the lid closed. Exposure was initially for 1 minute, after which the film was removed and developed, using a 1:10 dilution of Ilford PQ Universal developer (2 minutes) and fixed in a 1:5 dilution of Ilford Hypam fixer. If further exposures were not deemed necessary, the films were dried, scanned and the digital images were printed on paper. A standard curve from the marker track was produced by measuring the distance migrated (from the top of the gel) and plotting this against the \log_{10} of the known molecular weights of the standards. The molecular weights of the unknown samples may then be estimated by measuring their individual migration distance and taking the antilog_{10} where it crosses the plotted line.

2.4 Fluorescence microscopy

Tissue sections from a total of 39 blocks (as per Section 2.2) were initially viewed using a Zeiss epifluorescence microscope equipped with standard filter sets to check for FITC fluorescence. Favourable sections were further examined using a confocal laser scanning attachment (Biorad MRC 600) linked to a Zeiss Axiovert epifluorescence inverted microscope. This equipment utilized a reverse light path fibre-optic channelled Nomarski differential interference contrast (DIC) signal to the second detector, to allow comparison between immunofluorescent and refractive index (RI) related images of the same specimen. The DIC images are roughly equivalent to the more familiar phase-contrast images though the optical systems used to produce them differ. The software allows the two images (fluorescence and DIC) to be superimposed. The relationship between specimen RI and dry mass makes this a useful measure of the selectivity of the immunostaining. Images were recorded using Biorad Comos software version 6.05.8 and exported to Adobe Photoshop for labelling and print production.

2.5 Semi-thin (0.5 μ m) section light microscopy and transmission electron microscopy

For this study, 3 smooth, undamaged areas of the basal plates of 2 placentae were chosen, one each from the periphery, the centre and the intermediate zone. These were injected at a shallow angle with normal saline (137 mM aqueous sodium chloride) so that a blister was raised beneath the surface. The syringe was removed and replaced with one containing the glutaraldehyde fixative (*vid. inf.*), which was slowly introduced into the cavity. The surface was irrigated with more of the same fixative and the preparation was allowed to stand for some 15 minutes. A square with a side of ~15mm was cut around the injection site and the basal plate surface removed, by carefully

'carving' the underlying tissues away with a scalpel. These small excised pieces of basal plate were pinned onto an inert substrate (Sylgard ®Dow Corning) and immersion-fixed in 2.5% glutaraldehyde in phosphate buffer for a further 1 hour at room temperature. The buffer in this case was 0.1M sodium phosphate, pH 7.4, with 10% v/v of a 25% aqueous stock solution of glutaraldehyde. The tissue was then cut into smaller pieces (3 x 3 x 10 mm) and post-fixed for 1 hour in 1% w/v aqueous osmium tetroxide. After a thorough wash in distilled water, it was dehydrated through an ethanol series (75%, 90%, 2 x 100%, 20 minutes in each change), then transferred to 1, 2-epoxypropane (2 changes, 10 minutes each) and thence into a 50% v/v solution of Araldite resin in 1,2-epoxypropane. The glass vials containing the specimens were left uncapped in a fume hood overnight (the volatility of the solvent ensures that the concentration of the resin reaches >95% by the following morning). The resin was replaced 3 times, each change lasting 1 hour, before the specimens were transferred to polypropylene Beem capsules. Polymerisation of the resin was achieved by baking the capsules for 17 hours at 60°C. Semi-thin (0.5µm) sections were cut, using a glass knife on a Reichert-Jung Ultracut ultramicrotome. These sections were collected from the water-filled trough at the back of the knife edge and transferred to a droplet of water on a silane-coated glass slide, baked on a 90°C hotplate to increase adhesion and stained thereon for 1 minute with a mixture of 1% w/v toluidine blue and 2% w/v basic Fuchsin in 2% w/v borax. After washing in distilled water and drying, the sections were viewed and photographed using a Leitz Diaplan microscope equipped with a Vario-Orthomat camera system. A Zeiss x 100 oil-immersion objective lens was normally used and the images recorded on Kodak Technical-Pan film, with the film speed set at 32 ASA (16 DIN). After 10 minutes development at 20°C in 1: 20 Acutol (Paterson, Tipton, UK) the film was enlarged and printed on resin-coated paper. A montage covering a linear

stretch of the lining of the maternal blood space was produced, and a small area that included an anchoring villus (which interrupted the endothelium) was selected for ultrathin sectioning. These latter sections were cut at a thickness of 50–80 nm (silver or pale gold interference colour of reflected white light) using a diamond knife and picked up on 200-mesh carbon/formvar coated nickel grids and stained with saturated aqueous uranyl acetate and Reynolds' lead citrate (Reynolds, 1963). The sections were then viewed in a Siemens 102 electron microscope, photographed and printed on resin-coated paper.

2.6 Scanning electron microscopy

A further 6 samples for scanning electron microscopy were fixed initially by injecting sites on the basal plate of intact placentae with 2.5% glutaraldehyde in 0.1 M phosphate buffer, pH 7.4 as before (Section 2.5). The fixative was again applied to the exposed (abscission) surface itself, to prevent drying. When the tissue had hardened a little (15 minutes), a very thin layer of basal plate was excised using a scalpel (held almost horizontally) and pinned onto an inert elastomer substrate 'Sylgard' (Dow Corning GmbH, Wiesbaden, Germany), with the *inner* surface uppermost. Fixation was continued for 1 hour after immersing the whole preparation in the fixative. After washing in water, the tissue was removed from the substrate and post-fixed for 1 hour in 1% aqueous osmium tetroxide, thoroughly washed in several changes of distilled water and dehydrated through an ethanol series (70%, 90% and 2 changes of 100%, 15 minutes per change) then transferred to absolute acetone prior to being critical-point dried. For this technique, the specimens were placed in a pressure-resistant chamber with a transparent end-plate. The acetone was replaced by liquid CO₂ using the inlet and

exhaust valves on the chamber. Once all the acetone had been replaced, the temperature in the chamber was raised slowly until the liquid/vapour interface had disappeared (the critical point, at which temperature the liquid and vapour phases of CO₂ were in equilibrium). At this point, the pressure in the chamber was gradually released using the exhaust valve, until atmospheric pressure had been resumed. The specimens were then removed, attached to 1cm diameter aluminium stubs using a silver-based conductive adhesive, and stored in a vacuum desiccator. A thin layer of gold/palladium was sputter-coated onto the specimens, which were then viewed in a Hitachi F-3000 H scanning electron microscope, using a 5kV accelerating voltage. Digital images were stored on disc, and printed from Adobe Photoshop, Version 6.

2.7 Tissue preparation for methacrylate resin embedding

Five term placentae were obtained from the Maternity Unit at Leicester Royal Infirmary, following normal, uncomplicated (trans-vaginal or elective Caesarean) births. Informed consent was obtained according to local ethical guidelines in place at that time. Small pieces of basal plate (10 x 10 x 2 mm deep) were excised within minutes of delivery and fixed for 1 hour in 4% paraformaldehyde, 0.1% glutaraldehyde in phosphate-buffered saline (PBS). After this fixation step, the tissue was cut into 2mm wide strips, dehydrated through an ethanol series (70%, 90% and 2 changes of 100%, 1 hour each) and transferred to LR White resin (London Resin Company, London, England). The samples were left overnight in this, and then given 2 x 1-hour changes in fresh resin. Finally, the samples were placed in 7mm diameter gelatin capsules which were *completely* filled with the resin, in order to exclude oxygen which would inhibit total polymerisation. The capsules were incubated at 55°C for 18 hours.

2.8 Sectioning and immunogold labelling

The tissue blocks were trimmed and mounted *horizontally* on small brass stubs. This allowed a linear stretch of some 8-10mm of the basal plate lining surface to be cut at each pass of the block past the knife edge. Semi-thin (0.5-1.0 μ m) sections were baked onto glass slides, stained with 1% toluidine blue in 1% borax and viewed microscopically. Favourable regions of these sections were chosen, so that the (extremely) large block-face could be trimmed down to a size suitable for ultramicrotomy. Thin (80-100nm) diamond-cut sections from these were collected on 200-mesh nickel grids. These latter had been 'subbed' (made more tacky) by immersion in a solution of Sellotape™ adhesive: ~ 10cm of a 15mm width roll was placed in 5ml chloroform; when the adhesive had dissolved, the cellulose tape was removed. The grids were dipped in this solution and then immediately drawn along a piece of lint-free tissue until all the chloroform had evaporated. They were then used to collect the sections from the knife's water trough. When the sections were dry, they were stored in grid boxes until required.

For the incubations, a series of shallow depressions (in a square array) were pressed onto the surface of a sheet of dental wax using the rounded end of a 5mm glass rod. The arrangement is illustrated in Figure 2.3.

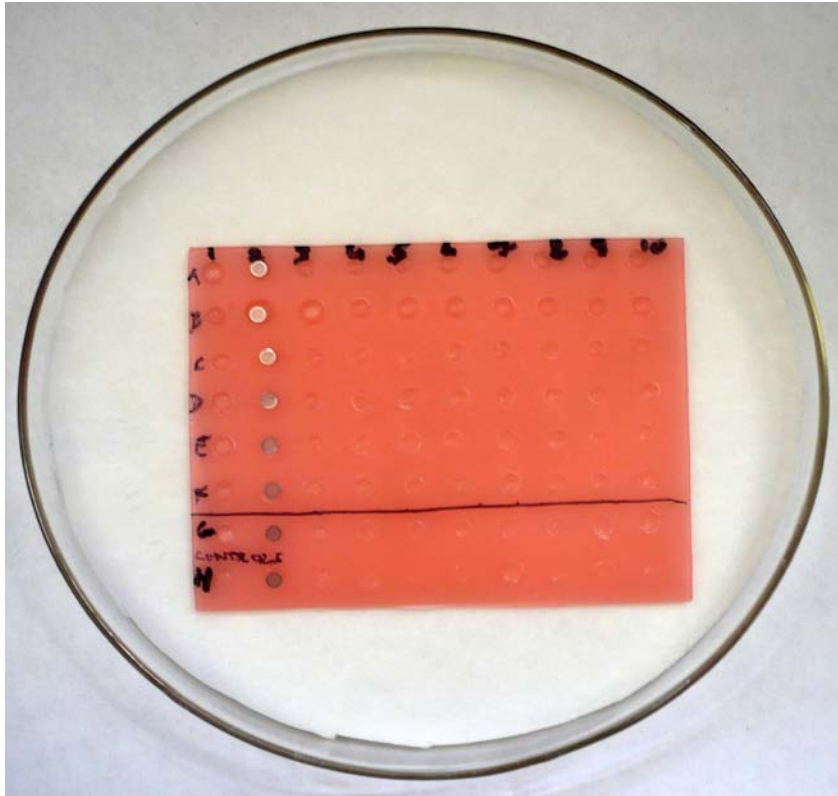


Figure 2.3 Apparatus for immunostaining of EM grids.

Grids in rows A - F were experimental grids; those in **G & H** were controls (no primary antibody).

Column 1 contained blocking buffer.

Column 2 contained 1:5 dilution of 1^o antibody in blocking buffer (except at positions **G & H**, which contained only blocking buffer).

Column 3 contained more blocking buffer.

Column 4 contained a 1:50 dilution of gold-conjugated 2^o antibody in blocking buffer.

Column 5 contained distilled water.

Column 6 contained 5% uranyl acetate in 9% isopropanol.

Column 7 contained distilled water.

Columns 8 – 10 were not used.

The wax sheet was placed in the lid of a large (14cm diameter) glass Petri dish containing a water-saturated disc of thick filter paper (Schleicher and Schuell, Catalogue number GB 005 – Sigma Aldrich, St. Louis, MO, USA). 10µl droplets of blocking solution, [2% v/v normal goat serum (NGS) /1% w/v bovine serum albumin (BSA) / 1% v/v Tween-20 in PBS] were placed in the 1st column of these depressions and the grids were floated, section-side down, on their surfaces and, when the base of the dish (which acted as a lid) had been replaced, were left at room temperature for 2 hours. The primary antibody was a rabbit anti-human caveolin-1 (Transduction Laboratories, C13630 *vid. sup.*), which was diluted 1:5 in the same blocking buffer. Grids were floated on droplets of this solution (in the 2nd column of depressions) and left at 4°C overnight. The grids were washed by dipping 20 times in TBST in 3 separate glass vials, then in TBS, before drying and returning (for 20 minutes to fresh 10µl droplets of blocking buffer in the 3rd column of depressions. The secondary antibody, a 10nm gold-conjugated goat anti-rabbit IgG (British Biocell International, Golden Gate, Cardiff, UK) was diluted 1:50 in blocking buffer and placed in the 4th column. The grids were floated, as before, on the surface of these and allowed to incubate for 2 hours at room temperature. The washing steps were identical to those used after the primary antibody, only after the third set of TBST washes, the grids were gently washed in a stream of distilled water from a wash-bottle before being dried. The sections were then placed on droplets of distilled water in the 5th column, prior to being passed to the next column and stained for 15 minutes in 5% uranyl acetate in 9% aqueous isopropanol (6th column). The grids were then quickly passed across onto the final (7th) column which contained distilled water. Finally, the grids were washed by dipping 20 times in 3 vials of distilled water. They were then blotted dry on lint-free tissue, air-dried and viewed using a Jeol 100 CX-II transmission electron microscope at c.10,000 x magnification.

2.9 Gold particles per unit area calculation

Film images from these were scanned and digitised before being imported into Adobe Photoshop for labelling and print production. A continuous sequence of all adequately preserved areas of tissue was imaged and used for area measurement and particle counting. For the polarity studies digital images were recorded directly from the TEM. Laser-jet printed photomicrographs were used for manual quantitation. In this case, a square of the paper having sides equal to the $1\mu\text{m}$ scale bar (included automatically on each image on this machine) was cut out of the print and weighed on a milligram balance. This *mass* then represented an area of $1\mu\text{m}^2$ on the paper. The masses of the various cell types and organelles cut out of the prints gave a very accurate estimation of their area, when compared to the standard $1\mu\text{m}^2$ mass. This method is an adaptation of one which was once commonly used to estimate the area under a complex curve before computer algorithms had been developed to do this task (see, for instance <http://www.uiowa.edu/~cmrf/methodology/stereology/index.html>). By these means, the number of gold particles per unit area for a given cell or organelle could be estimated with a high degree of confidence.

2.10 Cytogenetic study: Tissue collection and preparation.

Freshly delivered term placentae (n = 22, 19 from births of male babies, 3 from births of female babies) were obtained from Leicester Royal Infirmary maternity hospital following the birth of healthy babies after uncomplicated trans-vaginal and elective Caesarean deliveries. The basal plate (BP) was exposed and a smooth, undamaged area chosen for dissection. This area was initially injected with 10ml normal saline (137 mM NaCl, unbuffered) which diluted the blood in the maternal blood space and raised a

blister under the basal surface. The site was then injected with 10% unbuffered formal saline (4% formaldehyde in tap-water normal saline) and allowed to stand for 5 minutes; the exposed surface was irrigated with the same fixative to prevent drying. When the tissue became slightly firm, a square patch with a side of some 2cm was carefully excised using fine scissors and stored in fresh fixative in a universal bottle for 48 hours. After this the squares were cut into strips ~ 5mm wide. These were dehydrated using an alcohol series (70, 90, 100%: 2-3hours per change) of either ethanol or isopropanol. Xylene (20 minutes) was used as clearing agent. Tissues were impregnated with 56°C paraffin wax under vacuum before being orientated *on their edges* in plastic moulds and allowed to cool. For fluorescence *in-situ* hybridisation (FISH) studies, 5-7µm frozen sections were cut from Tissue-tek OCT embedding medium. Wax sections for enzyme labelling *in situ* hybridisation were cut at a thickness of 10µm (rather than the more usual 4-5 µm). These latter sections were floated out on warm (45°C) distilled water and mounted on coated slides. These were then dried overnight on a 45°C hotplate, de-waxed in two changes of xylene (10 minutes each), followed by rehydration through an ethanol series (100% for 5 minutes, 3% hydrogen peroxide (H₂O₂) in 90% methanol for 15 minutes, 90% for 5 minutes, 70% and 50%, 5 minutes each) to water or buffer. The peroxide step is included in this series to quench any endogenous peroxidase activity in the tissue.

2.11 Y-chromosome probe preparation and application

The labelled probe, pHY2.1, was synthesised by copying the template DNA carried on plasmid pBR328, (in this case a human Y-chromosome DNA sequence, restricted with Msp1), using Klenow large-fragment DNA polymerase in the presence of dinitrophenol (DNP)-labelled dUTP. The other nucleotides were not labelled. The reaction was

carried out overnight at room temperature. To facilitate the penetration of the probe into the section, pronase-E ($<150\mu\text{g ml}^{-1}$) or, more reliably, pepsin ($200\ \mu\text{g ml}^{-1}$ in 0.2M HCl) were used (Evans et al., 2003); this partially digested the sections without appreciably altering their morphology. The incubation time was limited to ~25 minutes. As an additional step, sections were pre-treated for 20-30 minutes with 10mM citrate buffer, pH 6.0 at 95°C , then 'rested' in fresh citrate buffer at room temperature for a further 20 minutes (Evans et.al., 2002). After digestion, the sections were pre-hybridised in a buffer containing 50% formamide and random DNA. This step ensured that non-specific DNA binding sites were saturated with unlabelled DNA. The probe (diluted in the same buffer) was applied to the sections, which were then incubated at 100°C for precisely 10 minutes. Once removed, they were maintained at 42°C for up to 48hr. All incubations were carried out in sealed, water vapour-saturated containers. Unbound labelled probe was removed from the sections by high stringency washing (2x SSC containing 50% formamide) followed by 0.1x SSC with 2mM MgCl_2 and 0.1% Triton X-100) at 42°C .

2.12. Visualisation of positive hybrids

To visualise the hybrids, a goat anti-DNP rabbit IgG, labelled with horseradish peroxidase (HRP) was used. The sections were incubated for 1 hour at room temperature with the antibody diluted 1:50 in 1% bovine serum albumin in Tris buffered saline, pH 7.6 containing 0.1% Tween-20 (TBST). Sections were then washed in 5 changes of TBST, 3 minutes each. An almost colourless substrate, diaminobenzidine tetrahydrochloride (DAB) was dissolved at a concentration of 1mg ml^{-1} in 0.2M Tris/HCl containing 7.5 mM nickel ammonium sulphate. Immediately before use $8.0\mu\text{l}$

of a 30% solution of hydrogen peroxide was added to each 10 ml of substrate, which was then applied to the sections through a 0.2 μ m syringe filter.

The HRP oxidised the substrate to produce an intense, insoluble black product at the hybridisation sites. After 3-7 minutes, when there was an overall purple/grey tinge on the sections, they were washed in distilled water, then counterstained with nuclear stains including methyl green, nuclear fast red or (preferentially) Kirkpatrick's carmalum, without acid-alcohol differentiation. Sections were rinsed in water, blotted dry, dehydrated in 90% and 100% alcohol, cleared briefly in xylene and coverslipped with the synthetic plastic mountant DPX.

For fluorescence signal visualisation, the sections were incubated with a FITC-labelled goat anti-rabbit IgG antibody (Sigma F0382) diluted 1:100 in TBST containing 1% BSA. This step replaced the DAB incubation in the immunohistochemical protocol. After 45 minutes, the sections were washed in TBST, counterstained with propidium iodide at a final concentration of 100ng ml⁻¹ during the last rinsing steps, then coverslipped in a polyvinyl alcohol (Mowiol) mountant: 10% w/v Mowiol 4-88 (Calbiochem 475904), 25% w/v glycerol, 2.5% w/v 1,4-diazobicyclo[2.2.2]octane (DABCO), 100mM Tris/HCl pH 8.0. (DABCO is a photo-bleaching retardant).

2.13 Microscopy

Sections were viewed and counts made by 3 independent observers using a Leitz Diaplan or a Zeiss Axioplan Imaging II fitted with a Zeiss AxioCam digital camera attachment. Fluorescence preparations were viewed using Zeiss epifluorescence microscope and a Biorad MRC 600 confocal laser scanning microscope (CLSM)

attached to a Zeiss Axiovert microscope. Images were recorded on Fujichrome Provia 400F film then scanned and digitised or recorded directly as digital image files. Digital images were processed using Zeiss Axiovision software, exported to Adobe Photoshop for labelling and processing. Stage mounted length standards were imaged under the same conditions as the specimen to calculate magnifications.

2.14. Statistical analysis.

Gold particle counts from printed digital electron micrographs allow the estimation of the number of particles per unit area for a particular cell type, or region within a cell. This is taken to equate to the amount of the target protein (caveolin-1) which is present in the area being examined. Because most (but not all) caveolin-1 is found close to the surface of cells, in the polarity study of endothelial cells, both villous capillary and basal plate, an arbitrary strip width of 150nm was set for the apical and basal surfaces. In those places where the total width of the endothelium was less than 300nm, the dividing line between these surfaces was placed equidistantly from each.

In consultation with Dr John Bennett FRSS, analysis of variance (ANOVA) was chosen as the statistical test for these counts as it allowed each of the areas to be compared with the others; Tukey's post hoc test was applied to these results to validate any apparently significant differences. Both tests were performed using SPSS version 12.0.

For the cytogenetic study, counts of labelled versus unlabelled nuclei were made with $n = 500$ for each of six tissue samples from each placenta obtained from a pregnancy giving rise to male offspring using bright field microscopy. Counts were imported to an

Excel spreadsheet and statistical and chart functions were applied for analysis and presentation of data. Tests of the 95% confidence intervals and p values for one proportion of these were estimated using MINITAB (version 15) for each of the six proportions. The test of the 95% confidence intervals and p values for two proportions was applied to the villus and basal plate labelled endothelial nuclear proportions.

Chapter Three

Caveolae: Immunofluorescence, scanning and transmission electron microscopy

3.1. Introduction

Directed transport of material enclosed within vesicles is of potential importance in endocytic, secretory and transepithelial transport processes. In the study of the human placenta, where these processes are obviously of paramount importance, emphasis has previously been placed on the receptor-mediated uptake and transport of compounds in 'coated' pits and vesicles where the major coat protein is clathrin (heavy chain) (Ockleford, 1976; Ockleford and Whyte, 1977). Caveolae are small invaginations of the plasma membrane of many cells (Yamada, 1955), which are prominently expressed in endothelial cells and have a similar size (50-100nm diameter) and shape to clathrin-coated micropinocytic vesicles; they also appear, in some situations, to mediate the uptake of proteins and other molecules (Montesano et al. 1982). Since the "placental barrier" is a multilayered structure histologically it seemed important to establish if and where such vesicles existed on the transplacental transport route.

The major family of proteins associated with caveolae, the caveolins (Rothberg et al., 1992), have a lower molecular mass than clathrin, and the ultrastructural appearance of the cytosolic face of their membrane is less substantial. However like clathrin, caveolin is capable of oligomeric complex formation (Sargiacomo et al., 1995) and it is these complexes which are thought, in part, to give rise to the fine spiral threads which surround caveolae viewed by scanning electron microscopy.

Sharing sequence identity with the protein VIP 21 (Glenney, 1992) caveolin-1 is a GPI-linked transmembrane protein. As well as its localisation to cell-surface caveolae,

caveolin is found in association with the trans-Golgi network region and contributes to apical and basal transport pathways (Kurzchalia et al., 1992).

Biochemically the caveolins include three forms encoded by three independent and separate genes (Tang, et al., 1996). They are denoted Caveolins -1, -2 and -3. Caveolin-3 is a distinct isoform apparently restricted to all classes of muscle cells (skeletal, cardiac and smooth muscle). The function of certain caveolae in skeletal muscle is thought to differ from that of caveolae found in other cells (Cohen et al., 2004). There appears to be a close association between sarcolemmal caveolae and the T-tubule system in adjacent underlying myofibrils; these 'static' caveolae are most noticeable at the tapered ends of the muscle fibres (Ockleford et al., 2007).

Caveolin-2 is predominantly found in adipocytes, which have a higher concentration of caveolae, per unit area of cell membrane, than any other cell type. It is probably the most ubiquitous of the three. Caveolin-1 is similarly widespread in its distribution, but is most strongly expressed in endothelial cells, fibroblasts, and smooth muscle (Scherer et al., 1997). Co-expression of two or occasionally all three caveolins by single cells has been reported elsewhere (Scherer et al., 1997). The two isoforms of caveolin-1 are thought to result from the use of alternative start sequences, with the full-length form being the α -isoform and the β -isoform the shorter translation product (Scherer et al., 1995).

In order to localise the α - and β -isoforms of caveolin-1 in human extraembryonic membranes, an indirect immunofluorescence protocol was used and 'Western' immunoblot analysis performed to validate the antibody. Both transmission and scanning

electron microscopy were used to visualise caveolae and to provide support for those interpretations based on the immunocytochemistry.

3.2 Results

3.2.1 Immuno-blotting

In order to confirm the specificity of the commercially obtained rabbit anti-human caveolin-1 (Transduction Laboratories, # C13630), protein extracts of amnion, basal plate, chorion, chorionic plate, umbilical chord, villous tree, a human epidermal/dermal skin sample from mammoplasty and an extract of human endothelial cells (supplied with the antibody as a positive control) were run on a 5-20% gradient SDS-PAGE gel and immuno-blotted with the antibody (Figure 3.2.1a). The samples were not taken from specific locations on the placenta or amnio-chorion but the umbilical cord samples were from a portion some 10cm distal from its insertion in the chorionic plate. Immunoblotting under non-reducing conditions (Figure 3.2.1a) confirmed the specificity of the antibody to a limited number of polypeptides with apparent molecular weights of 22 and 24 kD and simple multiples thereof. These lowest molecular weight species correspond to the molecular weights of the two caveolin-1 isoforms (α - and β -) which arise from the alternative start sites (Scherer et al., 1995) for this protein's transcription. The preponderance of the lower molecular weight isoform (caveolin-1 β) suggests that the shorter transcript is produced preferentially over the longer (caveolin-1 α). The pattern seen in the higher molecular weight region of this immunoblot most probably reflected the ability of these molecules to oligomerize up to at least the hexameric state (Sargiacomo et al., 1995).

This page has been left blank intentionally, so that samples run under non-reducing and reducing conditions can be compared more easily. See Page 52 (overleaf).

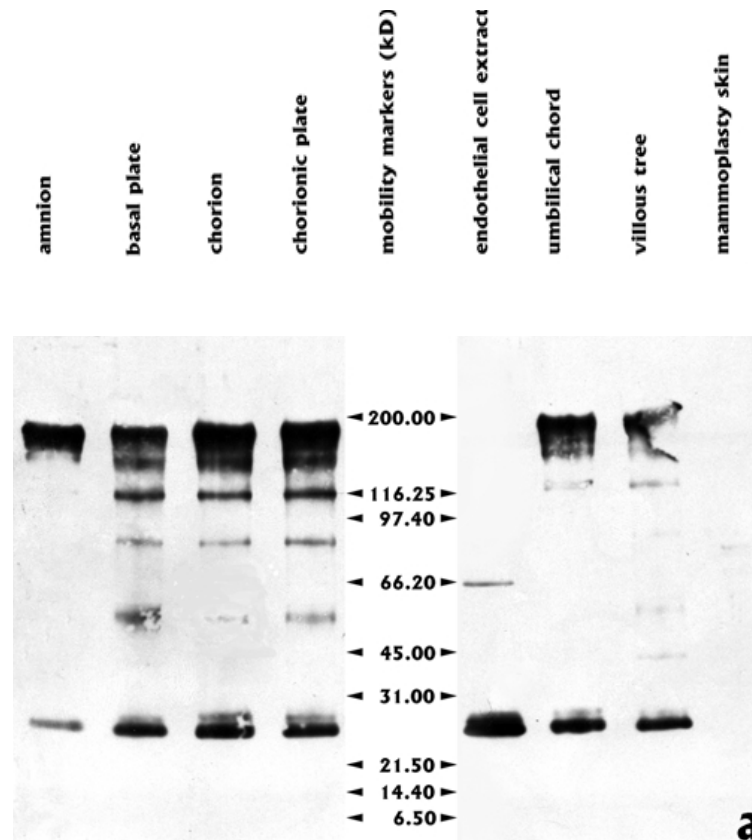


Figure 3.2.1 This panel (a) shows an immunoblot using the anti-caveolin-1 antibody to define immunoreactive polypeptides in protein extracts of amnion, basal plate, chorion, chorionic plate, umbilical cord, as well as a human epidermal/dermal skin sample and an extract of endothelial cells provided by the commercial supplier. This shows a blot of the proteins run under *non-reducing* conditions (i.e. in the absence of a sulphhydryl [S-H] reducing agent). The relative molecular masses were estimated from the mobility of a set of standard proteins electrophoresed in the same gel. The higher molecular weight proteins were thought to represent oligomeric forms of caveolin-1. In the basal plate sample, 6 discrete bands are easily discerned. The doublets seen at the bottom of the gel represent the α - and β -isoforms of this protein.

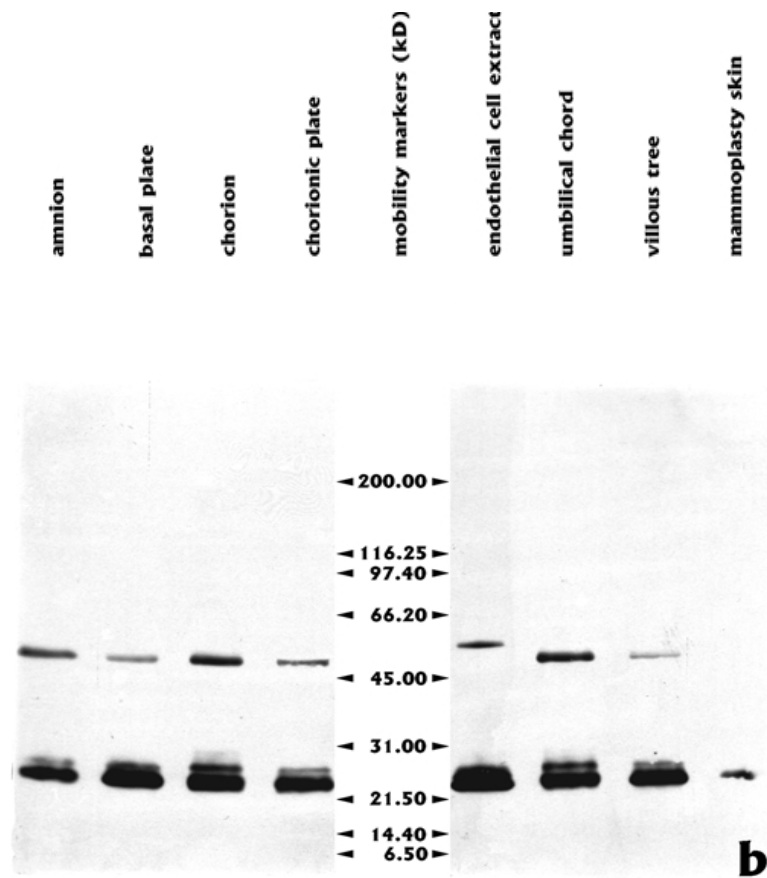


Figure 3.2.1 Panel (b) shows the same proteins as in Figure 3.2.1a, but electrophoresed in the presence of 5% v/v β -mercaptoethanol. Here, the reactive bands are restricted to the α - and β -isoforms of caveolin-1 and a possibly dimeric form of caveolin-1 which appears to be resistant to reduction to the monomeric form. The higher molecular weight species (other than this dimeric form) have all been reduced to the monomeric form.

When the proteins were electrophoresed in the presence of 5% v/v β -mercaptoethanol (Figure 3.2.1b), it was assumed that the oligomeric forms would *all* be reduced to the monomeric isoforms (α and β) yet in every case, except for the mammoplasty skin sample, there was evidence of a higher molecular weight species at about 48kD. This was interpreted as a dimeric form which was resistant to reduction under these conditions of digestion and is also present in the endothelial cell extract supplied by the antibody supplier as a positive control. It is interesting to speculate whether this dimer might represent the *soluble* form of caveolin-1, perhaps post-translationally modified, which allows it to resist reduction to the monomeric form (Liu et al., 2002). The slight difference in the apparent molecular weight of the dimeric form in the endothelial cell extract can be explained by the different composition of the sample buffer in which it was supplied.

3.3 Immunofluorescence

The bright immunofluorescence signal seen in foetal endothelial cells confirmed that these were immuno-positive when stained with this same antibody. There was a suggestion that the other mesenchymal cells of the villus core may also be immunoreactive, though the plane of this particular section (Figure 3.3.1) is such that there were very few of these other cells present.

Syncytiotrophoblasts, which form the outermost layer of the chorionic villi, showed a very low level of immunoreactivity and it was unclear whether this was above the level of non-specific binding. Villous cytotrophoblasts, which are rare in these term samples might account for some of the fluorescence seen in the later images (Linton et al., 2003).

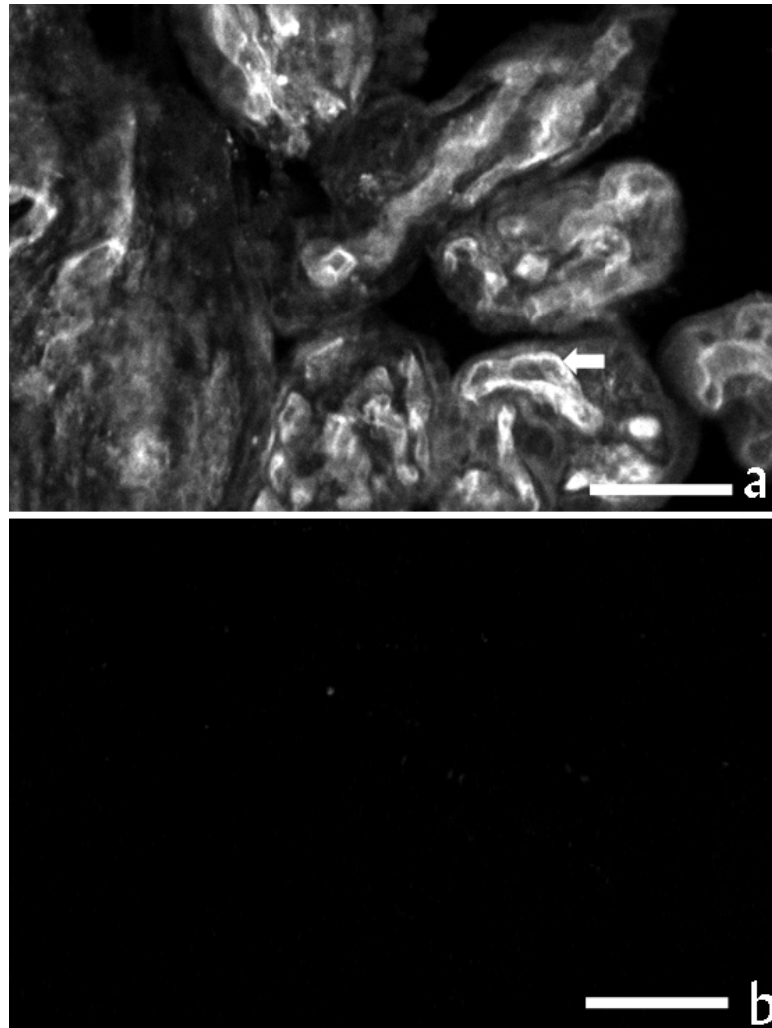


Figure 3.3.1(a). This image was from a frozen section of mid-cotyledonary term placental chorionic villi, using indirect immunofluorescence with the anti-caveolin primary antibody. The endothelial cells of the villus core capillaries were found to be intensely immunoreactive (arrow), the mesenchymal cells faintly so and the trophoblast barely more reactive than the background level of non-specific immunoreactivity. Scale bar: 50 μ m. **(b)** A similar section processed identically but without the specific anti-caveolin antibody. Following identical image-capture protocols there was virtually no evidence of non-specific staining in this control sample. Scale bar = 50 μ m.

The cells most immunoreactive to the anti-caveolin-1 antibody in sections of amnio-chorion roll (Figure 3.3.2) were located in the mesenchymal layers. The amniotic epithelium and decidua were both more immunoreactive than the trophoblast layers. Essentially all the immuno-labelling was cellular. The DIC images here reflected the variation in refractive index and 'dry-mass' of the section and were used to judge the specificity of the labelling where it was concentrated at particular sites within the tissue. The punctate nature of the basal surface labelling of the amniotic epithelium in the extended-focus projection image (Figure 3.3.2c) suggested that this may well be an indication of the location of individual caveolae or groups of caveolae.

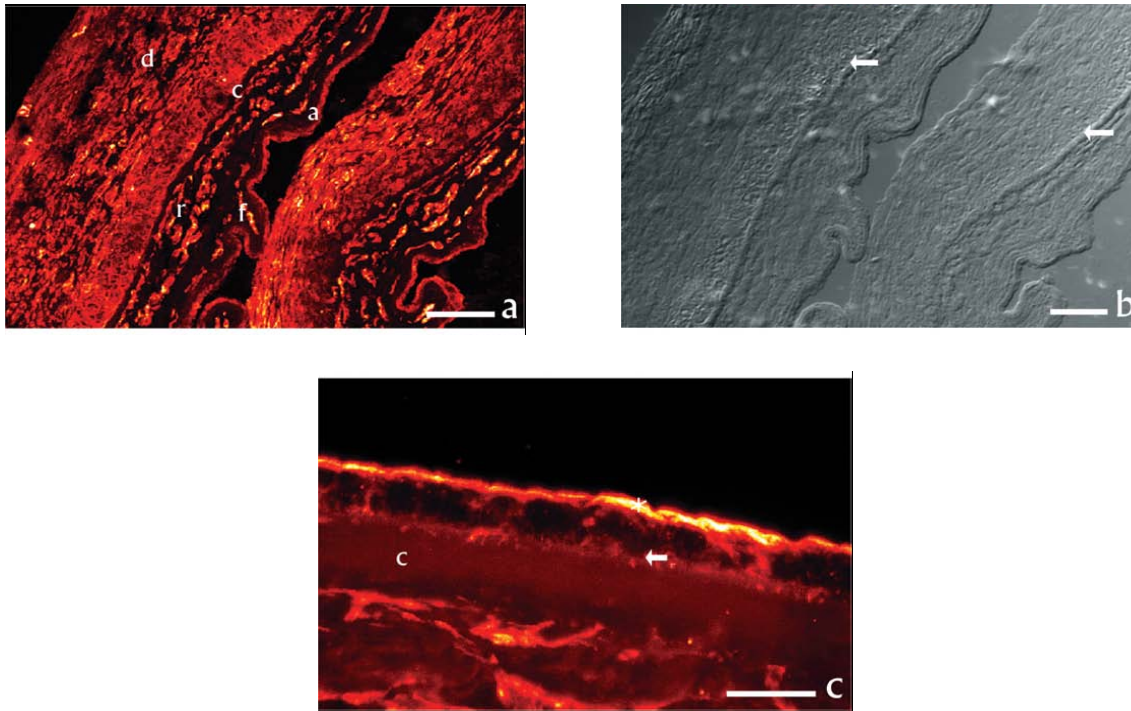


Figure 3.3.2 Foetal membranes: indirect immunofluorescence using the anti-caveolin-1 antibody on a frozen section of amniochorion roll.

(a) A frozen section of a human term amniochorion roll revealing two complete layers of amnion (a), chorion (c) and decidua (d). (f) is the fibroblast layer and (r) the reticular layer. Scale bar: 100 μ m. (b) Nomarski Differential Interference Contrast (DIC) micrograph of the frozen section shown in (a). The *chorion laeve* basal lamina (arrows) was of greater dry mass than the surrounding tissue, but in (a) showed no evidence of immunoreactivity. Scale bar: 100 μ m. (c) Extended-focus projection of 15 consecutive images through the thickness of a frozen section of human term amnion prepared using the anti-caveolin primary antibody in an indirect immunofluorescence protocol. The labelling was intense in the apical region of this simple cuboidal amniotic epithelium (*), but there was also basal surface immunoreactivity which was clearly punctate. Immunoreactive cells of the fibroblast layer were separated from the amniotic epithelium by the acellular compact layer (c). Scale bar: 25 μ m.

Placental morphologists have previously described the layer lining the maternal blood space at the basal plate as being syncytiotrophoblastic (Boyd and Hamilton, 1970), though others have suggested that it is entirely endothelial (Wanner, 1966). The observations made of this (Figure 3.3.3) and more particularly the following image (Figure 3.3.4), based solely on the evidence of the anti-caveolin-1 immunoreactivity, led to the supposition that neither is entirely true, but that this lining consists as a *mosaic* of *both* cell types. The extent of the endothelial lining was more strikingly obvious in this latter image (Figure 3.3.4) than in others. The organization of the basal plate region and adjacent chorionic villi were clearly demonstrated and a unicellular epi/endothelial morphology was seen in the lining of the intervillous space (maternal blood sinus).

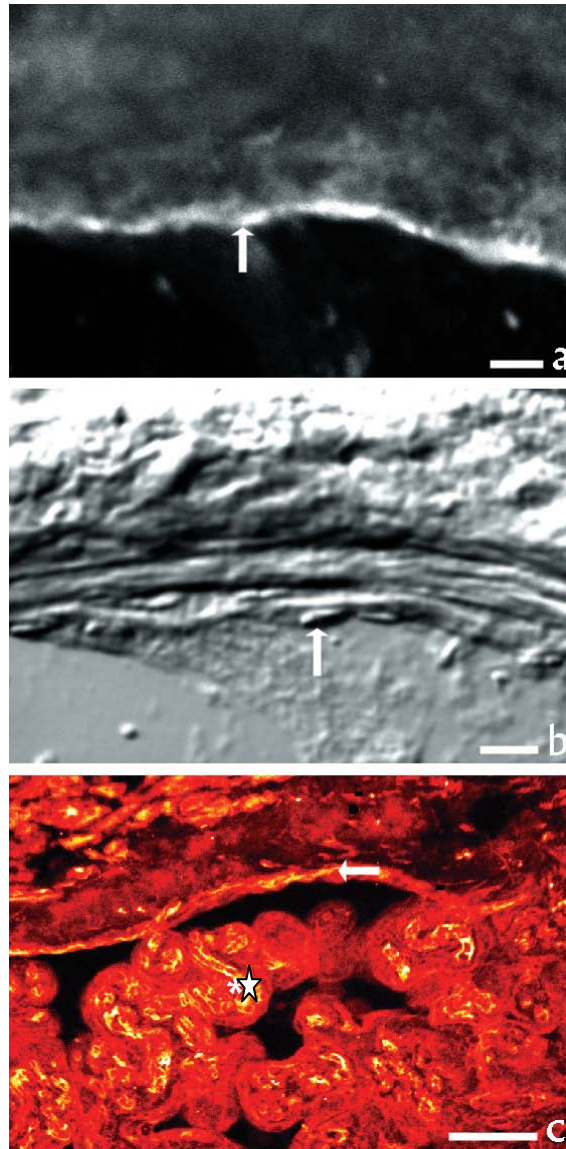


Figure 3.3.3(a) Term human placenta basal plate anti-caveolin immunocytochemistry. The thin bright line of immunofluorescence (arrow) was coincident with the lining of the maternal inter-villous space. Scale bar: 10 μ m.

(b) The same area of the section viewed in **(a)** but imaged using Nomarski DIC microscopy. The morphology of the lining cells associated with the strong immunofluorescence appeared similar to endothelium (arrow). Scale bar = 10 μ m.

(c) At lower magnification, revealed using the false colour look-up table (LUT) 'Autumn', it can be seen that the intensity of anti-caveolin-1 immunofluorescence in the basal plate was greatest at the margins of the intervillous space (arrow) and the intensity of the lining cells matched that of the sinusoidal capillary wall cells in the chorionic villi (*). The chorionic villus syncytiotrophoblast, on the other hand, exhibited a lower intensity of fluorescence. Scale bar = 100 μ m

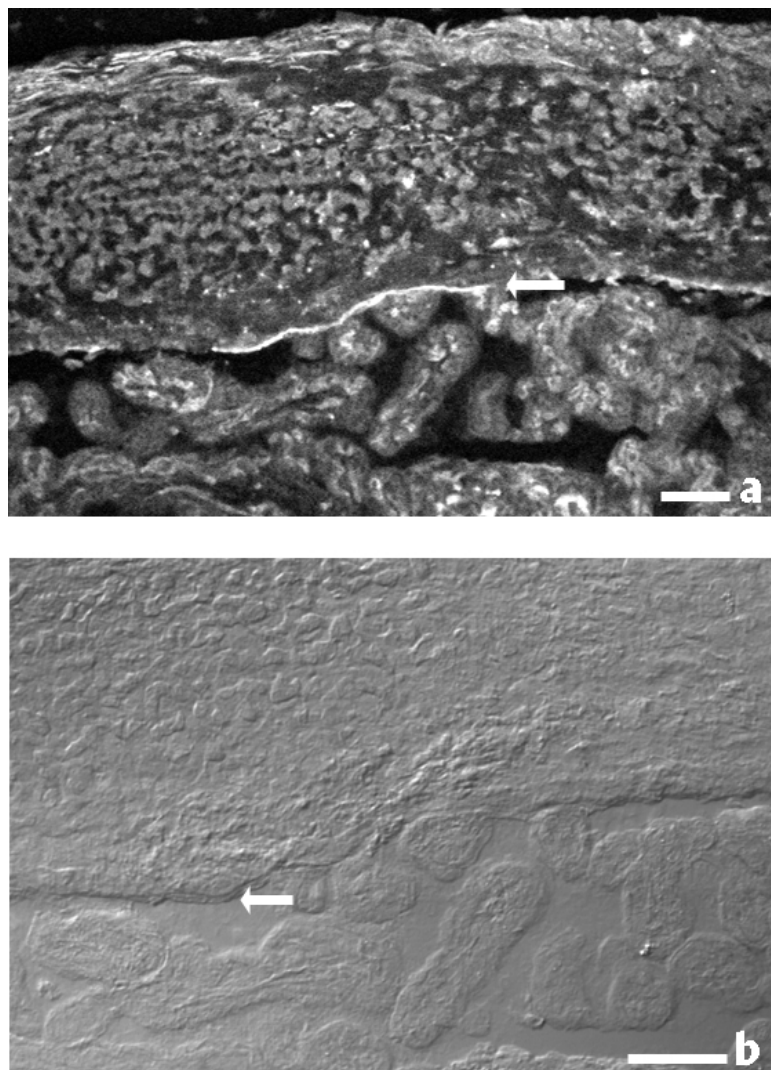


Figure 3.3.4 (a) Term human placental basal plate frozen section. This indirect immunofluorescence micrograph showed the pattern of anti-caveolin-1 immunoreactivity. The villus tree towards the bottom of the micrograph showed a strong immunofluorescence in the cores of the villi overlying the endothelia of blood vessels, but low fluorescence in the trophoblast. The narrow layer of the basal plate immediately adjacent to the intervillous space was intensely immunofluorescent (arrow), similar to that shown by the chorionic villus endothelial cells, but much brighter than the syncytiotrophoblast of chorionic villi. Some immunoreactivity of decidual cells was also observed. Scale bar: 100 μ m. (b) The same area of tissue as shown in (a) imaged using Nomarski DIC optics (to reveal the dry mass distribution of the tissue). The arrow in this image shows the start of the trophoblastic part of this lining. Scale bar = 100 μ m

Close to (and within) the *chorionic* plate, foetal blood vessels are generally larger, so that instead of being arterioles, venules and capillaries, (as in the smaller chorionic villi), they become true arteries and veins. The architecture of these larger vessels includes a more substantial *media* with a more developed smooth muscle layer, as well as a greater connective tissue component. Both smooth muscle cells and fibroblasts have been shown to express caveolin-1 and this was confirmed in sectioned material from this site. The labelling pattern in Figure 3.3.5 showed that the smooth muscle cells in the media of these larger blood vessels was clearly very positive. The differences between adjacent blood vessels in 3.3.5(b) reflected the fact that the central vessel was an artery and the flanking vessels were veins (arteries having a more substantial musculature than veins). This was reiterated in the umbilical vessel in 3.3.5(c), which is a vein.

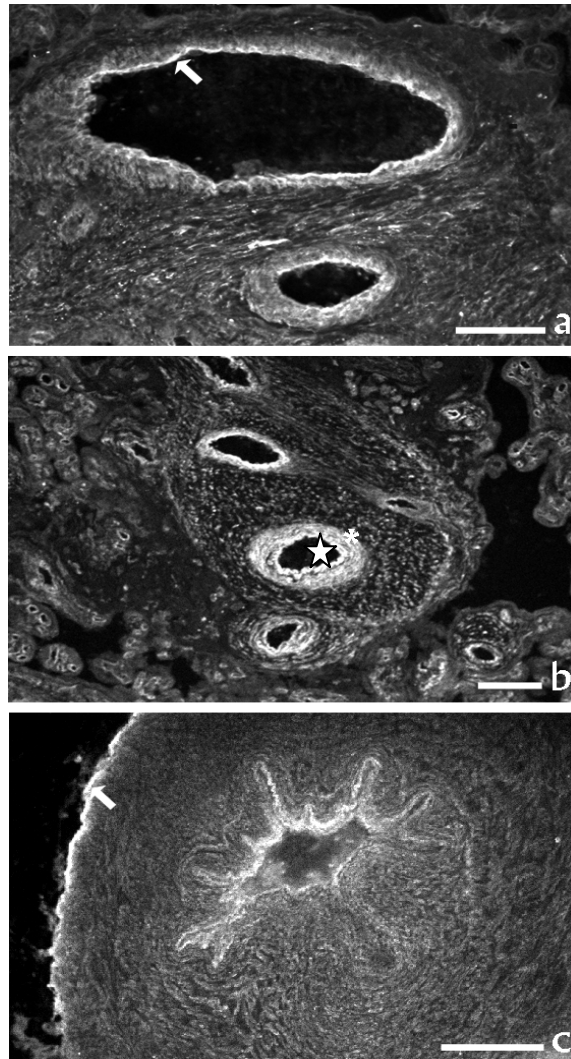


Figure 3.3.5 (a) Term human placental chorionic villus showing slightly oblique sections through foetal arterial and venous blood vessels. The frozen section was exposed to anti-caveolin antibody in an indirect immunofluorescence protocol. The *intima* of the foetal vessel walls was extensively immunoreactive (arrow). Scale bar: 100 μ m. (b) Frozen section of a stem villus close to the chorionic plate prepared using anti-caveolin antibody in an indirect immunofluorescence protocol. The endothelial cells of the transversely sectioned vessels (*) and the surrounding smooth muscle cells were labelled more intensely than the mesenchymal cells of the core. Least labelling was seen in the trophoblast. Scale bar: 100 μ m. (c) Frozen section of human term placental umbilical cord prepared for indirect immunofluorescence microscopy. Anti-caveolin immunoreactivity was predominant in the amniotic epithelial sleeve externally (arrow) and in the walls of the large diameter umbilical blood vessels, particularly in the intimal layer. The mesenchymal cells of Wharton's jelly are less intensely labelled. Scale bar: 250 μ m

3.4 Light and Electron Microscopy

The morphological detail afforded by plastic-embedded sections was found to be superior to that observed when frozen sections were used. Both in the inter-villous space and in the lumina of the villous capillaries, erythrocytes were clearly visible (Figure 3.4.1 *et seq.*) Cryo-fixation is unable to preserve these cells, which, because of their lack of a cytoskeleton, are lysed by ice-crystal formation.

Basal plate endothelial cells showed the typical morphology of squamous cells, with their flattened, tapered nuclei, and very thin, extensive cytoplasm. The morphology of the trophoblast layer was very different; though not very clearly shown in some light micrographs, the rough, microvillous apical surface could often be seen and the rounder nuclei (often clustered together as a syncytial knot precursors) were very apparent. These features were better illustrated in the electron micrographs 3.4.3 and 3.4.4.

Caveolae were a frequent feature of the endothelial cells lining the maternal blood space (Figures 3.4.4b&c) and their ultrastructural appearance is very similar to that seen in the vascular endothelium lining the villous capillaries (Figure 3.4.4a). It was often observed that the endothelial cells grew on top of the adjacent trophoblasts and in these cases the underlying apical microvilli were seen to be in an apparent state of regression.

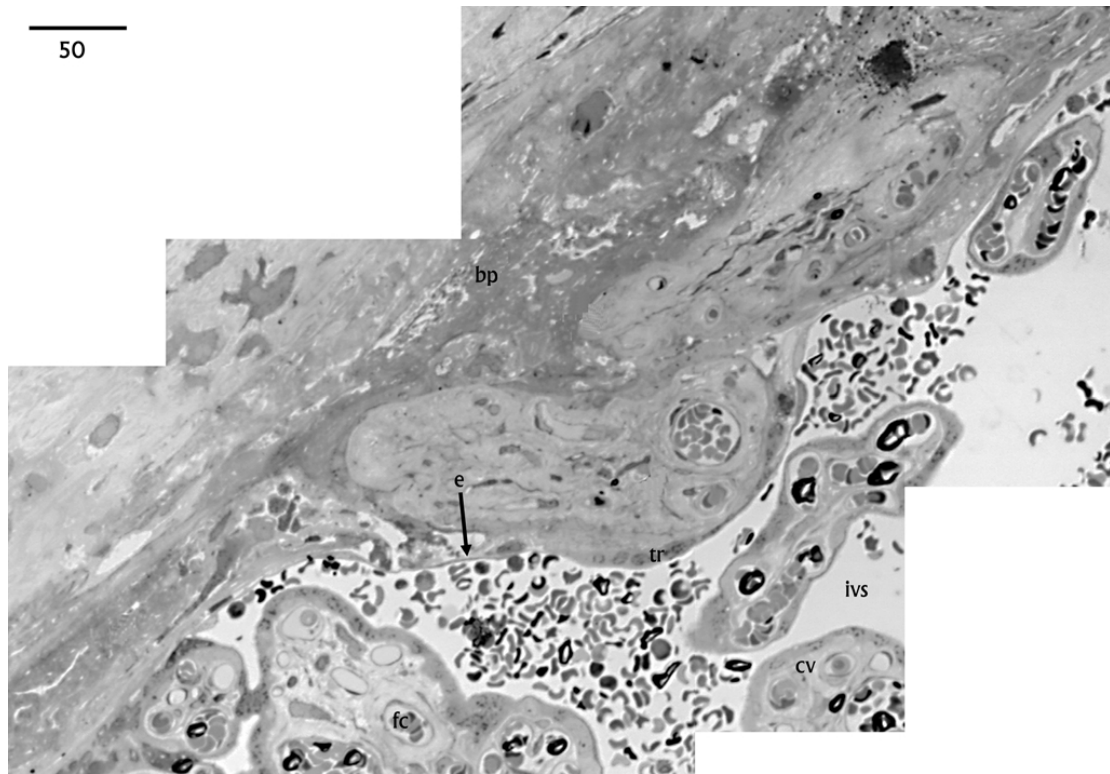
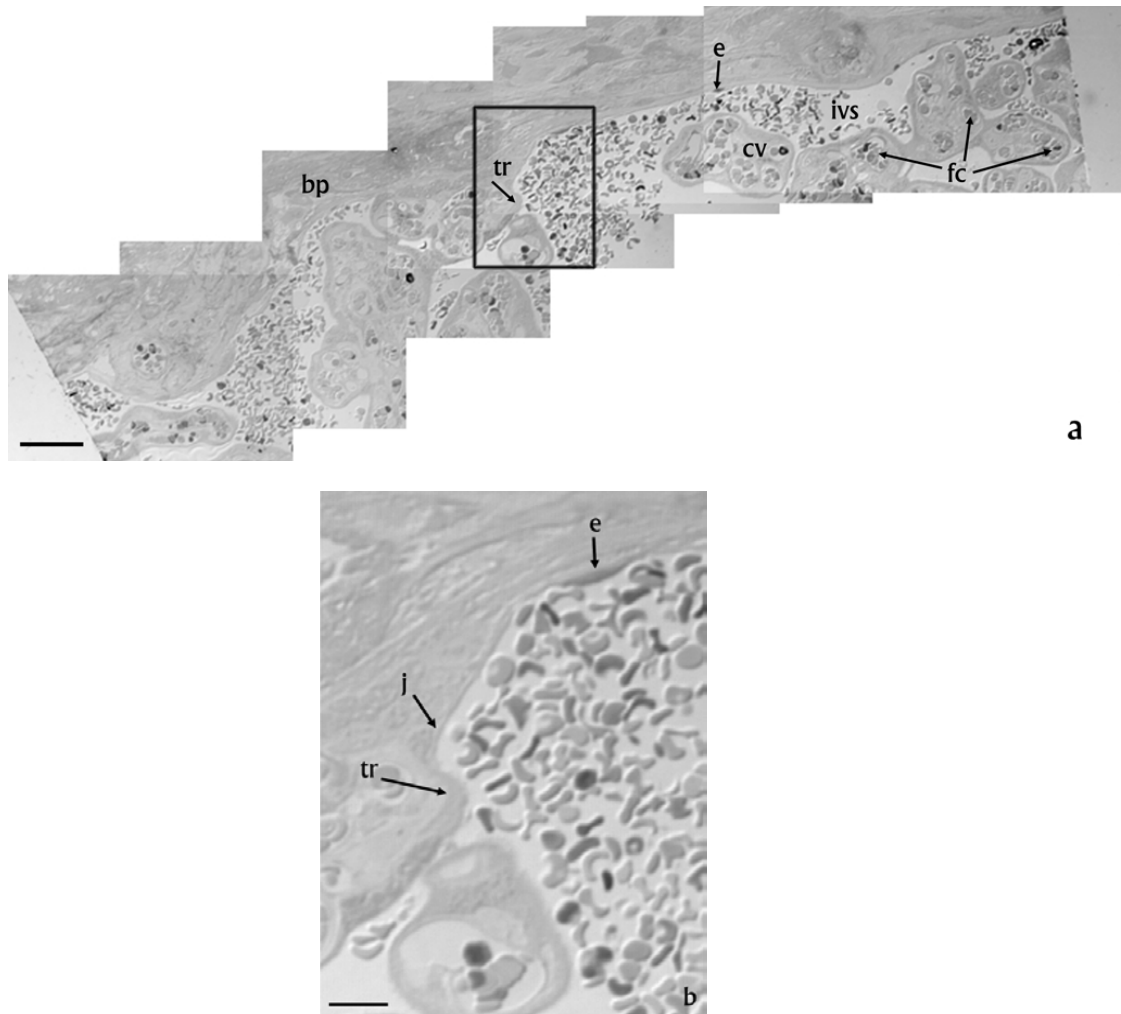


Figure 3.4.1. Semi-thin (0.5 μ m) plastic section of a basal plate (bp) specimen showing the attachment point of an anchoring villus. A clear transition from trophoblast (tr) to endothelial (e) morphology was apparent. Within the inter-villous space (ivs) several chorionic villi (cv) were sectioned which revealed the foetal capillaries (fc) of the villus core. Scale bar (top left) = 50 μ m.



25

Figure 3.4.2(a) Light micrograph of a plastic section of basal plate, showing the putative endothelial lining (e) of the inter-villous space (ivs) at this location. Anchoring chorionic villi (cv) originating in the basal plate (bp) are only approached by this outer covering at their base; syncytiotrophoblast (tr) forms their outer covering at all other locations. Foetal capillaries (fc) are clearly discernible in the cores of the villi. Scale bar=50 μm . **(b)** A higher magnification view of the boxed area in **(a)** that includes both syncytial and endothelial types of lining cells and the area where these two surfaces make contact. e = endothelium; j = junction; tr = trophoblast. Scale bar = 25 μm .



2

Figure 3.4.3 Transmission electron micrograph showing the endothelial-like inner lining of the decidua of the basal plate corresponding to the junctional area in Figure 3.4.2(b). At the origin of the anchoring villi, the endothelial layer made contact with syncytiotrophoblast and tight junctions were sometimes detectable. e = endothelium; j = junctional zone; tr = trophoblast. Scale bar = 2 μ m.

(This section was taken from the same place in the same tissue block as that in Figure 3.4.2(b), but is not quite a 'serial' section.)

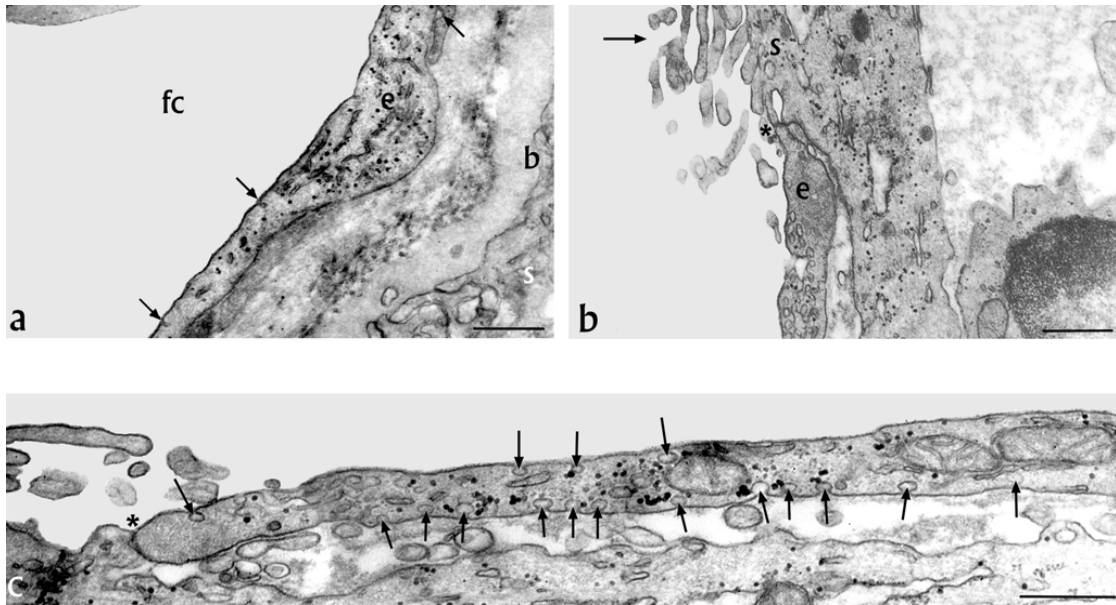


Figure 3.4.4(a) A transmission electron micrograph of an ultrathin epoxy-embedded section of a chorionic villus from a term placenta showing a foetal capillary (fc) endothelial cell (e) adjacent to the syncytiotrophoblast (s) and its shared basal lamina (b). Arrows show caveolae. Scale bar = 0.5 μm . **(b)** A region of the basal plate which is lined by both syncytiotrophoblast (s) and endothelium (e) is shown in this transmission electron micrograph. The arrow shows the microvilli on the apical surface of the trophoblast and the asterisk a junction between the two different cell types. Scale bar = 0.5 μm . **(c)** A transmission electron micrograph showing the inner lining of the basal plate where it bounds the inter-villus space. Caveolae are indicated by arrows and a junction by the asterisk. Scale bar = 0.5 μm .

Morphologically, the endothelial cells lining the foetal capillaries (3.4.4a) were seen to be extremely similar to the endothelial-like cells lining the basal plate (3.4.4b&c). They contained electron-dense glycogen granules as well as caveolae. The basal plate trophoblast surface was very different from that of the adjacent endothelial cells, in that it bore extensive microvilli and exhibited no obvious caveolae. The endothelial cells, by contrast, showed a great number of caveolae, particularly on their basal surface though the ratio of apical to basal caveolae was not calculated. The overall frequency of caveolae in any particular linear stretch of these endothelial cells was a variable phenomenon; certain areas of both the apical and basal surfaces were densely populated whereas other parts more sparsely so.

The occasional observation of junctions between these very different cell types was a surprising finding. The endothelial cells did not appear to have a basal lamina proper, but were typically seen in loose association with a strip of underlying material of moderate electron density staining characteristics. Although many vesicles were seen in the underlying and adjacent syncytiotrophoblast, there was no compelling evidence for the presence of any caveolae.

3.5. Scanning Electron Microscopy

Images from the scanning electron microscopic study (Figures 3.5 et seq.) showed that individual microvilli on the apical surface of syncytiotrophoblasts lining part of the basal plate could be clearly resolved; also, the endothelial cells at this location had a completely different surface topography from these trophoblasts. They were entirely devoid of any surface projections, the only features visible on the otherwise completely flat face were numerous small circular depressions. These, because of their size and distribution were interpreted as representing caveolar pori. (A porus is the *opening* of a caveola at the plasmalemmal surface).

Fibrin plaques in the scanning electron micrographs were characterised by their fibrous fringes and the absence of any obvious topographical features other than a smooth, undulating surface; the surface often appeared to be stratified, as though the layers of fibrin fibres had been added sequentially. This (subjective) impression is illustrated in the inset to Figure 3.5.3.

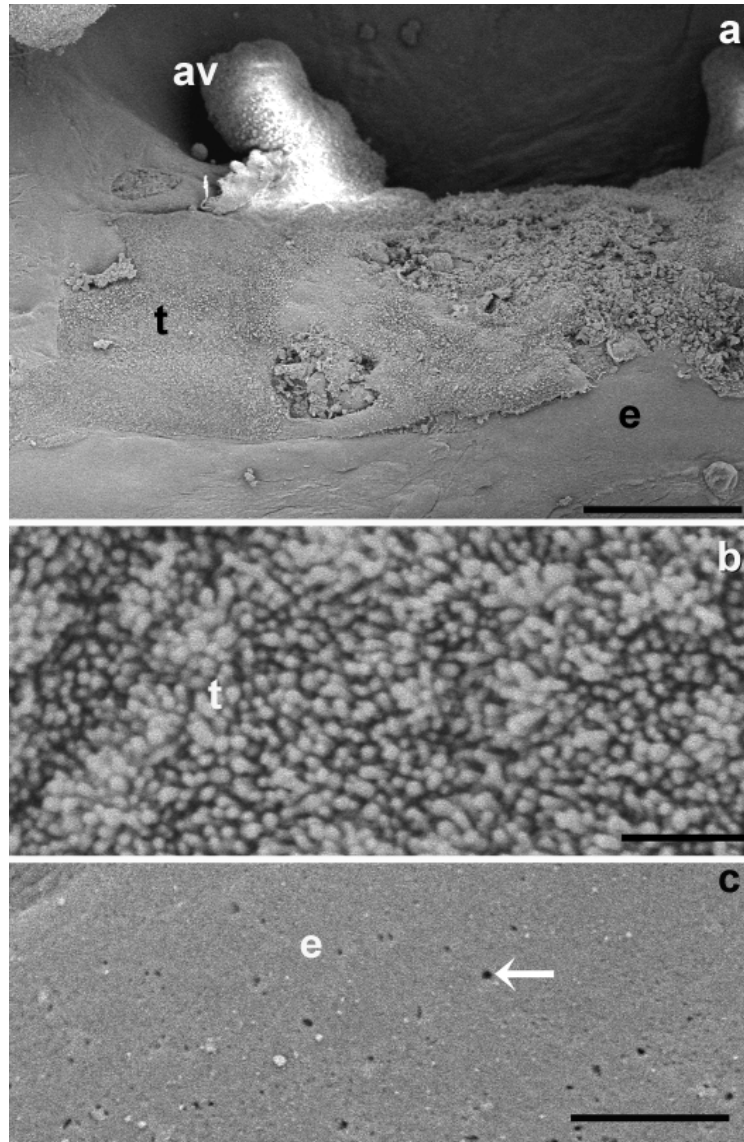


Figure 3.5.1 Scanning electron micrographs of the internal surface of the basal plate as viewed from the intervillous space. **(a)** anchoring villi (av) were seen to be covered by syncytiotrophoblast which extended down onto the flattened surface to which they attach. This part of the surface (t) showed typically trophoblastic (microvillous) surface morphology. Slightly further out from these anchorage points, the surface morphology became more characteristic of endothelium (e). Scale bar = 200 μ m. **(b)** A portion of the basal plate covered by trophoblast (t) seen at a higher magnification. Scale bar = 10 μ m. **(c)** Making edge-to-edge contact and lying in the same plane were much flatter cells (e) without microvilli. The small pits (arrow) in their surface were similar in size and distribution to caveolar pori. Scale bar = 1 μ m.

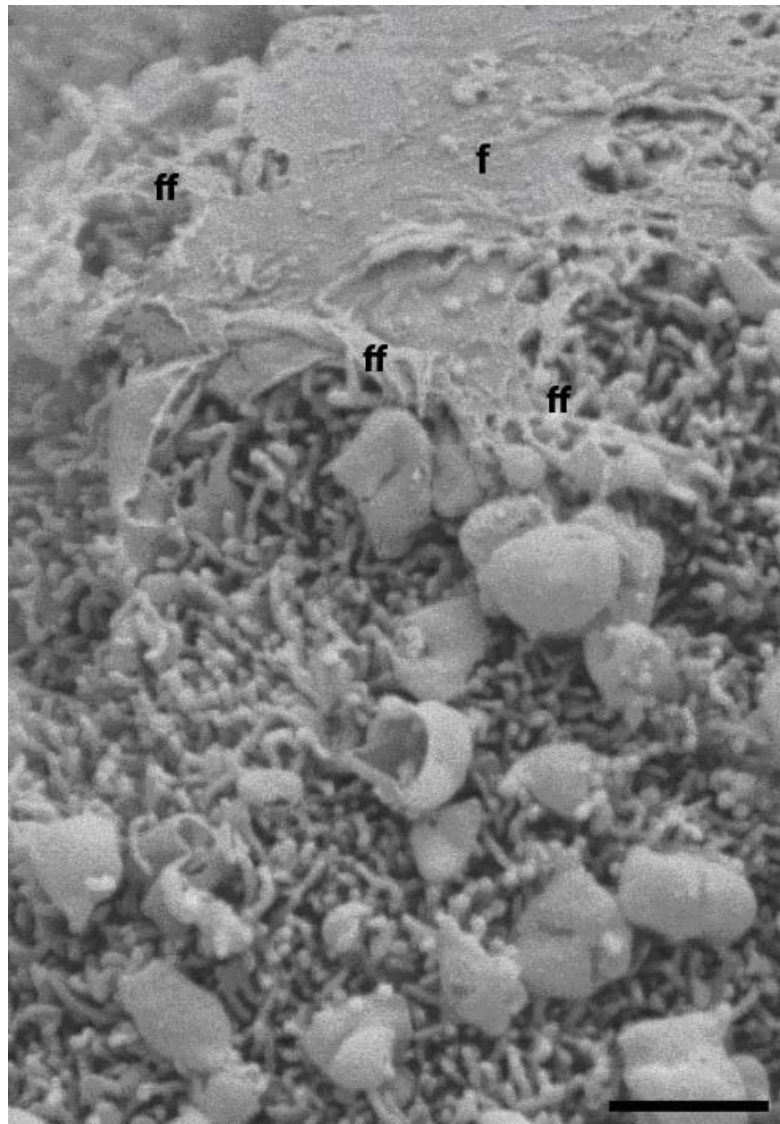


Figure 3.5.2 In this scanning electron micrograph, the deposition of fibrin (f) was seen to give a local flat coating over the surface of trophoblastic microvilli. Fibrin fibres (ff) were usually visible at the edges of the plaques with the fibrin overlying the trophoblasts. The debris covering the trophoblast in the lower half of the image is likely to be partially lysed maternal erythrocytes. Scale bar = 5 μ m.

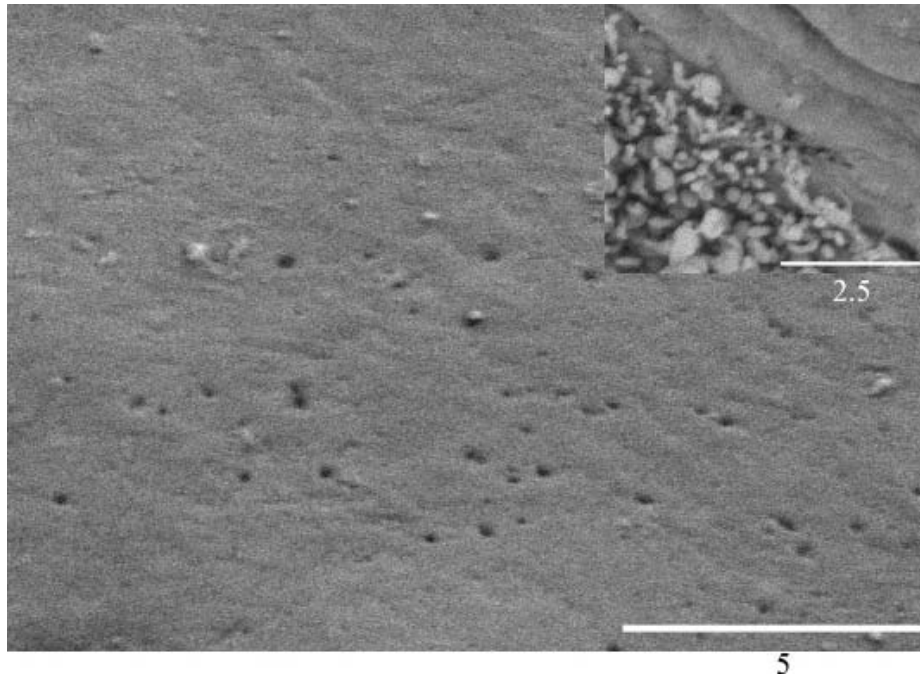


Figure 3.5.3 Direct comparison of the morphology of the three different types of surface seen when viewing the lining of the basal plate by scanning EM. Main picture is the endothelium. Inset is trophoblast (bottom left) partially covered by fibrin (top right). Endothelium showed clear evidence of caveolar pori; trophoblast was covered by microvilli and fibrin was comparatively smooth and undulating. Scale bar = 5 μ m.

3.6 Quantitation of fluorescence (pixel) intensity across line-scans

One of the features of the software of the BioRad CLSM is a function allowing the user to describe a line between any two points on an image and to display the pixel intensity ('brightness') along this line. Where there are multiple examples of a particular feature as, for instance, in Figure 3.6.1, which shows several chorionic villi, cut in cross-section, this line-scan feature allows comparative data to be collected with great ease. The pixel intensity, in arbitrary units, is displayed on the vertical axis and the distance covered by the described line (in μm) on the horizontal axis.

Although the pixel intensity is displayed in arbitrary units and is seen to vary from one preparation to another, the *pattern* of the graphical representation was found to be consistent. This is illustrated in Figure 3.6.2.

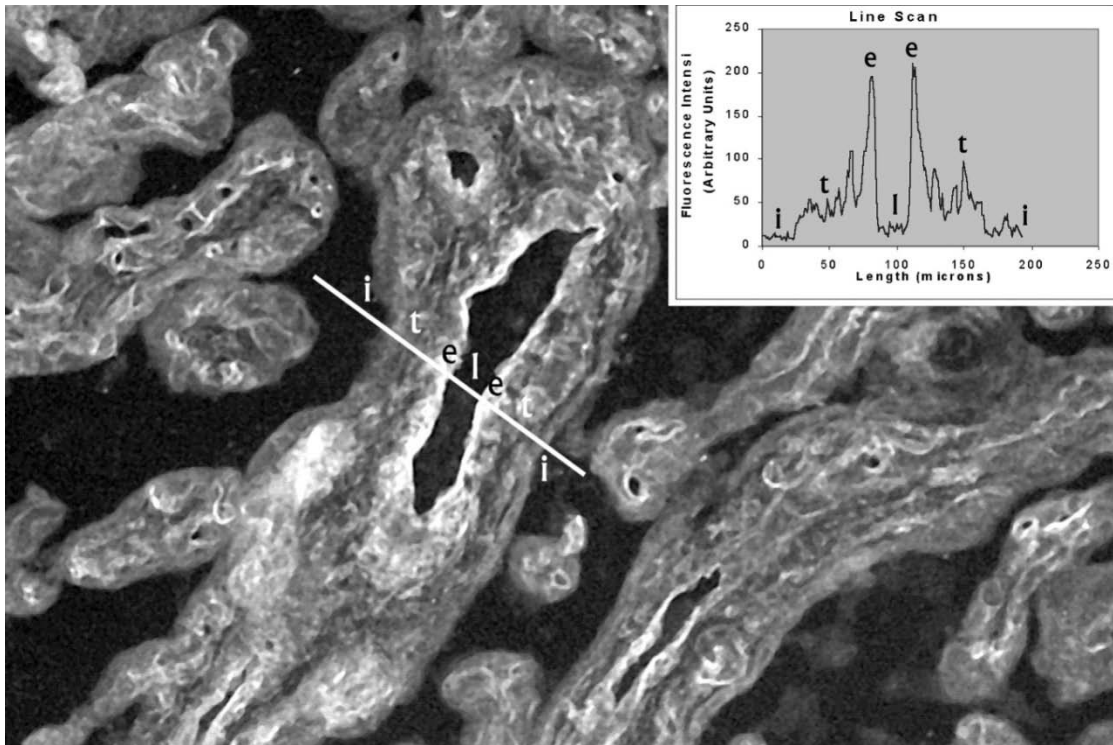


Figure 3.6.1 A representative section through an area of the chorionic villus tree. The frozen section was prepared for indirect immunofluorescence microscopy using anti-caveolin-1 antibody. The white line shows the position of the scan across a branch villus. The plot of relative fluorescence intensity against length in microns along the scan (inset) shows the variation at various positions along the line as follows: (i) intervillus space, (t) trophoblast, (e) endothelium, (l) lumen of foetal blood vessel.

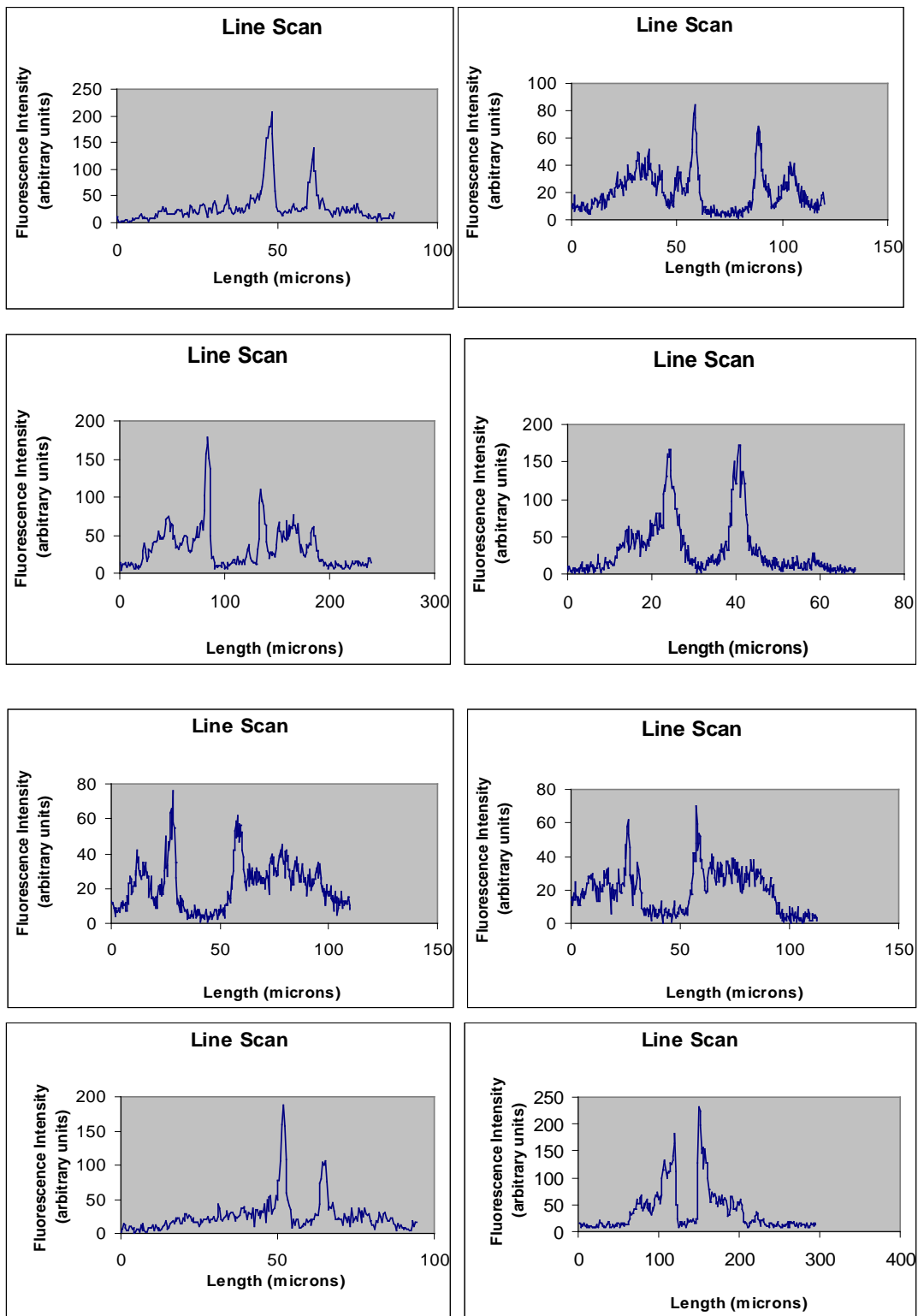


Figure 3.6.2 Eight further line-scans across transverse sections of chorionic villi, showing the similarity of the pattern when these are probed with the anti-caveolin-1 antibody

3.7 Summary of results

- The anti-caveolin-1 antibody recognised proteins with the same molecular weights as those published for the 2 isoforms of caveolin-1.
- This antibody recognised foetal capillary endothelial cells and fibroblasts.
- Amniotic epithelium was found to be immunoreactive, as were smooth muscle cells in the media of larger foetal blood vessels.
- Immunoreactive cells on the lining of the maternal blood space at the basal plate were shown to have an endothelial-like morphology.
- Scanning electron microscopy confirmed the endothelial nature of these lining cells.
- Junctions exist between this endothelium and the epithelium of the trophoblasts, which makes this layer a possibly unique allo-endo/epithelium.
- There was a small, but significant rise in the basal plate area fraction occupied by endothelium when pre-eclamptic placentae were compared to normal placentae.

3.9 Discussion

3.9.1 The distribution of caveolin-1 and its functional role in the placenta

The role of caveolae as internalization intermediaries has been emphasized in the light of an historical association with studies of endocytosis (e.g. Benlimame et al., 1998) but some caveolae (for example those associated with the sarcolemma in striated muscle) appear to be more or less permanently associated with the cell surface (Ralston and Ploug, 1999, Ockleford et al., 2007). Clearly other roles are served and certain research has given greater emphasis to these (Shaul and Anderson, 1998). In the words of these reviewers ‘Once the identification of the marker protein caveolin made it possible to isolate and purify this specialized membrane domain it was discovered that caveolae also contain a variety of signal transduction molecules. This includes G protein- coupled receptors, G proteins and adenylyl cyclases, molecules involved in the regulation of intracellular Ca^{2+} homeostasis, and their effectors including the endothelial isoform of nitric oxide synthase (eNOS), multiple components of the tyrosine kinase–mitogen-activated protein kinase pathway and numerous lipid signalling molecules’. This list can be extended to include olfactory signalling (Schreiber et al., 2000), effects on motility, migration and metastasis (Galbiati et al., 1998; Galbiati et al., 1999; Segal et al., 1999; Zhang et al., 2000), participation in tight-junctions (Nusrat et al., 2000), a role in shear-stress signalling (Rizzo et al., 1998; Park et al., 2000), disease progression in tumours (Nasu et al., 1998; Yang et al., 1999), muscular dystrophy (Razani et al., 2000) and toxin uptake (Skretting et al., 1999). Apart from these one can cite evidence for caveolar participation in SV40 virus infection (Chen and Norkin, 1999), formation of the cleavage furrow in cytokinesis (Kogo and Fujimoto, 2000), prion infection (Naslavsky et al., 1999), membrane retrieval following exocytosis (Valentijn et al., 1999), multi-drug resistance (Yang et al., 1998; Ikezu et al., 1998), apoptosis suppression (Timme et

al., 2000) and nuclear translocation of the VEGF receptor (Feng et al., 1999). With respect to the low level of expression of caveolin in trophoblast described here, the downregulation of caveolin by oestradiol (synthesized in the trophoblast) and the positive regulation of the oestrogen receptor-alpha are of interest (Schlegel et al., 1999; Pelligrino et al., 2000). This study showed that a molecule sharing immunological identity with caveolin-1 is present in and is found at a number of locations in term human extraembryonic membranes. The most consistently strong expression was in the foetal blood vessel endothelial cells of the chorionic villi, and in fibroblasts in both amnion and chorion laeve. These two main sites of expression probably reflect differences in the type of transport processes being used by the two cell types. Fibroblasts, situated in comparative isolation from their neighbours, are highly biosynthetic cells that may need to exploit any mechanism that assists in the uptake of substrates from their surroundings. The possession of many caveolae on their cell surface has been described elsewhere (Röhlich and Allison, 1976; Bretscher and Whytock, 1977), and is confirmed in this study. In endothelial cells, on the other hand, the possession of caveolae is believed to subserve transendothelial transport purposes. Expression in syncytiotrophoblast was very low and this is in agreement with the findings of Lyden et al. (Lyden et al., 2002). These authors were unable to detect caveolae or caveolins-1 or -2 either in this tissue or in cytotrophoblast. This latter finding is at variance with the work of Linton et al. (Linton et al., 2003) who showed that residual cytotrophoblast continues to express caveolin-1 even after syncytialisation.

In mesenchymal cells of chorionic villi, amnion and chorion expression was generally high. Expression in the amniotic epithelium indicated a stronger association with apical as opposed to baso-lateral membranes. This association extended to the amniotic sleeve

of the umbilical cord. The most remarkable finding was a strong immunoreactivity in parts of the thin lining layer of the maternal blood space of the basal plate. This layer has previously been defined as generally trophoblast (Boyd and Hamilton, 1970). Its immunoreactivity as defined in this and other studies appears in places more typical of endothelium (Lang et al., 1993).

3.9.2 The morphology of basal plate inter-villus space lining cells

It is clear from careful morphological analysis that the cells lining the intervillous space are of two types and that these are probably endothelium and trophoblast. This was possibly the first report of horizontal-plane interaction between epithelial and mesenchymally derived cells in any naturally occurring human tissue. It is also conceivable that two distinct types of cells are derived from genetically different individuals. The trophoblast is foetally derived but the genetic origin of the endothelial cells had yet to be established. One strong possibility is that the endothelium is derived from the maternal blood supplying the inter-villus space and is thus genetically maternal. The existence of a mixed simple endo-epithelial layer, some squamous (endothelium) and some cuboidal (syncytiotrophoblast) is a histological novelty. It is also intriguing, implying as it does that epithelial and mesodermal derivatives may associate edge-on to form a continuous membrane. The origin of the endothelial cells lining the basal plate is the subject of Chapter 6 of this thesis.

Chapter Four

Immunoelectron microscopy using an anti-caveolin-1 antibody

4.1 Introduction

Part of the striated proteinaceous coat of caveolae has been shown to consist of caveolin (Rothberg et al., 1992). Caveolin-1 has been identified as a marker for type-I squamous epithelial cells in lung (Campbell et al., 1999) and as an endothelial and fibroblast marker in placental tissue (Byrne et al., 2001); it was localised to vascular endothelial cells, villous stromal cells, fibroblasts, vascular smooth muscle, amnionic epithelium and the endothelium lining the basal plate, using immunofluorescence confocal laser-scanning microscopy (CLSM) with an anti-caveolin-1 antibody that had been validated using Western blotting. This ultrastructural immunogold labelling study was performed using the same antibody to define the localisation of this scaffold protein more precisely. It was postulated that if this was close to the cell surface, where exposed receptors and signalling effector molecules may sample the external milieu (Feng et al., 1999, Chen and Norkin, 1999), caveolae may be available for signalling. Caveolin-1 itself is inserted only into the *inner*, cytosolic leaflet of the lipid bi-layer, so does not participate directly in signalling or other receptor-mediated events. If caveolae are internalised, the sensitivity of the cell to external autocrine, paracrine and endocrine events may be lessened. Some soluble caveolin-1 may be located by this antibody.

Immunoelectron microscopy was first used as a diagnostic tool in 1980 (Roth et al., 1980). Although this initial study employed a protein-A gold complex to locate the

antigen of interest on Epon-embedded sections, other studies failed to capitalise on these early results. Because the resins commonly used at this time were the hydrophobic epoxy resins and because the fixation regimes employed tended to have a deleterious effect on the antigenicity of the target proteins, much of the subsequent work in this field relied on cryo-ultramicrotome-cut sections. These were ultra-thin sections of rapidly frozen tissue which were picked up on coated EM grids prior to incubation with the primary and secondary antibodies. In order to avoid the deleterious effects of ice-crystal formation, specimens needed to be frozen extremely rapidly, in liquid nitrogen to produce a 'vitreous ice'; this meant that the specimens had to be vanishingly small in order to obtain useful data. In addition, the sectioning process required great skill and patience and was far from satisfactory in terms of its reproducibility.

The advent of low viscosity methacrylate resins, which were both stable in the electron beam and also hydrophilic meant that with a mild fixation regime, tissues could be embedded in these resins and sectioned using conventional ultramicrotomes, whilst retaining much of their antigenicity. The hydrophilic nature of these resins allowed more satisfactory penetration of the tissues by the aqueous antibody solutions than was possible using hydrophobic epoxy resins. The embedded tissue blocks could also be stored indefinitely at room temperature.

The methods used to prepare the specimens for immuno-gold electron microscopy are described in Chapter 2, Sections 2.7 and 2.8.

4.2 Results.

Gold particles were abundant in foetal capillary endothelial cells and were concentrated close to the cell surfaces. A lower colloidal gold anti-caveolin labelling was associated with the trophoblast. The gold particles were distributed to the basal and apical surfaces of the endothelium preferentially (Figure 4.2.1). The shared basal lamina between villous endothelia and syncytiotrophoblast was almost devoid of any labelling, as were occasional cytoplasmic inclusions. In rare cases, the pattern of gold labelling suggests caveolae, as in the inset to Figure 4.2.1; however, the poor preservation of membrane in these preparations allows only subjective observations to be made. Figure 4.2.2 shows a very similar staining pattern to that seen in the previous image. Figures 4.2.3 and 4.2.4 were less well stained by the uranyl acetate than either Figures 4.2.1 or 4.2.2, but this had the advantage of facilitating the discernment of gold labelling in relation to the tissue staining.

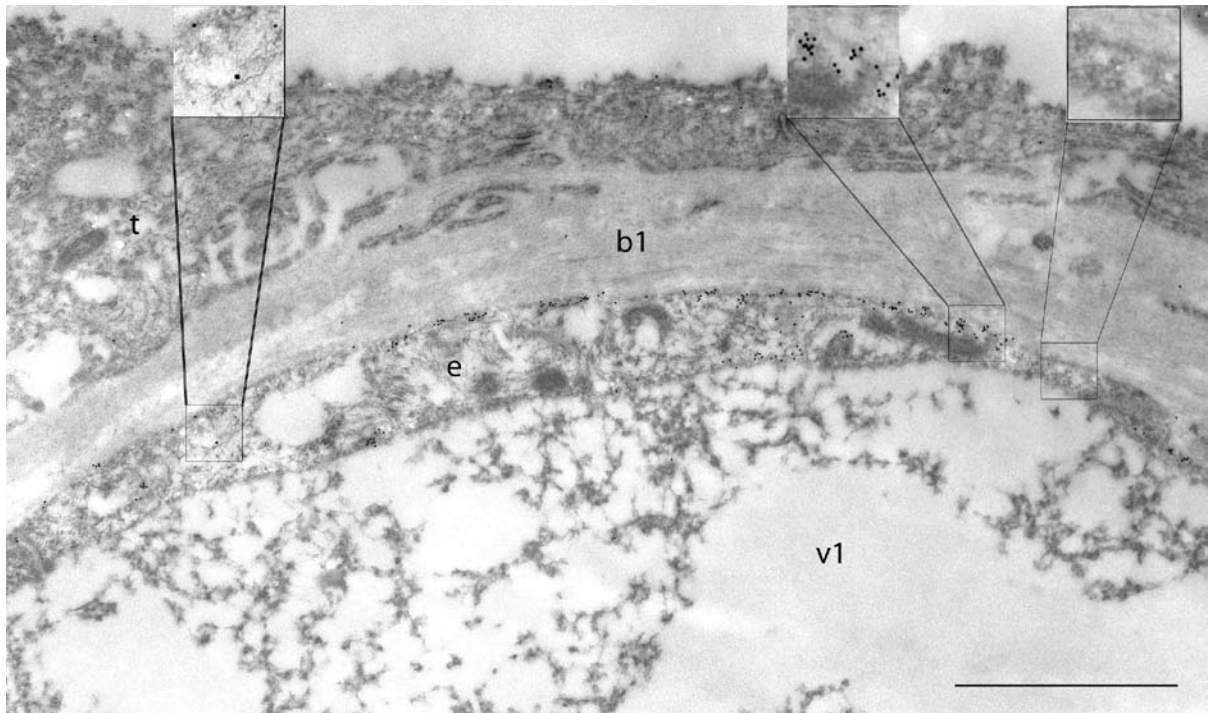


Figure 4.2.1 Anti-caveolin-1 immuno-gold labelling of an ultrathin cross-section through a terminal villus. The trophoblast (t) shows infrequent labelling compared with the foetal capillary endothelium (e). The band between the trophoblast and the endothelial cell is basal lamina (b1). v1 is the villous capillary lumen. The inset on the left of the image shows the boxed region at higher power so that the 10nm gold particles can be more clearly viewed; this is a region of intermediate labelling in the endothelium. The central inset shows an area of much greater labelling efficiency in the same cell, whilst the right-hand inset shows an area with no labelling at all. The electron-dense material within the capillary lumen is precipitated serum protein, often seen in tissues fixed in this way. The scale bar represents 1.0 μ m.

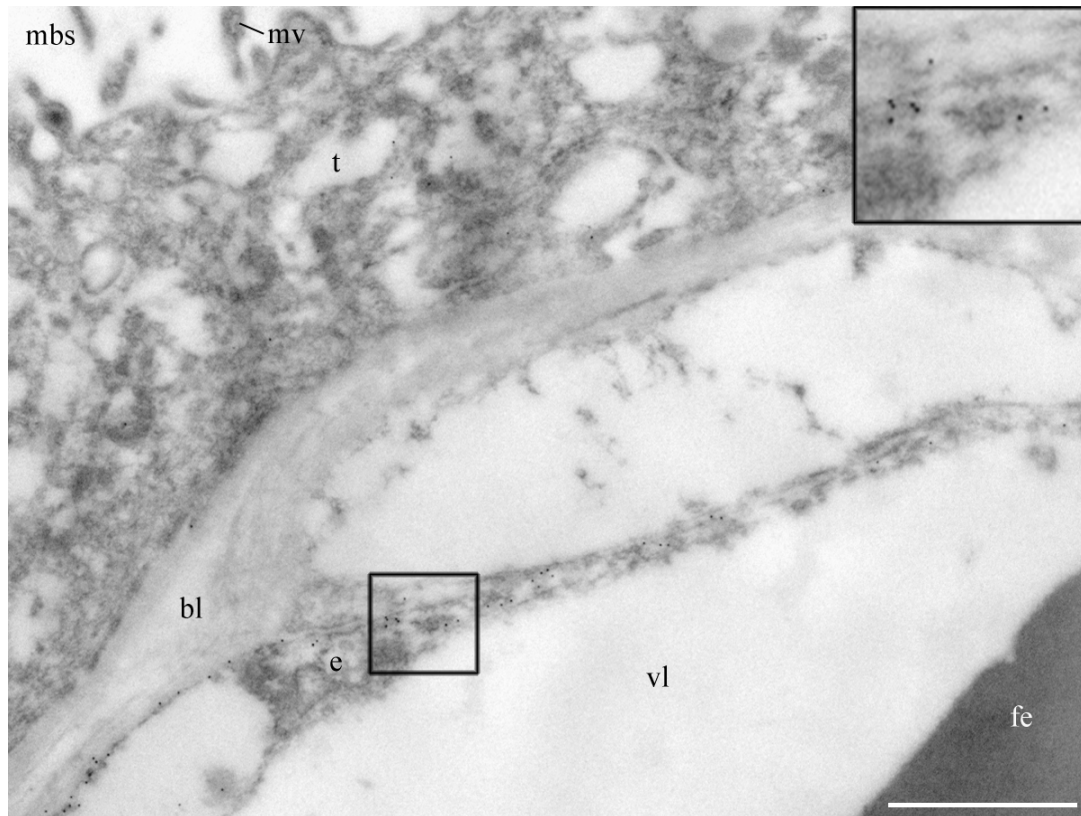


Figure 4.2.2 Anti-caveolin-1 immuno-gold labelling of an ultrathin cross-section through the full width of tissue separating maternal blood space (mbs) from foetal erythrocytes (fe). The trophoblast (t) with its microvillous (mv) border shows infrequent labelling compared with the foetal capillary endothelium (e). (vl) is the vessel lumen. The band between the trophoblast and the endothelial cell is basal lamina (bl). The inset shows the boxed region at higher power so that the 10nm particles can be more clearly viewed. The scale bar represents 1.0 μ m.

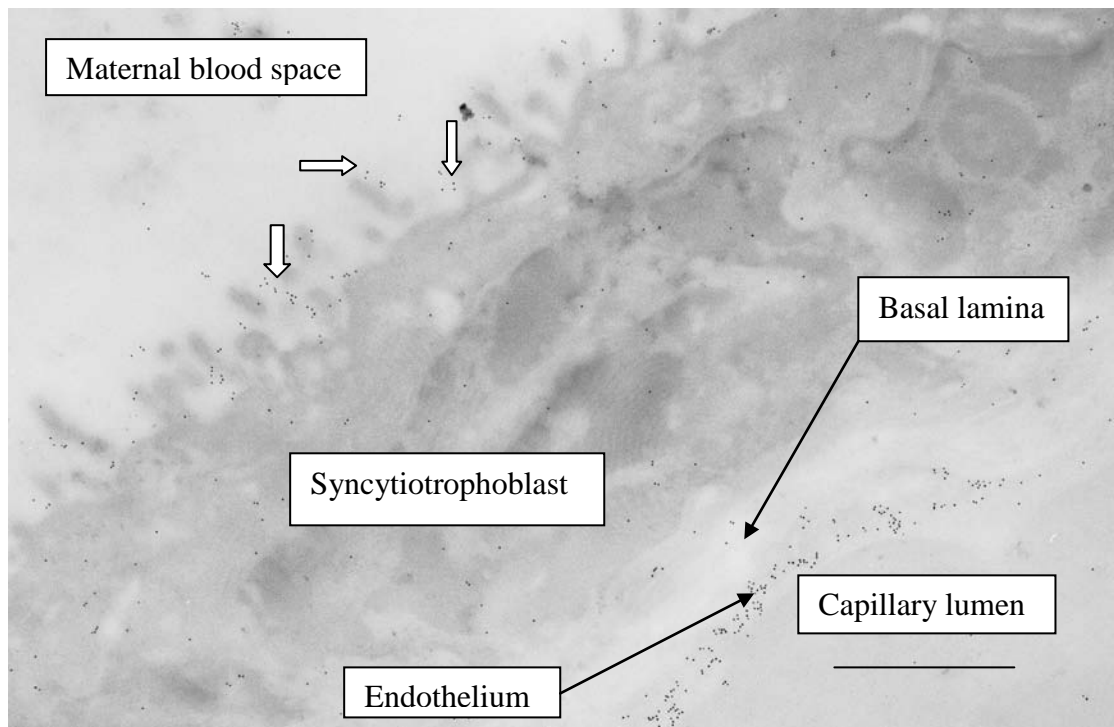


Figure 4.2.3 Anti-caveolin-1 immuno-gold. Villous trophoblast and underlying endothelium. Gold labelling is concentrated in the capillary endothelium. Gold is also associated with the microvilli of the syncytiotrophoblast, but seems often to be extracellular (white arrows). Scale bar = 1.0 μ m.

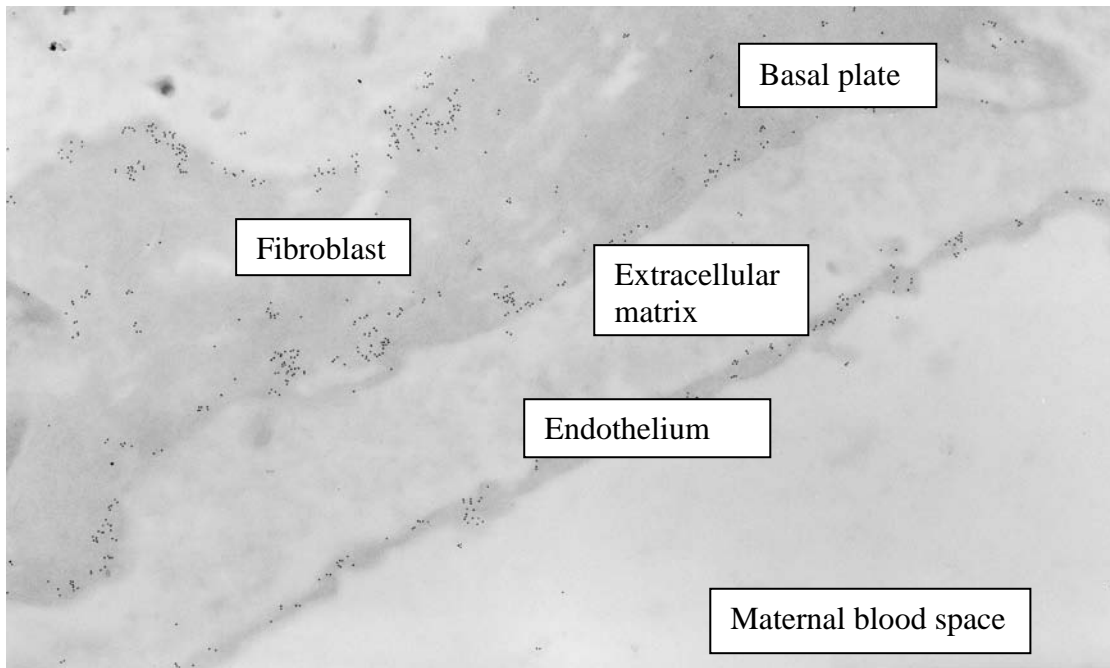


Figure 4.2.4 Basal plate lining the maternal blood space. Gold labelling is associated both with the endothelium and with the cortical region of the underlying cells in the basal plate. The morphology of these cells, especially at lower magnification, suggests that they are fibroblasts.

The single observation of a small foetal leucocyte (Figure 4.2.5) showed this cell to be highly immunoreactive to the anti-caveolin-1 antibody. Although some scattered nuclear labelling was observed, the majority of gold particles were seen to be associated with the cytoplasm/plasma membrane. The exceptionally high nuclear-cytoplasmic ratio of these cells may account for the unusual labelling density.

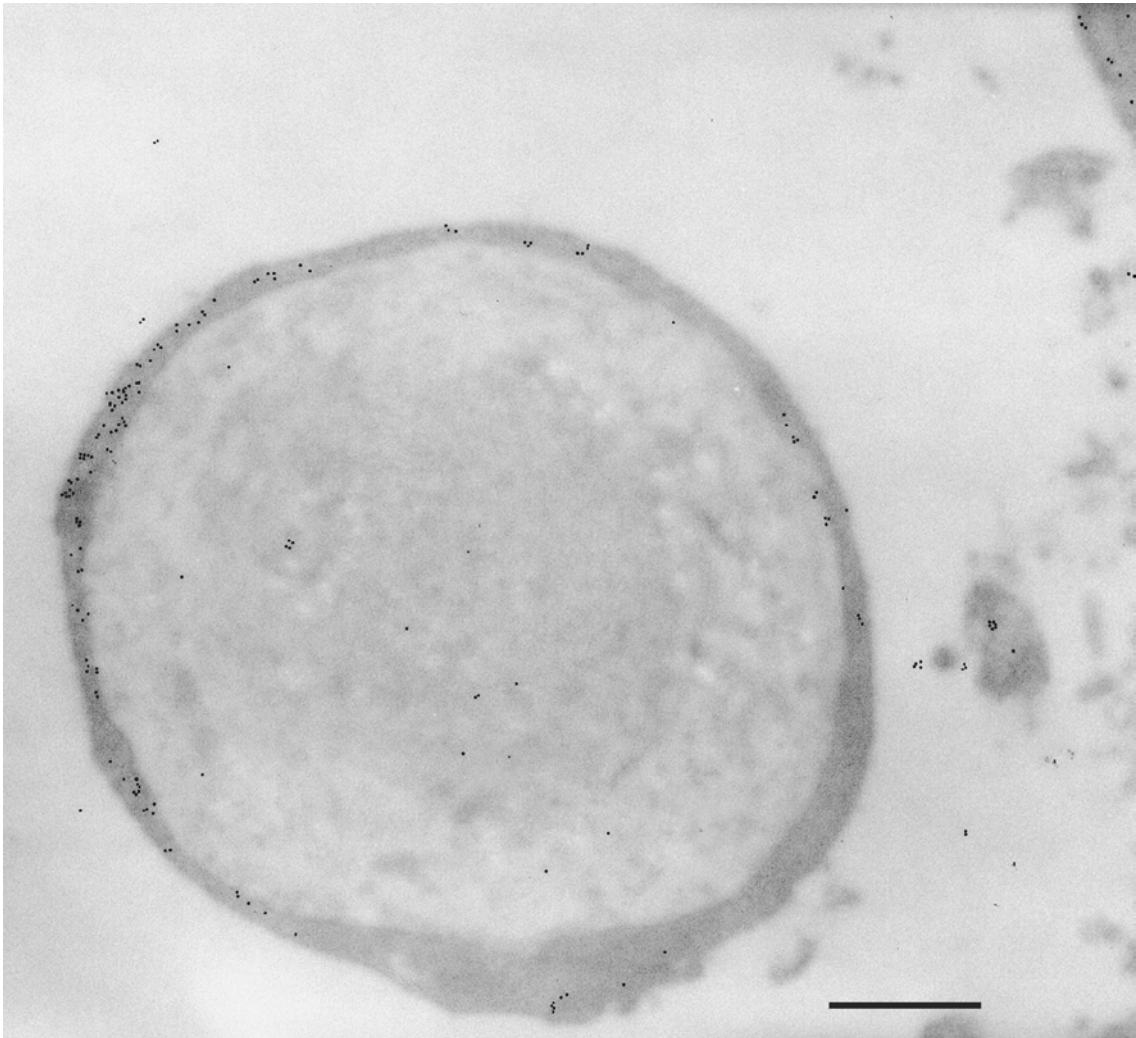


Figure 4.2.5 A small foetal leukocyte showing substantial cytoplasmic labelling with the anti-caveolin-1 antibody. Scale bar = 1.0 μ m.

The positive control (Figure 4.2.6), which employed an anti-pan-cytokeratin antibody, challenged an extra-villous trophoblast *from the same tissue block* as that used for the basal plate endothelial cell study, and had thus been prepared in an identical manner. In this case, little or no labelling was seen to be associated with the cell membrane. Filamentous keratin bundles, which preserved their electron density, were shown to be heavily labelled, whereas the nucleus, nucleolus and cellular inclusions were effectively negative.

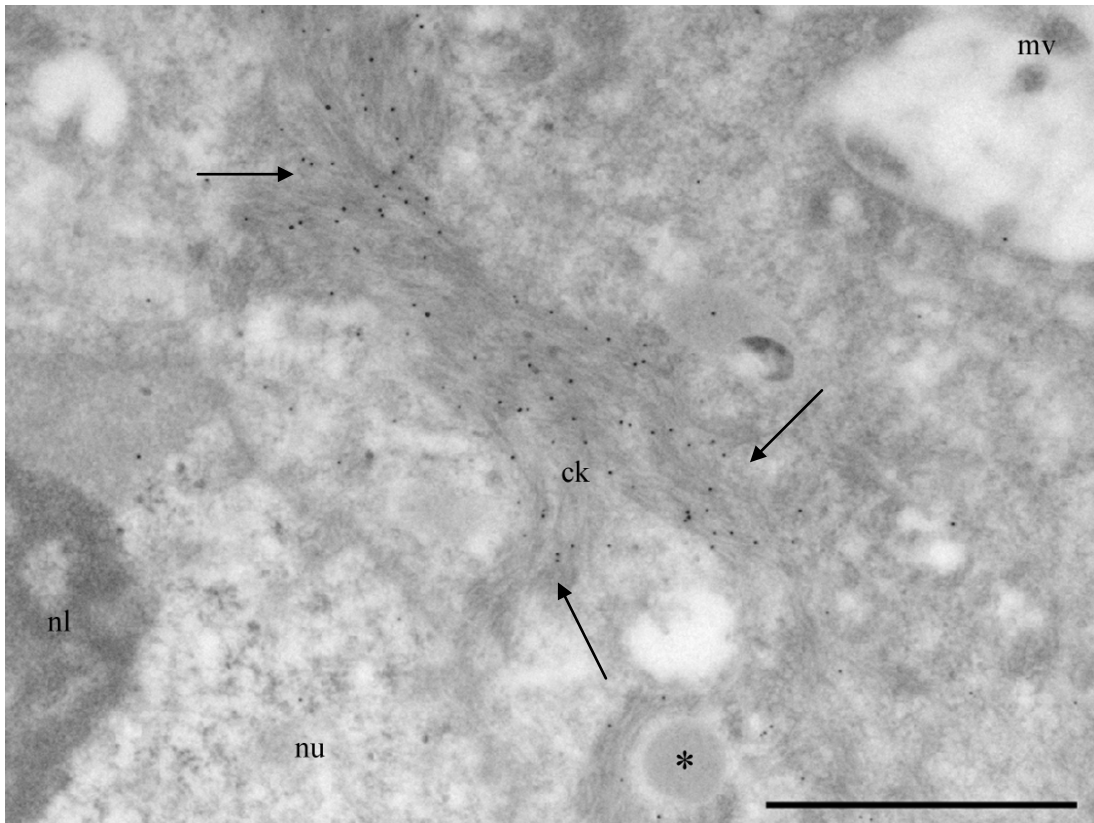


Figure 4.2.6 Positive control with anti-pan-cytokeratin immunogold labelling of an extra-villous trophoblast cell in the basal plate. Intermediate filament bundles (arrows), composed of cytokeratin (ck) are shown. (nu) is the nucleus and (nl) its nucleolus. (mv) are the microvilli which protrude into the extracellular matrix surrounding these cells. The asterisk (*) is a cytoplasmic inclusion. Scale bar = 1.0 μ m.

4.3 Statistical Analysis of Gold Particles per Unit Area

Analysis of the numerical data from different tissue types present in terminal villi (Figure 4.3.1) showed that the capillary endothelium was the only cell present which showed any significant immunoreactivity at this location. The inclusion of erythrocytes, extracellular matrix and capillary lumen in the counting regime was to establish the levels of non-specific binding at sites where *no* caveolin-1 is expected to be found. The fact that there appears to be some binding of the antibody by trophoblast which is *slightly* above the background level at these other sites may suggest that there is a low level of expression of caveolin-1 by this cell type, though some may be attributable to non-specific, extracellular binding as shown in Figure 4.2.4. Following analysis of variance using ANOVA in association with Tukey's HSD post-hoc test, the mean endothelial cell associated gold particle counts per μm^2 were shown to be significantly different from each of the other 4 means ($p = 0.0001$). The other 4 means were not significantly different from each other, although the trend shows an increase of labelling in trophoblast when compared with the three other areas (erythrocyte, vessel lumen and extracellular matrix). Differences in the labelling frequency of the differentiated cell types were obvious on qualitative inspection, with endothelium > trophoblast and trophoblast > maternal blood.

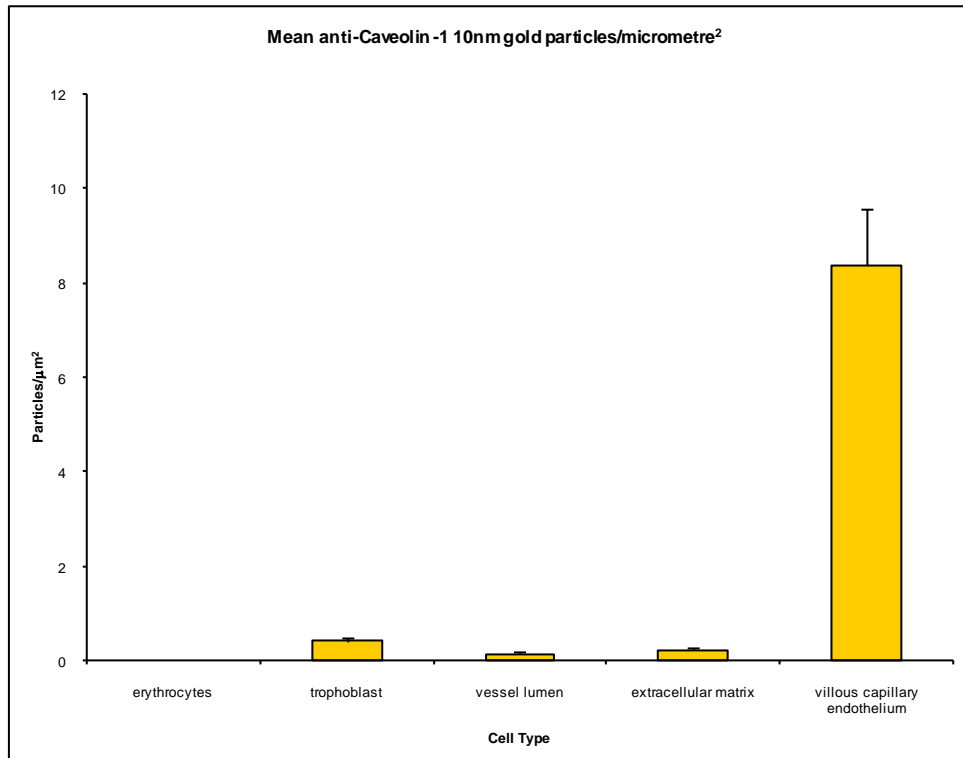


Figure 4.3.1 Anti-caveolin-1 immuno-gold. Numbers of gold particles per μm^2 of villous tissues including: erythrocytes, villous trophoblast, foetal vessel lumen, extracellular matrix and villous capillary endothelium. $n = 28$ areas counted for each tissue/cell type. ANOVA with Tukey's post hoc HSD. (Endothelial: all others $p < 0.0001$). Error bars = Standard error of the mean (SEM).

Zonal analysis of labelling density (Figure 4.3.2) compared the labelling density (expressed as gold particles per square micron) associated with a 150nm wide strip of the basal surface with a 150nm wide strip of the apical surface. These were then compared to the density of labelling in the more central parts of the endothelial cytoplasm. The basal mean count/ μm^2 was consistently higher than the apical. The apical mean, in turn, was higher than the central mean. The analysis of variance (ANOVA and Tukey's HSD post-hoc test) demonstrated significant differences between all 3 means. Apical versus basal significant difference was $p = 0.009$; for both apical and basal versus central $p = 0.0001$.

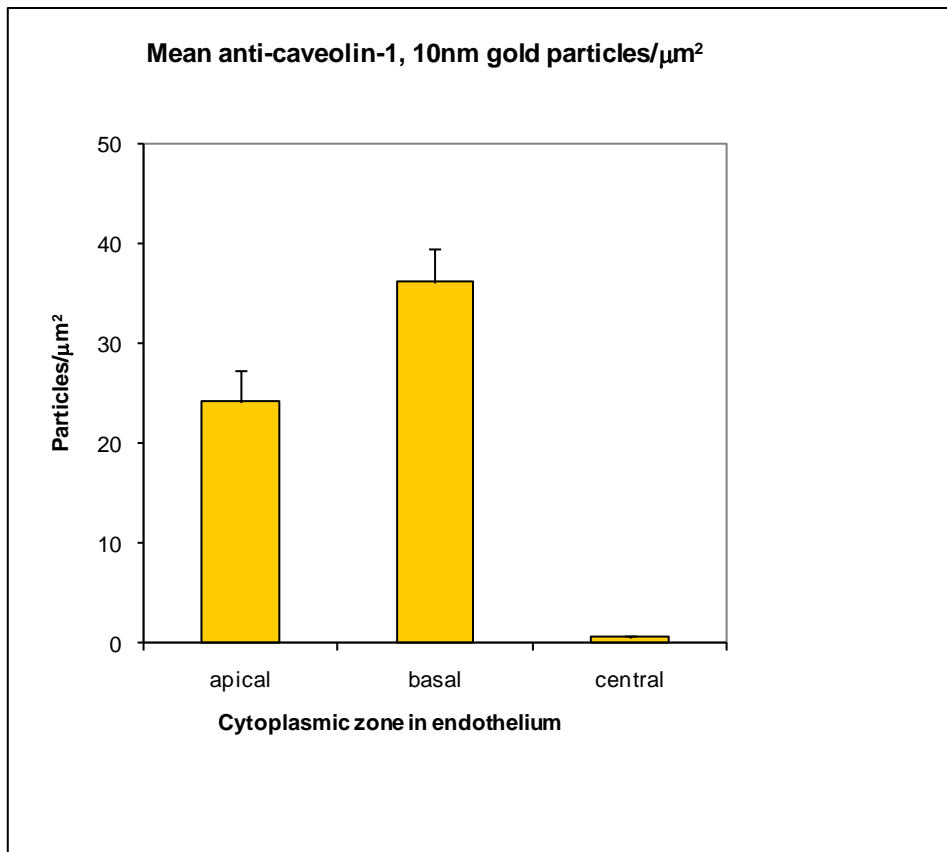


Figure 4.3.2 Zonal distribution of caveolin-1 label in foetal capillary endothelium.

The bar graph shows the mean anti-caveolin-1 10nm gold particle counts for the uniform width (150nm) apical, basal and central strips in foetal capillaries. For each zone, n = 15 separate areas were counted. ANOVA and Tukey's HSD. (Apical: basal $p < 0.009$; apical and basal: central $p < 0.0001$ for both). Error bars = SEM.

The interesting population of endothelial cells lining the basal plate and forming part of a mosaic there were investigated separately (Figure 4.3.3). The distribution of anti-cavolin-1 labelling reflected that of the chorionic villous endothelial cells with higher apical and basal labelling than central labelling. Using ANOVA and Tukey's HSD post hoc test, the only significant difference was between the apical and central zones ($p < 0.04$), probably owing to the limited sample size of adequate quality available and the greater scatter of the label in these cells. Figure 4.2.4 shows that these endothelial cells are frequently less than 150nm thick, which adds to the difficulty of differentiating between the apical and basal zones.

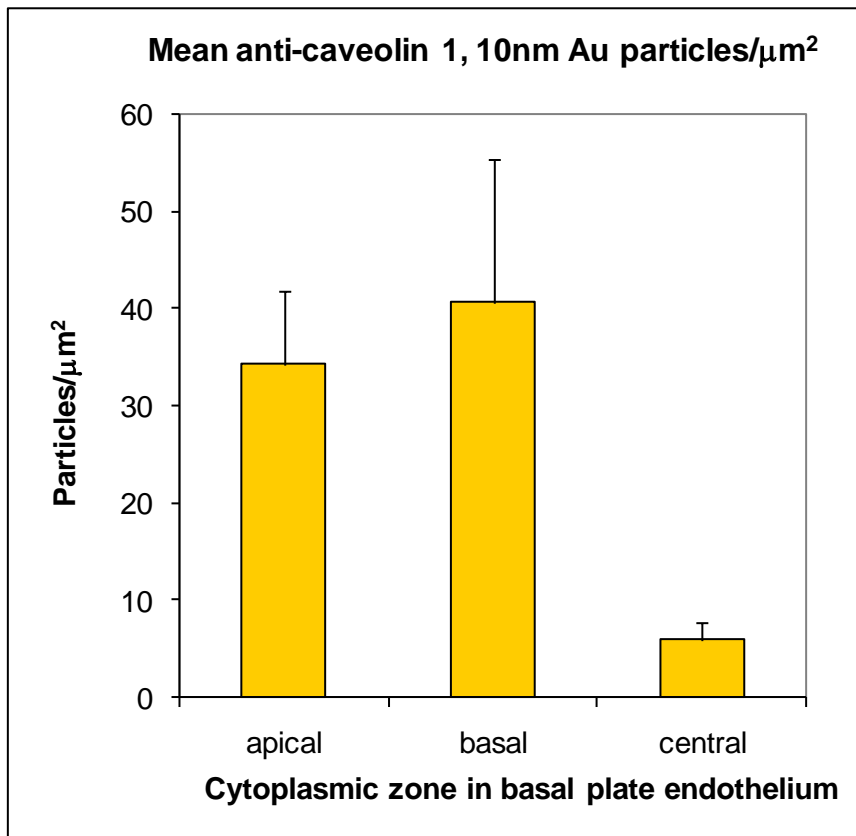


Figure 4.3.3 Zonal distribution of caveolin-1 label in basal plate endothelial lining.

This figure shows the mean counts per μm^2 in 150nm wide strips of the apical and basal surfaces of endothelial cells lining the basal plate and compares these with each other and with the counts from the central cytoplasmic zone in these cells. $n = 8$ for each zone. ANOVA and Tukey's HSD. (Apical: central $p < 0.04$). Error bars = SEM.

When the labelling densities of three different cell types found in chorionic villi were compared, there was a difference between the epithelial and each of the other mesenchymal cells counted, with the fibroblast and endothelial labelling being greater than that of the syncytiotrophoblast. The small population of villous cytotrophoblasts remaining at term may contribute to the overall “trophoblast” counts, but no distinction between these was made in this present study. The position of fibroblasts (i.e. in the central, stromal part of the villi), as well as their distinctive ultrastructural morphology, makes them easy to identify.

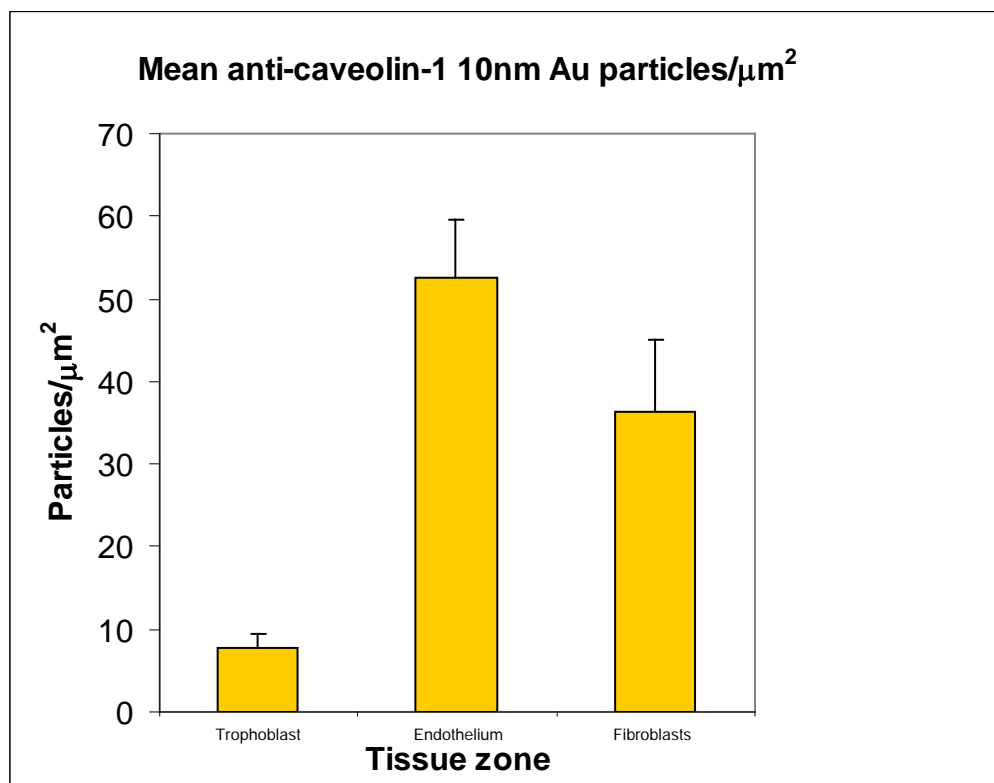


Figure 4.3.4 Caveolin-1 labelling densities in different villous cell types

In this figure, the epithelial villous trophoblast anti-caveolin labelling was compared with the labelling of two mesenchymal cell types of the villous core, the fibroblasts and endothelial cells. n = 23 for each cell type. ANOVA and Tukey's HSD. (Endothelium and fibroblasts: trophoblast p<0.001) Error bars= SEM.

When basal plate fibroblasts were examined, the majority of the anti-caveolin-1 gold labelling was confined to the 150nm wide cortical zone. The small percentage found elsewhere was either non-specific binding or binding associated with the soluble cytoplasmic form of this protein.

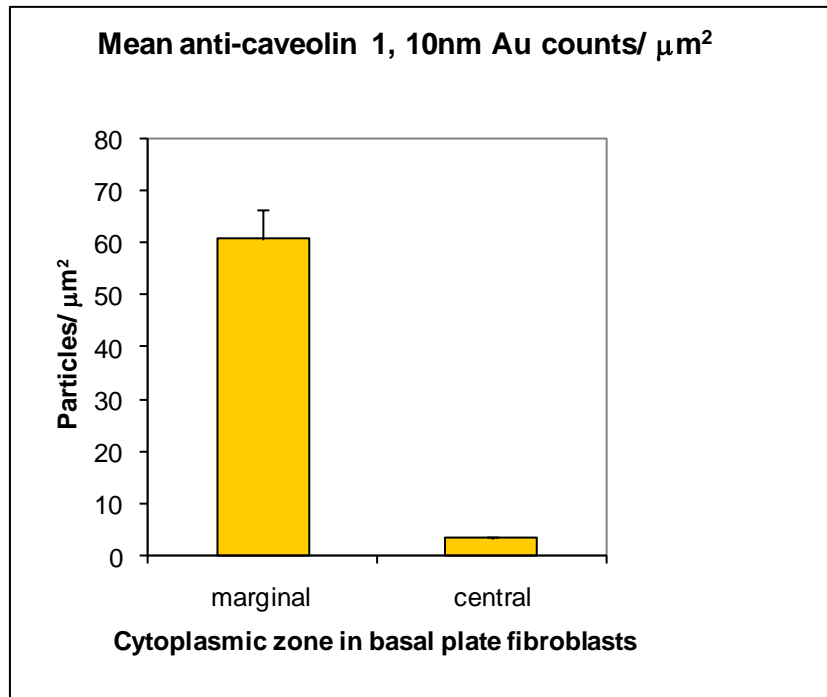


Figure 4.3.5 Zonal distribution in basal plate fibroblasts.

A significantly higher level of labelling by anti-caveolin 10nm gold particles was found in the cortical strip of cytoplasm 150nm wide as compared with the central cytoplasm in sections of fibroblasts. $n=16$ areas counted. ANOVA with Tukey's HSD post-hoc test. ($p < 0.0001$). Error bars= SEM.

The highest density of anti-caveolin-1 gold labelling was associated with villous endothelium (Table 4.3.2). Villous fibroblasts had a lower level of labelling, but substantially more than trophoblasts, some of which may be attributed to cytotrophoblast labelling, which is higher than syncytiotrophoblast (Linton et al., 2003). Both foetal and maternal erythrocytes were effectively unlabelled.

TISSUE	n	Min. Au/ μm^2	Max. Au/ μm^2	Mean (SEM)
Trophoblast	10	0.34	18.21	7.84 (1.63)
Endothelium	29	5.79	148.82	52.48 (7.1)
Foetal erythrocyte	11	0	7.42	2.31 (0.72)
Fibroblast	10	11.09	88.8	36.22 (8.9)
Maternal erythrocyte	31	0	1.86	0.67 (0.12)

Table 4.3.1 Mean gold counts/ μm^2 over different tissues

This table shows the mean colloidal gold particle counts per unit area overlying different tissues of terminal villi and neighbouring maternal erythrocytes. (n = number of areas counted, SEM = Standard error of the mean in the range of areas counted.)

4.4 Summary of results from the immuno-gold study.

- Cells showing the brightest anti-caveolin-1 immunofluorescence in the frozen section study (Chapter 3 - endothelial cells and fibroblasts), were similarly immuno-reactive in the plastic-embedded immuno-gold results.
- Immuno-negative cells (erythrocytes and syncytiotrophoblast) were similarly less reactive in this study.
- Foetal capillary cells were strongly positive.
- The labelling pattern in all cells, particularly in fibroblasts, was largely confined to a cortical band some 150nm wide.
- In both foetal capillary and in basal plate endothelial cells, the label was concentrated towards the basal, rather than the apical surface.
- A foetal leucocyte was shown to be highly immuno-reactive to this antibody.

4.5 Discussion

4.5.1 Specificity

The selective labelling of differentiated cell types and the increase of labelling frequency in the presence of the primary (anti-human caveolin-1) antibody demonstrated in this study supported the specificity of the labelling technique. The specificity of the antibody had been tested previously using Western blotting and immunofluorescence microscopy (Byrne et al., 2001). The intensity of labelling (strongest in endothelium, weak in syncytiotrophoblast) paralleled that found previously with immunofluorescence microscopy (Byrne et al., 2001; Linton et al., 2003), and was consistent with the ultrastructural data describing caveolae and micropinocytic vesicles in these and related tissues (Ockleford and Whyte 1977; Ockleford and Clint, 1980; Linton et al. 2003). Immuno-electron microscopy is an independent localisation method with higher resolution than the immunofluorescence used previously. It confirmed the previous results and extended these as it was the first ultrastructural immuno-labelling study that demonstrated the sub-cellular as well as cellular distribution of anti-caveolin immunoreactivity in placental tissue.

Available methods for ultrastructural immunocytochemistry include low-temperature embedding and cryo-ultramicrotomy. The latter is favoured where freeze fixation and cryo-embedding are better able to preserve antigenicity, in cases where resin embedding is deleterious (Griffiths, 1993). In this instance it appeared that caveolin-1, a detergent-resistant scaffold protein, was sufficiently robust to survive the embedding procedures used and that sufficient epitopes were preserved for interaction with the polyclonal antibody.

4.5.2 Tissue distribution.

It was not surprising that mature erythrocytes, with no known micropinocytic or caveolar association, exhibited only background labelling. Likewise, extracellular matrix was not expected to label with an antibody to an intracellular antigen. The two transporting cells - the foetal capillary endothelial cells and the syncytiotrophoblasts - are essential components of the materno-foetal exchange system. Cytotrophoblasts, which are very sparse at term, cease to play a significant role in this process; during the earlier trimesters, where they form an inner lining to the villi, this is not the case and may explain why their previously high caveolin-1 expression is down-regulated in the later stages of pregnancy. From this evidence it would appear that macromolecular handling by transcytotic processes and/or the uptake, secretion and receptor display systems, are very different in the two cell types. The bias of syncytiotrophoblast to the clathrin-coated pit (Ockleford and Whyte, 1977) as the predominant organelle of its type and of the foetal endothelial cells to the caveola described in the earlier work of Mongan and Ockleford, (Mongan and Ockleford, 1995), is re-emphasised by these findings.

The high labelling density in the cortical region of fibroblasts was not unexpected. These cells, which are often separated from neighbouring blood vessels by a considerable distance, and which reside in the extracellular matrix which they themselves synthesise, have to exploit whatever means at their disposal to take from their external milieu the nutrients, and other molecules essential for their survival.

4.5.3 Intracellular distribution

Membrane-associated labelling is expected of the caveolar stage of both signalling and micropinocytic processes; deeper intracellular labelling may be explained by the presence here of closed, internalised caveolar vesicles. It may also indicate sites of synthesis, storage or degradation of the protein. The soluble form of caveolin-1 would likewise be predicted to be present throughout the cytoplasm. The *basal* cortical band of intense labelling in villous endothelial cells was an unexpected finding. Its concentration at this, rather than the apical surface, could reflect the net transport (and signalling) requirements of the foetus. Maternal macromolecules (in the intervillous space) need to be taken up and transported *to* the foetus, so it seems logical that the surface closest to the source of these molecules (i.e. the basal surface of the villous capillary endothelium) would be invested with a higher number of caveolae per unit area than the apical surface. The anabolic requirements of the foetus outweigh its need to eliminate products of catabolism, which will generally be simpler and less transport-dependent.

The preponderance of caveolin-1 at the surface (particularly the basal surface) of the villous endothelial cells may simply be explained by the proximity of this surface to the source of the molecules whose transport *is* caveolin-dependent (the maternal blood). Control over processes at this level is known to take place in other circumstances as in the nitric oxide synthase interacting protein (NOSTRIN)/ nitric oxide synthase trafficker (NOSIP) system (Feng et al., 1999; García-Cardena et al., 1997; Zimmermann, et al., 2002). The association of these control molecules with the caveolar complexes makes them strong candidates as participants in such regulatory processes. Why the relatively large amount of labelling is intracellular in this tissue is a matter of conjecture. It may

reflect physiological or pathological processes, or be simply attributable to a fixation artefact. The distribution of the label using this technique does not always concur with what might be expected; the use of other anti-caveolin-1 antibodies may help to eliminate this problem.

The “barrier” that prevents the fatal mixing of maternal and foetal blood is thinnest at term. However it still constitutes two cellular layers, the endothelium and the syncytiotrophoblast. As indicated here by the diversity of the distribution of the structural platforms on which caveolae depend, there appear to be distinctive cell physiological properties associated with the two cellular layers of the “barrier”. Different physiological conditions affect maternal, placental and foetal compartments separately (Ganapathy et al., 2000). Two complete layers are required to separate three compartments and the signalling at the basal endothelial membrane might be expected, on this basis, to differ at least quantitatively and possibly to relate the placental physiology to the foetal demand that drives several aspects of pregnancy physiology. In terms of the signalling requirements of the foetus, it would make sense that caveolae should be concentrated closest to the source of such signals – the *basal* surface of villous endothelial cells.

The distribution of caveolin-1 labelling in the endothelial lining of the basal plate is something of an enigma; until more is known about the *raison d’etre* of these cells, one can only conjecture that signals which arise in the basal plate (on the basal surface of these cells) need to be relayed to the maternal compartment preferentially over those arriving *from* this compartment.

Chapter 5

Healthy and pre-eclamptic placental basal plate lining cells: quantitative comparisons based on confocal laser scanning microscopy.

5.1.1 Introduction

The embryonic development of higher primates is dependent on a haemo-chorial placenta, where foetal tissue is in direct contact with maternal blood. At term, the thinnest part of the barrier between the maternal and foetal blood consists of only two cellular layers – the syncytiotrophoblast and the villous capillary endothelium (Benirschke and Kaufmann, 2000). Mediating invasion of the uterine wall is an ectodermal, extra-embryonic derivative of the blastocyst, the trophoblast; this is the tissue of the conceptus that makes first contact with the uterine epithelium during the attachment phase. The maternal epithelium and underlying endometrium is excavated by a combined process of proteolysis and apoptosis, thereby creating an intervillous space. In advance of the primary villus invasion, a wave of trophoblast penetrates ahead of the remainder of the conceptus modifying the uterine spiral arterioles which will eventually supply the growing placenta with maternal blood (Feng et al., 2001). Although the vascular supply is initially plugged by the invading cytotrophoblasts, it will, by approximately the 12th week of gestation, be irrigated by whole maternal blood (Burton et al., 2001). Those cytotrophoblast cells which are not engaged in the invasion and occlusion of the spiral arteries become resident amongst the decidual cells in the basal plate tissue underlying the implantation site. These are the extravillous trophoblast cells.

A number of histological, cell and molecular pathological studies have revealed that there are measurable quantitative differences between healthy and pre-eclamptic uteroplacental (and specifically basal plate) parameters. These have been characterised using several different criteria. Firstly, the percentage of placental bed spiral arteries that exhibit a failure of physiologic transformation is higher at term in patients with pre-eclampsia than in normal pregnancies ($P = 0.0001$) (Kim et al., 2003a,b). The basal plate of the normal decidua contains numerous CD14 (+), HLA-DR (bright), mannose receptor (ManR) (+) tissue macrophages but virtually none of these phagocytic cells can be found in pre-eclamptic placentae (Burk et al., 2001; Williams et al., 2009). Placentae of pre-eclamptic pregnancies show villous cytotrophoblast proliferation, increased syncytial knot formation, and impaired trophoblast invasion (Gratton et al., 2002). Cytotrophoblasts from foetal growth retarded (FGR) placentae differ from healthy placentae with respect to proliferation markers. These placentae were osteopontin (OPN)-positive until 30 weeks, unless pre-eclampsia accompanied the FGR where cytotrophoblasts were OPN positive at 24–40 weeks. In pre-eclampsia, OPN immunoreactivity was detected at 24–40 weeks (Gabinskaya et al., 1998). Insulin-like growth factor binding protein 1 (IGFBP-1) expression was present only in the decidua of the basal plate and membranes and this expression decreased significantly in pre-eclamptic placentae (Gratton et al., 2002). Endothelin-1 (ET-1) is known to play an important role as a modulator of vascular tone in the utero-placental and foeto-placental units and may participate in the pathogenesis of pre-eclampsia (Barros et al., 2001). Patients with pre-eclampsia exhibited an attenuated vasodilatory response to bradykinin, compared to those with normal pregnancies ($P < 0.0001$) (Ong et al., 2003). It has also been shown that certain molecules induced by low oxygen tension, e.g., the ‘protein regulated by oxygen at 1%’ (PROXY-1), are elevated in certain tissues from pre-

eclamptic pregnancies, such as chorionic villi of peri-infarct regions, basal plate and membrane decidua, as well as in the chorion itself (Graham et al., 2000). Immunofluorescence techniques revealed that the thickness of Nitabuch's membrane (a fibrinoid-rich layer of the basal plate extracellular matrix) was significantly greater in the study (pre-eclamptic) group compared with the control group: 157.48 pixels vs. 63.80 pixels, $P = 0.006$, respectively (Balducci et al., 1997). There is also a published study suggesting that in pre-eclampsia, haemosiderin depositions were not correlated quantitatively with impaired foetal growth (Sherer and Salafia, 2000).

To hold the placenta to the uterine wall, some tertiary terminal villi bridge to the uterus. These are known as anchoring villi. At their junctions, the anchoring villous cores contain cytotrophoblast cells similar to the extravillous trophoblasts (Figure 5.1 overleaf). These are probably the source of the cells of the extravillous trophoblast lineage. Between the anchoring villi and lining the intervillous space is a thin unicellular layer that is the focus of this Chapter. Its cells are the basal plate intervillous-space lining cells (Byrne et al., 1998, 2001 and Chapters 3, 4 and 6 of this thesis).

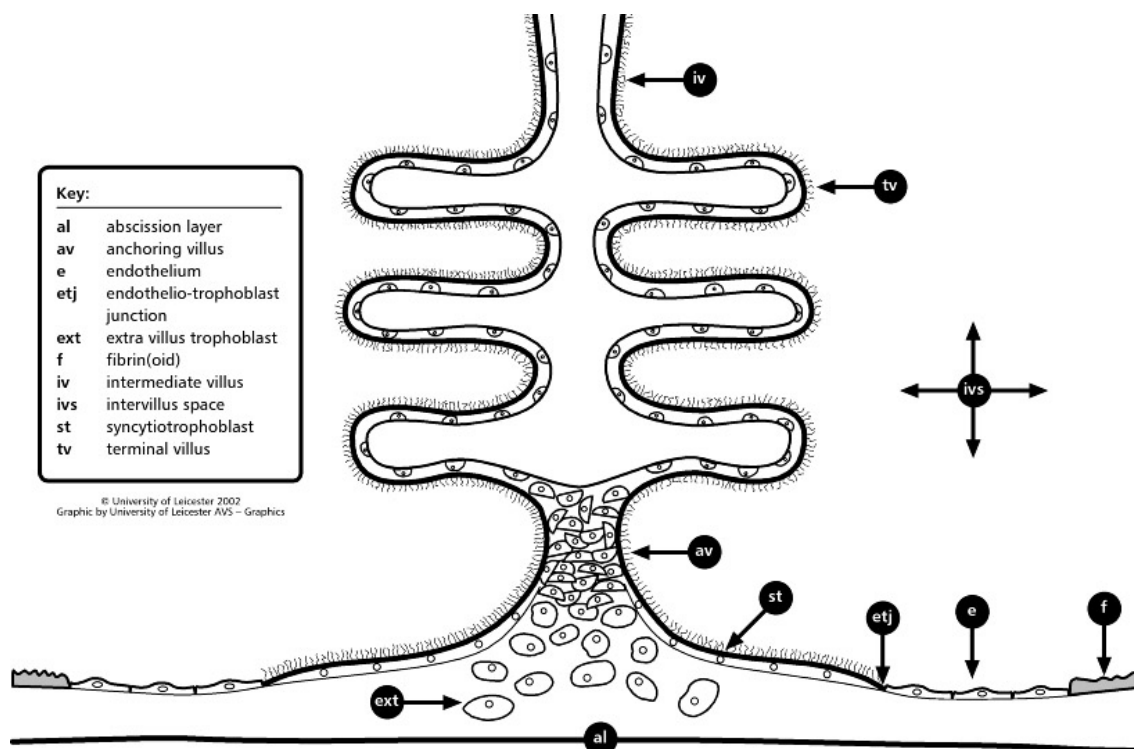


Figure 5.1 Diagram showing basal plate lining cells and an anchoring villus

The syncytiotrophoblast (st) covers the anchoring villi (av) and continues onto the surface of the basal plate. It then encounters either fibrin/fibrinoid (f) or endothelium. Junctions are sometimes seen between the syncytium and the endothelial cells (etj). Also shown are the resident extravillous trophoblasts (ext) which are derived from cytotrophoblasts in the core of the anchoring villus.

5.1.2 Cytoskeletal and other markers

Antibodies to cytoskeletal proteins were first used to identify and describe the structural importance to the architecture of extra-embryonic tissues (Ockleford et al., 1981, 1984, 1990, 1993; Ockleford, 1990). Anti-cytokeratins were recognised as useful ectodermal lineage markers and have become widely used to assist identification of cell populations in the basal plate alongside markers directed against the products of placental endocrine glycoprotein secretion. Placental villus endothelial cells which were initially characterised by staining with antibodies that recognised the presence of vimentin (Ockleford et al., 1990) have more recently been defined by the signalling platform

membrane protein caveolin-1 (Byrne et al., 1998, 2001) and by a wide range of other markers (Dye et al., 2001).

5.1.3 The intervillous space

In earlier years, the conventional view had been that the intervillous space was lined entirely by trophoblast or fibrin/fibrinoid (Boyd and Hamilton, 1970), but recent studies of proteolysis and apoptosis during implantation have thrown light on the development of blood spaces including vascular sinuses especially the intervillous space, its tributaries and its draining vessels. In particular, modifications to currently orthodox views concerning the lining of the inter-villus space at term have been proposed (Byrne et al., 1998, 2001, Chapter 3, this thesis). There is now evidence that at least part of the surface of this vascular sinus is an endothelial cell sheet that abuts laterally to trophoblast which is continuous with the surface layer of anchoring villi (Chapter 3). This view has been supported by others (Lang et al., 1993; Wanner, 1966) and this new insight presents an opportunity to re-interpret the nature of the formation and function/dysfunction of the blood-spaces supporting the haematotrophic nutrition of the foetus.

5.1.4 Pre-eclampsia and maternal vascular remodelling

To appreciate the medical importance of pre-eclampsia (Cunningham and Lindheimer, 1992) it is worth considering the World Health Organization (WHO) statistics for 1996 (WHO, 1996). In some developing countries there is a mortality rate of 1:12 as a result of a pregnancy-related problem (the equivalent risk in the developed world is 1:4,000). It is estimated that approximately 12% of these deaths are as a result of pre-eclampsia. As well as the mother, the baby is also at mortal and morbid risk in pre-eclampsia, primarily from intra-uterine growth retardation. In the pathology of this disease, much

attention has been given to the activity of the trophoblastic cells that enter and modify the uterine vasculature (Davey and Macgillivray, 1998). In a healthy gestation, this “plugging” trophoblast appears to deny blood access to the fully formed intervillous space until about week 12 of gestation (Burton and Caniggia, 2001). By this time, the diameter of the vessels opening into the intervillous space should have been widened and the medial smooth muscle layer effectively ablated. Such an adaptation is interpreted as allowing the presence of the Borelli jets of oxygenated blood that perfuse the intervillous space to be at a reduced pressure, effectively slowing the flow rate of blood over the absorptive villi. One of the key histopathological features of pre-eclampsia is a *failure of the spiral arterioles to be appropriately dilated*. The studies described in this chapter compare the area percent of the basal plate lining epi/endothelium occupied by endothelium, trophoblast and acellular material in normal term placentae. These data are then compared with that of pre-eclamptic tissue to determine whether this may be a significant factor in implantation failure in pre-eclampsia.

5.2 Results

5.2.1 Identification of cell types in the placenta by immunofluorescence

In cross-sections of mid-cotyledonary term placentae (Figure 5.2.1) cyokeratin staining was confined to villous trophoblast where the most intense staining was associated with the apical surface. von Willebrand factor staining was most prominent in the villous capillaries but was also present to a lesser extent in the stromal cells of the villi and in leucocytes and possibly platelets both in foetal capillaries and in the maternal blood space.

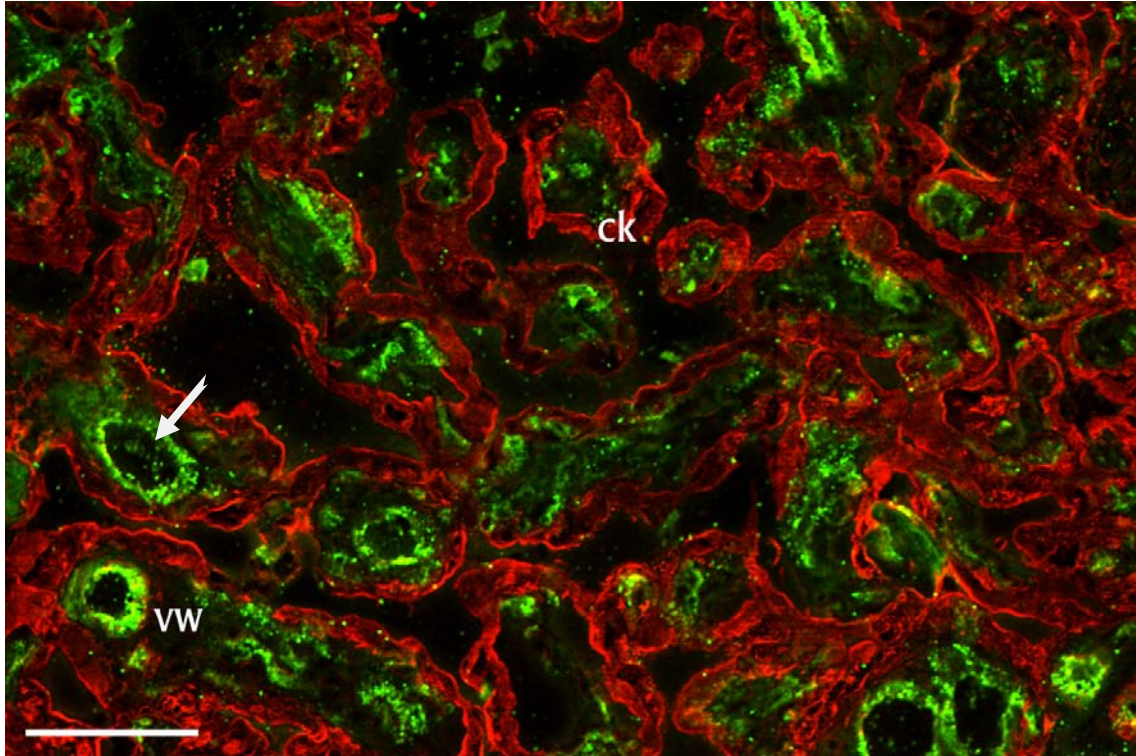


Figure 5.2.1 Normal chorionic villi labelled with anti-pancytokeratin and anti-von Willebrand factor

Pancytokeratin (red) and von Willebrand factor (green) dual-channel indirect immunofluorescence detected using confocal laser scanning microscopy. The red labelling of the trophoblastic epithelium (ck) and the green of the foetal capillary endothelium (vW) distinguishes them. White arrow is a foetal capillary. Scale bar = 100 μ m.

Much of the lining of the basal plate in healthy placentae was found to be positive for endothelial cell marker antibodies such as anti-PECAM-1. Where anti-pan-cytokeratin antibodies were used as trophoblast markers, a clear distinction was made between villous and extravillous cells, with the latter being always more strongly stained (Figure 5.2.2).

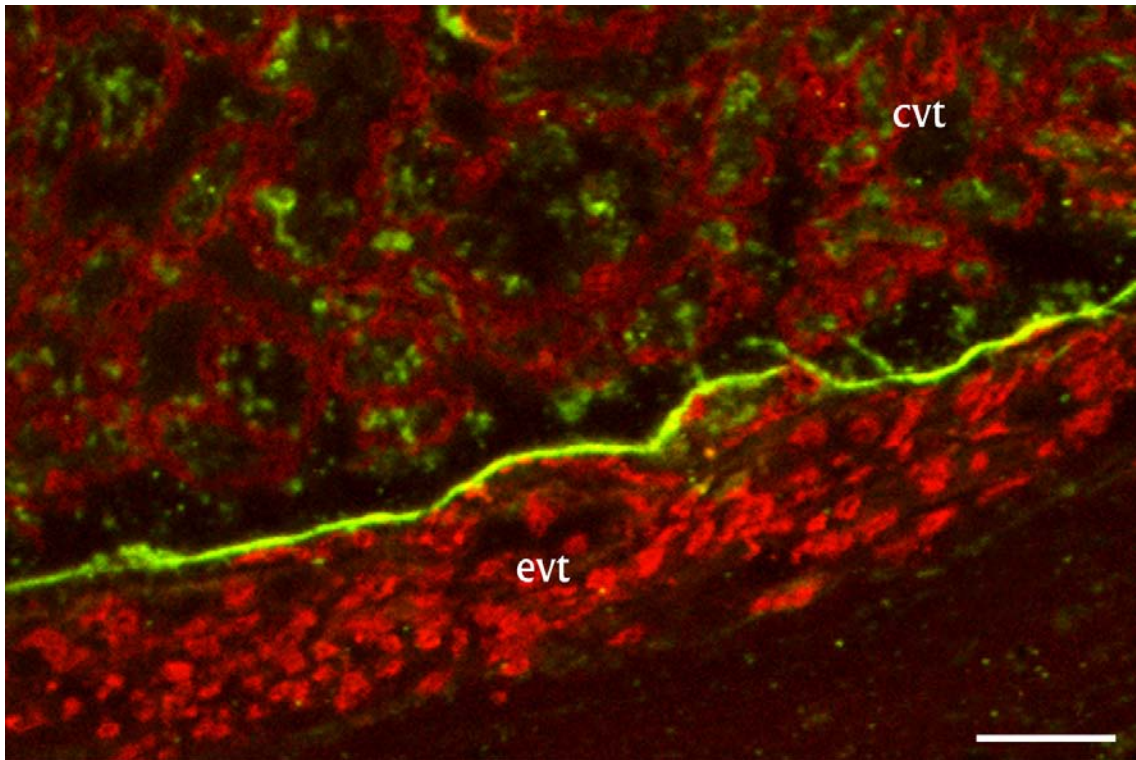


Figure 5.2.2 Anti- PECAM-1 and anti-pancytokeratin in normal basal plate

A section of healthy human placental basal plate. The intervillous space lining the basal plate was strongly positive for the endothelial cell marker PECAM-1 (green). A large proportion of this layer was shown to be endothelial. The trophoblast marker is anti-pancytokeratin and the staining in extravillous trophoblasts (evt) is considerably more intense than that seen in chorionic villous trophoblast (cvt). Scale bar = 100 μ m.

It was seen that the trophoblast and endothelium were continuous laterally and did not substantially overlap; where they do, the endothelial cells appear to overlie the syncytiotrophoblast (Figure 5.2.3).

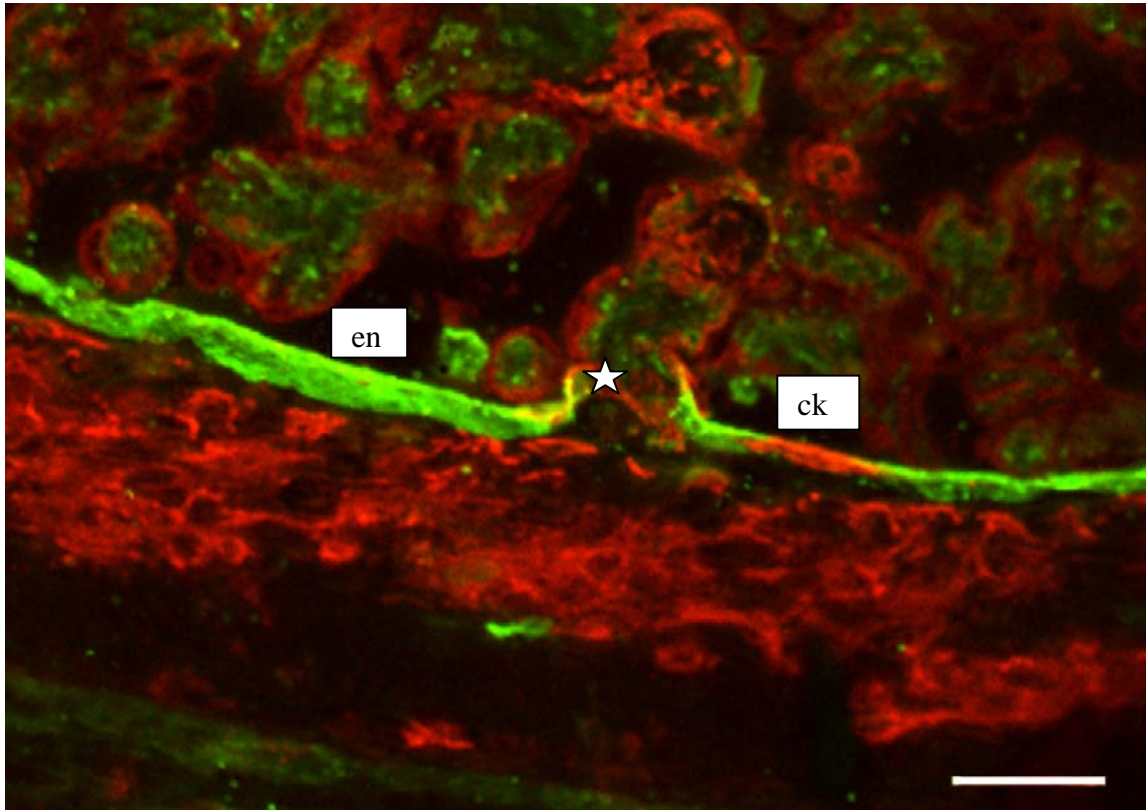


Figure 5.2.3 Anti-pancytokeratin and anti-PECAM-1 in the normal basal plate

In this cross-section of basal plate the anti-PECAM-1 (green) is seen to stain the endothelial cells lining the majority of the intervillous space (en). This layer is interrupted by a short section of pancytokeratin labelling (ck) close to the point of attachment of an anchoring villus (*). The oblique plane of this section makes the endothelial layer appear thicker than usual. Scale bar = 100 μ m.

Trophoblast-specific antibodies, such as anti-human chorionic gonadotrophin, were seen to bind to their expected target cells (villous and extravillous trophoblast) but there was also evidence that the protein was bound to other cells in the basal plate (perhaps by receptor-mediated adsorption), notably to the basal plate lining endothelium and the fibroblasts and smooth muscle cells associated with the media of maternal vessels resident at this site (Figure 5.2.4).

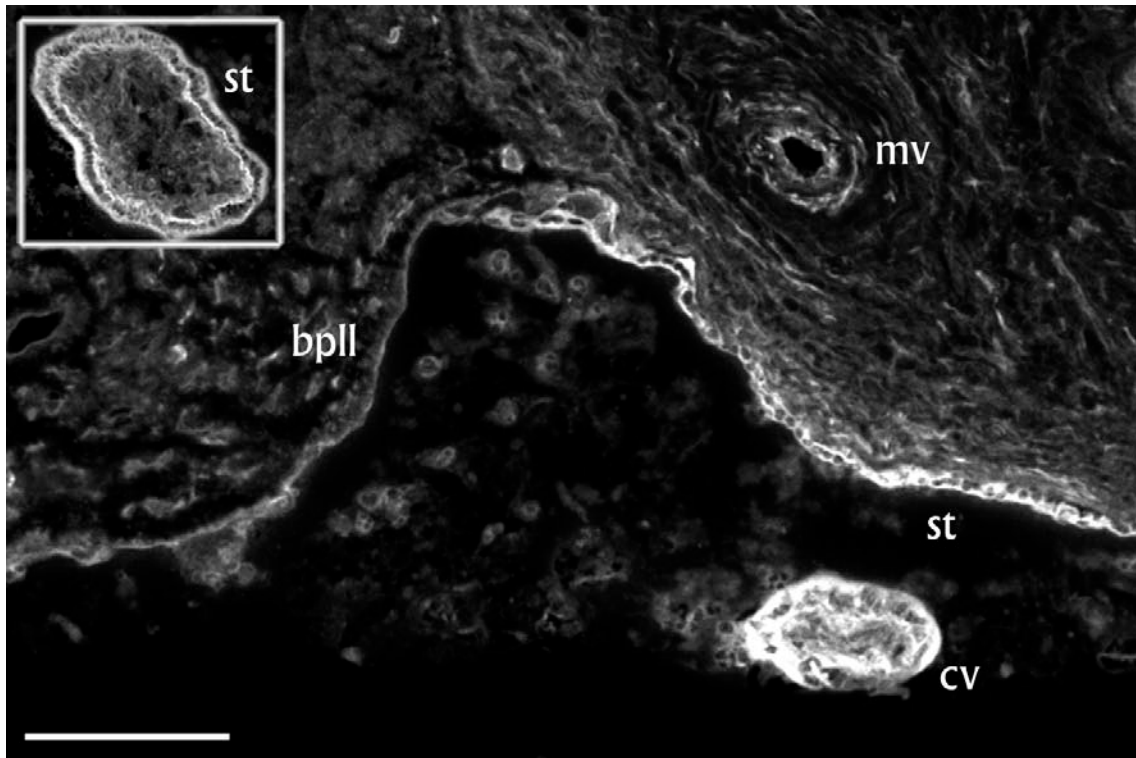


Figure 5.2.4 Anti-human chorionic gonadotrophin (hCG) in the normal basal plate

The epithelial (trophoblastic) component of the basal plate lining cells (st) exhibited strong immunoreactivity with the trophoblast marker anti-hCG. The thinner cellular lining layer to the left (bpll), however, had a faint, largely apical labelling pattern, possibly due to hCG being adsorbed from the blood. The obliquely sectioned villus (cv) and a trophoblast-lined maternal vessel (mv) were also positive for hCG. **Inset:** Cross-section through a terminal villus in the same section (though not in the field of the main image) shows anti-hCG staining the apical and basal surfaces of the syncytiotrophoblast contrasting with the less reactive villous core. Scale bar = 100µm.

5.3 Measurement of basal plate length percentages in healthy and pre-eclamptic placentae

Analysis of digital images of the basal plate lining (excluding anchoring villi) gave measured length ratios of endothelial: trophoblastic: other component (61% endothelium, 19% trophoblast, 20% other) in sections of healthy placenta (Fig. 5.3.1a and b). The other component probably consists of regions of fibrin deposition. The mean (61%) percentage length of healthy basal plate occupied by endothelium rises to 68% in the pre-eclamptic group. A statistically significant difference was demonstrated between the medians (67.4% and 71.7% Mann-Whitney Rank Sum test, $p = 0.033$) in the endothelial compartment in pre-eclampsia. Although this is the most appropriate test for significant difference between the two groups of measurements of this type, it applies only to medians and not to means. Since the isotropic uniform random (IUR) sampling procedures adopted allow this, the stereological sample of basal plate lining-length-percentages can be used as an estimate of the area percentages.

The key point to note in both Figures 5.3.1a and 5.3.1b (where these data are represented graphically) is the rise in the proportion of endothelium at the expense of trophoblast in the pre-eclamptic placentae in all but the earliest (34 week) placentae.

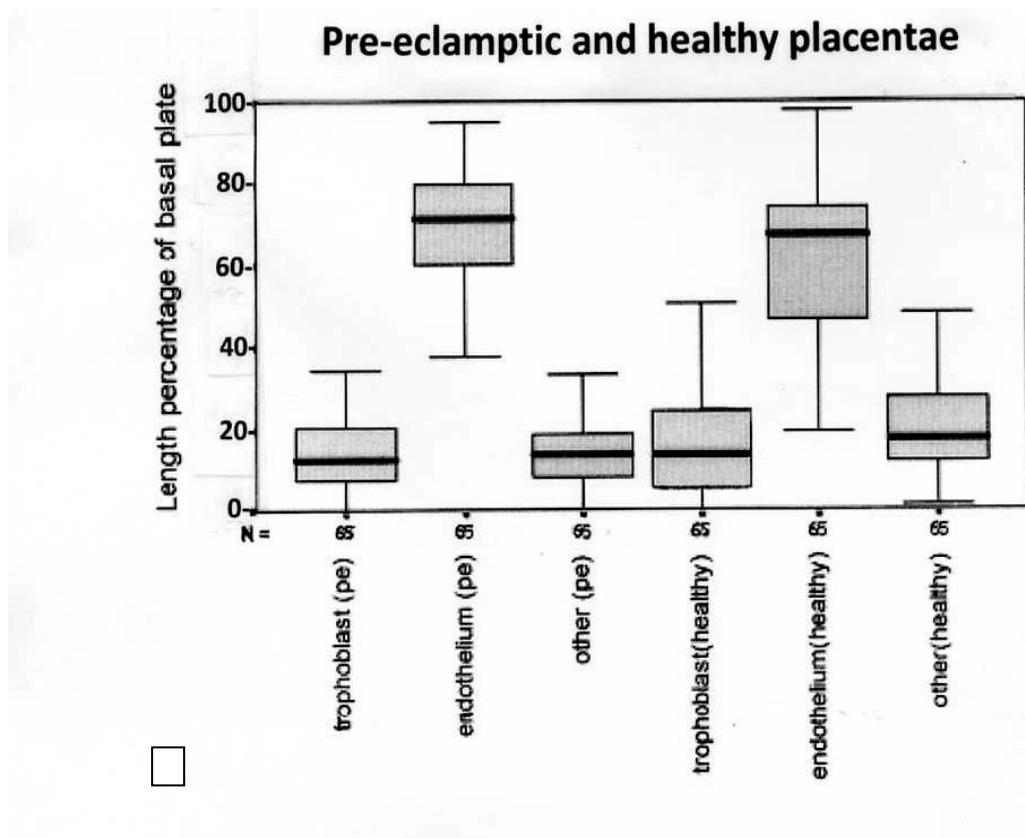


Figure 5.3.1a Analysis of the length percentage of the basal plate lining occupied by trophoblast, endothelium and other (acellular) material

Box plot showing the median (horizontal black bar) and inter-quartile range (grey boxes) of the length percentages of the sectioned basal plate. The differences in each of the areas in both healthy and pre-eclamptic placental basal plate intervillous space lining layer composed of endothelium, trophoblast, and other materials (e.g. fibrin/fibrinoid) are shown.

Healthy and preeclamptic placentae

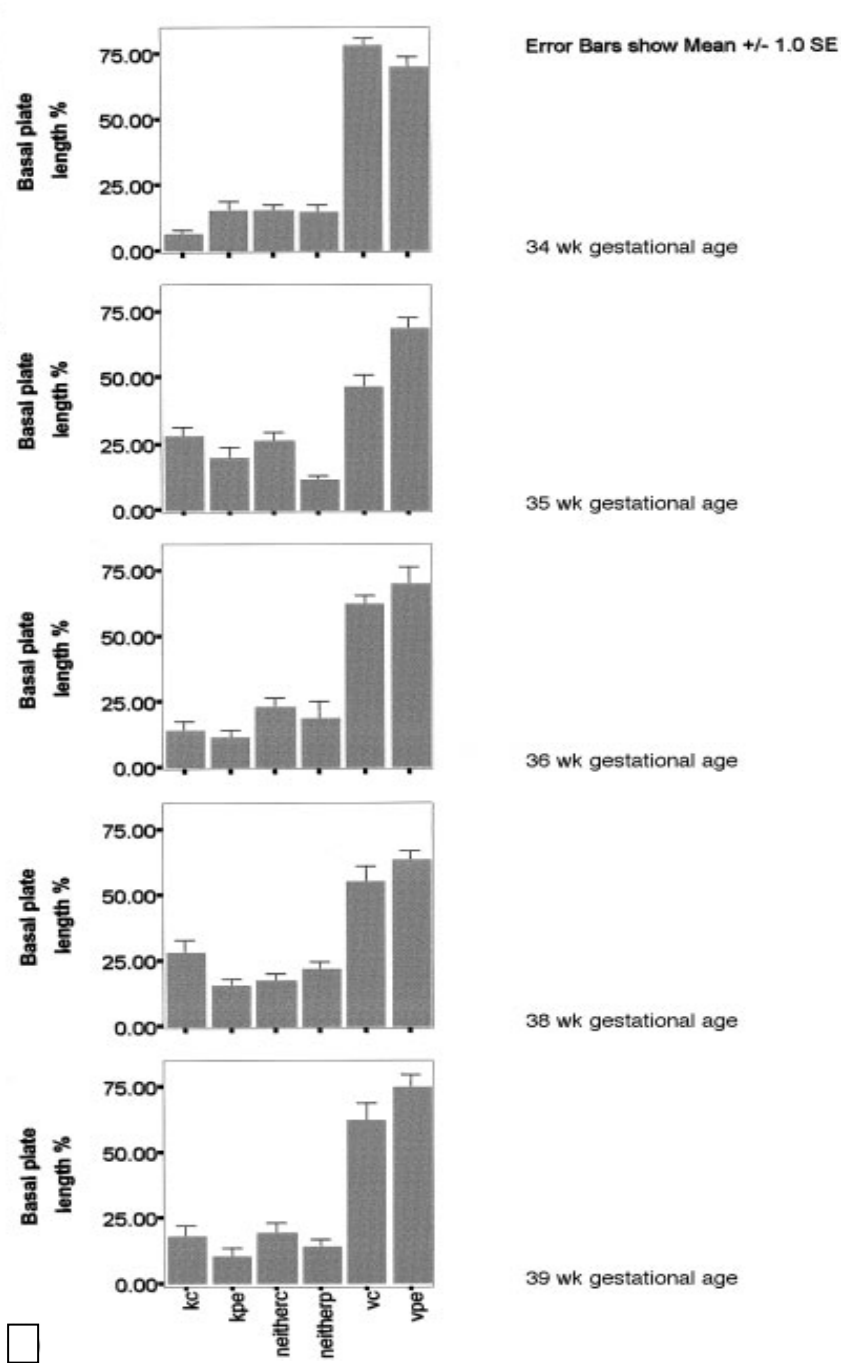


Figure 5.3.1b The same data as in Figure 5.3.1a, but segregated according to gestational age

kc = healthy placenta trophoblast; vc = healthy placenta endothelium; neither = other healthy placenta; kpe = preeclamptic trophoblast; vpe = pre-eclamptic endothelium; neither = other pre-eclamptic. No statistical gestational age-related trend was apparent in the differences between healthy and pre-eclamptic samples.

5.4 Discussion

5.4.1 The basal plate lining

The results shown earlier clearly identified the thin cellular boundary overlying the basal plate and lining the intervillous space to be composed of a mosaic of syncytiotrophoblast, endothelium and fibrin. This extended over the surface between the attachment points of anchoring villi (Chapters 3 and 4). The single cell layer could be divided into regions that labelled with antibodies identifying either endothelial-specific or trophoblast-specific markers, but crucially it was found that there was little overlap between the different cell types (Figures 5.2.2-5.2.4). The endothelial markers anti-caveolin-1, anti-platelet/endothelial cell adhesion molecule (PECAM-1), anti-vimentin, and anti-thrombomodulin all labelled the thinner endothelial part of the lining whereas trophoblast markers (anti-pancytokeratin, anti-human chorionic gonadotrophin (hCG), and anti-human placental lactogen (hPL)) consistently labelled areas with greater thickness and a more irregular surface.

As an internal control, chorionic villous capillary endothelium and villous syncytiotrophoblast (the lineage of which is beyond dispute) were positively stained with the appropriate markers and there was no significant cross-reactivity (Figure 5.2.1). Dual-channel confocal images (the images from the separate channels can be merged electronically by the confocal microscope's software) revealed continuity between the trophoblast and endothelial marker-labelled regions of the single cell layer. Where the layer was discontinuous, it appeared acellular. Unpublished experiments using anti-fibrin/fibrinogen markers have indicated that these are fibrin-rich "patches" of the basal plate.

5.4.2 Markers defining heterogeneity

Antibodies specific for endothelial markers (e.g. anti-von Willebrand factor and anti-PECAM-1) consistently bound to villous endothelium, uterine vessel endothelium and to endothelial-like parts of the basal plate lining but did not label villous or basal plate lining syncytiotrophoblast (Figures 5.2.1–5.2.3). Antibodies raised against the trophoblast marker pancytokeratin invariably labelled the chorionic villous and basal plate trophoblast but not the chorionic capillary endothelium nor the endothelium lining the basal plate (Figure 5.2.1 – 5.2.3).

5.4.3 Anchoring villi

Chorionic villi at term are mainly tertiary villi with an epithelial syncytiotrophoblast covering and an entirely mesenchymally derived core containing (foetal) fibroblasts, capillary endothelial cells and macrophages. This is reflected in the patterns of vimentin and cytokeratin antibody binding (Ockleford et al., 1981, 1984, 1990, 1993; Ockleford, 1990). This pattern is disturbed at the points of attachment that connect some villi to the basal plate. Such “anchoring villi” display trophoblastic antibody staining characteristics in a solid core of cytotrophoblast cells close to the basal plate. These cells exhibit the bright immunofluorescent anti-cytokeratin characteristic of the extravillous trophoblast and differ from the relatively less intense staining observed in the chorionic villus covering syncytiotrophoblast (Ockleford et al., 2004) (Figures 5.2.2 and 5.2.3).

5.4.4 Endothelial and trophoblast markers in pre-eclamptic tissue

The immunofluorescence patterns obtained with the endothelial- and trophoblast-specific antibodies were qualitatively similar in both healthy and pre-eclamptic tissue

samples. The fact that the basal plate lining is a heterogeneous mosaic of cells that may produce different secretions raises the possibility that the proportion of the different cell types varies in pre-eclampsia from that seen in healthy placentae. Whilst these morphometric studies have focussed on antibody markers which identify and differentiate between trophoblast and endothelium in normal and pre-eclamptic placentae, the patterns of staining (i.e. the area percent occupied by endothelium) may possibly reflect changes in the pattern of secreted hormonal-like factors which have profound effects on local blood pressure in this location.

5.4.5 Heterogeneity of cell types contributing to the basal plate lining

The findings described here demonstrate that the layer lining the intervillous space is a simple (unicellular) mosaic consisting of endothelium and trophoblast; this corroborates the findings described in Chapters 2 and 3 (Byrne et al., 1998, 2001). This layer is of mixed foetal and maternal origin (Byrne et al., 2010; Chapter 6) and reacts with the marker antibodies used in this study as expected of a layer of mixed mesenchymal and ectodermal embryonic origin, both in healthy and pre-eclamptic placentae. The present chapter presents quantitative data revealing the extent of endothelium and trophoblast. These data exclude the possibility that endothelium is a rare component or one only found immediately adjacent to vessel entry and exit points. The foetal trophoblast must meet side-by-side with maternal endothelium at some point and this report shows where this occurs and what the mean relative contributions to this lining layer are (61% endothelium, 19% trophoblast, 20% other) in healthy placenta. The interpretation of the basal plate lining morphology is thus intermediate between the “all trophoblast” view still portrayed in some embryology textbooks and the alternative extreme view of Wanner (1966), that apart from anchoring villus attachment sites, this is “all

endothelial.” This alternative view is based not only on the length quantitation of endothelial/ trophoblast marker studies described in this chapter, but also on semi-thin section histology, scanning and transmission electron microscopy from data described in earlier studies (Byrne et al., 1998, 2001; Lang et al., 1993).

5.4.6 Basal plate composition changes in pre-eclampsia

The most important conclusion with regard to pre-eclampsia is that there is an increase in the endothelium component of the intervillous space/basal plate lining layer (61% rises to 68%, $p = 0.033$ of the medians) at the expense of trophoblast (19% drops to 15.5%). The residual acellular fibrinoid-covered areas constitute a further proportion of the total in both healthy and pre-eclamptic gestations (20% and 17%).

A number of hormonal-like molecules synthesised by endothelial cells affect vascular physiology and this has been seen as a major feature of pre-eclamptic pathophysiology (Bosio et al., 1999; Carter and Charnock-Jones, 2001; Dekker and Sibai, 1998; Lyall and Myatt, 2002; Roberts et al., 1995; Walker, 2000). These include prostacyclin (a vasodilator and inhibitor of platelet aggregation); endothelial nitric oxide synthase (eNOS) and its product nitric oxide (a vasodilator and inhibitor of platelet adhesion and aggregation); haemoxygenase and its product carbon monoxide (a vasodilator and inhibitor of platelet aggregation); tissue plasminogen activator (tPA), an activator of fibrinolysis in blood vessels and amniotic fluid; thrombomodulin (an anticoagulant); thromboplastin (a promoter of blood coagulation); platelet activating factor (activation of platelets and neutrophils); and von Willebrand factor (promoter of platelet adhesion and activator of blood coagulation).

In the light of the data presented, it is proposed that an increase in the proportion of non-proliferative endothelium at the materno-foetal interface in pre-eclampsia may contribute to hypertensive changes in vascular physiology mediated by endothelial signalling. Signalling interactions subtended by caveolin platforms may prove to be an important aspect of the development of our understanding of the placental pathology of this condition.

5.4.7 Developmental aspects of pre-eclampsia

Identification of the cause of pre-eclampsia will require further data. There are genetic and immunological dimensions to the disease indicating paternal imprinting and partner change effects, respectively, on incidence (Moffett-King, 2002). These are as yet unlinked to the present findings.

There are likely to be genetic aspects to the predisposition to preeclampsia and environmental triggers such as paternal antigenicity that release these. To reproductive endocrinologists, the influence of the steroid hormones oestrogen and progesterone on the signalling systems operative is of great interest. The nuclear translocation processes of receptor- bound oestrogen and the control and activation of caveolar platforms indicate that this is a disease with many potential levels of control and signalling pathways to be explored.

An interesting feature of the disease is its progressive nature with symptoms worsening as pregnancy progresses through the second and third trimester and, ultimately, with more severe cases presenting earlier than the mild cases. In this respect, the role of endothelial caveolin-1 may be relevant (Lala and Desoye, 2001; Liu et al., 1999;

Ramirez et al., 2002). This protein is available to meet its caveolar cell-signalling role in the non-proliferative endothelial cell but sequestered in the cleavage furrow zone of the dividing (proliferative) cells. The greater area percent at term in pre-eclamptic patients indicates a greater population of endothelial cells. Whilst this population is expanding, its effect on blood pressure will be held in check as signalling platforms will be disassembled. Only later, once quiescent, will the down-regulation of, e.g., NOS, feed through to affect blood pressure. The improvement in maternal health following parturition is understandable given the model presented here as the basal plate is expelled during the third stage of labour.

Any complete explanation of the cause of the disease will need to include a reason for the cytokeratin-based cytoskeletal aspects described recently (Ockleford et al., 2004, Ahenkorah et al., 2008). These observations are a useful step in understanding how alterations in the developmental programme of transcription (Beck et al., 1995; Knöfler et al., 2001) lead to the implantation deficits typical of pre-eclampsia. Structural, anchorage failure or motility deficits could all explain features of the pathology such as shallow implantation, and the change in the endothelium: trophoblast area ratio in the basal plate lining-layer described here.

Chapter Six

A cytogenetic study of cells at the maternal/foetal interface of the basal plate, to establish their derivation

6.1 Introduction

The basal lining of the intervillous space is histologically unique. Its simple epithelial (single-cell thick) tissue layer is formed as a *mosaic* of two types of cells. It was established that one type was a trophoblastic (foetal) epithelial derivative and the other was an endothelium derived from the mesenchymal lineage (Byrne et al., 2001; Byrne et al., 2003; Ockleford et al., 2003; Smith et al., 2004). To test the possibility that this mosaic was made up of cells from different individuals (foetus and mother), an *in situ* hybridisation study was performed using a human Y-chromosome-specific probe on basal plate tissues from placentae obtained following the birth of children of *known gender*.

In situ hybridisation (ISH), in this context, is based on Southern hybridisation (Southern, 1975), where DNA is hybridised to a labelled synthetic DNA probe which is complementary to the DNA of interest (a cDNA probe). In Southern's original work, the DNA was extracted from cells, electrophoresed in an agarose gel and transferred to a nitrocellulose membrane. In ISH, the same principles apply, only in this case the DNA remains within the nuclei of tissues which have been sectioned and picked up on a glass slides.

The probe used in this study was derived from a tandemly repeated, α -satellite DNA from the untranslated region of the human Y-chromosome, first discovered by Cooke

(Cooke et al., 1978). This sequence, designated pHY2.1, is located at Yq2.1 on this chromosome. Although this sequence is also located on at least half of the autosomal chromosomes in humans, the copy number of the tandem repeats in these other locations is negligibly small when compared to the 2000+ copies found on the Y-chromosome.

This piece of DNA carries two sites for the restriction endonuclease Msp-1 (CCGG); this allowed it to be inserted into the plasmid pBR328 and it was in this form that the potential probe was presented. The plasmid was grown up in its host *E.coli* and was then restriction digested with the same enzyme to release the template DNA. This was then gel purified from an agarose gel prior to being labelled. The labelling reaction involved the use of the Klenow 'large fragment' *E.coli* DNA polymerase. This enzyme, in the presence of random hexanucleotide primers will copy the template DNA; inclusion of a labelled nucleotide in the substrate mixture allows a labelled probe to be synthesised. The mechanism is illustrated in Figure 6.1.1.

The labelled nucleotide used in this study was DNP-11 dUTP, where dUTP is labelled with dinitrophenol (DNP), with an eleven carbon-atom spacer between the nucleotide and the label. This spacer ensures that the label molecule does not interfere with the incorporation of the nucleotide into the nascent DNA chain; it also allows better access for the antibody during its subsequent detection. Although dUTP is not a normal nucleotide substrate for the DNA polymerase, it is nevertheless incorporated into the cDNA probe with adequate efficiency. Dinitrophenol, like the other more commonly-used non-radioactive label, digoxigenin, is a molecule which does not occur naturally in mammals; indeed both are potentially toxic; they share the property of being very immunogenic, which is why they are useful as reporters in genetic studies.

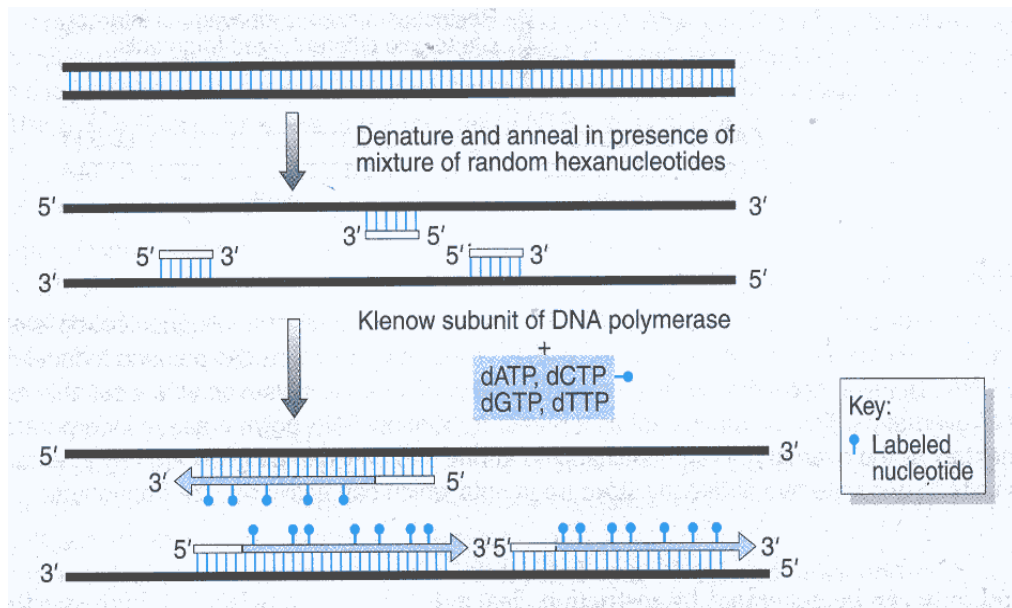


Figure 6.1.1 Diagram illustrating c-DNA probe synthesis

Denaturation of the template at high temperature causes the two strands of the template DNA to separate. This allows the random hexanucleotides to anneal to both strands when the temperature is lowered. These small duplexes are the recognition sites for the polymerase and it is from these sites that the synthesis of *de novo* complementary DNA (cDNA) is initiated. (This image from Strachan and Read, *Human Molecular Genetics* 2nd Edition, 1999 page 67).

Many placentologists formerly thought that the lining of the basal plate (i.e. the cells which form a barrier between the *decidua basalis* and the maternal blood space) was of foetal origin and consisted only of syncytiotrophoblast (Boyd and Hamilton, 1970). Though this is true for *parts* of this lining, it is certainly not true for all of it. It seems likely that earlier investigators simply did not look carefully enough at this layer. The morphology of parts of this lining are so different from syncytiotrophoblast that it is puzzling why these investigators chose to ignore it. In those parts of the lining adjacent to anchoring villi, syncytiotrophoblast is seen to spread out like the bark of a tree at its root. Where there are many anchoring villi, the parts of the lining layer which are trophoblastic may become the majority; conversely, where anchoring villi are sparse, most of the intervening surface may be invested with fibrin or the endothelial cell layer.

Although the work of Wanner (Wanner, 1966) pre-dates that of Boyd and Hamilton, these latter authors, though aware of its existence, chose not to investigate it further. Wanner not only described this endothelial layer, but went so far as to state, based on Barr-body staining, that it was of maternal origin. Barr bodies are only normally found in interphase female nuclei, and are thought to be an unusual sub-domain of these nuclei, which represents their inactivated ('Lyonised') second X-chromosome. This condensed chromatin, which lies close to the nuclear envelope, takes up slightly more stain than the rest of the nucleus and appears as a darker patch. The quality of the illustration of Wanner's work was far from compelling and the fact that this paper was published exclusively in German may have hampered its acceptance by the wider scientific community.

Stark and Kaufmann (1971, 1973) had suggested that the lining cells of the basal plate were all of trophoblastic origin, regardless of their morphology. Later research by

Nikolov and Schiebler (Nikolov and Schiebler, 1973), again published only in German, indicated the close association between trophoblasts and endothelium, particularly at the openings of the maternal spiral arteries. The overlapping of the two cell types at these places was demonstrated using transmission electron microscopy.

Using a panel of endothelial cell marker antibodies, Lang et al. (1993) were able to demonstrate a marked phenotypic heterogeneity in both foetal and maternal endothelial cells. The basal plate lining endothelium, which she refers to as “residual cells” is strongly reactive with many of these markers, which led her to favour an endothelial, rather than a trophoblastic lineage for these cells.

Chapters 3 and 4 of this thesis mapped the distribution of caveolin-1 in all parts of the human term placenta and drew attention to an unexpectedly strong immunoreactivity to the antibody over much of the maternal blood space lining adjacent to the basal plate. Further investigations of this area, using transmission and scanning electron microscopy, as well as immunocytochemistry, led to the conclusion that much of this layer was indeed endothelial, or at least had an endothelial phenotype. It was also shown in Chapter 3 that junctions existed between these endothelial cells and neighbouring syncytiotrophoblast, though this observation was not examined in further detail. In order to establish whether these cells were of foetal or maternal derivation, a Y-chromosome specific probe was used, in an *in situ* hybridisation context, on sectioned material of the placentae from neonates of known gender. The dinitrophenol-labelled dUTP used to synthesise the probes was located by a rabbit anti-dinitrophenyl primary antibody; a goat anti-rabbit IgG horseradish peroxidase (HRP)-conjugated secondary antibody allowed the label to be visualised in the sectioned material. The

conjugated HRP, in the presence of hydrogen peroxide (and nickel ions) catalyses the oxidation of the almost colourless substrate diaminobenzidine (DAB) to an insoluble black product. For counterstaining, in Figures 6.2.1- 6.2.8, Kirkpatrick's carmalum was used, without acid differentiation.

6.2 Results from the cytogenetic study

The first step in this series of experiments was to demonstrate that the probe binds in a specific manner and that the post-hybridisation washes were of adequate stringency. This latter was achieved by probing the placentae from pregnancies that produced a female baby. In such cases there should be no evidence of any hybridisation, as no Y-chromosomes are expected to be present. The absence of hybridisation signal in the negative control, (which was from a female child's placenta) confirmed that the probe did not bind in a non-specific manner and that the stringency of the post-hybridisation washes was adequate (Figure 6.2.1).

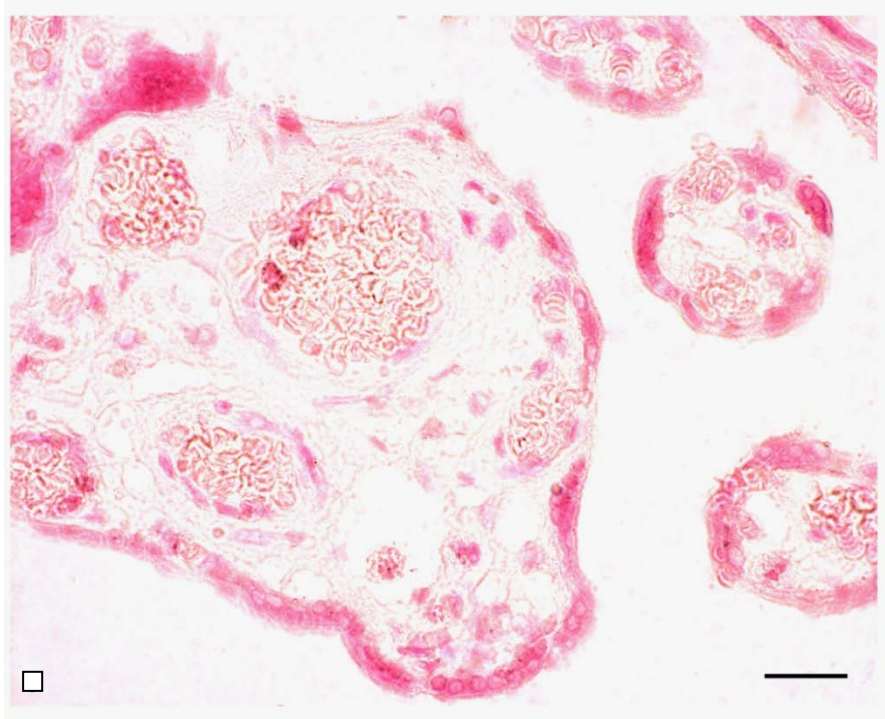


Figure 6.2.1 Negative control.

This placenta, from a *female* baby, failed to show any hybridisation of the Y-chromosome-specific probe to nuclei in the chorionic villi of this placenta. The trophoblast, endothelial cells and mesenchymal cells in this region are *all* unlabelled. Scale bar = 20µm.

Where the placentae from pregnancies that produced a male baby were probed, it became clear that most nuclei of foetal origin were labelled by the Y-chromosome probe. This showed that the probe was specific to male (Y-chromosome bearing) nuclei (Figures 6.2.2 et seq.). Erythrocytes both in the maternal blood space and in villous capillaries appeared brown, due to the residual endogenous peroxidase activity of these cells, despite attempts to quench this during processing (Figures 6.2.2, 6.2.3, 6.2.6 and 6.2.7).

The endothelial lining of the basal plate was consistently negative (Figure 6.2.2) when challenged with the Y-chromosome probe.

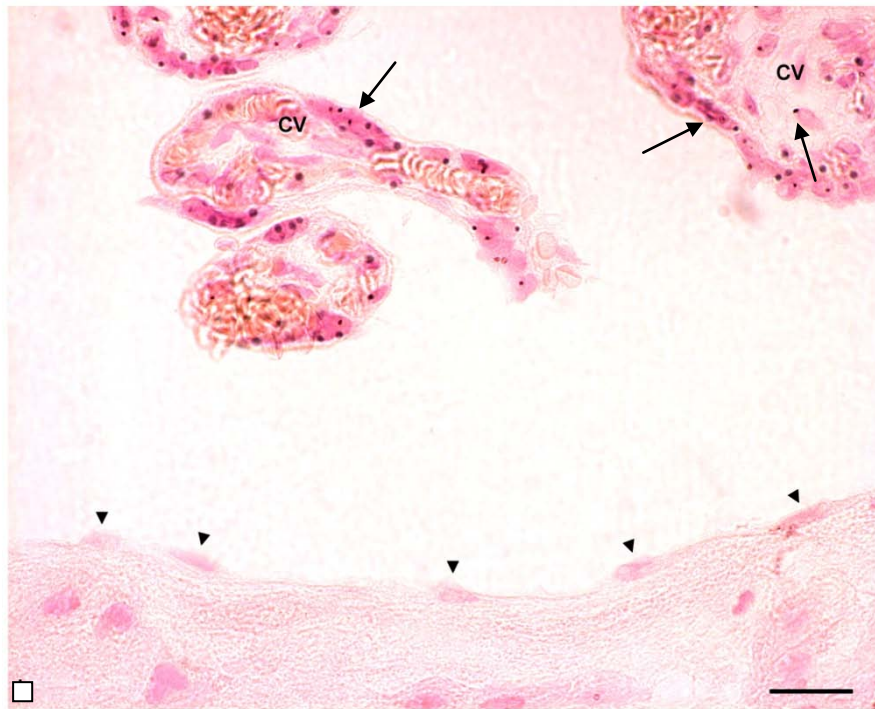


Figure 6.2.2 Absence of labelling in basal plate lining cells: labelling in villous trophoblasts.

In situ hybridisation (ISH) of the Y-chromosome specific probe to nuclei in the basal plate region was revealed by the dark dots within the *male* nuclei (arrows) in this placental tissue obtained following the birth of a male baby. A high labelling efficiency of the trophoblastic and mesenchymal cells of the chorionic villi (cv) in the upper part of the field was shown. The endothelial cells lining the basal plate in this region were unlabelled (arrowheads) as were the underlying decidual (maternally-derived) nuclei. Scale bar = 20 μ m.



Figure 6.2.3 Labelling of trophoblast and mesenchymal cells in chorionic villi

Hybridisation of the Y-chromosome-specific probe to nuclei in the basal plate region is revealed by the dark dots overlying the male nuclei in this placental tissue obtained following the birth of a *male* baby. There is a high labelling efficiency of the trophoblastic and mesenchymal cells of the chorionic villi in the upper and right part of the field. The endothelial cell nuclei lining the basal plate in this region are unlabelled (arrowhead) whereas the nuclei of the trophoblast continuous with this layer at the anchoring villus (top left) *are* labelled (arrow). (evt) represents labelled extravillous trophoblast. Unlabelled are the decidual nuclei, the foetal and maternal erythrocytes
Scale bar = 20 μ m.

In placentae from male babies, wherever foetally derived cells were examined, there was a strong chance (70% or more in most cases) that they would be labelled. This was very obvious in sections of chorionic villi (Figures 6.2.2 and 6.2.3). Within the basal plate, however, there is a mixed population of cells; the extravillous trophoblasts are foetally derived while the decidual cells and fibroblasts are maternal. This was reflected in the pattern of labelling in this tissue when it was subjected to Y-chromosome in situ hybridisation (Figure 6.2.4).

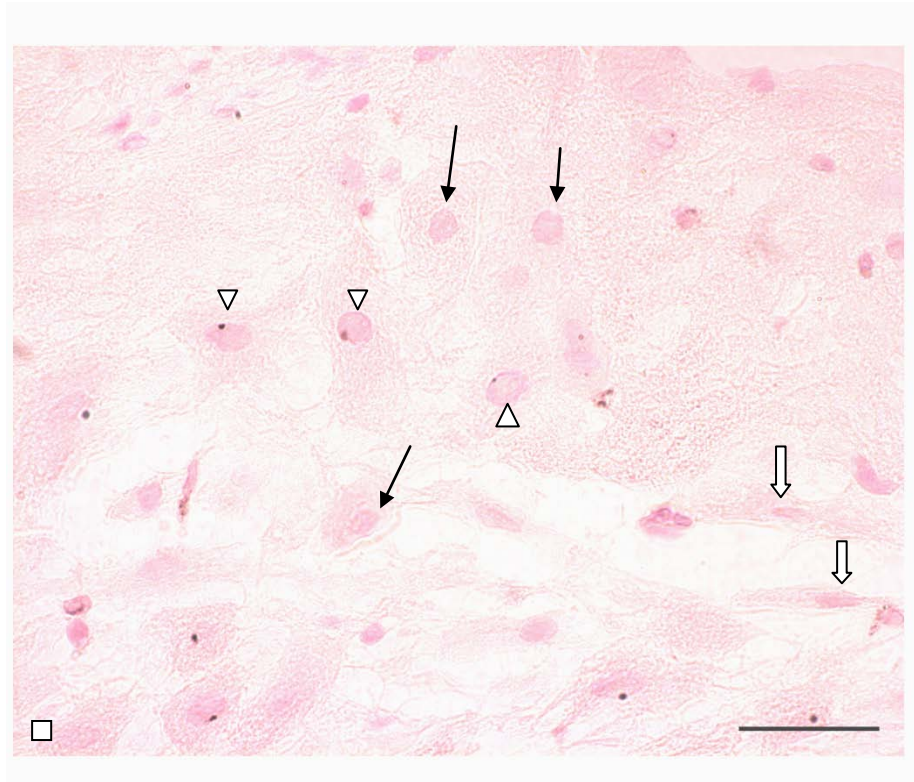


Figure 6.2.4 Extravillous trophoblast labelling within in the basal plate.

ISH of the decidual layer of the basal plate shows labelling of the extravillous trophoblast that has penetrated this layer (white arrowheads) but *not* of the resident decidual cells (black arrows) or fibroblasts (white arrows), which are genetically maternal. Scale bar = 20 μ m.



Figure 6.2.5 Absence of labelling in basal plate lining endothelial cells

ISH of the decidual layer of the basal plate shows labelling of the extravillous trophoblasts (arrows) that have penetrated this layer but not of the endothelial cells comprising the *lining* layer of the intervillous space (ivs). These, being unlabelled (arrowheads), are genetically maternal. Scale bar = 20 μ m.

It was important to check that the villous capillary endothelial cells were labelled, otherwise a lack of labelling in the basal plate lining endothelium might have been construed as a morphological feature peculiar to these squamous cells. Figure 6.2.6 showed that this was clearly not the case, as these villous endothelial cells were labelled with the same efficiency as the other foetally derived cells.

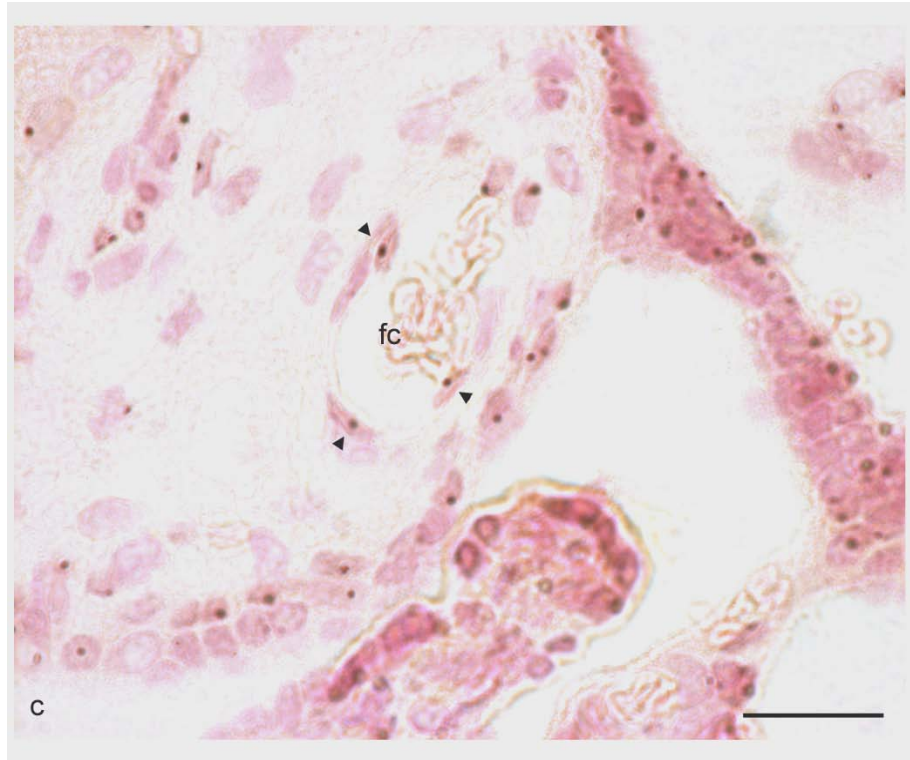


Figure 6.2.6 Labelling of endothelial cells in villous capillaries

In situ hybridisation of this villous region of a male child's placenta reveals a *foetal* capillary (fc) containing erythrocytes. These capillary endothelial cells *are* labelled (arrowheads). Scale bar = 20 μ m.

The syncytial covering of the anchoring villi was sometimes seen to continue for a small distance across the surface of the basal plate at its insertion. The endothelial lining was often seen to abut directly onto the syncytium. Whereas the syncytium was always labelled, the adjacent endothelium remained unlabelled. This is illustrated in Figure 6.2.7.

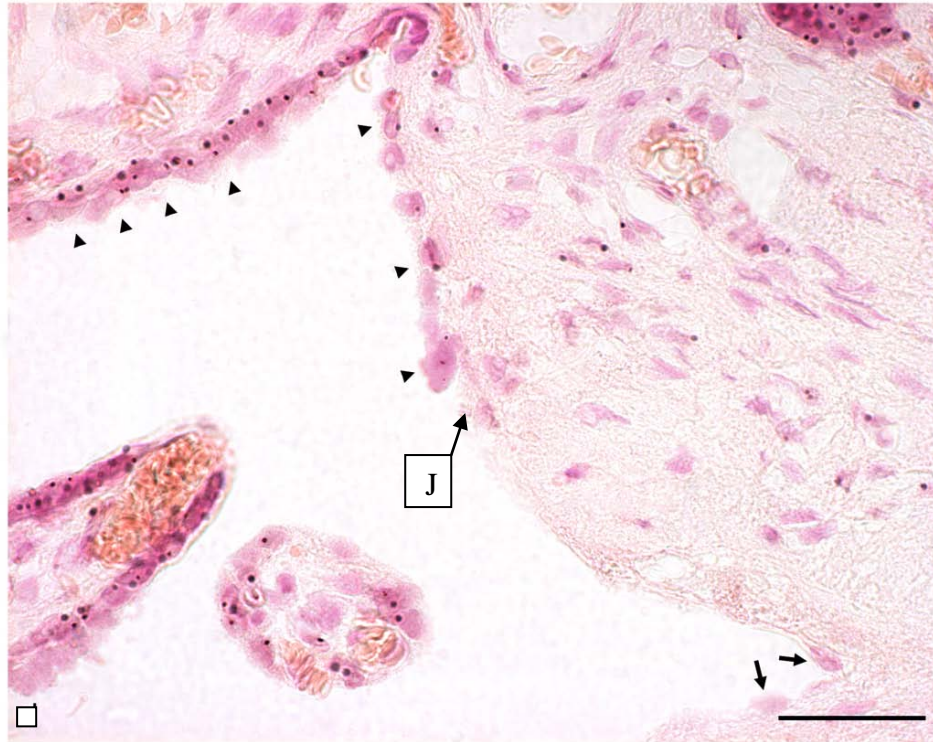


Figure 6.2.7 Junction between lining trophoblasts and endothelial cells.

This section shows a junctional region (J) in the single-cell thick layer lining the intervillous space at the basal plate. The upper part of the lining in this image is trophoblast (of foetally genetic origin), which is heavily labelled with the Y-chromosome probe (arrowheads). The nuclei of the endothelial part of the lining (bottom right) are unlabelled and therefore of maternal origin (arrows). Scale bar = 20 μ m.

Within the body of the basal plate, mononucleate interphase cells were sometimes seen to possess two hybridisation signals within the same nucleus. These cells often occurred in clusters (though always separated from their neighbours by some small distance) and were understood to be trophoblast giant cells, which have long been thought to be polyploidy. A representative sample of these cells is shown in Figure 6.2.8.

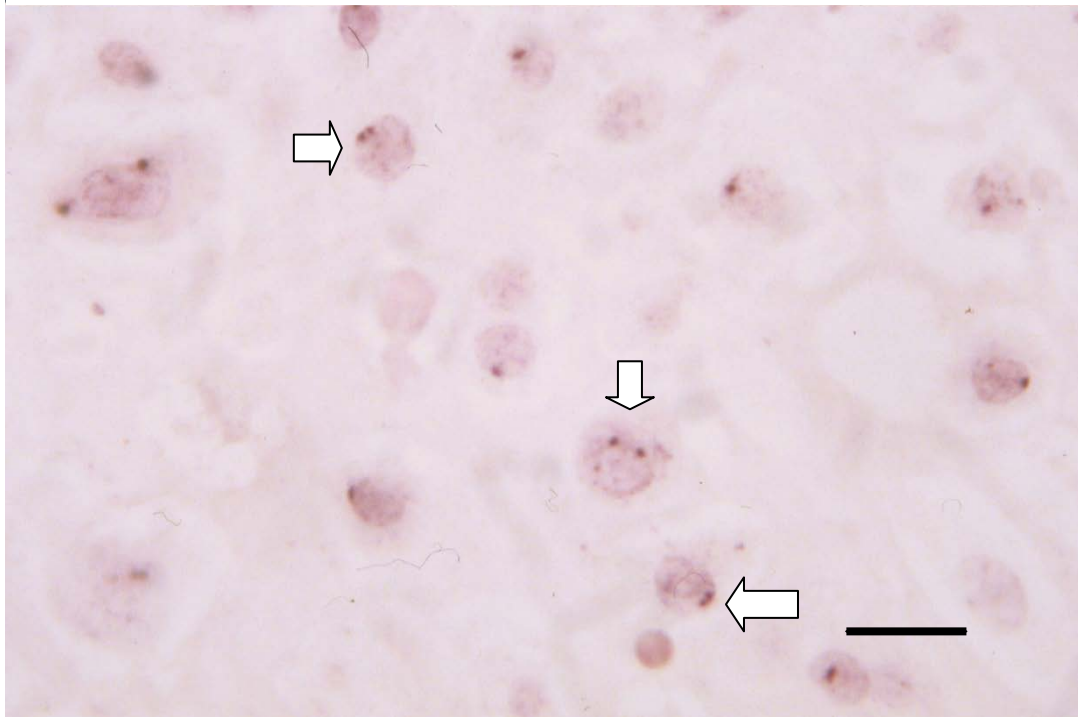


Figure 6.2.8 Polyplloid cells in the basal plate

Trophoblast giant cells were occasionally seen in small clusters among the decidual cells and extravillous trophoblasts of the basal plate. These cells, though mononucleate, showed clear evidence of possessing 2 Y-chromosomes (white arrows). Scale bar = 10 μ m.

The image in figure 6.2.9 is a true-colour film image from an epifluorescence microscope and *not* from a CLSM. The latter instrument possesses a monochrome detector only, so the wavelength (and thus the colour) of the detected fluorescence emission cannot be discerned, only its *intensity*. The false-colour images from the CLSM are generated by the use of 'look-up' tables which ascribe false colours (on a sliding scale) to pixels of a given intensity in the range 1-255 (zero – maximum saturation); these may be confused with true colour images by those unaware of this facility.

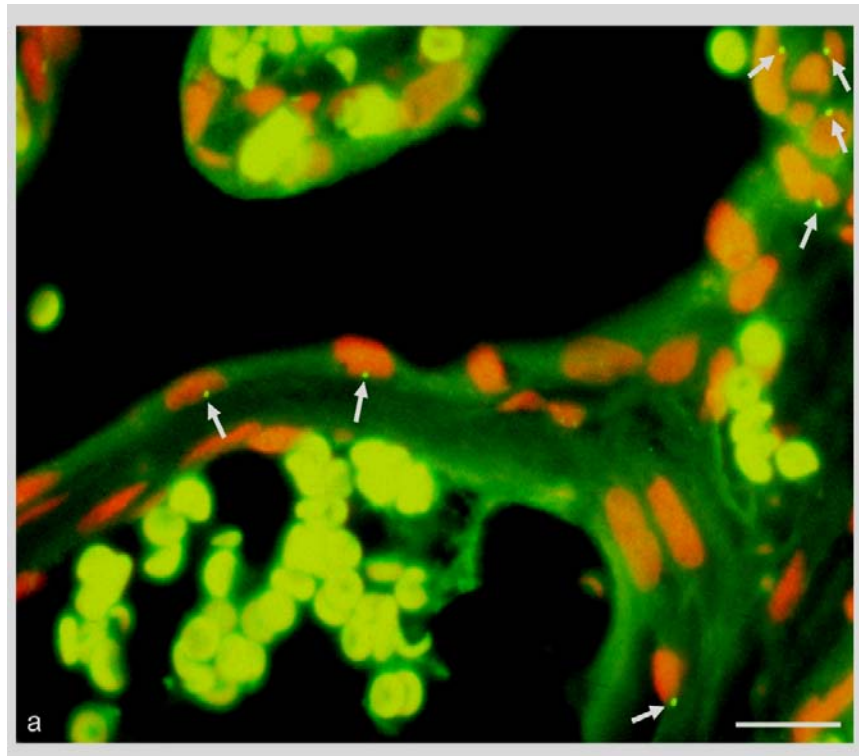


Figure 6.2.9 Fluorescence *in situ* hybridisation (FISH) using a Y-chromosome-specific probe

This placenta is from the birth of a male child and some of the chorionic villous nuclei (containing a Y-chromosome) are labelled with bright green dots (arrows). Erythrocyte autofluorescence is yellow-green; non-specific cytoplasmic autofluorescence is dark green; nuclear label is orange (propidium iodide); Y-chromosomes label green with FITC-conjugated mouse anti-rabbit IgG. Scale bar = 20 μ m.

A total of 500 nuclei from each of five different cell types were scored for the presence or absence of a positive hybridisation signal. The cell types were villous endothelium, villous trophoblast, villous stromal cells (mesenchymal fibroblasts and Hofbauer cells), basal plate lining endothelium and cells from within the basal plate (= basal plate “other”); these latter consisted of both the maternal decidual cells and fibroblasts, as well as the foetally derived extravillous trophoblasts. These data were tabulated as percentages of nuclei giving a positive signal and are presented graphically in Figure 6.2.10.

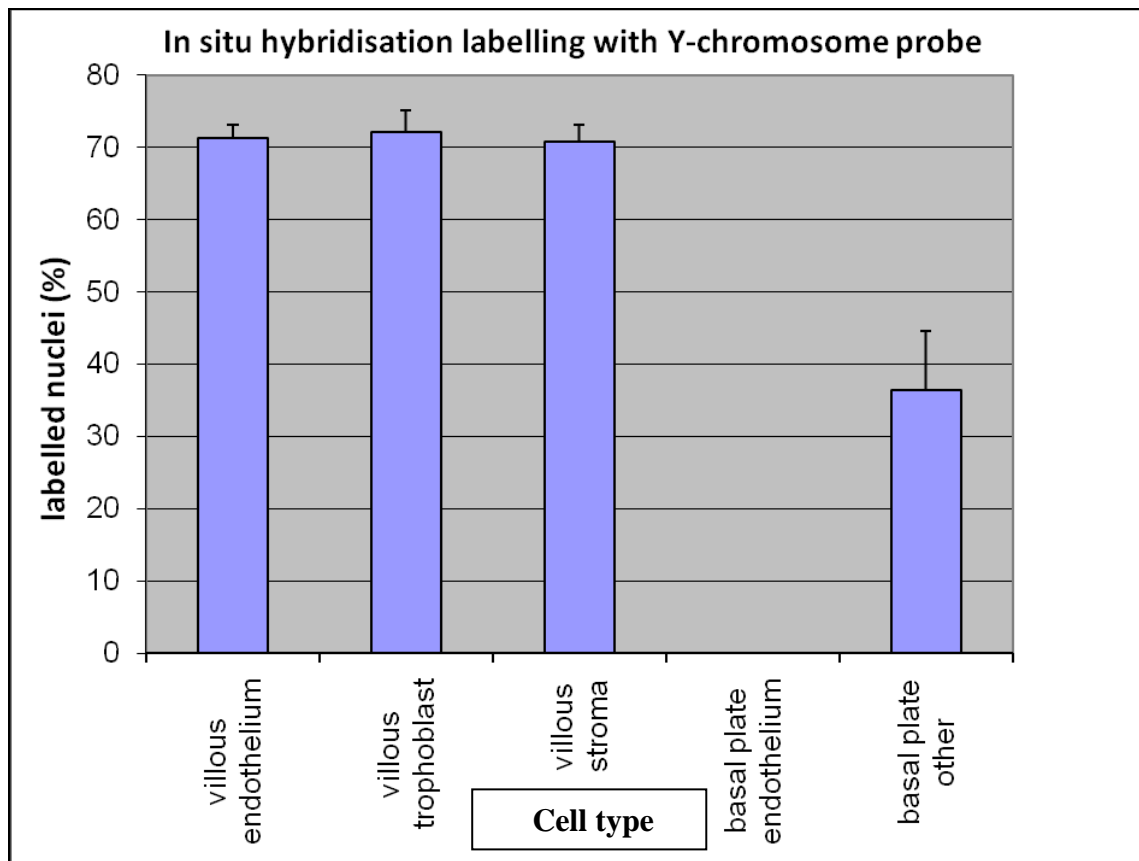


Figure 6.2.10 This bar chart shows the mean labelled (with Y-chromosome probe) nuclear counts from 10 healthy placentae from male babies. The error bars show the standard deviations of the counts. For each of the cell types $n = 500$ nuclei were scored for the presence of a positive hybridisation signal. Test and confidence intervals for one proportion test of $p = 0.5$ versus $p \neq 0.5$ reveals that $p < 0.0005$ for all cell types except basal plate trophoblast, where $p = 0.011$.

6.3 Summary of Results from the Y-chromosome Cytogenetic study

- The Y-chromosome probe showed a high labelling efficiency (>70% in most instances) to sectioned nuclei known to be derived from male babies.
- The probe failed to hybridise to *any* sectioned nuclei known to be from female babies.
- Endothelial cells *lining the basal plate* were consistently negative in placentae from births of *male* babies.
- Syncytiotrophoblast lining the basal plate was consistently positive in these same placentae.
- Villus endothelial cells from these placentae were also consistently positive.
- Extravillous trophoblasts resident in the basal plate of placentae from male babies were positive.
- A small proportion of these extravillous trophoblasts were seen to have two separate hybridisation signals within the same interphase nucleus, suggesting polyploidy.

6.4 Discussion.

The nuclear labelling frequency with the Y-chromosomes in the $\sim 7\mu\text{m}$ frozen section was lower than in the $10\mu\text{m}$ paraffin sections of other male baby placentae. With samples so thin, the Y-chromosome label appears in only some 40% of nuclear profiles. In earlier experiments, using wax sections of thicknesses varying between $4\mu\text{m}$ and $15\mu\text{m}$, the labelling efficiency was tested (results not shown); a compromise was reached between those sections which were too thick ($>10\mu\text{m}$) to allow clear photomicrography, due to depth-of-focus considerations and those thinner sections ($<10\mu\text{m}$) which did not sample a sufficient *volume* of the nuclei resident in the section. The hybridisation site itself occupies probably less than one hundredth of the total nuclear volume, so in thinner sections, the chance of including this site is greatly reduced.

The Y-chromosome probe was synthesised using dinitrophenol-labelled dUTP; the same rabbit anti-dinitrophenyl antibody as used on the paraffin sections located the *probe* but, for the frozen sections, a FITC-labelled goat anti-rabbit IgG showed where the rabbit antibody had bound (and thus the sites of hybridisation).

The tissue was taken from the maternal-foetal junction. There are five distinct areas of the tissue: foetal *chorionic villous* endothelium, foetal chorionic villous trophoblastic epithelium, foetal villous-core stromal cells (mesenchymal, Hofbauer etc.), basal plate “other” cells (decidua from the mother and extra-villous trophoblast from the foetus) and the endothelial cells of *basal plate*, lining the inter-villous space. Labelling of basal plate trophoblast was similar to the labelling of chorionic villous trophoblast. On the basis of these data from $10\mu\text{m}$ sections, the labelling efficiency is in excess of 70% and the first three tissues were evidently male (and therefore genetically foetal). As it

contained both decidual *and* extravillous trophoblast, the category “Basal plate other” is a mixture of cells.

There were no significant counts in the basal plate endothelial nuclei, reflecting a genetically maternal origin. The “basal plate other” cell counts were intermediate between the trophoblast and basal plate endothelial values, reflecting the mixed population of foetally-derived extravillous trophoblast and the maternally-derived cells such as those of the decidua. The higher standard deviation here reflects irregular clustering of the extravillous trophoblast within the basal plate.

The short term survival of maternal blood-borne apoptotic trophoblastic emboli from the placenta (syncytial knots), the leakage of foetal leukocytes and the migration of extravillous trophoblast into the basal plate maternal circulation are all events taking place in an immuno-compromised pregnant physiology; they serve to make the maternal-foetal interface one that is anatomically complex. Cells originating from a male foetus and extracted from the mother’s blood can be identified using the Y-chromosome with fluorescence microscopy using the high affinity of quinacrine dyes which stain the repetitive DNA on the Y-chromosomes long arm (Hatfield et al., 1975).

On the one hand, hyper-proliferative trophoblast (in the maternal spiral arteries) may contribute to the accumulation of foetally derived cells and cell debris in the maternal circulation, or on the other hand, the fragility of the villous syncytiotrophoblast, as evidenced in Ahenkora’s study (Ahenkorah et al., 1997) may equally be held to account.

At one time, most placentologists believed that at term the intervillous space (the maternal blood filled sinus from which chorionic villi receive nutrients and oxygen) was lined exclusively by trophoblast, reflected from the sleeves of syncytiotrophoblast covering the villi onto the surface of the basal plate (at the attachment points of anchoring villi). Data presented here and by Byrne et al. (Byrne et al., 2010) clearly reveals the genetic mosaic nature of this layer. Coupled with published immunocytochemical, histological and ultrastructural data this gives clear evidence for the unique composition of this cell layer.

Analysis of the statistical data presented (Figure 6.2.10) demonstrated the maternal genetic nature of the basal plate lining endothelium and the foetally genetic nature of the villous endothelium which both contribute to this mosaic. Basal plate lining trophoblast exhibits labelled nuclear counts typical of foetal genetic origin. The data were consistent with all components of the villus tree being of foetal genetic origin and the basal plate lining cells as being of mixed maternal and foetal origin.

By defining the endothelial component of the basal plate lining as maternal, the view that this may be derived from the linings of the maternal uterine blood vessels connected to the intervillous space was supported. The *intima* of these vessels is continuous with the basal-plate lining layer at the openings of the uterine veins and spiral arterioles.

However, it seems more likely that this endothelium originates from circulating maternal endothelial progenitor cells (EPC) (Werner et al, 2005). These authors correlated the outcome of patients with cardiovascular disease to the number of circulating endothelial progenitor cells. It seemed possible that the hypertensive disease pre-eclampsia may cause a similar rise in the numbers of these cells. However, Matsubara et al. (Matsubara et al., 2006) showed that although the numbers of EPC were not significantly different in pre-eclamptic compared to normal pregnancies, their

proliferative capacity was raised. Disturbance of the area ratio between the elements of the mosaic has been noted in the hypertensive disease of pregnancy, pre-eclampsia (Smith et al., 2004). This may go some way towards explaining the increased area fraction occupied by endothelial cells lining the basal plate of placentae from pre-eclamptic mothers. Taking the results of this cytogenetic analysis into account and combining them with the previously published data (Byrne et al., 2001) and those of others (Lang, et al., 1993), it seems probable that the basal plate-lining layer of the human placenta at term is a histologically unique *allo-epi-endothelium*. With the unusual relationship identified here, a new dimension is added to the complexity of the human maternal-foetal interaction. The data demonstrate a co-operative histological relationship where in the extra-embryonic membranes cells from two individuals and two germ layers form a monolayer lining a vascular sinus (the intervillous space) that maintains the foetus *in-utero*.

Chapter seven: Conclusions

7.1 General discussion

The results from the anti-caveolin-1 antibody study confirmed that this protein was distributed in the human term placenta in all cells where previous research had suggested it might be found (fibroblasts, smooth muscle and endothelium).

The continuous lines of bright immuno-fluorescence seen in some areas of the basal plate were an unexpected finding, as these were at variance with historical descriptions still (erroneously) current at the time, concerning the composition of this lining layer (Boyd and Hamilton, 1970); these authors, of this highly-acclaimed and carefully detailed work, considered it to be entirely trophoblastic. Although the earlier work by Wanner (Wanner, 1966) had disputed the morphological nature of this lining, claiming that it was *exclusively* endothelial, it was not until Lang had made a more detailed survey of this area, using a panel of both endothelial and trophoblast marker antibodies, that the heterogeneous nature of this lining layer began to be apparent (Lang et al., 1993). Thus it was decided to investigate the cells contributing to this lining in more detail, using both conventional and immuno-gold electron microscopy.

What emerged from this was unprecedented: two cells from different germ lines – the epithelial trophoblast and the mesenchymal endothelial cells - were seen to abut and in some instances to form tight junctions.

The immuno-electron microscopy, apart from confirming the specificity of the antibody by a separate technique, was able to demonstrate a significant difference between the

apical and basal labelling density in foetal capillary endothelial cells. Perhaps surprisingly, the basal surface was shown to have a greater concentration of anti-caveolin-1 immuno-reactivity (and thus, presumably, a greater number of caveolae) than the apical surface in these cells.

It seems probable that this might reflect a functional role for caveolae in this unusual situation. Whereas in the normal (postnatal) systemic circulation, the net flow of materials (nutrients, signalling molecules and other macromolecules carried in the blood) is *from* the blood, through the apical surface and thence through the basal surface, in the foetal circulation, the situation runs *in reverse*. Here, materials in the maternal blood (space) must first cross the syncytiotrophoblast, covering the chorionic villi, using, if necessary the abundant coated pits as a transport mechanism. Only when these same materials have passed through this first barrier can they be transported into the foetal capillary endothelial cells. As these two different barriers often share the same basement membrane, it would seem more important, in the foetal endothelium, to have a greater concentration of caveolae at this basal surface, where more nutrients, etc. are arriving, ready to be transported across this second barrier and into the foetal circulation. Some of this cargo may be used by the endothelial cells themselves and there may also be some storage of this material before it completes its trans-endothelial journey, via the caveolae seen at the apical surface and enters the foetal circulation.

The observation of the small leucocytes which were caveolin-1 positive was serendipitous. Its significance was not appreciated when the images were captured; they were merely recorded as being a clear indication of how caveolin-1 positive cells

sometimes appear. With their very high nuclear-cytoplasmic ratio, the signal appears to be concentrated within the cytoplasm.

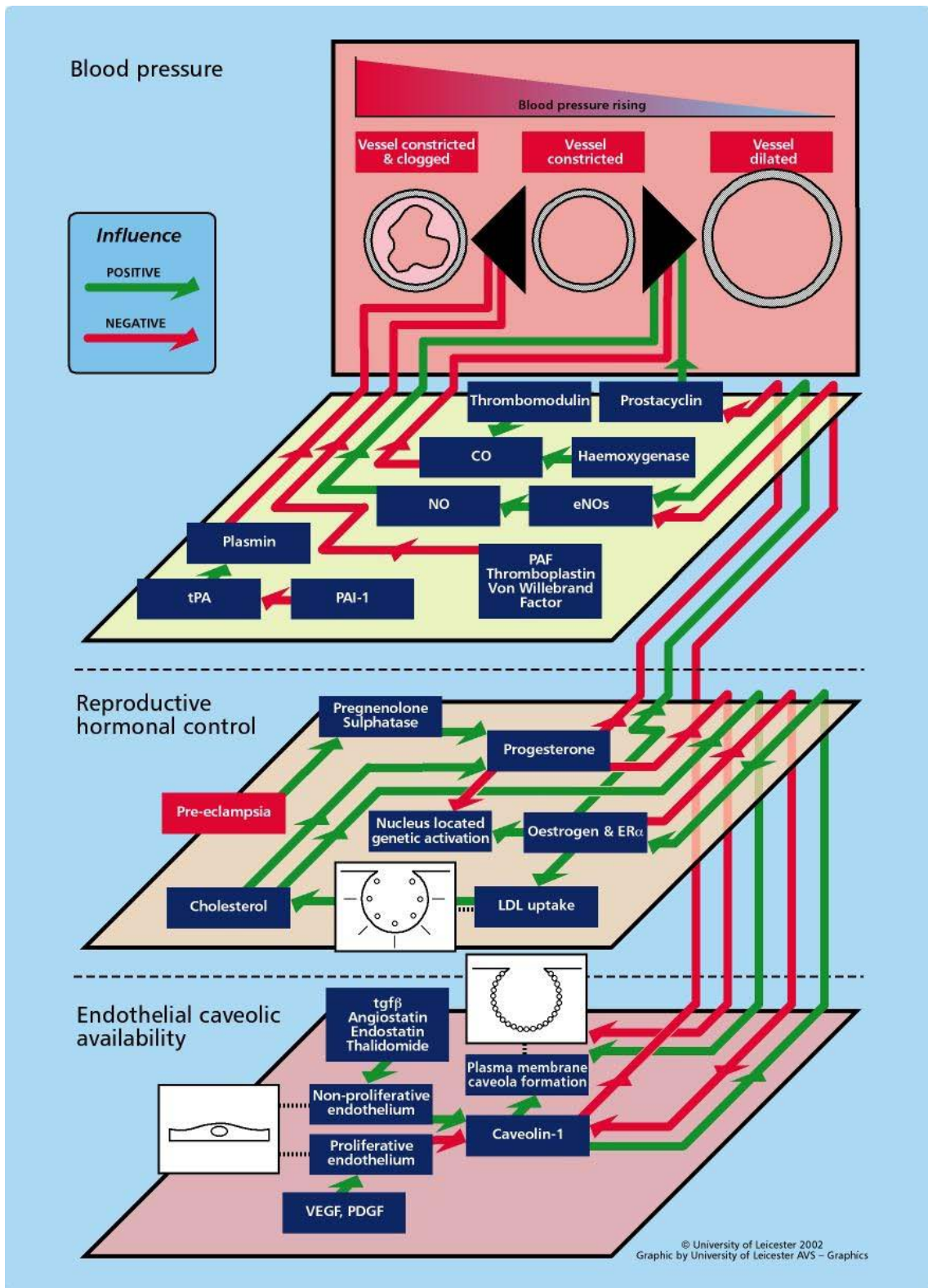
The identity of these cells has not been unambiguously established, but their size and morphology is indicative of lymphocytes. These cells have been reported as neither expressing caveolin-1 nor caveolae (Fra et al., 1995). Similarly, Sengelov et al. stated categorically that neutrophils were devoid of caveolin (Sengelov et al., 1998) yet Kiss et al. (Kiss et al., 2002) were able to show a clear induction of caveolin-1 in non-resident rat macrophages which were responding to an inter-peritoneal challenge by Freund's adjuvant. In this same paper, resident macrophages (those which had not migrated into the peritoneum) were shown to have very few caveolae; they constitutively express coated vesicles. It would seem, therefore, that the genes responsible for driving caveolae formation are inducible, in some leucocytes, according to whether the cells are quiescent or active. Whether this is applicable to all leucocytes is, as yet, a matter for conjecture.

The cytogenetic study, using the human Y-chromosome probe, established that the endothelial cells lining the basal plate were maternally derived. The source of these cells is not clear but it would seem most likely that they originate from the circulating maternal endothelial cells rather than from the spiral arteries themselves. It is conceivable that this endothelium acts as a protective barrier to the fragile adjacent trophoblastic lining. In some instances the endothelial cells are seen to have migrated over the top of trophoblast already resident at the site.

The results from the pre-eclamptic study (Smith et al., 2004), which were a sequel to the first caveolin-1 paper (Chapter 3) introduced a new dimension to the possible clinical significance of the maternally-derived endothelial lining to the basal plate. Whether these cells proliferate more in pre-eclampsia as a means of protecting the fragile syncytiotrophoblasts (Ahenkorah et al., 2009), or whether they play a more sinister role in exacerbating the symptoms of this condition remains an enigma.

A schematic diagram illustrating the possible links between the increase in the area fraction of the basal plate occupied by endothelium in the placentae of pre-eclamptic pregnancies and the aetiopathology of this disease is presented in Figure 7.1.1. This figure is taken from a presentation given by Professor Colin Ockleford and is reproduced with his permission. This is an attempt to link the increased proportion of basal plate lining endothelial cells seen in pre-eclampsia to the manifestation of hypertension. The various hormonal elements which may influence the progression of the disease are identified as having a positive or negative effect and the regulators of vascular tone and vessel calibre are detailed.

Figure 7.1 Possible links between caveolae and pre-eclampsia



7.2 Future work

In this study, the mapping of caveolin-1 immuno-reactivity in the normal human term placenta has only been covered using one rabbit polyclonal anti human caveolin-1 antibody. The results obtained by Bush et al. (2006), who used several different antibodies, both monoclonal and polyclonal, (some raised against the whole caveolin-1 molecule, others against specific epitopes within the molecule) produced some unexpected results. They showed that the different antibodies stained different sub-cellular populations of caveolin-1 within cultured Madin Darby canine kidney (MDCK) cells. It seems likely that a similar study performed on the placental tissues used in this study might also yield further information concerning the distribution of non-caveolar caveolin-1 in the placental context.

It would also be interesting to establish which caveolae-associated molecules are co-expressed or co-localise with caveolae. These would include several pregnancy-related molecules and the blood-pressure regulating NOS/NOSIP/NOSTRIN system. Numerous receptors and ligands are found in association with caveolae; where these may be related to pregnancy, both normal and pathological, similar immunological studies could be undertaken. This would involve dual-labelling experiments, with caveolin-1 being labelled using, say, a FITC-labelled anti-rabbit IgG as the secondary antibody and a mouse monoclonal anti-ligand antibody with a Texas red-/phycoerythrin-/cy3-labelled goat anti-mouse IgG secondary.

Immuno-electron microscopy has been shown to be a powerful and accurate indicator of the presence of antigens at a sub-cellular level. It has become a more accessible method since low-viscosity methacrylate resins were developed. Again, a similar approach

could be adopted to locate caveolae-associated ligands in placental tissues. For dual-labelling experiments in this context, the secondary antibodies used have to be conjugated to different sized gold particles. These normally fall in the range between 5 and 20nm diameter and are highly consistent: it is usual to use 5 and 15nm or 10 and 20nm in order to give an unambiguous difference in the final images.

One difficulty in researching placental tissues is the lack of available samples from the first and second trimesters of pregnancy, particularly if the area of interest is the basal plate. In the first trimester, placental tissues from terminations can sometimes be gathered (with informed consent), but often the material is very much fragmented by the methods used in its removal (curettage and/or vacuum aspiration). This is particularly deleterious to the integrity of the basal plate. The lack of these earlier specimens means that one is unable to map the first appearance of a particular phenomenon with any degree of accuracy. Access to archive material in the form of wax sections can only partially compensate for this shortfall. In any case, this material is extremely rare as virtually no new samples are currently being generated. Ethical guidelines, now strictly enforced, mean that this line of enquiry into developmental aspects of human placentology can never be adequately investigated.

Extrapolation of data obtained from the placentae of lower primates, whilst useful in this context, is sometimes misleading, as there are often large differences between the human situation and that pertaining in other primates.

The investigation of caveolin-1 and caveolae expression in human peripheral blood leucocytes by conventional transmission and immuno-electron microscopy is, by

comparison with the above, a relatively straightforward procedure. Density-gradient centrifugation of blood samples allows for the separation of the different sub-groups of these cells. These are easily embedded in the appropriate low-viscosity resin and the epoxy-embedded specimens should then yield information, at the ultrastructural level, concerning the vesicles (caveolae or coated pits) expressed by these cells. The methacrylate-embedded specimens, meanwhile, could be subjected to anti-caveolin-1 immuno-electron microscopy as described in Chapter Four and the results compared with their epoxy-embedded partners. These would represent the *quiescent* distribution of caveolae in these cells; their activation by an immunogenic agent may be achievable *in vitro*. If this is so, then these cells could then be prepared in an identical fashion and compared with the 'normal' cells.

It is the author's sincere hope that the reader may be encouraged to design better experiments, perhaps with a greater clinical bias, using the techniques outlined in this thesis in their own work; only then will the expenditure of so much effort be vindicated!

Bibliography

Ahenkorah J, Byrne S, Bosio P and Ockleford CD (2008) Immunofluorescence confocal laser scanning microscopy and immune-electron microscopic identification of keratins in human maternofetal interaction zone. *Journal of Cellular and Molecular Medicine*, **13**: 735-748.

Anderson RGW (1998) The caveolae membrane system. *Annual Review of Biochemistry*, **67**: 199-225.

Balducci J, Weiss PM, Atlas RO, Pajarillo MF, Dupree WB and Klasko SK (1997) Preeclampsia: immunologic alteration of Nitabuch's membrane? Clinical sequelae. *Journal of Maternal-Fetal Medicine*, **6**: 324–328.

Barros JS, Bairos VA, Baptista MG and Fagulha JO (2001) Immunocytochemical localization of endothelin-1 in human placenta from normal and pre-eclamptic pregnancies. *Hypertension in Pregnancy*, **20**: 125–137.

Beck F, Erler T, Russell A and James R (1995) Expression of Cdx-2 in the mouse embryo and placenta: possible role in patterning of the extra-embryonic membranes. *Developmental Dynamics*, **204**: 219–227.

Benirschke K and Kaufmann P (2000) Pathology of the human placenta. Early development of the human placenta, 4th edition. New York: Springer Verlag. p 1–968.

Benlimame N, Le PU and Nabi IR (1998) Localization of autocrine motility factor receptor to caveolae and clathrin-independent internalization of its ligand to smooth endoplasmic reticulum. *Molecular Biology of the Cell*, **9**: 1773–1786.

Bjerrum OJ and Schafer-Nielsen C (1986) in 'Analytical Electrophoresis' Editor MJ Dunn; Verlag Chemie, Weinheim, Germany: p. 315.

Bosio PM, McKenna PJ, Conroy R and O’Herlihy C (1999) Maternal central hemodynamics in hypertensive disorders of pregnancy. *Obstetrics and Gynecology*, **94**: 978–984.

Boyd JD and Hamilton WJ (1970) *The human placenta.* : Heffer and Sons, Cambridge.

Bretscher MS and Whytock S (1977) Membrane-associated vesicles in fibroblasts. *Journal of Ultrastructural Research*, **61**: 215–217.

Burk MR, Troeger C, Brinkhaus R, Holzgreve W and Hahn S (2001) Severely reduced presence of tissue macrophages in the basal plate of pre-eclamptic placentae. *Placenta*, **22**: 309–316.

Burton GJ and Cannigia I (2001). Hypoxia implications for implantation to delivery - a workshop report. *Placenta*, **22**: S83–S92.

Burton GJ, Hempstock, J and Jauniaux E (2001) Nutrition of the human fetus during the first trimester: a review. *Placenta*, **22**: S70– S76.

Byrne S, Cheent A, Dimond J, Fisher G and Ockleford CD (1998) Immunocytochemical localisation of Caveolin-1 in human term extraembryonic membranes using confocal laser scanning microscopy. *Journal of Anatomy*, **193**: 312-313.

Byrne S, Cheent A, Dimond J, Fisher G and Ockleford, CD (2001) Immunocytochemical localisation of a caveolin-1 isoform in human term extra-embryonic membranes using confocal laser scanning microscopy: Implications for the complexity of the materno-fetal junction. *Placenta*, **22**: 499-510.

Byrne S, Barber H, Mercer N, D’Lacey C and Ockleford CD (2003) ACE in the basal plate. *Placenta*, **24**: A43.

Byrne S, Ahenkorah J, Hottor B, Lockwood C and Ockleford CD (2007) Immunoelectron microscopic localisation of Caveolin-1 in human placenta. *Immunobiology*, **212**: 39-46.

Byrne S, Challis E, Williams JLR, Pringle JH, Hennessey JM and Ockleford CD (2010) A mosaic layer in human pregnancy. *Placenta*, **31**: 373-379.

Campbell L, Hollins AJ, Al-Eid A, Newman GR, von Ruhland C and Gumbelton M (1999) Caveolin-1 expression and caveolae biogenesis during cell transdifferentiation in lung alveolar epithelial primary cultures. *Biochemical and Biophysical Research Communications*, **262**: 744-751.

Carter AM and Charnock-Jones DS (2001) Angiogenesis and blood flow: implications for pathobiology: a workshop report. *Placenta*, **22**: S66-S68.

Chen Y and Norkin LC (1999) Extracellular simian virus 40 transmits a signal that promotes virus enclosure within caveolae. *Experimental Cell Research*, **246**: 83-90.

Cohen AW, Hnasko R, Schubert W and Lisanti MP (2004) Role of caveolae and caveolins in health and disease. *Physiological Reviews*, **84**:1341-1379.

Cooke HJ, Schmidtke J and Gosden JR (1982) Characterisation of a human Y chromosome repeated sequence and related sequences in higher primates. *Chromosoma*, **87**: 491-502.

Cunningham FG and Lindheimer M (1992) Hypertension in pregnancy. *New England Journal of Medicine*, **326**: 927-932.

Davey DA and Macgillivray I (1988) The classification and definition of the hypertensive disorders of pregnancy. *American Journal of Obstetrics and Gynecology*, **158**: 892-898.

Dekker GA and Sibai BM (1998) Etiology and pathogenesis of preeclampsia. Workshop report. *Trophoblast Research*, **16**: S142-S145.

Dye JF, Jablenska R, Donnelly JL, Lawrence L, Leach L, Clark P and Firth JA (2001) Phenotype of the endothelium in the human term placenta. *Placenta*, **22**: 32–43.

Evans MF, Mount SL, Beatty BG and Cooper K. (2002) Biotinyl-tyramide-based *in situ* hybridization signal patterns distinguish human papillomavirus type and grade of cervical intraepithelial neoplasia. *Modern Pathology*, **15**: 1339–1347.

Feng Q, Liu K, Liu Y-X, Byrne S and Ockleford C (2001) Plasminogen activators and inhibitors are transcribed during early macaque implantation. *Placenta*, **22**: 186–199.

Feng Y, Venema VJ, Venema RC, Tsai N and Caldwell RB (1999) VEGF induces nuclear translocation of Flk-1/KDR, endothelial nitric oxide synthase, and caveolin-1 in vascular endothelial cells. *Biochemical and Biophysical Research Communications*, **256**: 192–197.

Fielding CJ and Fielding PE (2001) Caveolae and intracellular trafficking of cholesterol. *Advanced Drug Delivery Reviews*, **49**: 251–264.

Gabinskaya T, Salafia CM, Gulle VE, Holzman IR and Weintraub AS (1998) Gestational age-dependent extravillous cytotrophoblast osteopontin immunolocalization differentiates between normal and preeclamptic pregnancies. *American Journal of Reproductive Immunology*, **40**: 339–346.

Galbiati F, Volonte D, Engelman JA, Watanabe G, Burk R, Pestell RG and Lisanti MP (1998) Targeted downregulation of caveolin-1 is sufficient to drive cell transformation and hyperactivate the p42/44 MAP kinase cascade. *European Molecular Biology Organisation Journal*, **17**: 6633–6648.

Galbiati F, Volonte D, Engelman JA, Scherer PE and Lisanti MP (1999) Targeted down-regulation of caveolin-3 is sufficient to inhibit myotube formation in differentiating C2C12 myoblasts. Transient activation of p38 mitogen-activated protein kinase is required for induction of caveolin-3 expression and subsequent myotube formation. *Journal of Biological Chemistry*, **274**: 30315–30321.

Ganapathy V, Prasad PD, Ganapathy ME and Liebach FH (2000) Placental transporters relevant to drug distribution across the maternal-fetal interface. *Pharmacology*, **294**: 413-420.

García-Cardena G, Martasek P, Masters BSS, Skidd PM, Couet J, Li S, Lisanti MP and Sessa,WC (1997) Dissecting the interaction between nitric oxide synthase (NOS) and caveolin. *Journal of Biological Chemistry*, **272**: 25437-25440.

Glenney JR (1992) The sequence of human caveolin reveals identity with VIP21, a component of transport vesicles. *Federation of European Biochemical Societies Letters*, **314**: 45–48.

Goldman-Wohl DS, Ariel I, Greenfield C, Lavy Y and Yagel S (2000) Tie-2 and angiopoietin-2 expression at the fetal-maternal interface: a receptor ligand model for vascular remodelling. *Molecular Human Reproduction*, **6**: 81-87.

Graham CH, Postovit LM, Park H, Canning MT and Fitzpatrick TE (2000) Adriana and Luisa Castellucci award lecture 1999: role of oxygen in the regulation of trophoblast gene expression and invasion. *Placenta*, **21**: 443–450.

Gratton RJ, Asano H and Han VK (2002) The regional expression of insulin-like growth factor II (IGF-II) and insulin-like growth factor binding protein-1 (IGFBP-1) in the placentae of women with preeclampsia. *Placenta*, **23**: 303–310.

Griffiths G (1993) Fine structure immunocytochemistry. Springer-Verlag, Berlin, Germany. pp 34-42.

Hanson CG and Nichols BJ (2010) Exploring the caves: cavins, caveolins and caveolae. *Trends in Cell Biology*, **24**: 177-186.

Hazra S, Waugh J and Bosio P (2003) 'Pure' pre-eclampsia before 20 weeks of gestation. *British Journal of Obstetrics and Gynecology*, **110**: 1034-1035.

Hill MM, Bastiani M, Luetterforst R, Kirkham M, Kirkham A, Nixon SJ, Walser P, Aloankwa D, Oorschot VMJ, Martin S, Hancock JF and Parton RG (2008) PTRF-cavin, a conserved cytoplasmic protein required for caveola formation and function. *Cell*, **132**: 113-124.

Hottor B, Bosio P, Waugh J, Diggle PJ, Byrne S, Ahenkorah J and Ockleford CD (2010) Variation in composition of the intervillous space lining in term placentas of mothers with pre-eclampsia. *Placenta*, **31**: 409-417.

Ikezu T, Ueda H, Trapp BD, Nishiyama K, Jing FS, Volonte D, Galbiati F, Byrd AL, Bassell G, Serizawa H, Lane WS, Lisanti MP and Okamoto T (1998) Affinity-purification and characterization of caveolins from the brain: Differential expression of caveolin-1, -2 and -3 in brain endothelial and astroglial cell types. *Brain Research*, **804**: 177-192.

Kim YM, Bujold E, Chaiworapongsa T, Gomez R, Yoon BH, Thaler HT, Rotmensch S and Romero R (2003a) Failure of physiologic transformation of the spiral arteries in patients with preterm labor and intact membranes. *American Journal of Obstetrics and Gynecology*, **189**: 1063-1069.

Kim YM, Chaiworapongsa T, Gomez R, Bujold E, Yoon BH, Rotmensch S, Thaler HT and Romero R (2003b) Failure of physiologic transformation of the spiral arteries in the placental bed in preterm premature rupture of membranes. *American Journal of Obstetrics and Gynecology*, **187**: 1137-1142.

Kiss AL, Turi Á, Müller B, Kántor O and Botos E (2002) Caveolae and caveolin isoforms in rat peritoneal macrophages. *Micron*, **33**: 75-93.

Kogo H and Fujimoto R (2000) Concentration of caveolin-1 in the cleavage furrow as revealed by time-lapse analysis. *Biochemical and Biophysical Research Communications*, **268**: 82–87.

Knöfler M, Vasicek R and Schrieber M (2001) Key regulatory factors involved in placental development: a review. *Placenta* **22**: S83–S92.

Kurzchalia TV, Dupree P, Parton RG, Kellner R, Virta H, Lehnert M and Simons K (1992) VIP21, A 21-kD Membrane Protein is an Integral Component of *Trans*-Golgi-Network-Derived Transport Vesicles. *Journal of Cell Biology*, **118**: 1003–1014.

Laemmli UK (1970) Cleavage of structural proteins during the assembly of the head of bacteriophage T4. *Nature*, **227**: 680–685.

Lala P and Desoye G (2001) Signal transductions: variants on developmental control from implantation to delivery. *Placenta*, **22**: S98–S100.

Lang I, Hartmann M, Blaschitz A, Dohr G, Skofitsch G and Desoye G (1993) Immunohistochemical Evidence for the Heterogeneity of Maternal and Fetal Vascular Endothelial Cells in Human Full-term Placenta. *Cell and Tissue Research*, **274**: 211–218.

Li S, Song KS and Lisanti MP (1996) Expression and characterization of recombinant caveolin. *Journal of Biological Chemistry*, **271**: 568–573.

Lindheimer M and Katz A (1997) The normal and diseased kidney in pregnancy. In: Schrieber RW and Gottshalk CW (editors) *Diseases of the Kidney*, 6th Edition, Boston: Little, Brown pp. 2063-2097.

Linton EA, Rodriguez-Linares B, Rashid-Doubell F, Ferguson, DJ and Redman CW (2003) Caveolae and caveolin-1 in human term villous trophoblast. *Placenta*, **7**: 745-757.

Lisanti MP, Scherer PE, Tang Z-L and Sargiacomo M (1994) Caveolae, caveolin, and caveolin-rich membrane domains: a signalling hypothesis. *Trends in Cell Biology*, **4**: 231–235.

Liu J, Razani B, Tang S, Terman BI, Ware JA and Lisanti MP (1999) Angiogenesis activators and inhibitors differentially regulate caveolin-1 expression and caveolae formation in vascular endothelial cells. Angiogenesis inhibitors block vascular endothelial growth factor-induced down-regulation of caveolin-1. *Journal of Biological Chemistry*, **274**: 15781–15785.

Lyall F and Myatt L (2002) The role of the placenta in pre-eclampsia. *American Journal of Obstetrics and Gynecology*, **179**: 1359–1375.

Lyden TW, Anderson CL and Robinson JM (2002) The endothelium but not the syncytiotrophoblast of human placenta expresses caveolae. *Placenta*, **23**: 640-652.

Mayhew TM and Burton GJ (1997) Sterology and its impact on our understanding of human placental functional morphology. *Microscopy Research and Technique*, **38**: 195–205.

Moffett-King A (2002). Natural killer cells and pregnancy. *Nature Reviews Immunology*, **2**: 656–663.

Mongan LC and Ockleford CD (1995) Behaviour of two IgG subclasses in transport of immunoglobulin across the human placenta. *Journal of Anatomy*, **188**: 43-51.

Mongan LC, Gormally J, Hubbard ARD, d’Lacey C and Ockleford CD (1998) Confocal microscopy: theory and applications. In: Lambert D, editor. Calcium signalling protocols. Totowa, NJ: Humana Press, New Jersey. pp.1–39.

Montesano R, Roth J, Robert A and Orci L (1982) Non-coated membrane invaginations are involved in binding and internalization of cholera and tetanus toxins. *Nature*, **296**: 651–653.

Naslavsky N, Shmeeda H, Friedlander G, Yanai A, Futerman AH, Barenholz Y and Taraboulos A (1999) Sphingolipid depletion increases formation of the scrapie prion protein in neuroblastoma cells infected with prions. *Journal of Biological Chemistry*, **274**: 20763–20771.

Nasu Y, Timme TL, Yang G, Bangma CH, Li L, Ren C, Sang HP, DeLeon M, Wang J and Thomson TC (1998) Suppression of caveolin expression induces androgen sensitivity in metastatic androgen-insensitive mouse prostate cancer cells. *Nature Medicine*, **4**: 1062–1064.

Nusrat A, Parkos CA, Verkade P, Foley CS, Liang TW, Innis-Whitehouse W, Eastburn KK and Madara JL (2000) Tight junctions are membrane microdomains. *Journal of Cell Science*, **113**: 1771–1781.

Ockleford CD (1976) A three dimensional reconstruction of the polygonal pattern on placental coated vesicle membranes. *Journal of Cell Science*, **23**: 83–91.

Ockleford CD (1990). A quantitative interference light microscope study of human first trimester chorionic villi. *Journal of Microscopy*, **157**: 225-237.

Ockleford CD (1995) Editorial: The confocal laser scanning microscope (CLSM). *Journal of Pathology*, **176**: 1–2.

Ockleford CD and Whyte A (1977) Differentiated regions of human placental cell surface associated with exchange of materials between maternal and foetal blood. The structure, distribution, ultrastructural cytochemistry and biochemical composition of coated vesicles. *Journal of Cell Science*, **25**: 293–312.

Ockleford CD, Wakely, J and Badley RA (1981) Morphogenesis of human placental chorionic villi: cytoskeletal, syncytioskeletal and extracellular matrix proteins. *Proceedings of the Royal Society (Biological Sciences)*, **212**: 305–316.

Ockleford CD, Dearden, L and Badley, RA (1984) Syncytioskeletons in choriocarcinoma in culture. *Journal of Cell Science*, **66**: 1–20.

Ockleford CD and Clint JM (1980) The uptake of IgG by human placental chorionic villi. A correlated autoradiographic and wide aperture counting study. *Placenta*, **1**: 91-111.

Ockleford CD, Malak T, Hubbard A, Bracken K, Burton S-A, Bright N, Blakey G, Goodliffe J, Garrod D, d’Lacey C (1993) Confocal and conventional immunofluorescence and ultrastructural localisation of intracellular strength giving components of human fetal membranes. *Journal of Anatomy*, **183**: 483–505.

Ockleford CD, Mongan L and Hubbard ARD (1997) Techniques of advanced light microscopy and their applications to morphological analysis of human extra-embryonic membranes. In: Danzer V, Leiser R, editors. Placenta, comparative and functional morphology by different methodological approaches. *Microscopy Research and Technique*, **38**: 153–164.

Ockleford CD, Smith R, Byrne S, Sanders R and Bosio P (2003) Human placental basal plate lining cells: significant changes associated with pre-eclampsia. *Annals of Anatomy* (Supplement to), **185**: 166-167.

Ockleford CD, Smith RK, Byrne S, Sanders R, Bosio P (2004) A confocal laser scanning microscope study of cytokeratin immunofluorescence dimming indicates a mechanism of trophoblast deportation and its upregulation in pre-eclampsia. *Microscopy Research and Technique*, **64**: 43–53.

Ockleford CD, Cairns H, Rowe AJ, Byrne S, Scott JJA and Willingale R (2007) The distribution of caveolin-3 immunofluorescence in skeletal muscle fibre membrane defined by dual channel confocal laser scanning microscopy, fast Fourier transform and image modelling. *Journal of Microscopy*, **206**: 139-151.

Ong SS, Moore RJ, Warren AY, Crocker IP, Fulford J, Tyler DJ, Gowland PA and Baker PN (2003) Myometrial and placental artery reactivity alone cannot explain reduced placental perfusion in preeclampsia and intrauterine growth restriction. *British Journal of Obstetrics and Gynaecology*, **110**: 909–915.

Park H, Go Y-M, Darji R, Choi J-W, Lisanti MP, Maland MC and Jo H (2000) Caveolin-1 regulates shear stress-dependent activation of extracellular signal-regulated kinase. *American Journal of Physiology*, **278**: H1285–H1293.

Parton RG, Way M, Zorzi N and Stang E (1997) Caveolin-3 associates with developing T-tubules during muscle differentiation. *Journal of cell Biology*, **136**: 137–154.

Pelligrino DA, Ye S, Tan F, Santizo RA, Feinstein DL and Wang Q (2000) Nitric-oxide-dependent pial arteriolar dilation in the female rat; Effects of chronic estrogen depletion and repletion. *Biochemical and Biophysical Research Communications*, **269**: 165–171.

Ralston E and Ploug T (1999) Caveolin-3 is associated with the T-tubules of mature skeletal muscle fibers. *Experimental Cell Research*, **246**: 510–515.

Ramirez M, Pollack L, Millien G, Yu X-C, Hinds A, Williams MC (2002) The isoform of caveolin-1 is a marker of vasculogenesis in early lung development. *Journal of Histochemistry and Cytochemistry*, **50**: 33–42.

Rashid-Doubell F, Tannetta D, Redman, CW, Sargent IL, Boyd, CA and Linton, EA (2007) Caveolin-1 and lipid rafts in confluent BeWo trophoblasts: Evidence for rock-1 association with caveolin-1. *Placenta*, **28**: 139–151.

Razani B, Schlegel A and Lisanti MP (2000) Caveolin proteins in signalling, oncogenic transformation and muscular dystrophy. *Journal of Cell Science*, **113**: 2103–2109.

Rizzo V, McIntosh DP, Oh P and Schnitzer JE (1998) In situ flow activates endothelial nitric oxide synthase in luminal caveolae of endothelium with rapid caveolin dissociation and calmodulin association. *Journal of Biological Chemistry*, **273**: 34724–34729.

Roberts JM, Hubel, CA and Taylor RN (1995) Endothelial dysfunction yes, cytotoxicity no! *American Journal of Obstetrics and Gynecology*, **173**: 978–979.

Röhlich P and Allison AC (1976) Oriented pattern of membrane-associated vesicles in fibroblasts. *Journal of Ultrastructure Research*, **57**: 94–103.

Roth J, Bendayan M and Orci L (1980) FITC-Protein A-gold complex for light and electron microscopic immunocytochemistry *Journal of Histochemistry and Cytochemistry*, **28**: 55-57.

Rothberg KG, Heuser JE, Donzell WC, Ying Y-S, Glenney JR and Anderson RGW (1992) Caveolin, a protein component of caveolae membrane coats. *Cell*, **68**: 673–682.

Salamonsen LA (1999) The role of proteases in implantation. *Reviews in Reproduction*, **4**: 11-22.

Sargiacamo M, Scherer PE, Tang Z-L, Kübler E, Song KS, Sanders MC and Lisanti MP (1995) Oligomeric structure of caveolin: Implications for caveolae membrane organization. *Proceedings of the National Academy of Sciences*, **92**: 9407–9411.

Scherer PE, Tang Z-L, Chun M, Sargiacamo M, Lodish HF and Lisanti MP (1995) Caveolin isoforms differ in their N-terminal protein sequence and subcellular distribution. *Journal of Biological Chemistry*, **270**: 16395–16401.

Scherer PE, Okamoto T, Chun M, Nishimoto I, Lodish HF and Lisanti MP (1996) Identification, sequence, and expression of caveolin-2 defines a caveolin gene family. *Proceedings of the National Academy of Sciences*, **93**: 131–135.

Scherer PE, Lewis RY, Volonté D, Engelman JA, Galbiati F, Couet J, Kohtz DS, van Dosselar E, Peters P and Lisanti MP (1997) Cell-type and tissue-specific expression of caveolin-2. *Journal of Biological Chemistry*, **272**: 29337–29346.

Schlegel A, Wang C, Katzenellenbogen BS, Pestell RG and Lisanti MP (1999) Caveolin-1 potentiates estrogen receptor alpha (ER alpha) signalling. Caveolin-1 drives ligand-independent nuclear translocation and activation of ER alpha. *Journal of Biological Chemistry*, **274**: 33551–33556.

Schnitzer JE, Oh P and McIntosh DP (1996) Role of GTP hydrolysis in fission of caveolae directly from plasma membranes. *Science*, **274**: 239–242.

Schreiber S, Fleischer J, Breer H and Boekhoff I (2000) A possible role for caveolin as a signaling organizer in olfactory sensory membranes. *Journal of Biological Chemistry*, **275**: 24115-24123.

Segal SS, Brett SE and Sessa WC (1999) Codistribution of NOS and caveolin throughout peripheral vasculature and skeletal muscle of hamsters. *American Journal of Physiology. Heart and Circulatory Physiology*, **277**: H1167–H1177.

Sengeløv H, Voldstedlund M, Vinten J, and Borregaard N (1998) Human neutrophils are devoid of the integral membrane protein caveolin. *Journal of Leukocyte Biology*, **65**: 563-566.

Shaul PW and Anderson RGW (1998) Role of plasmalemmal caveolae in signal transduction. *American Journal of Physiology*, **275**: L843–L851.

Sherer DM and Salafia CM (2000) Chronic intrauterine bleeding and fetal growth at less than 32 weeks of gestation. *Gynecologic and Obstetric Investigation*, **50**: 92–95.

Skretting G, Torgersen ML, Van Deurs B and Sandvig K (1999) Endocytic mechanisms responsible for uptake of GPI-linked diphtheria toxin receptor. *Journal of Cell Science*, **112**: 3899–3909.

Smith RK, Ockleford CD, Byrne S, Bosio P and Sanders R (2004) Healthy and pre-eclamptic basal plate lining cells: Quantitative comparisons based on confocal laser scanning microscopy. *Microscopy Research and Technique*, **64**: 54-62.

Song KS, Scherer PE, Tang Z-L, Okamoto T, Li S, Chafel M, Chu C, Kohtz DS and Lisanti MP (1996) Expression of caveolin-3 in skeletal, cardiac, and smooth muscle cells. *Journal of Biological Chemistry*, **271**: 15160–15165.

Southern E (1975) Detection of specific sequences among DNA fragments separated by electrophoresis. *Journal of Molecular Biology*, **98**: 503.

Stan RV (2005). Structure of caveolae. *Biochimica et Biophysica Acta*, **1746**: 334-348.

Stark J and Kaufmann P (1971) Protoplasmatische Trophoblastabschnürungen in den mütterlichen Kreislauf bei normaler und pathologischer Schwangerschaft, *Archiv für. Gynäkologie*, **210**: 375–385.

Strachan T and Read AP (1999) *Human Molecular Genetics, 2nd edition* New York: John Wiley and Sons, p.67.

Tang ZL, Scherer PE, Okamoto T, Song K, Chu C, Kohtz DS, Nishimoto I, Lodish HF and Lisanti MP (1996) Molecular cloning of caveolin-3, a novel member of the caveolin family expressed predominantly in muscle. *Journal of Biological Chemistry*, **271**: 2255–2261.

Timme TL, Goltsov A, Tahir S, Li L, Wang J, Ren C, Johnston RN and Thompson TC (2000) Caveolin-1 is regulated by c-myc and suppresses c-myc-induced apoptosis. *Oncogene*, **19**: 3256–3265.

Towbin H, Staehelin T and Gordon J (1979) Electrophoretic transfer of proteins from polyacrylamide gels to nitrocellulose sheets: procedure and some applications. *Proceedings of the National Academy of Sciences*, **76**: 4350-4356.

Valentijn KM, Gumkowski FD and Jamieson JD (1999) The subapical actin cytoskeleton regulates secretion and membrane retrieval in pancreatic acinar cells. *Journal of Cell Science*, **112**: 81–96.

Walker J (2000) Pre-eclampsia. *Lancet*, **356**: 1260–1265.

Wanner A (1966) Wird bei der Geburtsplacenta des Menschen die Basalplatte von Trophoblastzellen oder Zellen mütterlicher herkunft überzogen? *Acta Anatomica*, **63**: 545-548.

Werner N, Kosiol S, Schiegl T, Ahlers P, Walenta K, Link A, Böhm M and Nickenig G. (2005) Circulating endothelial progenitor cells and cardiovascular outcomes. *New England Journal of Medicine*, **353**: 999-1007.

Williams PJ, Bulmer JN, Searle RF, Innes BA and Robson SC (2009) Altered decidual leucocyte populations in the placental bed in pre-eclampsia and foetal growth restriction: a comparison with late normal pregnancy. *Reproduction* **138**, 177-184.

World Health Organization (1996) Revised 1990 estimates of Maternal Mortality. A new approach by WHO and UNICEF. *WHO/FRH/MSM96.11*. Geneva: WHO.

Yamada E (1955) The Fine Structure of the Gall Bladder Epithelium in the Mouse. *Journal of Biophysical and Biochemical Cytology*, **1**: 445–458.

Yang C-PH, Galbiati F, Volonte D, Horwitz SB and Lisanti MP (1998) Upregulation of caveolin-1 and caveolae organelles in taxol-resistant A549 cells. *Federation of European Biochemical Societies Letters*, **439**: 368–372.

Yang G, Truong LD, Wheeler TM and Thompson TC (1999) Caveolin-1 expression in clinically confined human prostate cancer: A novel prognostic marker. *Cancer Research*, **59**: 5719–5723.

Zhang W, Razani B, Altschuler Y, Bouzahzah B, Mostov KE, Petell RG & Lisanti MP (2000) Caveolin-1 inhibits epidermal growth factor-stimulated lamelli-pod extension and cell migration in metastatic mammary adenocarcinoma cells (MTLn3): Transformation suppressor effects of adenovirus-mediated gene delivery of caveolin-1. *Journal of Biological Chemistry*, **275**: 20717–20725.

Zimmermann K, Opitz N, Dedio J, Renne C, Muller-Esterl W and Oess S (2002)
Nostrin: a protein modulating nitric oxide release and subcellular distribution of endothelial nitric oxide synthase. *Proceedings of the National Academy of Science*, **26**: 17167-17172.

Electronic reference

<http://www.uiowa.edu/~cmrf/methodology/stereology/index.html>22/11/2010 10:18:18

Reference to paper weighing.

Appendices

1. Patient information letter for pre-eclampsia study

PATIENT INFORMATION LEAFLET

**PATIENT INFORMATION LEAFLET,
VERSION NO 2003CDO2,
Study No LGH 9161 LLREC 7144**

Study title: Pre-eclampsia: a disease that causes high blood pressure and protein in the urine of pregnant women and may lead to harm for their babies

Principle Investigators *Dr Colin
Ockleford PhD, FRCPath*
Mr Paul Bosio
MD MRCOG
Mr Jason
Waugh MRCOG



**University of
Leicester**

**Department of Infection, Immunity
and Inflammation**

*Director of Advanced Light Microscope
Facility & The Laboratory for
Developmental Cell Sciences*

Colin D. Ockleford PhD FRCPath ILTM

Medical Sciences Building

University Road

Leicester LE1 9HN UK

Tel: +44 (0)116 252 3021 (*Secretary*)

+44 (0)116 252 3020 (*Direct line*)

Fax: +44 (0)116 252 5072

E-mail: cxo@le.ac.uk

For further information you may contact Dr Ockleford at:-

The Advanced Light Microscope Facility

*Maurice Shock Medical Sciences Building
Leicester Warwick Medical School
University Road
Leicester LE1 9HN*

Tel: 0116 252 3020

Email: cxo@le.ac.uk

You are being invited to take part in a research study that will only require the donation of a few sugar-cube sized tissue samples of the after-birth (to be removed immediately prior to its disposal). Before you decide to participate it is

important for you to understand why the research is being done and what it will involve. Please take time to read the following information carefully and discuss it with others if you wish. Ask us if there is anything that is not clear or if you would like more information. Take time to decide whether or not you wish to take part.

1. What is pre-eclampsia?

Pre-eclampsia is a disease that can affect pregnant women. In mild cases it causes protein in the urine, swelling of tissues and slightly raised blood pressure. Untreated, the raised blood pressure can have severe effects. In these cases it can lead to eclampsia where the mother has fits and harm can come to her baby. Although the cause is not yet fully understood it is believed to involve afterbirth tissue as where that exhibits certain particular alterations pre- eclampsia is more common. Pre- eclampsia is obviously a disease where progress in understanding, if it leads to new treatments, could be very valuable.

2. What is the purpose of the study?

We have recently uncovered new information about the detailed structure of the tissues in the healthy human after-birth. The new information relates to a part of the placenta that develops abnormally when pre-eclampsia ensues. We now wish to study this area in detail comparing the normal and pre-eclamptic afterbirth very carefully to see what we can learn about the course of the disease. At some future stage this may help us to develop new rational strategies for treatment of the disease. The study (Leicester Research Ethics Committee ref. No. 6336) of which this is a development was originally sponsored by "The Pathological Society of Great Britain and Ireland". The work is to be carried out by staff at Leicester Warwick Medical Schools.

3. Why have I been chosen?

You have been chosen either

- a) because you have clinical signs of pre-eclampsia and we would like to examine small samples of afterbirth after it is delivered for changes associated with the disease. Or alternatively
- b) because your pregnancy is a healthy one and we wish to compare similar small samples of afterbirth taken after it is delivered so that we can be sure we have a good basis for comparison.

4. What will happen to me if I take part in the study?

- The whole study should be complete within 3 years of the start date in early April 2004
- The number of visits to hospital will not be increased beyond that expected for your normal treatment.
- Any tests to be carried out, e.g. physical examination, blood test etc. on you and your baby will be the normal routine ones for your own and your baby's benefit. In addition we would like you to give permission for use of samples of the afterbirth. These will be

obtained after the delivery of the afterbirth and baby for careful microscopic and cell-biological study. Subsequently the tissue of the afterbirth will be disposed of in the approved manner for human tissues. We do not plan to keep any tissue beyond the end of the study this will be at the latest 3 years from your giving consent.

- You will not be asked to keep any records specifically for this study.
- You will not be asked to fill in any questionnaires for the purposes of this study.
- The procedures for our research will all be carried out on the afterbirth after your baby has been delivered and special research staff will be handling the tissue. We do not therefore envisage any additional risk involved for you or your baby in helping with this research.
- No short-term benefits will accrue to you or your family. We hope and are working hard to try to ensure that there will be long term ones for others and babies affected by this condition in the future.

4. Will information obtained in the study be confidential?

As usual your treatment will be recorded in your medical records and these will be treated with the usual degree of confidentiality under the data protection act. Some relevant excerpts of your notes may be useful as raw research data to members of the research team. The consultant-in-charge of your welfare and that of your baby will arrange to transmit only any necessary information and then using a code number. *Your name and address will be removed so that you cannot be recognised from it.*

You will not be identified in any documents or published work relating to the research.

Normally the patient's GP is informed of the patient participation in a medical study. As this study is of the afterbirth only we do not intend to do so on this occasion. However should you wish to consult your GP please do so and show them the information you have been given. We will make ourselves available to discuss any issues with your GP if they think it valuable.

5. What if I and/ or my baby are harmed by the study?

We believe this to be extremely *unlikely* as we are only intending to study the afterbirth following your baby's birth. Nevertheless the research will be indemnified in the usual way. If you are harmed due to someone's negligence, then you may have grounds for a legal action but you may have to pay for it. Regardless of this, if you wish to complain, or have any concerns about any aspect of the way you have been approached or treated during the course of this study, the normal National Health Service complaints mechanisms are available to you.'

6. Will I receive out of pocket expenses for taking part in the study?

There will be no out of pocket expenses payment associated with this trial and there should be no additional travel involved. Neither will your doctor be paid for including you in this study; he is doing this in the hope that the work will benefit future patients.

7. Do I have to take part?

It is up to you to decide whether or not to take part. If you do decide to take part you will be given this information sheet to keep and be asked to sign a consent form. If you decide to take part you are still free to withdraw at any time and without giving a reason. A decision to withdraw at any time, or a decision not to take part, will not affect the standard of care you receive.

8. What will happen to the results of the research study?

We aim to publish the outcome of our work in peer-reviewed medical and scientific journals that are freely accessible so that they are most useful to the widest range of people. We cannot predict where they will appear, as acceptance for publication is an editorial decision, but this should be within 4 years and if any member of the team is contacted they undertake to indicate to participants where relevant results are to be, or have been published, so they can obtain a copy.

9. Who has reviewed the study?

All research that involves NHS patients or staff, information from NHS medical records or uses NHS patients or staff, information from NHS medical records or uses NHS premises or facilities must be approved by a Leicestershire Local Research Ethics Committee before it goes ahead. Approval does not guarantee that you will not come to any harm if you take part. However, approval means that the Committee is satisfied that your rights will be respected, that any risks have been reduced to a minimum and balanced against possible benefits and that you have been given sufficient information on which to make an informed decision to take part or not.

‘Thank you for reading this.’

2. Permission to reproduce Figure 1.8

ELSEVIER LICENSE TERMS AND CONDITIONS

Jan 29, 2011

This is a License Agreement between Simon Byrne ("You") and Elsevier ("Elsevier") provided by Copyright Clearance Center ("CCC"). The license consists of your order details, the terms and conditions provided by Elsevier, and the payment terms and conditions.

All payments must be made in full to CCC. For payment instructions, please see information listed at the bottom of this form.

Supplier	Elsevier Limited The Boulevard, Langford Lane Kidlington, Oxford, OX5 1GB, UK
Registered Company Number	1982084
Customer name	Simon Byrne
Customer address	Infection, Immunity & Inflammation Leicester, other LE1 9HN
License number	2562601259333
License date	Dec 05, 2010
Licensed content publisher	Elsevier
Licensed content publication	Trends in Cell Biology
Licensed content title	Exploring the caves: cavins, caveolins and caveolae
Licensed content author	Carsten G. Hansen, Ben J. Nichols
Licensed content date	April 2010
Licensed content volume number	20
Licensed content issue number	4
Number of pages	10
Start Page	177
End Page	186
Type of Use	reuse in a thesis/dissertation
Portion	figures/tables/illustrations
Number of figures/tables/illustrations	1
Format	both print and electronic

Are you the author of this Elsevier article?	No
Will you be translating?	No
Order reference number	
Title of your thesis/dissertation	The distribution of caveolin-1 in human term placenta and the derivation of the endothelial cells lining its basal plate
Expected completion date	Dec 2010
Estimated size (number of pages)	150
Elsevier VAT number	GB 494 6272 12
Permissions price	0.00 GBP
Value added tax 17.5%	0.0 USD / 0.0 GBP
Total	0.00 GBP
Terms and Conditions	

INTRODUCTION

1. The publisher for this copyrighted material is Elsevier. By clicking "accept" in connection with completing this licensing transaction, you agree that the following terms and conditions apply to this transaction (along with the Billing and Payment terms and conditions established by Copyright Clearance Center, Inc. ("CCC"), at the time that you opened your Rightslink account and that are available at any time at <http://myaccount.copyright.com>).

GENERAL TERMS

2. Elsevier hereby grants you permission to reproduce the aforementioned material subject to the terms and conditions indicated.

3. Acknowledgement: If any part of the material to be used (for example, figures) has appeared in our publication with credit or acknowledgement to another source, permission must also be sought from that source. If such permission is not obtained then that material may not be included in your publication/copies. Suitable acknowledgement to the source must be made, either as a footnote or in a reference list at the end of your publication, as follows:

“Reprinted from Publication title, Vol /edition number, Author(s), Title of article / title of chapter, Pages No., Copyright (Year), with permission from Elsevier [OR APPLICABLE SOCIETY COPYRIGHT OWNER].” Also Lancet special credit - “Reprinted from The Lancet, Vol. number, Author(s), Title of article, Pages No., Copyright (Year), with permission from Elsevier.”

4. Reproduction of this material is confined to the purpose and/or media for which permission is hereby given.

5. Altering/Modifying Material: Not Permitted. However figures and illustrations may be altered/adapted minimally to serve your work. Any other abbreviations, additions, deletions and/or any other alterations shall be made only with prior written authorization of Elsevier

Ltd. (Please contact Elsevier at permissions@elsevier.com)

6. If the permission fee for the requested use of our material is waived in this instance, please be advised that your future requests for Elsevier materials may attract a fee.

7. **Reservation of Rights:** Publisher reserves all rights not specifically granted in the combination of (i) the license details provided by you and accepted in the course of this licensing transaction, (ii) these terms and conditions and (iii) CCC's Billing and Payment terms and conditions.

8. **License Contingent Upon Payment:** While you may exercise the rights licensed immediately upon issuance of the license at the end of the licensing process for the transaction, provided that you have disclosed complete and accurate details of your proposed use, no license is finally effective unless and until full payment is received from you (either by publisher or by CCC) as provided in CCC's Billing and Payment terms and conditions. If full payment is not received on a timely basis, then any license preliminarily granted shall be deemed automatically revoked and shall be void as if never granted. Further, in the event that you breach any of these terms and conditions or any of CCC's Billing and Payment terms and conditions, the license is automatically revoked and shall be void as if never granted. Use of materials as described in a revoked license, as well as any use of the materials beyond the scope of an unrevoked license, may constitute copyright infringement and publisher reserves the right to take any and all action to protect its copyright in the materials.

9. **Warranties:** Publisher makes no representations or warranties with respect to the licensed material.

10. **Indemnity:** You hereby indemnify and agree to hold harmless publisher and CCC, and their respective officers, directors, employees and agents, from and against any and all claims arising out of your use of the licensed material other than as specifically authorized pursuant to this license.

11. **No Transfer of License:** This license is personal to you and may not be sublicensed, assigned, or transferred by you to any other person without publisher's written permission.

12. **No Amendment Except in Writing:** This license may not be amended except in a writing signed by both parties (or, in the case of publisher, by CCC on publisher's behalf).

13. **Objection to Contrary Terms:** Publisher hereby objects to any terms contained in any purchase order, acknowledgment, check endorsement or other writing prepared by you, which terms are inconsistent with these terms and conditions or CCC's Billing and Payment terms and conditions. These terms and conditions, together with CCC's Billing and Payment terms and conditions (which are incorporated herein), comprise the entire agreement between you and publisher (and CCC) concerning this licensing transaction. In the event of any conflict between your obligations established by these terms and conditions and those established by CCC's Billing and Payment terms and conditions, these terms and conditions shall control.

14. **Revocation:** Elsevier or Copyright Clearance Center may deny the permissions described in this License at their sole discretion, for any reason or no reason, with a full

refund payable to you. Notice of such denial will be made using the contact information provided by you. Failure to receive such notice will not alter or invalidate the denial. In no event will Elsevier or Copyright Clearance Center be responsible or liable for any costs, expenses or damage incurred by you as a result of a denial of your permission request, other than a refund of the amount(s) paid by you to Elsevier and/or Copyright Clearance Center for denied permissions.

LIMITED LICENSE

The following terms and conditions apply only to specific license types:

15. Translation: This permission is granted for non-exclusive world **English** rights only unless your license was granted for translation rights. If you licensed translation rights you may only translate this content into the languages you requested. A professional translator must perform all translations and reproduce the content word for word preserving the integrity of the article. If this license is to re-use 1 or 2 figures then permission is granted for non-exclusive world rights in all languages.

16. Website: The following terms and conditions apply to electronic reserve and author websites:

Electronic reserve: If licensed material is to be posted to website, the web site is to be password-protected and made available only to bona fide students registered on a relevant course if:

This license was made in connection with a course,

This permission is granted for 1 year only. You may obtain a license for future website posting,

All content posted to the web site must maintain the copyright information line on the bottom of each image,

A hyper-text must be included to the Homepage of the journal from which you are licensing at <http://www.sciencedirect.com/science/journal/xxxxx> or the Elsevier homepage for books at <http://www.elsevier.com> , and

Central Storage: This license does not include permission for a scanned version of the material to be stored in a central repository such as that provided by Heron/XanEdu.

17. Author website for journals with the following additional clauses:

All content posted to the web site must maintain the copyright information line on the bottom of each image, and

the permission granted is limited to the personal version of your paper. You are not allowed to download and post the published electronic version of your article (whether PDF or HTML, proof or final version), nor may you scan the printed edition to create an electronic version,

A hyper-text must be included to the Homepage of the journal from which you are licensing at <http://www.sciencedirect.com/science/journal/xxxxx> , As part of our normal production process, you will receive an e-mail notice when your article appears on Elsevier's online service ScienceDirect (www.sciencedirect.com). That e-mail will include the article's Digital Object Identifier (DOI). This number provides the electronic link to the published article and should be included in the posting of your personal version. We ask that you wait until you receive this e-mail and have the DOI to do any posting.

Central Storage: This license does not include permission for a scanned version of the

material to be stored in a central repository such as that provided by Heron/XanEdu.

18. **Author website** for books with the following additional clauses:

Authors are permitted to place a brief summary of their work online only.

A hyper-text must be included to the Elsevier homepage at <http://www.elsevier.com>

All content posted to the web site must maintain the copyright information line on the bottom of each image

You are not allowed to download and post the published electronic version of your chapter, nor may you scan the printed edition to create an electronic version.

Central Storage: This license does not include permission for a scanned version of the material to be stored in a central repository such as that provided by Heron/XanEdu.

19. **Website** (regular and for author): A hyper-text must be included to the Homepage of the journal from which you are licensing at

<http://www.sciencedirect.com/science/journal/xxxxx>. or for books to the Elsevier homepage at <http://www.elsevier.com>

20. **Thesis/Dissertation**: If your license is for use in a thesis/dissertation your thesis may be submitted to your institution in either print or electronic form. Should your thesis be published commercially, please reapply for permission. These requirements include permission for the Library and Archives of Canada to supply single copies, on demand, of the complete thesis and include permission for UMI to supply single copies, on demand, of the complete thesis. Should your thesis be published commercially, please reapply for permission.

21. **Other Conditions**:

v1.6

Gratis licenses (referencing \$0 in the Total field) are free. Please retain this printable license for your reference. No payment is required.

If you would like to pay for this license now, please remit this license along with your payment made payable to "COPYRIGHT CLEARANCE CENTER" otherwise you will be invoiced within 48 hours of the license date. Payment should be in the form of a check or money order referencing your account number and this invoice number RLNK10894678.

Once you receive your invoice for this order, you may pay your invoice by credit card. Please follow instructions provided at that time.

**Make Payment To:
Copyright Clearance Center
Dept 001
P.O. Box 843006
Boston, MA 02284-3006**

If you find copyrighted material related to this license will not be used and wish to cancel, please contact us referencing this license number 2562601259333 and noting

the reason for cancellation.

Questions? customercare@copyright.com or +1-877-622-5543 (toll free in the US) or +1-978-646-2777.

3. First author papers

(i) (From Chapter 3)

Byrne S, Cheent A, Dimond J, Fisher G and Ockleford, CD (2001) Immunocytochemical localisation of a caveolin-1 isoform in human term extra-embryonic membranes using confocal laser scanning microscopy: Implications for the complexity of the materno-fetal junction. *Placenta*, **22**: 499-510.

(ii) (From chapter 4)

Byrne S, Ahenkorah J, Hottor B, Lockwood C and Ockleford CD (2007) Immuno-electron microscopic localisation of Caveolin-1 in human placenta. *Immunobiology*, **212**: 39-46.

(iii) (From Chapter 6)

Byrne S, Challis E, Williams JLR, Pringle JH, Hennessey JM and Ockleford CD

(2010) A mosaic layer in human pregnancy. *Placenta*, **31**: 373-379.

4. Second author paper (From Chapter 5)

Smith RK, Ockleford CD, Byrne S, Bosio P and Sanders R. (2004) Healthy and pre-eclamptic basal plate lining cells: Quantitative comparisons based on confocal laser scanning microscopy. *Microscopy Research and Technique*, **64**: 54-62.

Immunocytochemical Localization of a Caveolin-1 Isoform in Human Term Extra-embryonic Membranes Using Confocal Laser Scanning Microscopy: Implications for the Complexity of the Materno–fetal Junction

S. Byrne, A. Cheent, J. Dimond, G. Fisher and C. D. Ockleford^a

Advanced Light Microscope Facility, Department of Pre-Clinical Sciences, Leicester Warwick Medical School, University Road, Leicester, LE1 9HN, UK

Paper accepted 23 March 2001

This immunochemical, immunocytochemical, histological and ultrastructural study demonstrates the presence of caveolin 1 in a number of locations in term human extra-embryonic membranes. Strong expression was observed in fetal blood vessel endothelial cells of chorionic villi (cv) and in cv, amniotic and chorionic plate mesenchymal cells, but weak expression was characteristic of trophoblast. Expression in the amniotic epithelium indicated a stronger association with apical as opposed to baso-lateral membranes. Strong immunoreactivity in the thin lining layer of the maternal blood space of the basal plate was a surprising finding. Previously defined as trophoblast, we argue that this is at least partly endothelium based on this new histological, ultrastructural and immunocytochemical data.

© 2001 Harcourt Publishers Ltd

Placenta (2001), 22, 499–510

INTRODUCTION

Directed transport of material enclosed within vesicles is of potential importance in endocytic, secretory and transepithelial transport processes. In the study of the human placenta where these processes are obviously of paramount importance, emphasis has previously been placed on the receptor-mediated uptake and transport of compounds in coated pits and vesicles where the major coat protein is clathrin heavy chain (Ockleford, 1976; Ockleford and Whyte, 1977). Caveolae (Yamada, 1955), which are prominently expressed in endothelial cells, have a similar size (50–100 nm diameter) and shape to clathrin-coated micropinocytic vesicles and also appear in some situations to mediate the uptake of proteins and other molecules (Montesano et al., 1982). Since the 'placental barrier' is a multilayered structure histologically, it is important to establish if and where such vesicles exist on the transplacental transport route.

The major family of proteins associated with caveolae, the caveolins (Rothberg et al., 1992), are smaller than clathrin, and the ultrastructural appearance of the cytosolic face of their membrane is less substantial. However like clathrin, caveolin is capable of oligomeric complex formation (Sargiacomo et al., 1995) and it is these complexes which are thought, in part, to give rise to the fine spiral threads which surround caveolae.

^a To whom correspondence should be addressed.

Sharing sequence identity with the protein VIP 21 (Glenney, 1992) caveolin-1 is a GPI-linked transmembrane protein (Lisanti et al., 1994; Li et al., 1996). As well as its localization to cell-surface caveolae, caveolin is found in association with the trans-Golgi network region and contributes to apical and basal transport pathways (Kurzychalia et al., 1992). Biochemically the caveolins include three forms encoded by three independent and separate genes (Tang et al., 1996). They are denoted caveolins 1, 2 and 3. Caveolin-3 is a distinct isoform apparently restricted to muscle cells (Song et al., 1996). Caveolin-2 is predominantly found in adipocytes, though it is probably the most ubiquitous of the three. Caveolin-1 is similarly widespread in its distribution, but is most strongly expressed in endothelial cells, fibroblasts, and smooth muscle (Scherer et al., 1997). Co-expression of two or occasionally all three caveolins by single cells has been reported elsewhere (Scherer et al., 1997). Two isoforms of caveolin-1 result from the use of alternative start sequences. The full-length form is the α isoform whereas the β isoform is the shorter translation product (Scherer et al., 1995).

In order to localize α and β forms of caveolin-1 in human extraembryonic membranes, we employed an indirect immunofluorescence protocol and Western blot analysis. Correlative scanning and transmission electron microscopy were used to visualize caveolae and to provide support for the interpretations based on the immunocytochemistry. This paper describes our findings.

MATERIALS AND METHODS

Tissue

A series of 13 human placentae, fetal membranes and umbilical cord specimens were obtained from Leicester Royal Infirmary Maternity Unit following either natural childbirth or elective caesarean section. Tissue for immunocytochemical studies was immersed in OCT cryo-embedding medium (Miles, Elkhart, IL, USA) and frozen-fixed in a slush of solid CO₂ and hexane, within minutes of delivery. Blocks were sectioned at 8–12 µm using a Leitz cryomicrotome. Sections were fixed in freshly prepared 3 per cent paraformaldehyde in phosphate-buffered saline (PBS; 10 mM phosphate buffer, 0.8 per cent NaCl, pH 7.3).

Immunocytochemistry

Frozen sections were exposed for 18 h at 4°C to a 1:100 dilution of the primary antibody in PBS containing 20 per cent non-immune goat serum. This was a rabbit polyclonal anti-human caveolin-1 (Cat. No. C13630 Transduction Laboratories, Lexington, UK). Following three 10-min PBS washes, sections were exposed to the FITC-conjugated second step antibody, a goat anti-rabbit IgG (Cat. No. F-1262, Sigma, Poole, UK), diluted 1:200 in PBS containing 20 per cent non-immune goat serum, for up to 2 h at 20°C. Finally three 10-min washes in PBS were followed by mounting under a No. 0 coverslip in a photobleach retardant, glycerol-based mountant (Citifluor, Canterbury, UK).

Immunoblotting

Samples of the following tissues: amnion, chorion, amnio-chorion, basal plate, chorionic plate, chorionic villi and umbilical cord were obtained following three deliveries of healthy babies. The tissues were rinsed in PBS, scissor-minced and frozen in liquid nitrogen prior to comminution using a pre-cooled mortar and pestle. An endothelial cell extract used as a positive control sample was supplied with the primary antibody. Digestion used Laemmli sample buffer (Laemmli, 1970), with or without β-mercaptoethanol. Samples were diluted to give a final protein concentration of 1 mg/ml. Then 25 µl aliquots of these protein solutions were loaded onto a 5–20 per cent polyacrylamide gradient gel. This was cast in the laboratory using a two-chamber gradient mixer containing at the outset solutions of 5 and 20 per cent acrylamide respectively both of these solutions were diluted from a 40 per cent stock solution of acrylamide (Sigma, Poole, UK) containing 1.067 per cent bis-acrylamide (BDH, Loughborough, UK). A standard molecular mass reference track was used. The proteins were transferred onto nitrocellulose using a semi-dry blotting system. Transfer was assured using Ponceau S staining and non-specific IgG binding sites were blocked using 5 per cent non-fat milk, 1 per cent bovine serum albumin, 0.5 M

glucose and 2.5 per cent glycerol in Tris-buffered saline/Tween (TBS-T; 10 mM Tris/HCl, 0.8 per cent NaCl, 0.1 per cent Tween-20, pH 7.6). Immunoreactivity was tested using a 1:10 000 dilution of the primary antibody (*vid. sup.*) in blocking buffer. After three 10-min washes in TBS-T, the blot was incubated with a 1:50 000 dilution of a peroxidase-conjugated mouse monoclonal anti-rabbit IgG (A-2074, Sigma, Poole, UK), in blocking buffer for a further 90 min at room temperature. After three 10-min washes in TBS/T, a chemiluminescent substrate (Pierce Super Signal) was applied to the blot, and visualized using Fuji medical x-ray film. After development, the films were scanned and the digital images processed using Biosoft Quantiscan software to estimate the molecular weights of the component polypeptides.

Fluorescence microscopy

Sections were viewed using a Zeiss epifluorescence microscope equipped with standard filter sets to check for FITC fluorescence. Favourable sections were further examined using a confocal laser scanning attachment (Biorad MRC 600) linked to a Zeiss Axiovert epifluorescence microscope. This equipment utilized a reverse light path fibre-optic channelled Nomarski DIC signal to the second detector, to allow comparison of immunofluorescent and refractive index (RI) related images of the same specimen. The relationship between specimen RI and dry mass makes this a useful measure of the selectivity of the immunostaining. Images were recorded using Biorad Comos software and exported to Adobe Photoshop for labelling and print production.

Semi-thin (0.5 µm) section light microscopy and transmission electron microscopy

Basal plate was immersion fixed with 2.5 per cent glutaraldehyde in phosphate buffer for 1 h at room temperature. The tissue was cut into smaller pieces (3 × 1 × 1 mm) and post-fixed in 1 per cent aqueous osmium tetroxide. After a thorough wash in water, it was dehydrated through an ethanol series, transferred to 1,2-epoxypropane, and embedded in Araldite resin. Semi-thin (0.5 µm) sections were collected on glass slides, baked to increase adhesion, and stained with a mixture of 1 per cent toluidine blue and 2 per cent basic fuchsin in borax. After washing and coverslipping in a synthetic mountant (DPX), the sections were viewed and photographed using a Leitz Diaplan microscope equipped with a Vario-Orthomat camera system. A Zeiss X-100 objective was used, and the images recorded on Kodak Technical-Pan film, with the film speed set at 32 ASA, 16 DIN. After 10 min development at 20°C in 1:20 Acutol (Paterson, Tipton, UK) the film was enlarged and printed on resin-coated paper. A montage covering a linear stretch of the putative endothelial lining of the maternal blood space was produced, and a small area that included an anchoring villus (which interrupts the

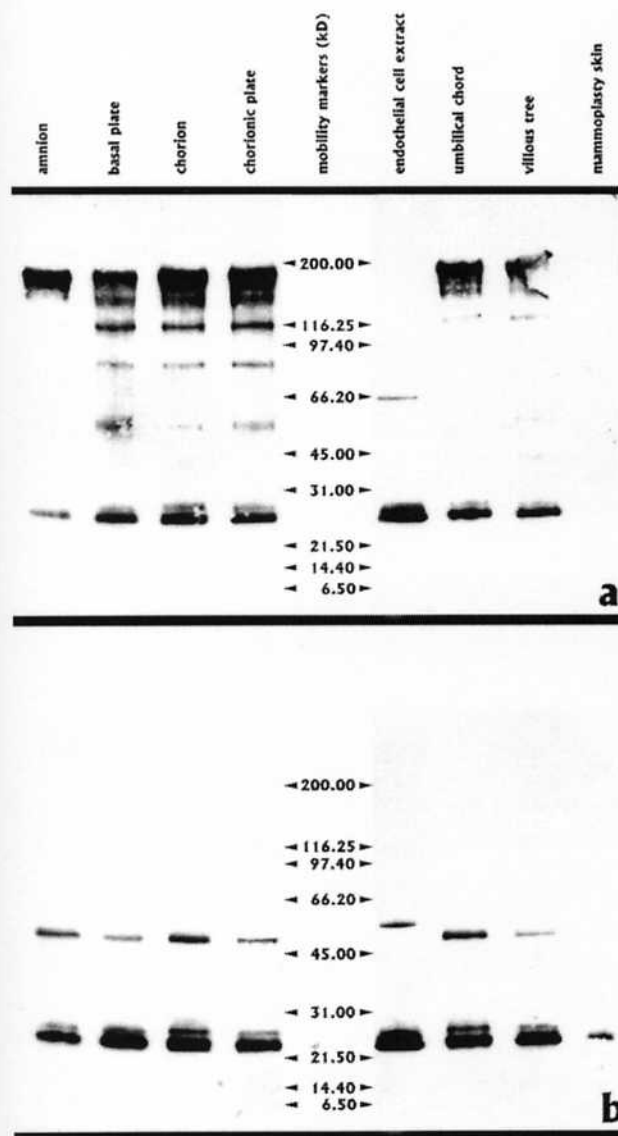


Figure 1. An immunoblot using the anti-caveolin antibody to define immunoreactive polypeptides in protein extracts of amnion, chorion and basal plate of human term fetal membranes and an extract of endothelial cells provided by the commercial supplier. Panel (A) shows the Western blot of the proteins run in unreduced form and panel (B) shows the reduced proteins following treatment with 5 per cent mercaptoethanol.

endothelium) was selected for ultrathin sectioning. These latter sections were cut at a thickness of 50–80 nm (silver or pale gold) and picked up on 200-mesh carbon/formvar coated nickel grids, stained with uranyl acetate and lead citrate, and viewed in a Siemens 102 electron microscope.

Scanning electron microscopy

Samples for scanning electron microscopy were fixed initially by injecting sites on the basal plate with 2.5 per cent glutar-

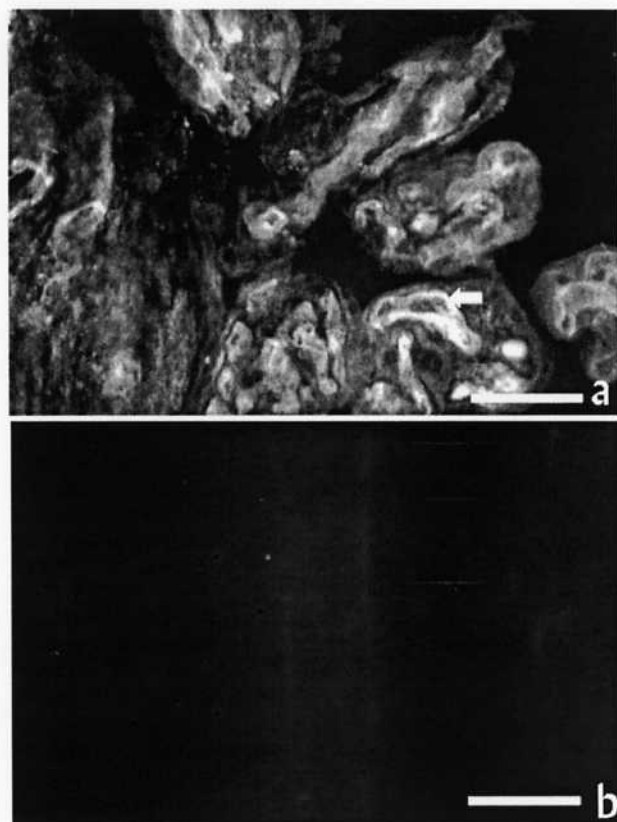


Figure 2. (A) A frozen section of mid-cotyledonary term placental chorionic villi. Indirect immunofluorescence using anti-caveolin antibody. The endothelial cells of the villus core are intensely immunoreactive (←), the mesenchymal cells faintly so and the trophoblast barely more reactive than the background level of non-specific staining. Scale bar=50 μm. (B) A similar section processed identically but without the specific anti-caveolin antibody. Following identical photographic protocols there is virtually no evidence of non-specific staining in this control sample. Scale bar=50 μm.

aldehyde in 0.1 M phosphate buffer. The fixative was also applied to the exposed surface itself, to prevent drying. When the tissue had hardened a little, a very thin layer of basal plate was dissected and pinned onto an inert elastomer substrate, with the inner surface uppermost. Fixation was continued for 1 h. After washing in water, the tissue was post-fixed in 1 per cent aqueous osmium tetroxide, dehydrated through an ethanol series, transferred to absolute acetone and critical-point dried. A thin layer of gold/palladium was sputter-coated onto the specimens, which were then viewed in a Hitachi F-3000 H scanning electron microscope, using a 5 kV accelerating voltage. Digital images were stored on disc, and printed from Adobe Photoshop.

RESULTS

Immunocytochemistry

The immunoblot of the unreduced polypeptides isolated from term extra-embryonic membranes shown in Figure 1 confirms

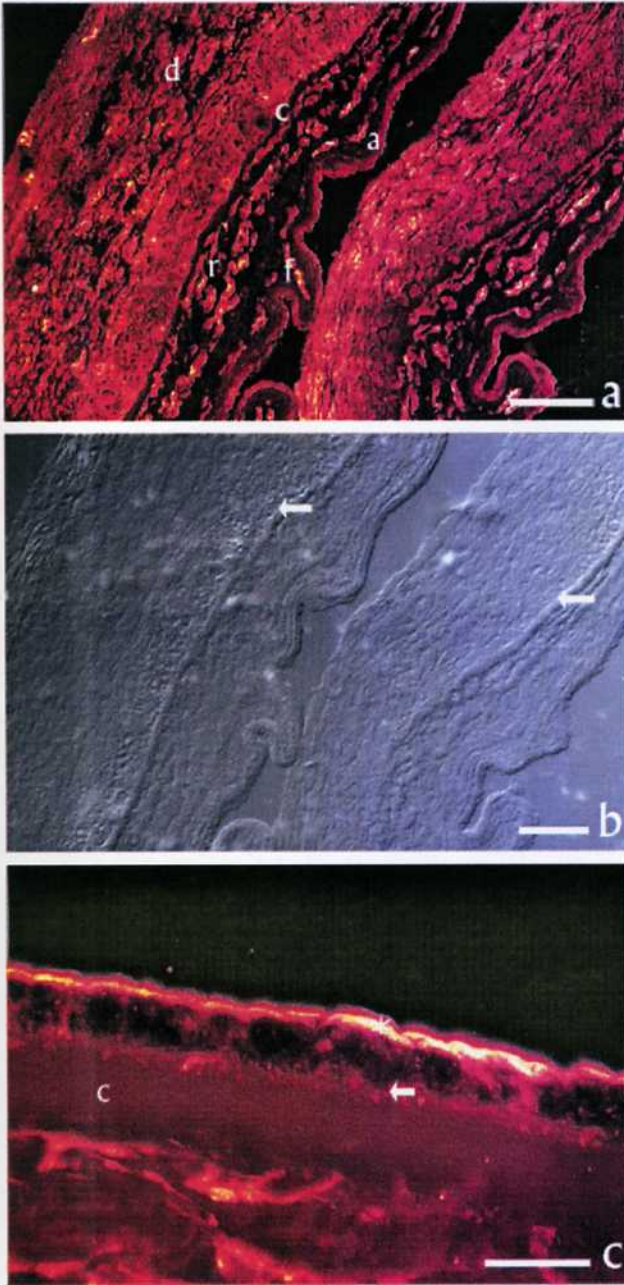


Figure 3. (A) A frozen section of a human term amniochorion roll revealing two complete layers of amnion (a), chorion (c) and decidua (d). Indirect immunofluorescence was accomplished using anti-caveolin antibody. The most immunoreactive cells are the mesenchymal layers—the fibroblast (f) and reticular (r) layers. The amniotic epithelium and decidua are both more immunoreactive than the trophoblast layers. Essentially all the immunolabelling is cellular. Scale bar=100 μ m. (B) Nomarski Differential Interference Contrast micrograph of the frozen section showed in (a). The image reflects the variation in refractive index and dry mass of the section and can be used to judge the specificity of the labelling which is concentrated at particular locations within the tissue. The chorion laeve basal lamina (\leftarrow) is of greater dry mass than the surrounding tissue, but in (A) shows no evidence of immunoreactivity. Scale bar=100 μ m. (C) Extended focus projection of 15 consecutive images through a frozen section of human term amnion prepared using anti-caveolin primary antibody in an indirect immunofluorescence protocol. The labelling is intense in the apical region of the simple cuboidal amniotic epithelium (*), but interestingly there is basal and baso-lateral immunoreactivity also which is clearly visible in the basal membrane infoldings (\leftarrow). Immunoreactive cells of the fibroblast layer are separated from the amniotic epithelium by the acellular compact layer (c). The labelling of the former is punctate in places and may indicate the presence of separated vesicles. Scale bar=25 μ m.

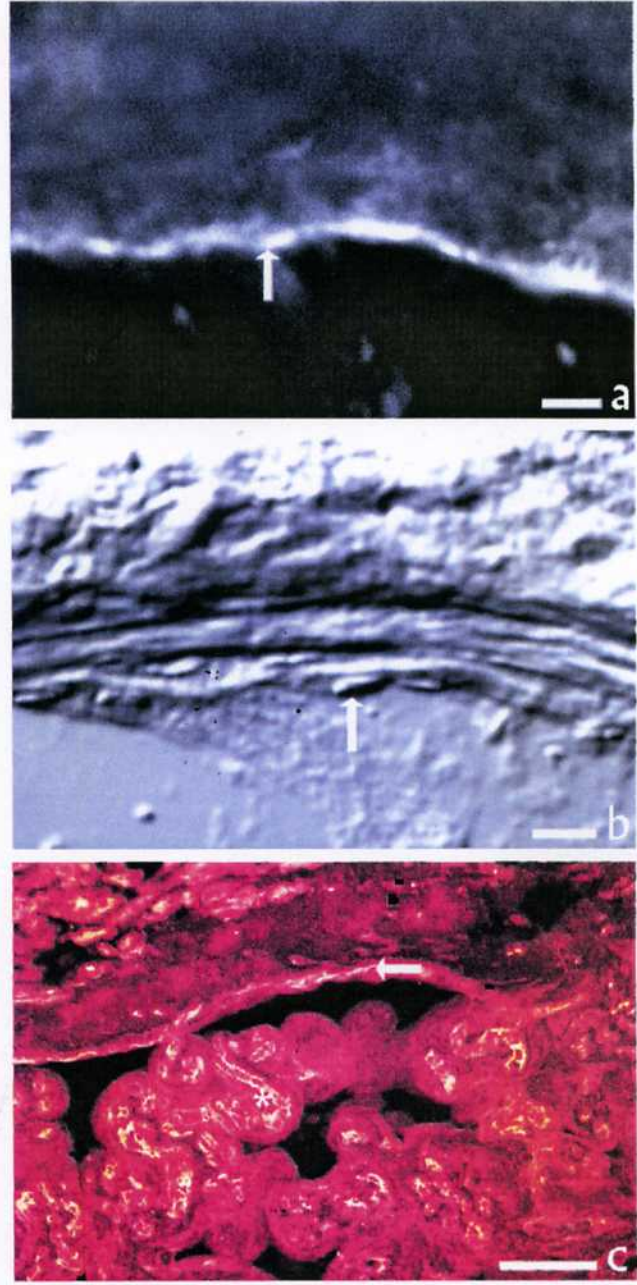


Figure 4. (A) Term human placenta basal plate anti-caveolin immunocytochemistry. The thin bright line of immunofluorescence (\leftarrow) is coincident with the lining of the maternal inter-villous space which is filled with maternal blood in vivo. Placental morphologists have previously described this layer as being syncytiotrophoblastic. Scale bar=10 μ m. (B) The same area of the section viewed in (A) but imaged using Nomarski DIC microscopy. The morphology of the lining cells associated with the strong immunofluorescence appears similar to endothelium (\leftarrow). Scale bar=10 μ m. (C) At lower magnification, revealed using the false colour look-up table (LUT) autumn, it can be seen that the intensity of anti-caveolin immunofluorescence in the basal plate is greatest at the margins of the intervillous space (\leftarrow) and the intensity of the lining cells matches that of the sinusoidal capillary wall cells in the chorionic villi (*). The chorionic villus syncytiotrophoblast on the other hand exhibits lower intensity of fluorescence. Scale bar=100 μ m.

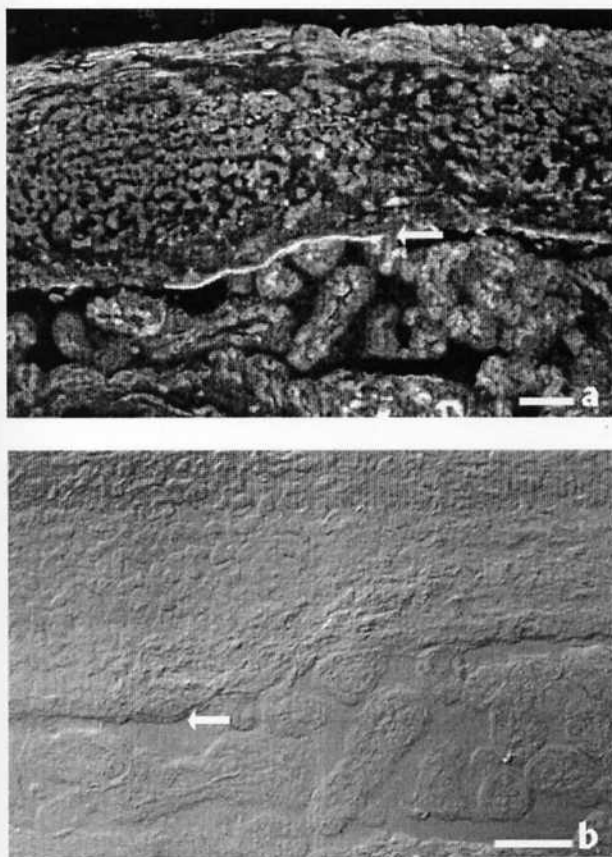


Figure 5. (A) Term human placental basal plate frozen section. This indirect immunofluorescence micrograph shows the pattern of anti-caveolin immunoreactivity. The villus tree towards the bottom of the micrograph show strong immunofluorescence in the cores of the villi overlying the endothelia of blood vessels, but low fluorescence in the trophoblast. The narrow layer of the basal plate immediately adjacent to the intervillus space is intensely immunofluorescent (\leftarrow), similar to the chorionic villus endothelial cells, but much brighter than syncytiotrophoblast of chorionic villi. Some immunoreactivity of decidual cells is also observed. Scale bar=100 μ m. (B) The same area of tissue as shown in (A) imaged using Nomarski DIC optics to reveal the dry mass distribution of the tissue. The organization of the basal plate region and adjacent chorionic villi are clearly demonstrated and a unicellular epi/endothelial morphology (\leftarrow) is seen in the lining of the intervillus space (maternal blood sinus). Scale bar=100 μ m.

the specificity of the antibody to a limited number of polypeptides with apparent relative molecular masses of 22–24 kD and simple multiples thereof. This pattern most probably reflects the ability of these molecules to oligomerize up to at least the hexamer state [Figure 1(A)]. When reduced, the reactive species are limited to the lowest molecular weight forms. These include the putative monomeric isoforms α and β and a β -mercaptoethanol resistant dimeric form that is also preserved under these conditions [Figure 1(B)]. There is a distinct but small difference in the apparent molecular weight of the putative dimeric form when the fetal-derived samples are compared with the supplied endothelial cell extract from adult tissue. This difference in mobility was eliminated when care was taken to ensure precise equivalence of the conditions of solubilization of all the protein samples.

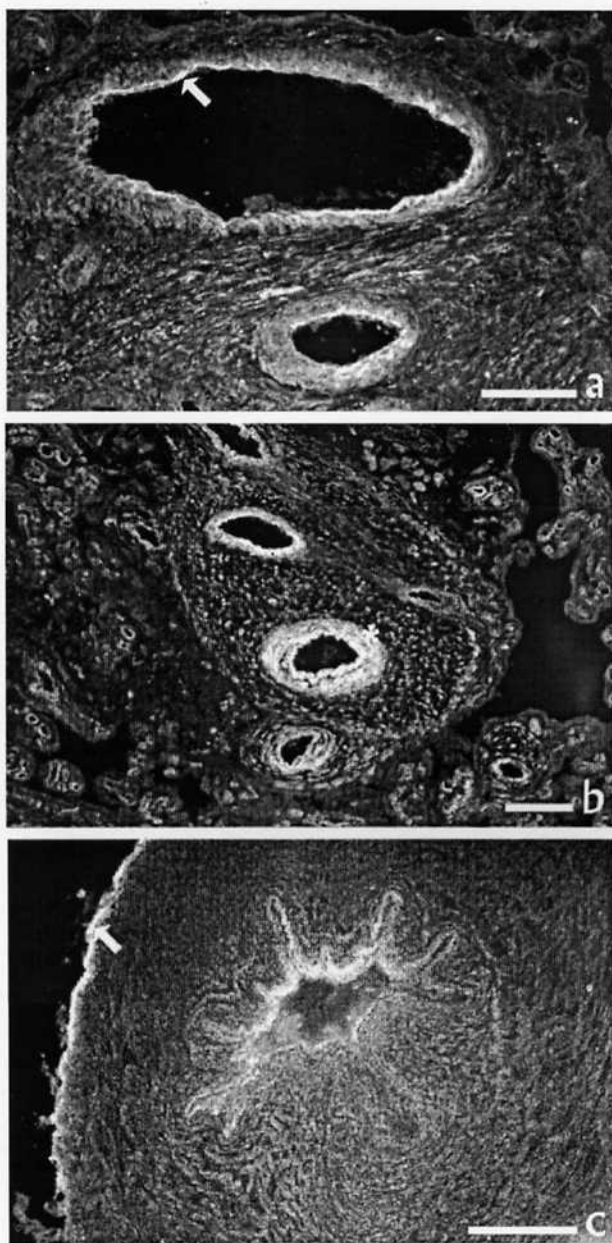
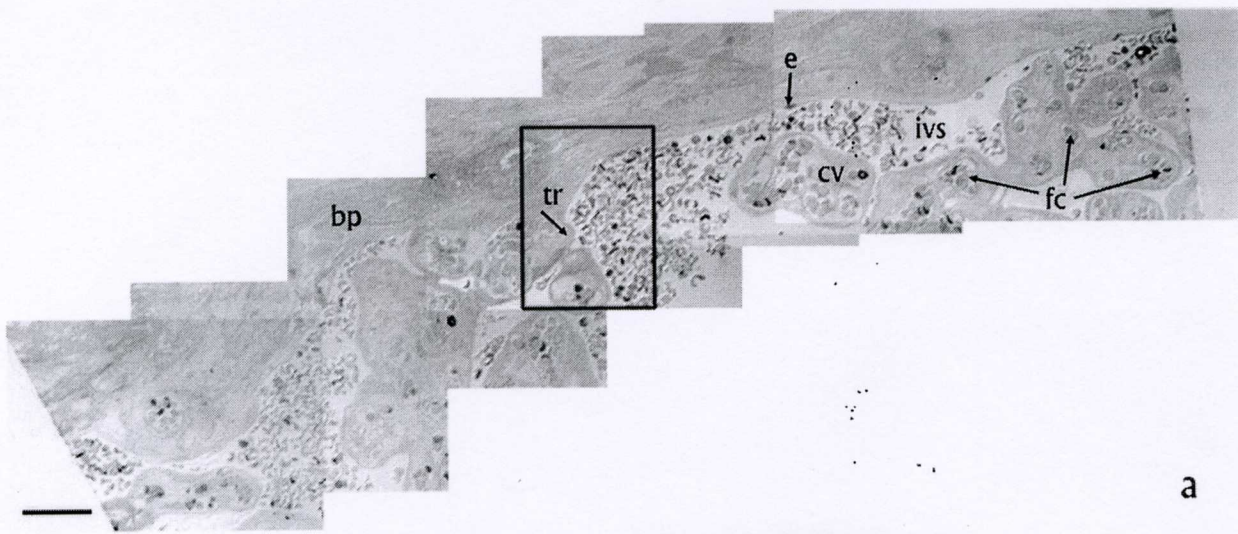


Figure 6. (A) Term human placental chorionic villus showing oblique sections through fetal arterial and venous blood vessels. The frozen section has been exposed to anti-caveolin antibody in an indirect immunofluorescence protocol. The intima of the fetal vessel walls are extensively immunoreactive (\leftarrow). Scale bar=100 μ m. (B) Frozen section of a stem villus close to the chorionic plate prepared using anti-caveolin antibody in an indirect immunofluorescence protocol. The endothelial cells of the transversely sectioned vessels (*) and the surrounding smooth muscle cells are labelled more intensely than the mesenchymal cells of the core. Least labelling is seen in the trophoblast. Scale bar=100 μ m. (C) Frozen section of human term placental umbilical cord prepared for indirect immunofluorescence microscopy. Anti-caveolin immunoreactivity is predominant in the amniotic epithelial sleeve externally (\leftarrow), and in the walls of the large diameter umbilical blood vessels, particularly in the intimal layer. The mesenchymal cells of Wharton's jelly are less intensely labelled. Scale bar=250 μ m.



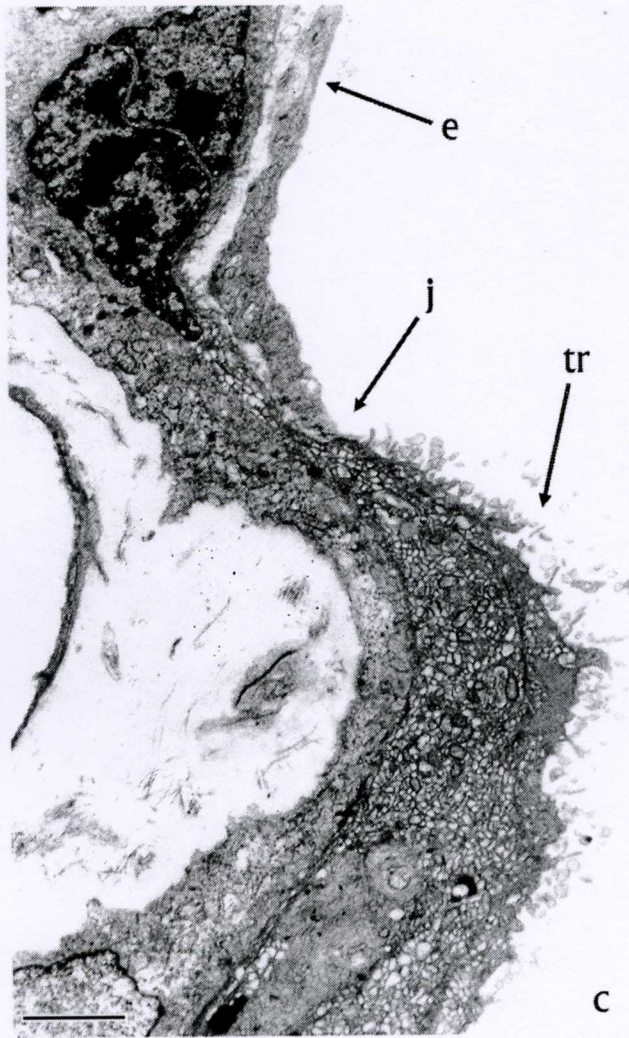
a

50



b

25



c

2

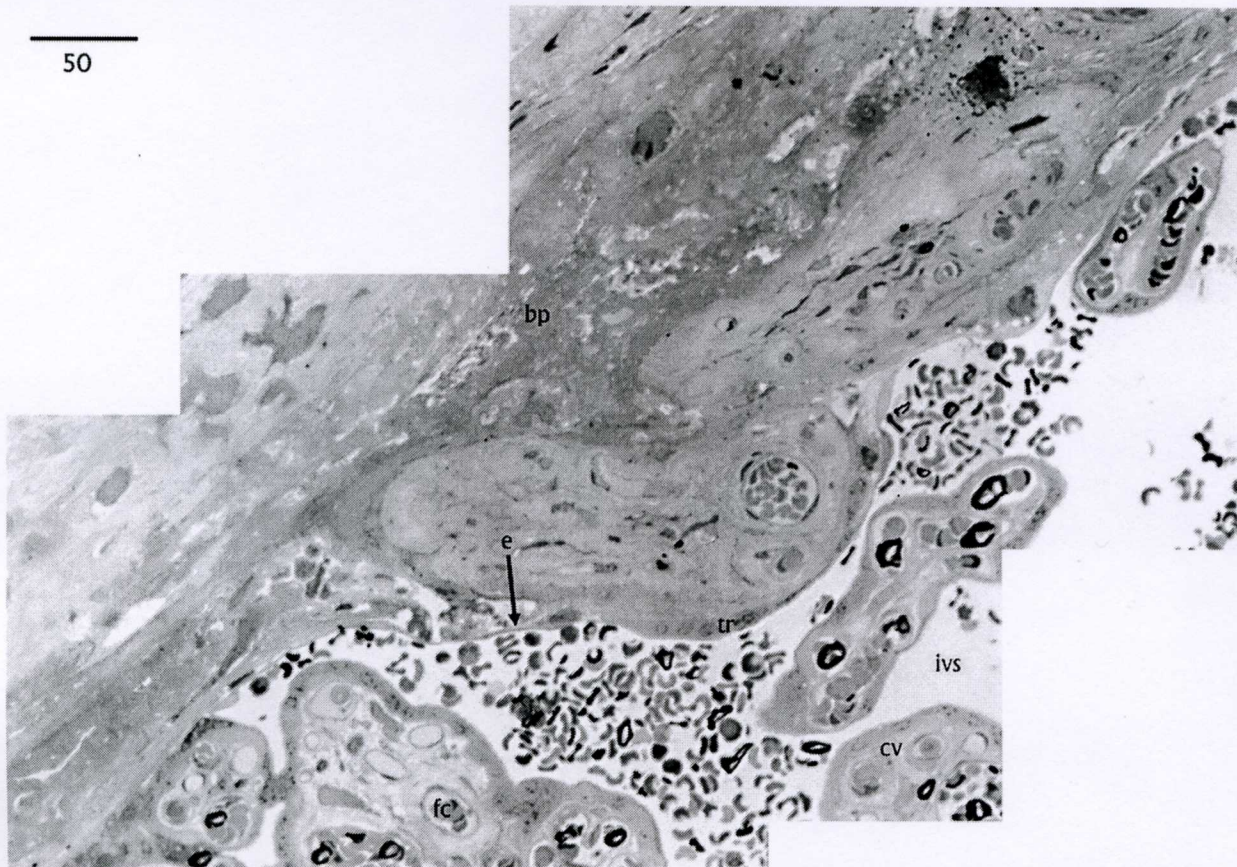


Figure 8. Semi-thin section of basal plate (bp) showing the attachment point of an anchoring villus. A clear transition from trophoblast (tr) to endothelial (e) morphology is apparent. Within the intervillous space (ivs) are sectioned chorionic villi (cv) revealing the fetal vessels (fc) of the villus core. Scale bar=50 μ m.

Immunocytochemistry

The immunofluorescence patterns were consistent and specific as determined by comparison with the negative control preparations containing an excess of non-immune same-species serum. Immunoreactive sites were mapped in the chorionic villus tree (Figures 2, 4 and 6) and these were semiquantitated using line scans of fluorescence intensity (Figure 11), amniochorion (Figure 3) basal plate (Figures 4 and 5), chorionic plate and umbilical cord (Figure 6). The mesenchymal cells of the amnion and chorion were considerably more immunoreactive than the amniotic epithelium and clearly more-so than the decidua basalis and parietalis [Figure 3(C)]. There was a pattern of cytological distribution observed in extended focus images of amniotic epithelial cells which

showed strong apical labelling (punctate in places) and baso-lateral labelling particularly in the basal projections into the underlying basal lamina. The amniotic epithelium was more immunoreactive than the chorion laeve trophoblast epithelium, which showed the lowest intensity of any cellular layer. The fluorescence intensity was low or undetectable in the trophoblast cells of the chorionic villi, but the endothelial cells of the chorionic villus core were strongly immunoreactive and the mesenchymal cells were also labelled but to a lesser extent than the endothelial cells. The chorionic plate was generally most immunoreactive in the mesenchymal layers, but the chorionic plate amniotic epithelium was also to some extent immunofluorescent. The lining layer of the intervillous space in the gaps between stem villi was not strongly immunofluorescent. Stem villi containing thicker-walled blood vessels

Figure 7. (A) Light micrograph of basal plate showing the putative endothelial lining of the maternal blood space(ivs) at this location. These cells (e) have the typical morphology of squamous cells, with their flattened, tapered nuclei, and very thin, extensive cytoplasm. Chorionic villi (cv) originating in the basal plate (bp) are only approached by this outer covering at their base; syncytiotrophoblast (tr) forms their outer covering at all other locations. Fetal capillaries (fc) are clearly discernible in the cores of the villi. Scale bar=50 μ m. (B) An higher magnification view of the boxed area in (a) that includes both syncytial and endothelial types of lining cells and the area where these two surfaces make contact. e, endothelium; j, junction; tr, trophoblast. Scale bar=25 μ m. (C) Electron micrograph showing the endothelial-like inner lining of the decidua of the basal plate corresponding to the boxed area in (B). Caveolae are a frequent feature of these cells and their ultrastructural appearance is almost identical to that seen in the vascular endothelium lining the villous capillaries. At the origin of the stem villi, the endothelial layer makes contact with syncytiotrophoblast and tight junctions are detectable. e, endothelium; j, junction; tr, trophoblast. Scale bar=2 μ m.

exhibited low levels of immunoreactivity in the medial smooth muscle layer (Figure 6) as did the umbilical cord. The umbilical cord also exhibited intense layers of immunofluorescence corresponding to the position of the cord amnion and intimal lining of umbilical vessels. A similar pattern of fluorescence was observed in the basal plate with generally low immunofluorescence but where the marginal layer to the intervillus space was evident, an intense immunoreactivity was present (Figure 4).

Ultrathin and semi-thin sections

Extensive areas of basal plate were examined in montages and high-resolution images of sections [Figure 7(A–C)]. These clearly demonstrated that the ultimate layer of the basal plate that made contact with the blood filling the inter-villus space was composed of two cell types. Associated with the distal portions of anchoring villi, one type of cells reflected onto the surface and bore similar characteristics to syncytiotrophoblast. They were apparently syncytial, bore extensive apical microvilli and contained nuclei that were irregular in outline and heterochromatic. A significant part of the surface of the blood space however was made up of cells rather typical of the cells expected to be forming the lining of a sinus. These bore the characteristic features of endothelium [Figure 12(A–C)]. They were thin, smooth surfaced and large in surface area. One substantial component of the limiting cell boundary was endothelial cells. It was repeatedly noted that the trophoblast and endothelial cells formed different parts of the same tissue layer. They made close contact edge to edge [Figures 7(C) and 12(C)] and appeared to form shared junctional organelles at their extremities.

Scanning electron microscopy

High resolution scanning electron microscope analysis of the internal surface of the basal plate allowed the characteristic differences between two cell types to be imaged [Figure 9(A–C)]. The endothelium was generally smooth but at a higher magnification [Figure 9(C)], the endothelial cell surfaces show many small depressions, some of which appear to penetrate the cell membrane. These are almost certain to be the caveolae which are so frequently observed in transmission electron microscope images of ultrathin sections. The trophoblastic component was indistinguishable from the syncytiotrophoblast on the surface of the chorionic villi. The trophoblast surface was densely covered with irregular microvilli [Figure 9(A,B)]. Areas where there were junctions between these two clearly distinct types of surface were observed close to the point of contact of anchoring villi with the basal plate [Figure 9(A)]. It is unlikely that the smooth areas interpreted below as endothelium are an artefact resulting from images of fibrin covering layers as these are morphologically distinct (Figure 10).

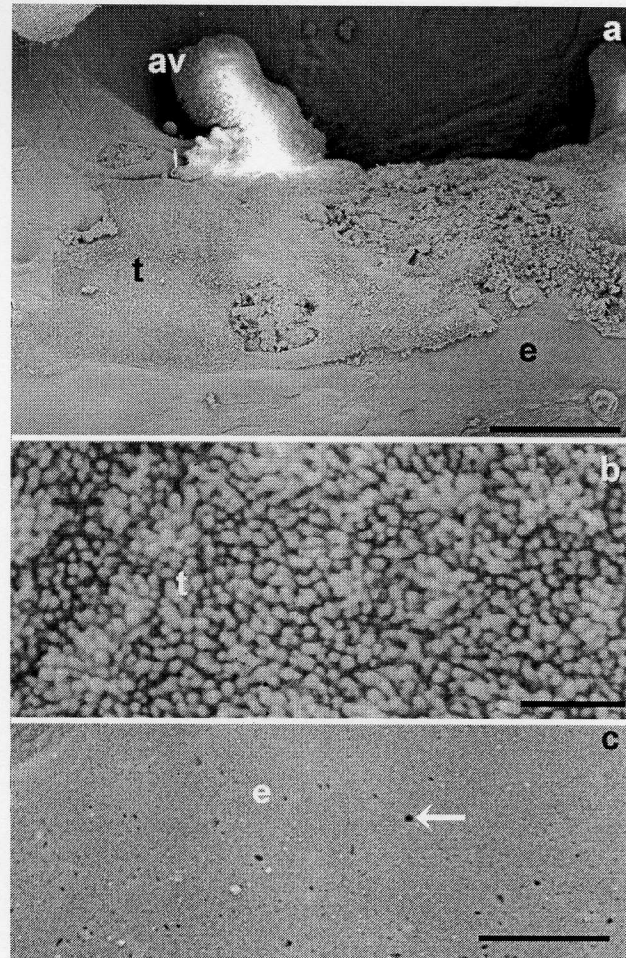


Figure 9. Scanning electron micrographs of the internal surface of the basal plate viewed as from the intervillus space. (A) The anchoring villi (av) are covered by syncytiotrophoblast that extend down onto the flattened surface to which it make contact. The surface is trophoblastic (t) and this is characteristically microvillous. Scale bar = 200 μm . (B) A portion of the surface of the basal plate coated with trophoblast (t). Note the microvillous surface. Scale bar = 10 μm . (C) Making edge to edge contact with trophoblast cells and lying in the same plane are much flatter cells bearing no microvilli. These have the morphological characteristics of endothelium (e) and contain small pits in the surface similar to caveolar apertures (arrow). Scale bar = 10 μm .

DISCUSSION

Variant caveolin-1 isoform?

The interpretation of the differing mobility of the putative form of caveolin-1 could have reflected:

- (1) an altered form of processing in the endothelial cells used;
- (2) a difference in preparative technique;
- (3) the expression of an altered molecular weight early 'fetal' form of the gene.

Re-running polyacrylamide gels using identical preparation conditions for solubilization of commercially supplied molecular weight marker protein and extra-embryonic proteins

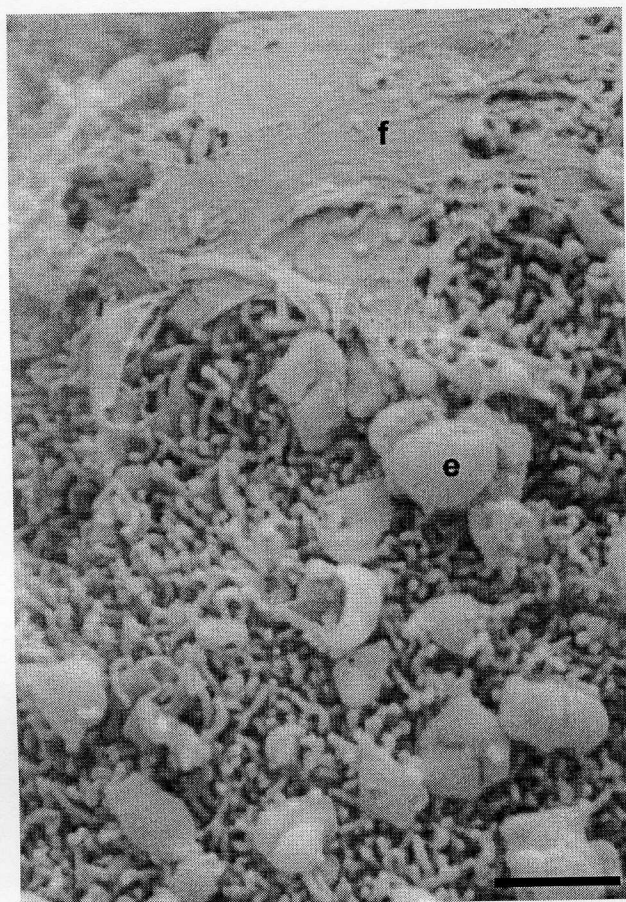


Figure 10. The deposition of fibrin can give a local flat coating over the surface of trophoblastic microvilli (f) as shown in this scanning electron micrograph. Fibrin fibres are usually visible at the edges of the plaques and the fibrin overlies the trophoblastic microvilli. As such they represent a morphologically distinct form easy to distinguish from the endothelium shown in Figure 9(C). Scale bar=5 μ m.

gave rise to a convergence in apparent molecular weight of the immunoreactive band. This ruled out options (1) and (3) and made option (2) the probable explanation for the discrepancy noted in the mobilities in Figure 1.

Distribution of the protein and its functional role

The role of caveolae as internalization intermediaries has been emphasized in the light of a historical association with studies of endocytosis (e.g. Benlimame et al., 1998) but some caveolae (for example those associated with the sarcolemma in striated muscle) appear to be more or less permanently associated with the cell surface (Ralston and Ploug, 1999). Clearly other roles are served and recent research has given greater emphasis to these (Shaul and Anderson, 1998). In the words of these reviewers 'Once the identification of the marker protein

caveolin made it possible to isolate and purify this specialized membrane domain it was discovered that caveolae also contain a variety of signal transduction molecules. This includes G protein-coupled receptors, G proteins and adenylyl cyclases, molecules involved in the regulation of intracellular Ca^{++} homeostasis, and their effectors including the endothelial isoform of nitric oxide synthase, multiple components of the tyrosine kinase-mitogen-activated protein kinase pathway and numerous lipid signalling molecules'. This list can be extended to include olfactory signalling (Schreiber et al., 2000), effects on motility, migration and metastasis (Galbiati et al., 1998; Galbiati et al., 1999; Segal et al., 1999; Zhang et al., 2000), participation in tight-junctions (Nusrat et al., 2000), a role in shear-stress signalling (Rizzo et al., 1998; Park et al., 2000), disease progression in tumours (Nasu et al., 1998; Yang et al., 1999) muscular dystrophy (Razani et al., 2000) and toxin uptake (Skretting et al., 1999). Apart from these one can cite evidence for caveolar participation in SV40 virus infection (Chen and Norkin, 1999), formation of the cleavage furrow in cytokinesis (Kogo and Fujimoto, 2000), prion infection (Naslavsky et al., 1999), membrane retrieval following exocytosis (Valentijn et al., 1999), multi-drug resistance (Yang et al., 1998; Ikezu et al., 1998), apoptosis suppression (Timme et al., 2000) and nuclear translocation of the VEGF receptor (Feng et al., 1999).

With respect to the low level of expression of caveolin in trophoblast described here, the downregulation of caveolin by oestradiol (synthesized in the trophoblast) and the positive regulation of the oestrogen receptor alpha are of interest (Schlegel et al., 1999; Pelligrino et al., 2000).

This study showed that a molecule sharing immunological identity with caveolin-1 is present in and is found at a number of locations in term human extraembryonic membranes. The most consistently strong expression is in the fetal blood vessel endothelial cells of the chorionic villi, and in fibroblasts in both amnion and chorion laeve. These two main sites of expression probably reflect differences in the type of transport processes being used by the two cell types. Fibroblasts, situated in comparative isolation from their neighbours, are highly biosynthetic cells that may need to exploit any mechanism that assists in the uptake of substrates from their surroundings. The possession of many caveolae on their cell surface has been described elsewhere (Röhlich and Allison, 1976; Bretscher and Whytock, 1977), and is confirmed in this study. In endothelial cells, on the other hand, the possession of caveolae is believed to subservise transendothelial transport purposes. Expression in trophoblast was generally low, but in mesenchymal cells of chorionic villi, amnion and chorion, generally high. Expression in the amniotic epithelium indicated a stronger association with apical as opposed to baso-lateral membranes. This association extended to the amniotic sleeve of the umbilical cord.

The most remarkable finding is a strong immunoreactivity in parts of the thin lining layer of the maternal blood space of the basal plate. This layer has previously been defined as entirely trophoblast (Boyd and Hamilton, 1970). Its

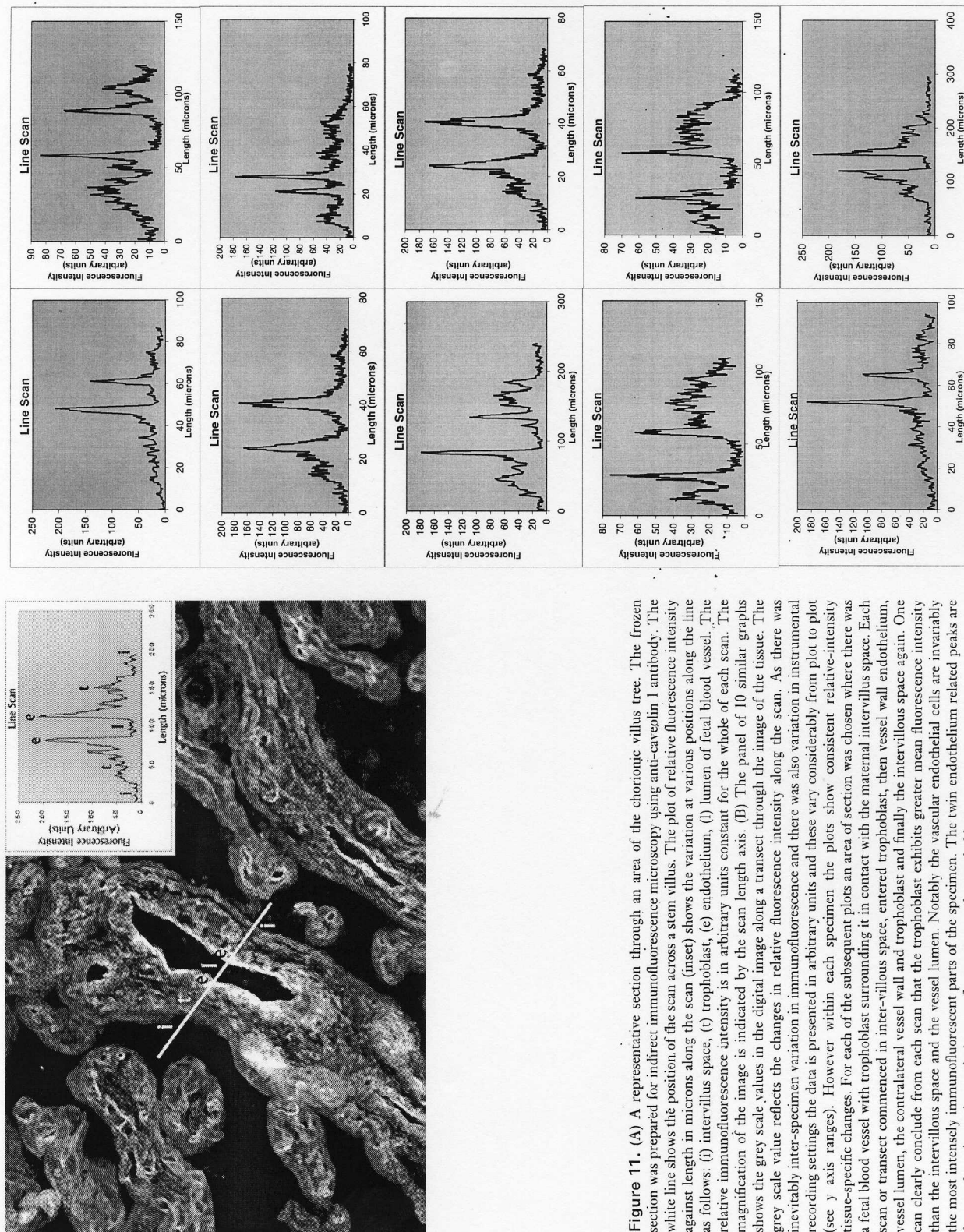


Figure 11. (A) A representative section through an area of the chorionic villus tree. The frozen section was prepared for indirect immunofluorescence microscopy using anti-caveolin 1 antibody. The white line shows the position of the scan across a stem villus. The plot of relative fluorescence intensity against length in microns along the scan (inset) shows the variation at various positions along the line as follows: (f) intervillous space, (t) trophoblast, (e) endothelium, (l) lumen of fetal blood vessel. The relative immunofluorescence intensity is in arbitrary units constant for the whole of each scan. The magnification of the image is indicated by the scan length axis. (B) The panel of 10 similar graphs shows the grey scale values in the digital image along a transect through the image of the tissue. The grey scale value reflects the changes in relative fluorescence intensity along the scan. As there was inevitably inter-specimen variation in immunofluorescence and there was also variation in instrumental recording settings the data is presented in arbitrary units and these vary considerably from plot to plot (see y axis ranges). However within each specimen the plots show consistent relative-intensity tissue-specific changes. For each of the subsequent plots an area of section was chosen where there was a fetal blood vessel with trophoblast surrounding it in contact with the maternal intervillous space. Each scan or transect commenced in inter-villous space, entered trophoblast, then vessel wall endothelium, vessel lumen, the contralateral vessel wall and trophoblast and finally the intervillous space again. One can clearly conclude from each scan that the trophoblast exhibits greater mean fluorescence intensity than the intervillous space and the vessel lumen. Notably the vascular endothelial cells are invariably the most intensely immunofluorescent parts of the specimen. The twin endothelium related peaks are frequently twice as intensely immunofluorescent as the trophoblast.

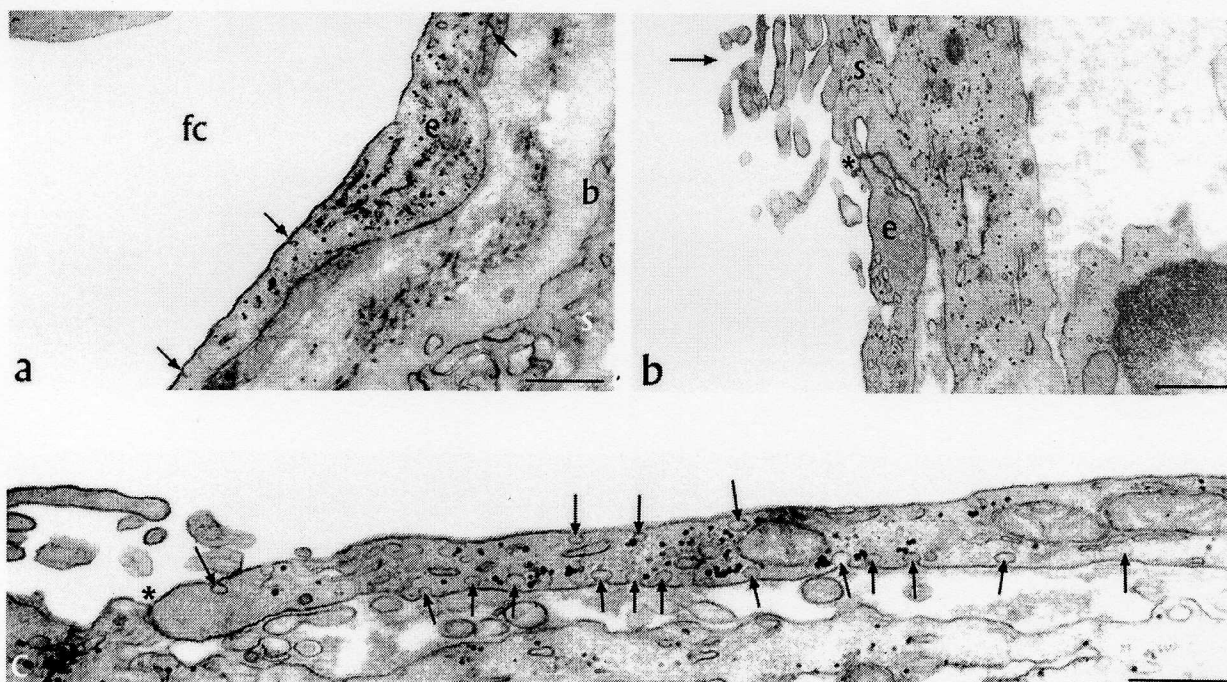


Figure 12. (A) A transmission electron micrograph of an ultrathin section of portion of a chorionic villus from a term placenta showing a fetal capillary (fc) adjacent to the syncytiotrophoblast (s) and its basal lamina (b). The endothelial cell (e) bounding the capillary is extremely similar to the basal plate cell with endothelial characteristics shown in (C). It contains electron dense glycogen and caveolae (arrows). Scale bar=0.5 μ m. (B) A region of basal plate syncytiotrophoblast cell surface is shown in this transmission electron micrograph (s). The basal plate trophoblast surface (arrow) is very different from that of the endothelial cells shown (e) in that it bears extensive microvilli and exhibits few if any caveolae. Note the junction between the cells (*) and the large number of caveolae in the endothelial cell as compared to the trophoblast. Scale bar= 0.5 μ m. (C) A transmission electron micrograph showing the inner lining of the basal plate where it bounds the intervillous space. Caveolae are a frequent feature of these cells and their ultrastructural appearance is indistinguishable from that seen in the vascular endothelium lining the villous capillaries. At the distal attachment of the anchoring villi to the basal plate the endothelial layer makes contact with the syncytiotrophoblast and intercellular junctions can be observed (*). The endothelial cells do not appear to have a basal lamina proper, but are typically seen in loose association with a strip of underlying material of moderate electron density staining characteristics. In the 3 μ m length of endothelium shown here, some 12 caveolae can be counted on the basal surface, compared to four on the apical surface (arrows). The ratio of apical to basal caveolae is not constant, however, nor is the overall frequency of caveolae in any particular linear stretch. Although many vesicles can be seen in the underlying syncytiotrophoblast shown here, there is no compelling evidence for the presence of any caveolae. If they are indeed present, they must be present at low frequency. Scale bar=0.5 μ m.

immunoreactivity as defined in this and other studies appears in places more typical of endothelium (Lang et al., 1993).

The morphology of basal plate inter-villous space lining cells

It is clear from careful morphological analysis that the cells lining the intervillous space are of two types and that these are probably endothelium and trophoblast respectively. This is probably the first report of horizontal-plane interaction between epithelial and mesenchymally derived cells in any naturally occurring human tissue. It is also conceivable that two distinct types of cells are derived from genetically different individuals. The trophoblast is said to be fetally derived. The

genetic origin of the endothelial cells is yet to be established but one strong possibility is that the endothelium has migrated from the maternal blood vessels supplying or draining the inter-villous space and is thus genetically maternal.

The existence of a mixed endo-epithelial simple squamous layer is a histological novelty. It is also intriguing, implying as it does that epithelial and mesodermal derivatives may associate edge-on to form a continuous membrane. If one were to anticipate the elucidation of their genetic origin as being maternal then it would be an exciting outcome. The trend over recent years of increase in our appreciation of the complex intermixing of cells at the materno-fetal junction would be further augmented by the realization that a materno-fetal mixed cellular layer lines the intervillous space basal plate.

ACKNOWLEDGEMENTS

CDO thanks the Wellcome Trust, The Royal Society and the Chinese National Academy of Natural Sciences for support. We are grateful to C. d'Lacey for his skilful assistance with preparation of the plates.

REFERENCES

- Benlimame N, Le PU & Nabi IR (1998) Localization of autocrine motility factor receptor to caveolae and clathrin-independent internalisation of its ligand to smooth endoplasmic reticulum. *Mol Biol of the Cell*, **9**, 1773–1786.
- Boyd JD & Hamilton WJ (1970) *The Human Placenta*. Cambridge: Heffer.
- Bretscher MS & Whytock S (1977) Membrane-Associated Vesicles in Fibroblasts. *J Ult Res*, **61**, 215–217.
- Chen Y & Norkin LC (1999) Extracellular simian virus 40 transmits a signal that promotes virus enclosure within caveolae. *Exp Cell Res*, **246**, 83–90.
- Feng Y, Venema VJ, Venema RC, Tsai N & Caldwell RB (1999) VEGF induces nuclear translocation of Flk-1/KDR, endothelial nitric oxide synthase, and caveolin-1 in vascular endothelial cells. *Biochem Biophys Res Comm*, **256**, 192–197.
- Galbiati F, Volonte D, Engelman JA, Watanabe G, Burk R, Pestell RG & Lisanti MP (1998) Targeted downregulation of caveolin-1 is sufficient to drive cell transformation and hyperactivate the p42/44 MAP kinase cascade. *EMBO Journal*, **17**, 6633–6648.
- Galbiati F, Volonte D, Engelman JA, Scherer PE & Lisanti MP (1999) Targeted down-regulation of caveolin-3 is sufficient to inhibit myotube formation in differentiating C2C12 myoblasts. Transient activation of p38 mitogen-activated protein kinase is required for induction of caveolin-3 expression and subsequent myotube formation. *J Biol Chem*, **274**, 30315–30321.
- Glenny JR (1992) The Sequence of Human Caveolin Reveals Identity with VIP21, a Component of Transport Vesicles. *FEBS Lett*, **314**, 45–48.
- Ikezu T, Ueda H, Trapp BD, Nishiyama K, Jing FS, Volonte D, Galbiati F, Byrd AL, Bassell G, Serizawa H, Lane WS, Lisanti MP & Okamoto T (1998) Affinity-purification and characterization of caveolins from the brain: Differential expression of caveolin-1, -2 and -3 in brain endothelial and astroglial cell types. *Brain Research*, **804**, 177–192.
- Kogo H & Fujimoto R (2000) Concentration of caveolin-1 in the cleavage furrow as revealed by time-lapse analysis. *Biochem Biophys Res Comm*, **268**, 82–87.
- Kurzchalia TV, Dupree P, Parton RG, Kellner R, Virta H, Lehnert M & Simons K (1992) VIP21, A 21-kD Membrane Protein is an Integral Component of *Trans*-Golgi-Network-Derived Transport Vesicles. *J Cell Biol*, **118**, 1003–1014.
- Laemmli UK (1970) Cleavage of Structural Proteins during the Assembly of the Head of Bacteriophage T4. *Nature*, **227**, 680–685.
- Lang I, Hartmann M, Blaschitz A, Dohr G, Skofitsch G & Desoye G (1993) Immunohistochemical Evidence for the Heterogeneity of Maternal and Fetal Vascular Endothelial Cells in Human Full-term Placenta. *Cell and Tissue Res*, **274**, 211–218.
- Li S, Song KS & Lisanti MP (1996) Expression and Characterization of Recombinant Caveolin. *J Biol Chem*, **271**, 568–573.
- Lisanti MP, Scherer PE, Tang Z-L & Sargiacomo M (1994) Caveolae, Caveolin, and Caveolin-rich Membrane Domains: a Signalling Hypothesis. *Trends in Cell Biology*, **4**, 231–235.
- Montesano R, Roth J, Robert A & Orci L (1982) Non-coated Membrane Invaginations are Involved in Binding and Internalization of Cholera and Tetanus Toxins. *Nature*, **296**, 651–653.
- Naslavsky N, Shmceda H, Friedlander G, Yanai A, Futerman AH, Barenholz Y & Taraboulos A (1999) Sphingolipid depletion increases formation of the scrapie prion protein in neuroblastoma cells infected with prions. *J Biol Chem*, **274**, 20763–20771.
- Nasu Y, Timme TL, Yang G, Bangma CH, Li L, Ren C, Sang HP, DeLeon M, Wang J & Thomson TC (1998) Suppression of caveolin expression induces androgen sensitivity in metastatic androgen-insensitive mouse prostate cancer cells. *Nature Medicine*, **4**, 1062–1064.
- Nusrat A, Parkos CA, Verkade P, Foley CS, Liang TW, Innis-Whitehouse W, Eastburn KK & Madara JL (2000) Tight junctions are membrane microdomains. *J Cell Sci*, **113**, 1771–1781.
- Ockleford CD (1976) A three dimensional reconstruction of the polygonal pattern on placental coated vesicle membranes. *J Cell Sci*, **23**, 83–91.
- Ockleford CD & Whyte A (1977) Differentiated regions of human placental cell surface associated with exchange of materials between maternal and foetal blood. The structure, distribution, ultrastructural cytochemistry and biochemical composition of coated vesicles. *J Cell Science*, **25**, 293–312.
- Park H, Go Y-M, Darji R, Choi J-W, Lisanti MP, Maland MC & Jo H (2000) Caveolin-1 regulates shear stress-dependent activation of extracellular signal-regulated kinase. *Am J Physiol*, **278**, H1285–H1293.
- Pelligrino DA, Ye S, Tan F, Santizo RA, Feinstein DL & Wang Q (2000) Nitric-oxide-dependent pial arteriolar dilation in the female rat; Effects of chronic estrogen depletion and repletion. *Biochem Biophys Res Comm*, **269**, 165–171.
- Ralston E & Ploug T (1999) Caveolin-3 is associated with the T-tubules of mature skeletal muscle fibers. *Exp Cell Res*, **246**, 510–515.
- Razani B, Schlegel A & Lisanti MP (2000) Caveolin proteins in signalling, oncogenic transformation and muscular dystrophy. *J Cell Sci*, **113**, 2103–2109.
- Rizzo V, McIntosh DP, Oh P & Schnitzer JE (1998) In situ flow activates endothelial nitric oxide synthase in luminal caveolae of endothelium with rapid caveolin dissociation and claudulin association. *J Biol Chem*, **273**, 34724–34729.
- Röhlich P & Allison AC (1976) Oriented Pattern of Membrane-Associated Vesicles in Fibroblasts. *J Ultrastruct Res*, **57**, 94–103.
- Rothberg KG, Heuser JE, Donzell WC, Ying Y-S, Glenney JR & Anderson RGW (1992) Caveolin, a Protein Component of Caveolae Membrane Coats. *Cell*, **68**, 673–682.
- Sargiacomo M, Scherer PE, Tang Z-L, Kübler E, Song KS, Sanders MC & Lisanti MP (1995) Oligomeric Structure of Caveolin: Implications for Caveolae Membrane Organization. *PNAS (USA)*, **92**, 9407–9411.
- Scherer PE, Tang Z-L, Chun M, Sargiacomo M, Lodish HF & Lisanti MP (1995) Caveolin Isoforms Differ in Their N-Terminal Protein Sequence and Subcellular Distribution. *J Biol Chem*, **270**, 16395–16401.
- Scherer PE, Okamoto T, Chun M, Nishimoto I, Lodish HF & Lisanti MP (1996) Identification, Sequence, and Expression of Caveolin-2 Defines a Caveolin Gene Family. *J Biol Chem Proc Natl*, **93**, 131–135.
- Scherer PE, Lewis RY, Volonté D, Engelman JA, Galbiati F, Couet J, Kohtz DS, van Dosselaar E, Peters P & Lisanti MP (1997) Cell-type and Tissue-specific Expression of Caveolin-2. *J Biol Chem*, **272**, 29337–29346.
- Schlegel A, Wang C, Katzenellenbogen BS, Pestell RG & Lisanti MP (1999) Caveolin-1 potentiates estrogen receptor alpha (ERalpha) signalling. Caveolin-1 drives ligand-independent nuclear translocation and activation of ER alpha. *J Biol Chem*, **274**, 33551–33556.
- Schreiber S, Fleischer J, Breer H & Boekhoff I (2000) A possible role for caveolin as a signaling organizer in olfactory sensory membranes. *J Biol Chem*, **275**, 24115–24123.
- Segal SS, Brett SE & Sessa WC (1999) Codistribution of NOS and caveolin throughout peripheral vasculature and skeletal muscle of hamsters. *Am J Physiol*, **277**, H1167–H1177.
- Shaul PW & Anderson RGW (1998) Role of plasmalemmal caveolae in signal transduction. *Am J Physiol*, **275**, L843–L851.
- Skretting G, Torgersen ML, Van Deurs B & Sandvig K (1999) Endocytic mechanisms responsible for uptake of GPI-linked diphtheria toxin receptor. *J Cell Sci*, **112**, 3899–3909.
- Song KS, Scherer PE, Tang Z-L, Okamoto T, Li S, Chafel M, Chu C, Kohtz DS & Lisanti MP (1996) Expression of Caveolin-3 in Skeletal, Cardiac, and Smooth Muscle Cells. *J Biol Chem*, **271**, 15160–15165.
- Tang ZL, Scherer PE, Okamoto T, Song K, Chu C, Kohtz DS, Nishimoto I, Lodish HF & Lisanti MP (1996) Molecular Cloning of Caveolin-3, a Novel Member of the Caveolin Family Expressed Predominantly in Muscle. *J Biol Chem*, **271**, 2255–2261.
- Timme TL, Goltsov A, Tahir S, Li L, Wang J, Ren C, Johnston RN & Thompson TC (2000) Caveolin-1 is regulated by c-myc and suppresses c-myc-induced apoptosis. *Oncogene*, **19**, 3256–3265.
- Valentijn KM, Gumkowski FD & Jamieson JD (1999) The subapical actin cytoskeleton regulates secretion and membrane retrieval in pancreatic acinar cells. *J Cell Sci*, **112**, 81–96.
- Yamada E (1955) The Fine Structure of the Gall Bladder Epithelium the Mouse. *J Biophys Biochem Cytol*, **1**, 445–458.
- Yang C-PH, Galbiati F, Volonte D, Horwitz SB & Lisanti MP (1998) Upregulation of caveolin-1 and caveolae organelles in Taxol-resistant A549 cells. *FEBS Lett*, **439**, 368–372.
- Yang G, Truong LD, Wheeler TM & Thompson TC (1999) Caveolin-1 expression in clinically confined human prostate cancer: A novel prognostic marker. *Cancer Res*, **59**, 5719–5723.
- Zhang W, Razani B, Altschuler Y, Bouzahzah B, Mostov KE, Petell RG & Lisanti MP (2000) Caveolin-1 inhibits epidermal growth factor-stimulated lamelli-pod extension and cell migration in metastatic mammary adenocarcinoma cells (MTLn3): Transformation suppressor effects of adenovirus-mediated gene delivery of caveolin-1. *J Biol Chem*, **275**, 20717–20725.

Immuno-electron microscopic localisation of caveolin 1 in human placenta

Simon Byrne, John Ahenkorah, Bismarck Hottor, C. Lockwood, Colin D. Ockleford*

Laboratory for Developmental Cell Sciences, Department of Infection Immunity and Inflammation, School of Medicine and Biological Sciences, University of Leicester and Warwick Medical Schools, University Road, Leicester LE1 9HN, UK

Received 28 July 2006; received in revised form 22 September 2006; accepted 27 September 2006

Abstract

We have localised the placental endothelial marker caveolin-1 at the ultrastructural level using indirect immunogold labelling. The particulate label has been quantified to assess the distribution of the target protein within term placental chorionic villi. The mesodermal compartment of the tissue was more heavily labelled than the ectodermally derived trophoblast. Basal plate lining endothelium and villous endothelium had similar immunoreactivity with anti-caveolin-1 antibody. A polarised distribution of the caveolin within chorionic villous capillary endothelial cells was observed. As evidenced by immuno-reactivity, the protein was statistically significantly more concentrated in the region associated with the basal membrane than the apical membrane. The latter region contained in turn significantly more anti-caveolin-1 immunoreactivity than the central region. These differences are discussed in the light of possible transport and signalling platform rôles for villous and basal plate endothelium.

© 2006 Elsevier GmbH. All rights reserved.

Keywords: Caveolin-1; Chorionic villi; Gold labelling; Materno-foetal interaction; Placental transport; Signalling

Introduction

Caveolae are small invaginations of the plasma membrane of many cells (Yamada, 1955). Part of their striated proteinaceous coat has been shown to consist of caveolin (Rothberg et al., 1992), a family of three similar proteins, which are usually expressed as specific pairs in different cell types (Scherer et al., 1997; Anderson, 1998). Caveolin-1 has been identified as a marker for type-I squamous epithelial cells in lung (Campbell et al., 1999) and as an endothelial and fibroblast marker in placental tissue (Byrne et al., 2001; Lyden et al., 2002;

Linton et al., 2003). In our previous study caveolin-1 was localised using immunofluorescence confocal laser-scanning microscopy (CLSM). We used an anti-caveolin-1 antibody that was validated by Western blotting that showed oligomeric aggregates extracted from placental tissue. On reduction the blots showed evidence of monomer and dimer only. In cell culture protein isolates extracted by the manufacturer the sole band seen was at the expected monomer molecular weights.

This paper describes an ultrastructural immunogold labelling study, which has been performed using the same antibody to define the localisation of this scaffold protein more precisely. If this is at the cell surface, where exposed receptors and signalling effector molecules may sample the external milieu (Feng et al., 1999; Chen and Norkin, 1999), it may be available for signalling. If internalised, the sensitivity of the cell to external autocrine, paracrine and endocrine events may be lessened.

*Corresponding author. Present address: Clinical Anatomy Learning Centre, Department of Medicine, Faraday Building, Lancaster University, Bailrigg, Lancaster LA1 4YWT UK.
Tel.: +44 1524 594515.

E-mail address: c.ockleford@lancaster.ac.uk (C.D. Ockleford).

Materials and methods

Tissue samples and fixation

Eight placentae were obtained from the Maternity Unit at Leicester Royal Infirmary, following normal, uncomplicated births. Informed consent was obtained according to local ethical committee guidelines. Small pieces of basal plate (10 × 10 × 2 mm) were excised within minutes of delivery and fixed for 1 h in 4% paraformaldehyde, 0.1% glutaraldehyde in phosphate-buffered saline (PBS), dehydrated through an ethanol series and embedded in LR White (London Resin Company).

Thin sectioning and TEM immuno-labelling

Semi-thin (0.5–2.0 μm) sections were baked onto glass slides, stained with 1% toluidine blue and viewed microscopically. Favourable regions of these sections were chosen, so that the large block face could be trimmed down to a size suitable for ultramicrotomy. Thin (60–80 nm) sections from these were collected on 200-mesh nickel grids. When the sections were dry, they were ‘blocked’ against non-specific antibody binding by flotation on droplets of 2% normal goat serum (NGS)/1% bovine serum albumin (BSA)/1% Tween-20 in PBS at 4 °C overnight. The experimental primary antibody was a rabbit anti-human caveolin-1 (Transduction Laboratories # C13630), which was diluted 1:5 in the same blocking buffer. The anti-cytokeratin 18 was a mouse monoclonal (clone number CY-90: product number C8541; Sigma). Grids were floated on droplets of this solution at 4 °C overnight. After three 2 h washes in blocking buffer, the sections were incubated, as before, in a 1:50 dilution of the secondary antibody, a 10 nm gold-conjugated goat anti-rabbit IgG (British Biocell International) or in a 1:100 dilution of goat anti-mouse IgG whole molecule conjugated to 10 nm gold particles (Sigma 777). Positive and negative control experiments were carried out and these and the outcomes of these are described in the Results section.

After a thorough washing first in blocking buffer, then in distilled water, the sections were stained in 5% uranyl acetate in 9% aqueous isobutanol, washed again in distilled water, air-dried and viewed in Jeol 100 CX-II or Jeol 1200 CX transmission electron microscopes at 10 000 × magnification.

Particle counting

Film images from these were scanned and digitised before being imported into Adobe Photoshop for labelling and print production. A continuous sequence of all adequately preserved areas of tissue was imaged

and used for area measurement and particle counting. Numbers of gold particles per μm² for different cell/tissue types were estimated using an electronic planimeter and Kontron Elektronik Videoplan software. For the polarity studies digital images were recorded directly from the TEM. Ink-jet printer photomicrographs were used for manual quantitation.

Investigating polarity

In order to establish whether any polarity of caveolin expression existed in endothelial cells, strips of cytoplasm 150 nm in width were outlined. For each endothelial cell section there were three of these: apical (marginated along the apical plasma membrane), basal (marginated along the basal plasma membrane) and central (midway between the other two). A similar procedure was carried out for fibroblasts. As these are non-polar cells, a peripheral zone 150 nm wide and a central zone (all cytoplasm) within this were identified. Gold particle counts were then carried out in each of these strips denoted a, b and c and expressed as counts per μm². Specific descriptions of statistical tests applied to measure the significance of differences between different data sets were applied with advice of a statistician (J. Beckett) and are the most appropriate tests in each case for the data sets investigated.

Results

Ultrastructure of endothelium

Transmission electron microscopy of ultrathin sections of villus endothelial cells reveals the expected ultrastructural appearance and caveolar profiles. These are frequently observed in association with villous endothelial cell surfaces (Fig. 1). Similar membranous endothelial cell ultrastructure has been described previously in the plate lining endothelial cell population (Byrne et al., 2001).

Specificity of labelling

The 10 nm gold particles were most frequently observed associated with the tissue rather than the embedding medium alone, where background levels could be established (Figs. 2–5 and Table 1). Labelling over negative control section tissue, where the primary antibody was omitted from the procedure or an isotope control (in the case of the monoclonal) was substituted, were so low as to be conveniently unquantifiable. No difficulty was experienced with the control experiments using the blocking regime described in the Materials and methods. Outcomes in these control sections were similar

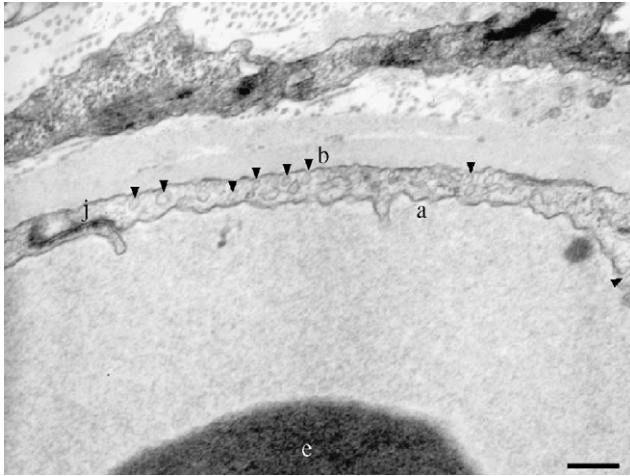


Fig. 1. This transmission electron micrograph shows the cross section of an endothelial cell in a chorionic villus. The apical (a) and basal (b) endothelial cell surfaces are identified and the endothelial cell-cell junction (j). A foetal erythrocyte is indicated (e). The arrowheads show sections through caveolae and possible vesicles, there are many more caveolar profiles in the endothelial basal surface than the apical surface. It is structures with this type of appearance that have previously been shown to be associated with caveolin-1. The standard procedures required to visualise the caveolar membranes in such specimens are not compatible with the processing for immunogold labelling used here where preservation of antigen detection, not morphology has had to be prioritised. The scale bar represents 200 nm.

over all parts of the tissue to the levels defined as background in the labelled sections where caveolin was not thought to be present. Generally, these areas of tissue not expected to be associated with caveolae such as extracellular matrix, red blood cells and serum-filled-compartments exhibited very low counts when exposed to the anti-caveolin and gold detection reagents. When immunogold-bearing antibody with different specificity (anti-cytokeratin) was applied a different pattern of labelling from that seen with anti-caveolin-1 particles occurred. With anti-cytokeratin antibody a strong labelling was seen in epithelial as opposed to endothelial cells (Figs. 4 and 5). This contrasted with the anti-caveolin 1 pattern that gave labelling with the opposite distribution (Figs. 2 and 3). This outcome creates a neat positive control for both procedures. In addition the ultrastructural association of the anti-pan cytokeratin with the intermediate filament-rich areas of trophoblast (epithelial) cytoplasm is an independent confirmation of that antibody's specificity. In appropriately oriented sections membranes were preserved but at low contrast in our regime. This was unimportant because we are not claiming localisation with respect to caveolae only quantitating the regional (not organellar) distribution of the protein caveolin. This may include protein in the synthetic or catabolic phases as well as organelle attached.

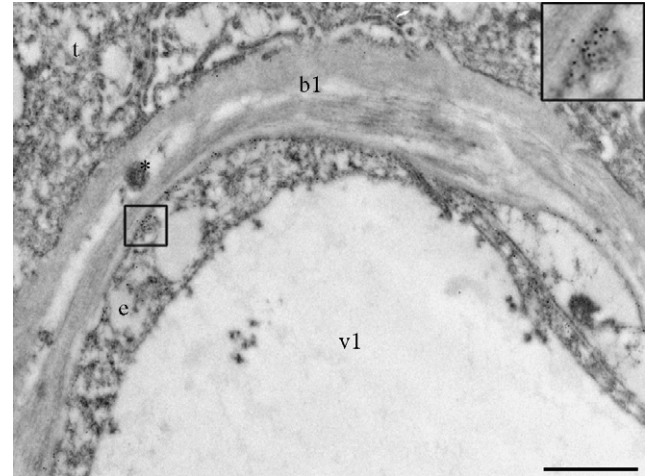


Fig. 2. Anti-caveolin-1 immunogold labelling of a transmission electron microscope ultrathin cross-section is evident in this section through the basal region of the syncytiotrophoblast and a margined capillary. The trophoblast (t) shows infrequent labelling (arrow) compared with the foetal capillary endothelium (e) and its vessel lumen (vl). The band between the trophoblast and the endothelial cell is basal lamina (bl) that contains an inclusion (*). The gold particles are distributed to the basal and apical surfaces of the endothelium preferentially. Very low levels or an absence of labelling are found over foetal capillary lumen and basal lamina. The scale bar represents 1.0 μm. The inset shows the boxed region at higher power so that the 10 nm gold particles can be clearly viewed.

Differences in the labelling frequency of the differentiated cell types were obvious on qualitative inspection and the quantitative data gained support from the subjective impressions. The anti-caveolin immunogold labelling showed preferential association with endothelial cells: much lower levels with trophoblast, erythrocytes and extracellular matrix in the villus core (Fig. 6). The differences in the counts per unit area of tissue were also significant as assessed in an entirely independent experiment using slightly different area comparison criteria by Student's *t*-test: Endothelium > trophoblast, $p < 0.001$; Trophoblast > maternal blood, $p < 0.002$ (Table 1).

Caveolae were observed in the foetal villous capillaries and the maximum Feret diameter of these profiles was of the order of 100 μm. The thicker walled clathrin-coated pits, which were common in the trophoblastic cells, were unlabelled (Fig. 3).

Pattern and polarity of endothelial labelling

One interesting feature of the villous endothelial cell labelling was that the label appeared to be most concentrated toward the external band of the cells' cytoplasm close to the basal surface. The outer basal

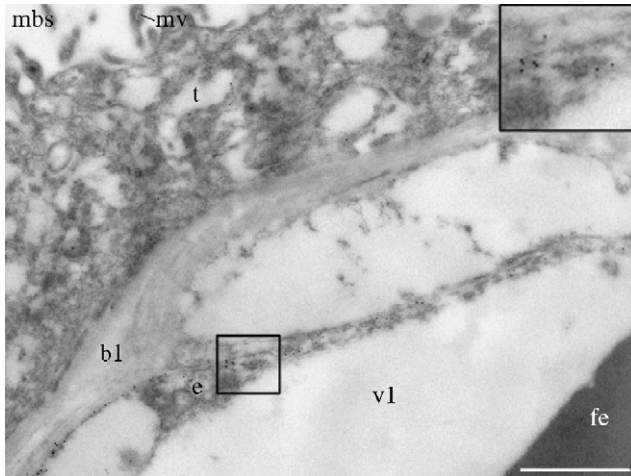


Fig. 3. Anti-caveolin-1 immunogold labelling is shown in this transmission electron micrograph of an ultrathin cross-section through the full width of tissue separating maternal blood space (mbs) from foetal blood erythrocytes (fe). The trophoblast (t) with its microvillous (mv) border shows infrequent labelling compared with the foetal capillary endothelium (e) and its foetal vessel lumen (vl). The band between the trophoblast and the endothelial cell is basal lamina (bl). The gold particles are distributed to the basal and apical surfaces of the endothelium preferentially. Very low levels or an absence of labelling are found over foetal capillary lumen and basal lamina. The inset shows the boxed region at higher power so that the 10 nm particles can be clearly viewed. The scale bar represents 1.0 μm .

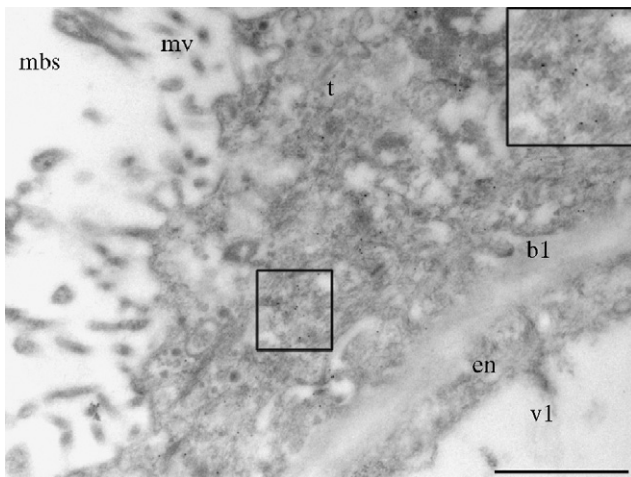


Fig. 4. Positive control with anti-cytokeratin 18 immunogold labelling shows extensive labelling of the trophoblast with 10 nm particles. The distribution of labelling is quite different from the anti-caveolin-1 and is concentrated in the trophoblast (t) associated with the cytoplasmic intermediate filament bundles (inset) not the microvilli (mv) endothelial cell (en), the vessel lumen (vl), maternal blood space (mbs) or basal lamina (bl). An unlabelled coated pit is visible towards the top of the syncytiotrophoblast cell surface bearing microvilli. The scale bar represents 1.0 μm .

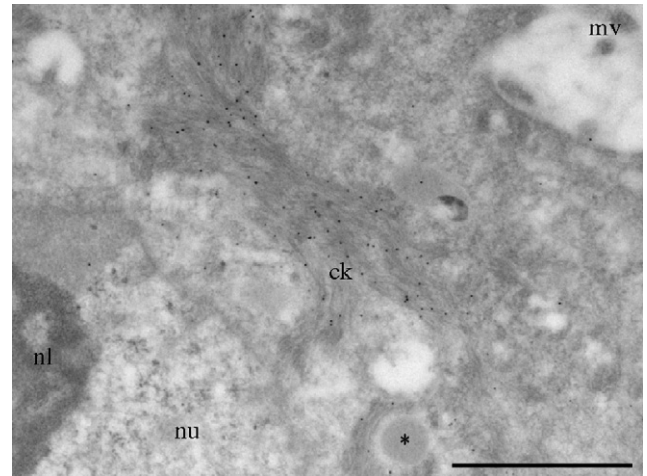


Fig. 5. Positive control with anti-cytokeratin 18 immunogold labelling shows extensive labelling of the trophoblast with 10 nm particles. The distribution of labelling is concentrated in the trophoblast associated with the cytoplasmic intermediate filament bundles (ck) not the cytoplasmic inclusion (*), the nucleus (n) or nucleolus (nl). The scale bar represents 1.0 μm .

membrane is associated with a basal lamina on the surface furthest from the foetal/umbilical cord blood. This labelling extended deeper than the membrane and occupied a cortical region of cytoplasm. Counts are shown as bar graphs (Figs. 7 and 8).

Fibroblasts

Observations of fibroblasts in the cores of chorionic villi and the basal plate showed that they were well labelled with anti-caveolin 10 nm gold but not anti-cytokeratin 10 nm gold (Figs. 9–11 and Table 1). In one instance a series of closely related gold particles were observed in a curved line gestalt. This array was in a similar size range and radius of curvature to caveolae. Mean anti-caveolin gold fibroblast labelling per μm^2 was increased in the cortical 150 nm strip associated with the plasma membrane as compared with the interior of the cell (Figs. 9–11).

Discussion

Specificity

The selective labelling of differentiated cell types and the increase of labelling frequency in the presence of the primary antibody support the specificity of the labelling technique. The specificity of the antibody has been tested previously using Western blotting (Byrne et al., 2001). The intensity of labelling (strongest in

Table 1. Mean colloidal gold particle counts per unit area overlying different tissues

Tissue	<i>N</i>	Minimum Au particles/ μm^2	Maximum Au particles/ μm^2	Mean Au particles/ μm^2	SEM
Trophoblast	10	0.34	18.21	7.84	1.63
Endothelium	29	5.79	148.82	52.48	7.10
Erythrocyte	11	0.00	7.42	2.31	0.72
Fibroblast	10	11.09	88.80	36.22	8.90
Maternal blood	31	0.00	1.86	0.67	0.12

N = number of areas counted, SEM = standard error of the mean in the range of areas counted. The term erythrocyte refers to fetal erythrocytes contained within villus blood vessels. The term maternal blood refers to the maternal blood space (i.e. blood space in contact with the syncytiotrophoblast). The latter is a measure of particle background labelling showing counts in red blood cells and maternal serum combined. Labelling efficiency differences between the experiments and sample size changes account for differences in measurements and significance levels shown in Fig. 6 and Table 1 and the relevant text. The overall pattern of labelling is consistent and repeatable and the background levels are low in both experiments.

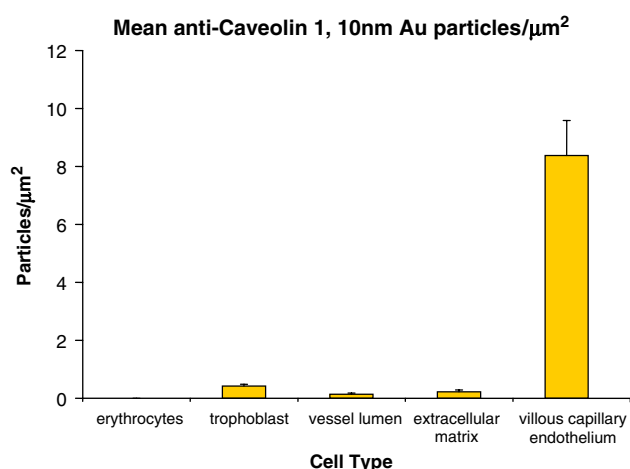


Fig. 6. Numbers of gold particles/ μm^2 of tissues including: erythrocytes, villous trophoblast, maternal vessel lumen, extracellular matrix and villous capillary endothelium. Following analysis of variance using ANOVA in association with Tukey's HSD post hoc test the mean endothelial cell associated gold particle counts/ μm^2 were shown to be significantly different from each of the other four means (significance $p < 0.0001$). The other four means were not significantly different from each other although the trend shows an increase of labelling in trophoblast when compared with three areas (erythrocyte, vessel lumen and extracellular matrix).

endothelium, weak in trophoblast) parallels that found previously with immunofluorescence and bright field immunocytochemical microscopy (Byrne et al., 2001; Linton et al., 2003), and is consistent with the ultrastructural data describing caveolae and micropinocytic vesicles in these and related tissues (Ockleford and Whyte, 1977; Ockleford and Clint, 1980; Linton et al., 2003). This is an independent localisation method with higher resolution than the immunofluorescence we used previously. It confirms previous results and extends them as it is the first immunogold labelling study that demonstrates the subcellular as well as cellular distribu-

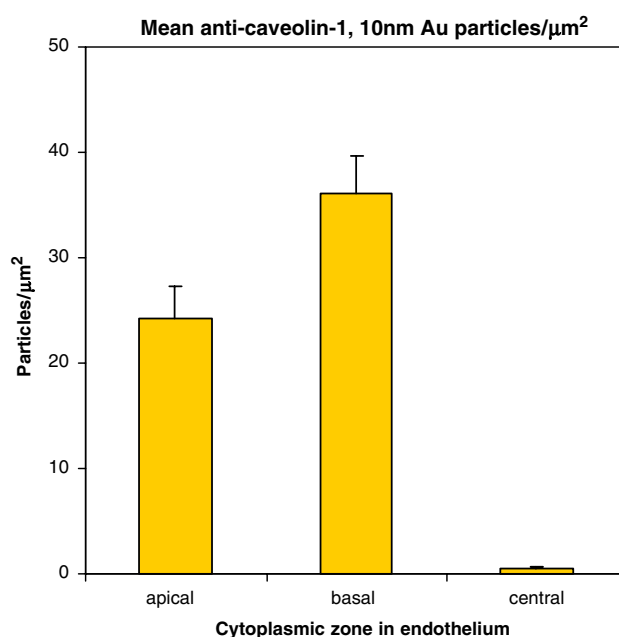


Fig. 7. The bar graph shows the mean anti-caveolin1 10 nm gold particle counts for the uniform width (150 nm) apical, basal and central strips. The basal mean count/ μm^2 was consistently higher than the apical. The apical mean in turn was higher than the central mean. The analysis of variance (ANOVA and Tukey HSD post hoc test using SPSS) demonstrated significant differences between all three means. Apical versus basal significant difference was $p < 0.009$; apical and basal versus central both $p < 0.0001$.

tion of anti-caveolin-1 and pancytokeratin immunoreactivity in placental tissue.

Available methods for ultrastructural immunocytochemistry include low-temperature embedding and cryoultramicrotomy. The latter is favoured where freeze fixation and cryo-embedding are better able to preserve antigenicity, in cases where resin embedding is deleterious (Griffiths, 1993). In this instance it appears that caveolin-1, a scaffold protein, is relatively resistant to

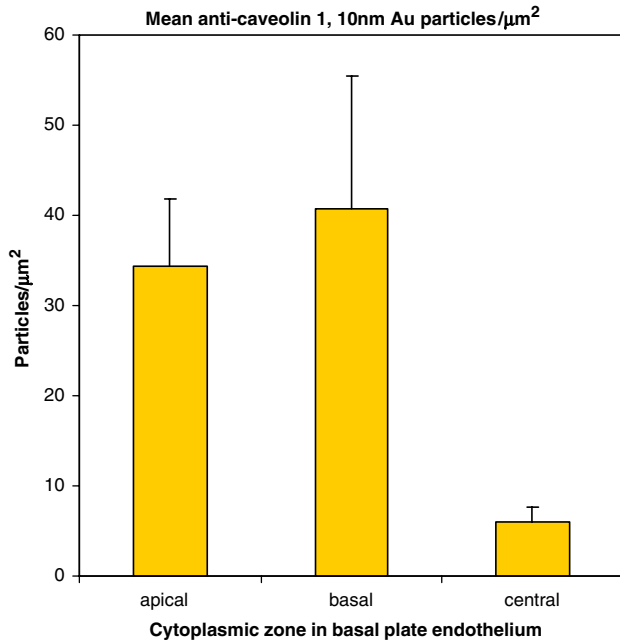


Fig. 8. The interesting population of endothelial cells lining the basal plate and forming part of a monolayer mosaic also containing trophoblast were investigated separately. The distribution of anti-caveolin-1 labelling reflected that of the chorionic villous endothelial cells with higher apical and basal labelling than central labelling. Using ANOVA and Tukey’s HSD post hoc test only the difference between the mean counts/μm² for basal and central strips were significantly different ($p < 0.04$), probably owing to greater scatter of the data in immunogold counts for endothelial cells at this site.

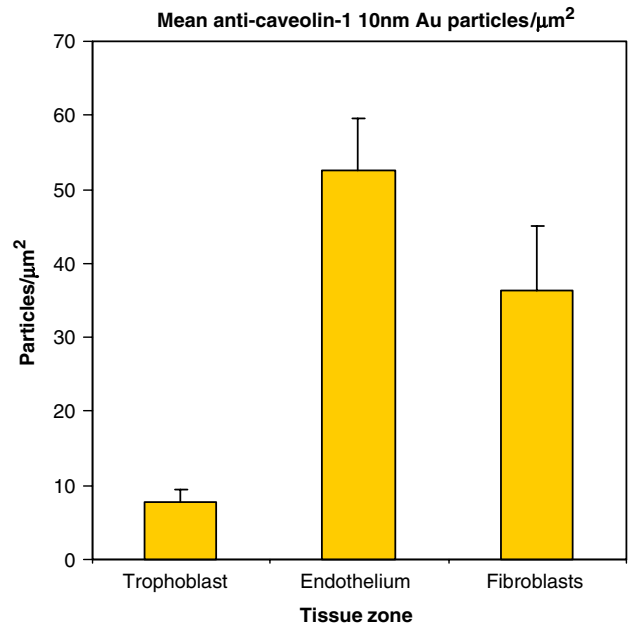


Fig. 10. In this set of observations the epithelial villous trophoblast anti-caveolin labelling was compared with the labelling of two mesenchymal cell types of the villous core, the fibroblasts and endothelial cells. There was a significant difference between the epithelial and each of the mesenchymal tissues with the fibroblast and endothelial labelling being greater.

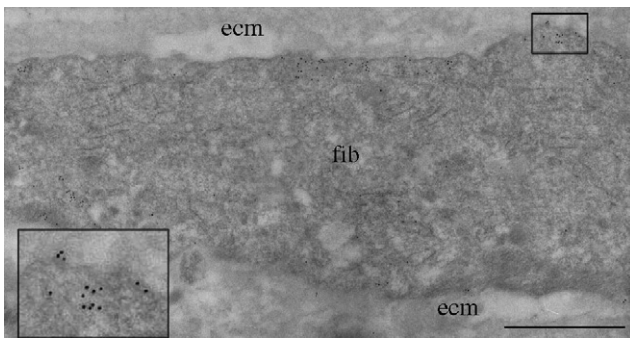


Fig. 9. This micrograph shows the distribution of anti-caveolin-1 immunogold labelling in a transmission electron micrograph of a portion of fibroblast cytoplasm. The fibroblast (fib) was located in the extracellular matrix (ecm) of the basal plate. Note the heavier labelling with the highly electron dense 10 nm gold particles close to the cell surface as compared with the interior of the cell. The inset shows the boxed region at higher power so that the 10 nm particles can be clearly viewed. The scale bar represents 1.0 μm.

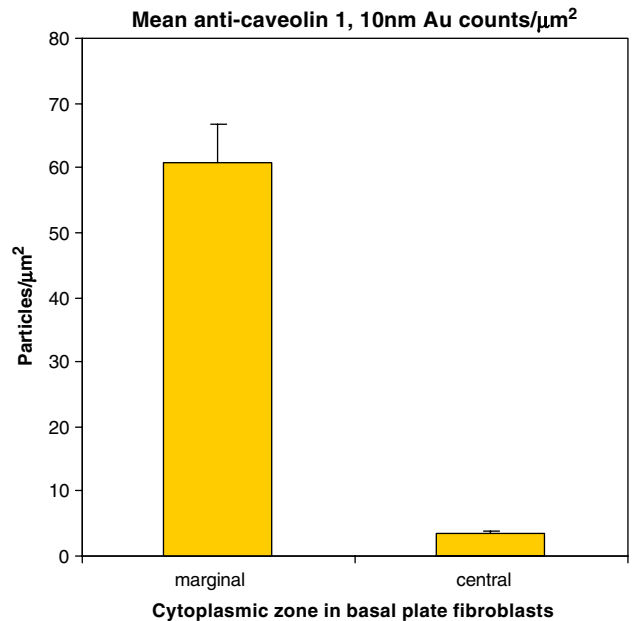


Fig. 11. A significantly higher level of labelling (significance $p < 0.0001$, ANOVA with Tukey HSD post hoc test) by anti-caveolin 10 nm Au gold particles was found in the cortical strip of cytoplasm 150 nm wide as compared within the central cytoplasm in sections of fibroblasts.

the embedding procedures used and that epitopes are preserved for interaction with the polyclonal anti-serum.

Tissue distribution

It is unsurprising but a useful confirmation of specificity in our technique that mature erythrocytes, with no known micropinocytic or caveolar association, exhibit only background anti-caveolin-1 labelling. Likewise, extracellular matrix should not be expected to label with an antibody to an intracellular antigen. The two transporting cells—the foetal capillary endothelial cells and the trophoblast—are essential steps in the materno-foetal exchange system. From this evidence it would appear that macromolecular handling by transcytotic processes and or the uptake, secretion and receptor display systems, are very different in the two cell types. The bias of trophoblast to clathrin-coated pits (Ockleford and Whyte, 1977) as the predominant organelle of its type and the foetal endothelial cells to the caveolae described in our earlier work (Mongan and Ockleford, 1995) is re-emphasised by these findings.

Intracellular distribution

Membrane associated labelling is expected of the caveolar stage of the micropinocytic process; deep intracellular labelling may be typical of the closed, internalised caveolar vesicle or the synthesis, storage or degradation of the protein. The basal cortical band of intense labelling (Figs. 7 and 8) was an unexpected finding. Its basal-cortical emphasis could reflect the net transport requirement. In order to ensure foetal growth, maternal macromolecules need to be taken up and transported to the foetus more frequently than macromolecules used need to be exported from the foetus. The anabolic requirements of the foetus outweigh its need to eliminate products of catabolism, which will generally be simpler and less transport-dependent. The preponderance of caveolin at the surface (particularly the basal surface) of the villous endothelial cells may simply be explained by the proximity of this surface to the source of the molecules whose transport is caveolin-dependent (the maternal blood). Another consideration is the possibility that there is a ‘holding zone’ for caveolae or nascent caveolar vesicles (just beneath the membrane) that can be deployed into the basal cell surface for endocytic and receptor signalling when these processes require rapid upregulation. Control over processes at this level is known to take place in other circumstances as in the NOSTRIN/NOSIP system (Feng et al., 1999; García-Cardena et al., 1997; Zimmermann et al., 2002). The association of these control molecules with the caveolar complexes makes them candidates as participants in such regulatory processes. Why the relatively

large amount of labelling is intracellular in this tissue is a matter of conjecture. It may reflect physiological or pathological processes, or be attributable to fixation. GFP-caveolin-1 vital-imaging, with high-resolution, low-phototoxicity methods may give insight into the dynamic aspects of the accumulation of the protein indicated by the present findings.

The degree to which these observations reflect uptake, signalling or possibly other cell physiological processes such as transcytosis is unclear from these observations as rates of cell physiological processes and the local levels of possible triggering cargo or ligand molecules have not yet been investigated in this context. Co-labelling live cell imaging studies for caveolin-1 with receptor and ligand are required to address these questions. These can be supported at the ultrastructural level using different size-clones of colloidal gold particles in time course experiments.

The finding that caveolin distribution in basal plate lining endothelium (Byrne et al., 2001) reflects that in villous endothelial cells lining more orthodox blood vessels indicates that they bear the protein signature of the signalling platforms that in other circumstances affect vascular control of blood pressure. This supports a possible role for these cells in pre-eclampsia where this population of cells is known to be upregulated in area (Ockleford et al., 2004; Smith et al., 2004) and the disease has its immuno-genetic origins at the very early stages of implantation in abnormal vascular development but expresses its greatest effect later in pregnancy as a systemic hypertensive maternal disease.

The “barrier” that prevents the fatal mixing of maternal and foetal blood is thinnest at term. However it still constitutes two cellular layers, the endothelium and trophoblast. As indicated here by the diversity of the distribution of the structural platforms on which caveolae depend, there appear to be distinctive cell physiological properties associated with the two cellular layers of the “barrier”. Distinctive physiological conditions affect maternal, placental and foetal compartments separately (Ganapathy et al., 2000). Two complete layers are required to separate three compartments and the signalling at the basal endothelial membrane might be expected, on this basis to differ at least quantitatively, and possibly to relate the placental physiology to the foetal demand that drives several aspects of pregnancy physiology.

Mori et al. (2006) have recently shown that cryo-ultrathin section preparations examined using immunofluorescence and confocal laser scanning microscopy (CLSM) yield resolution improvement over viewing 5–10 µm thick cryosections with the CLSM. Their findings include that a different antibody from that applied here, but similarly specific for caveolin-1, shows marginal distribution of the protein. It confirms data presented here and supports our view that our antibody

specifically shows a basal emphasis of caveolar labelling that conforms with the luminal/apical emphasis of CD31/PECAM 1. Despite the technical excellence of their recent series of publications in this area (Takizawa et al., 2003; Takizawa and Robinson, 2003) these authors did not measure or discuss any core/cortex or basal/apical distribution emphasis of caveolin-1 as we have done here.

Acknowledgements

Colin Ockleford is a member of the EMBIC consortium funded under EU Project no. 512040. We thank David Dinsdale for the loan of equipment and Chris d'Lacey for image rendering.

References

- Anderson, R.G.W., 1998. The caveolae membrane system. *Annu. Rev. Biochem.* 67, 199–225.
- Byrne, S., Cheent, A., Dimond, J., Fisher, G., Ockleford, C.D., 2001. Immunocytochemical localisation of a caveolin-1 isoform in human term extra-embryonic membranes using confocal laser scanning microscopy: implications for the complexity of the materno-fetal junction. *Placenta* 22, 499–510.
- Campbell, L., Hollins, A.J., Al-Eid, A., Newman, G.R., Von Ruhland, C., Gumbelton, M., 1999. Caveolin-1 expression and caveolae biogenesis during cell transdifferentiation in lung alveolar epithelial primary cultures. *Biochem. Biophys. Res. Commun.* 262, 744–751.
- Chen, Y., Norkin, L.C., 1999. Extracellular simian virus-40 transmits a signal that promotes virus enclosure within caveolae. *Exp. Cell Res.* 246, 83–90.
- Feng, Y., Venema, V.J., Tsai, N., Caldwell, R.B., 1999. VEGF induces nuclear translocation of Flk-1/KDR, endothelial nitric oxide synthase and caveolin-1 in vascular endothelial cells. *Biochem. Biophys. Res. Commun.* 256, 192–197.
- Ganapathy, V., Prasad, P.D., Ganapathy, M.E., Liebach, F.H., 2000. Placental transporters relevant to drug distribution across the maternal–fetal interface. *Pharmacology* 294, 413–420.
- García-Cardena, G., Martasek, P., Masters, B.S.S., Skidd, P.M., Couet, J., Li, S., Lisanti, M.P., Sessa, W.C., 1997. Dissecting the interaction between nitric oxide synthase (NOS) and caveolin. *J. Biol. Chem.* 272, 25437–25440.
- Griffiths, G., 1993. *Fine Structure Immunocytochemistry*. Springer, Berlin, Germany.
- Linton, E.A., Rodriguez-Linares, B., Rashid-Doubell, F., Ferguson, D.J., Redman, C.W., 2003. Caveolae and caveolin-1 in human term villous trophoblast. *Placenta* 24, 745–757.
- Lyden, T.W., Anderson, C.L., Robinson, J.M., 2002. The endothelium but not the syncytiotrophoblast of human placenta expresses caveolae. *Placenta* 23, 640–652.
- Mongan, L.C., Ockleford, C.D., 1995. Behaviour of two IgG subclasses in transport of immunoglobulin across the human placenta. *J. Anat.* 188, 43–51.
- Mori, M., Ishikawa, G., Takeshita, T., Goto, T., Robinson, J.M., Takizawa, T., 2006. Ultrahigh-resolution immunofluorescence microscopy using ultrathin cryosections: subcellular distribution of caveolin-1 α and CD31 in human placental endothelial cells. *J. Electron Microsc.* 55, 107–112.
- Ockleford, C.D., Clint, J.M., 1980. The uptake of IgG by human placental chorionic villi. A correlated autoradiographic and wide aperture counting study. *Placenta* 1, 91–111.
- Ockleford, C.D., Whyte, A., 1977. Differentiated regions of human placental cell surface associated with exchange of materials between maternal and foetal blood. The structure, distribution, ultrastructural cytochemistry and biochemical composition of coated vesicles. *J. Cell Sci.* 25, 293–312.
- Ockleford, C.D., Smith, R.K., Byrne, S., Sanders, R., Bosio, P., 2004. A confocal laser scanning microscope study of cytokeratin immunofluorescence differences between villous and extravillous trophoblast: cytokeratin downregulation in pre-eclampsia. *Microsc. Res. Tech.* 64, 43–53.
- Rothberg, K.G., Heuser, J.E., Donzell, W.C., Ying, Y.S., Glenney, J.R., Anderson, R.G.W., 1992. Caveolin, a protein component of caveolae membrane coats. *Cell* 68, 673–682.
- Scherer, P.E., Lewis, R.Y., Volonte, D., Engelman, J.A., Galbiati, F., Couet, J., Kohtz, D.S., van Donselaar, E., Peters, P., Lisanti, M.P., 1997. Cell-type and tissue-specific expression of caveolin-2. Caveolins 1 and 2 co-localize and form a stable hetero-oligomeric complex in vivo. *J. Biol. Chem.* 272, 29337–29346.
- Smith, R., Ockleford, C.D., Byrne, S., Bosio, P., Sanders, R., 2004. Healthy and pre-eclamptic placental basal plate lining cells: quantitative comparisons based on confocal laser scanning microscopy. *Microsc. Res. Tech.* 64, 54–62.
- Takizawa, T., Robinson, J.M., 2003. Ultrathin cryosections: an important tool for immunofluorescence and correlative microscopy. *J. Histochem. Cytochem.* 51, 707–714.
- Takizawa, T., Anderson, C.L., Robinson, J.M., 2003. A new method to enhance contrast of ultrathin cryosections for immunoelectron microscopy. *J. Histochem. Cytochem.* 51, 31–39.
- Yamada, E., 1955. The fine structure of the gall bladder epithelium of the mouse. *J. Biophys. Biochem. Cytol.* 1, 445–458.
- Zimmermann, K., Opitz, N., Dedio, J., Renne, C., Muller-Esterl, W., Oess, S., 2002. Nostrin: a protein modulating nitric oxide release and subcellular distribution of endothelial nitric oxide synthase. *Proc. Natl. Acad. Sci.* 99, 17167–17172.



A Mosaic Cell Layer in Human Pregnancy

S. Byrne^a, E. Challis^a, J.L.R. Williams^a, J.H. Pringle^b, J.M. Hennessy^c, C.D. Ockleford^{a,d,*}

^a *Laboratory for Developmental Cell Sciences, Department of Infection Immunity and Inflammation, School of Medicine and Biological Sciences, University of Leicester Medical School, University Road, Leicester, LE1 9HN, UK*

^b *Department of Cancer Studies & Molecular Medicine, School of Medicine and Biological Sciences, University of Leicester Medical School, University Road, Leicester, LE1 9HN, UK*

^c *Department of Genetics, School of Medicine and Biological Sciences, University of Leicester Medical School, University Road, Leicester, LE1 9HN, UK*

^d *School of Health and Medicine, Division of Medicine, Faraday Building, Lancaster University, Bailrigg, Lancaster, LA1 4YB, UK*

ARTICLE INFO

Article history:
Accepted 3 February 2010

Keywords:
Germ layers
Placenta
Pregnancy
Basal plate
Extra-embryonic membranes
Materno-fetal interaction

ABSTRACT

We present evidence for a novel histological and embryological relationship at the human materno-fetal interface. Here an epi-endothelium forms an integrated unicellular layer lining the intervillous space in between the anchoring villi that attach the placenta to the uterus. This layer appears to be derived from two different germ layers (mesoderm and ectoderm). The data presented here reveals that when a probe for the Y-chromosome is used to test the gender of placental cells following the birth of male or female babies, the cell-sheet is a genetic mosaic derived from two individuals (mother and baby). The endothelium is maternally derived; the epithelium is fetal derived. This new allo-epi-endothelium model is relevant to theories of germ layer separation in development, reproductive immunology and the endocrinology of implantation and placentation. It demonstrates cooperative intercellular interactions that are fundamental to achieving a major goal of human interstitial implantation the establishment of a blood sinus for haematotrophic nutrition. Poor implantation is a fundamental cause of pregnancy pathology and this knowledge will be useful in development of our understanding of pregnancy diseases.

© 2010 Elsevier Ltd. All rights reserved.

1. Introduction

The first suggestion that the intervillous space lining was a mosaic monolayer was presented at an International tripartite meeting of South African, Dutch and British Anatomical Societies held in Rolduc, The Netherlands [1]. Shortly thereafter similar ideas were included in the then new edition of a text book, but with no attribution [2]. The first full original refereed paper describing the mosaic [3] included the proposal that the mosaic was a genetic mixture of maternal and fetal cells. The first demonstration of the genetics of the allo-epi-endothelium was an *in situ* hybridisation study presented at a meeting in Malinska, Croatia in June 2005 [4]. This initial study was published in the proceedings of that meeting which were refereed. The initial measurements of the area fractions of the mosaic using immunofluorescence [5] were followed by the publication of data supporting the notion that the mosaic was extensive using immunoenzyme cytochemistry [6]. Accepting

that the basal lining of the intervillous space is an epi-endothelium, an histologically unique single-cell thick tissue layer formed as a mosaic of trophoblastic epithelium and endothelium we were intrigued to define its origin. We suggested at that time that the endothelial component could be derived from maternal mesenchyme [1,3–5]. With this series of experiments we have chosen a cytogenetic approach to critically examine the origin of the mosaic endothelial cells. To do this we aimed to carry out *in situ* hybridisation using a probe for human Y-chromosomes [4,7,8] to analyse the nuclei in the materno-fetal interaction zone of placentae obtained following the birth of children of known gender.

Following the birth of a male child, probes to identify the Y-chromosome will indicate whether the monolayer mosaic cells with endothelial morphology exhibit no male chromosome nuclear labelling and whether cells with characteristic trophoblast morphology have nuclei with a high level of labelling. If so the data will be consistent with the conclusion that the trophoblast-like component is genetically fetal (♂) and that the endothelial layer is in contrast maternal (♀). We can use a female child's placenta as a negative control because when it is probed there should be no significant labelling as the fetal trophoblast (♀) and the maternal endothelium (♀) should both contain no significant Y-chromosomal

* Corresponding author. School of Health and Medicine, Division of Medicine, Faraday Building, Lancaster University, Bailrigg, Lancaster, LA1 4YB, UK. Tel.: +44 1524 594515; fax: +44 1524 593747.

E-mail address: c.ockleford@lancaster.ac.uk (C.D. Ockleford).

labelling. The same sections that include basal plate endothelium also contain endothelial cells lining fetal blood vessels in the core of chorionic villi. These we suggest form an excellent positive control for effective labelling of endothelial nuclei as in the placenta of male (δ) babies they are predicted to be strongly labelled as they lie deep within the fetal compartment and develop from the fetal side. We have carried out the necessary experiments to determine the genetic origin of the mosaic endothelial population.

2. Materials and methods

2.1. Tissue

Freshly delivered term placentae ($n = 22$, 19 from a male conceptus, 3 from a female) were obtained from Leicester Royal Infirmary maternity hospital following the birth of healthy babies after uncomplicated deliveries. The tissue was obtained with informed consent using procedures given approval by the Leicestershire Research Ethics Committee (Reference Nos. 6336 and 7144) and the University Hospitals of Leicester NHS Trust (Project Nos. 7180, 9161). From the maternal facing surface of the placenta the cobbled pattern showing the cotyledons is clearly discernible. The tissue taken from this surface was examined. There were five distinct areas of the tissue studied from each placenta to ensure extensive sampling from central, peripheral and intermediate parts of the discoid placenta. The superficial layer, the basal plate (BP), was examined and smooth, undamaged areas chosen for dissection. These areas were initially injected at a low angle from one side with about 10 mL normal saline. This was slowly injected to lift the basal plate and to clear the blood from beneath it so that the basal plate swelled to form a transparent dome, like a blister. In this way, as it held the fluid, its continuity could be demonstrated and irrigation was said to be complete.

The site was injected with 10% unbuffered formal saline in tap water, allowed to stand for 5 min and the exposed surface was fixed. When the tissue became slightly firm, blocks were carefully excised using fine scissors (position indicated by the rectangles in Supplementary data, Diagram 1). These contained the intervillous space lining and were stored in fresh fixative in a universal bottle for 48 h prior to dehydration and embedding.

This was accomplished using an alcohol series (70, 90, 100%: 2–3 h) of either ethanol or isopropanol. Xylene (20 min) was used as clearing agent.

Tissues were impregnated with 60 °C melting temperature paraffin wax under vacuum before being orientated in plastic moulds so that the plane of the intervillous basal plate lining was orthogonal to the plane of sectioning and allowed to cool. For fluorescence *in situ* hybridisation (FISH) studies, 5 μ m frozen sections were cut from Tissue Tek embedding medium. Wax sections for enzyme labelling *in situ* hybridisation were cut at a thickness of 10 μ m. The thicker sections used for *in situ* hybridisation Y-chromosome signal scoring allowed greater efficiency of labelling. As section thickness increased from 5 to 10 μ m the proportion by volume of any nuclei included within a single section increased. As there is only 1 Y-chromosome which occupies a small fraction of each nucleus by volume it is more likely to be included within a given section and so detected as nuclear volume fraction within that section rises. Sections were floated out and attached to subbed slides. These were then dried overnight on a hotplate, dewaxed in two changes of xylene (10 min each), followed by rehydration through an alcohol series (5 min each) to water or citrate buffer (see below). The sections used for antibody-HRP conjugate histochemistry were pre-incubated for 15 min in 3% H₂O₂ in MeOH following the 100% EtOH step. These sections were also pre-digested for 25 min at 37 °C in 200 μ g/ml pepsin in 200 mM HCl to assist probe penetration [9].

2.2. Y-probe preparation and application

Labelled probe [7,8] pHY21 was synthesised by copying the template DNA carried on plasmid pBR328, in this case a human Y-chromosome DNA sequence, restricted with MspI, using Klenow fragment DNA polymerase in the presence of dinitrophenol (DNP)-labelled dUTP. The other nucleotides are not labelled. The reaction was carried out overnight at room temperature. To facilitate the penetration of the probe into the section, Pronase-E (< 150 μ g mL⁻¹) or more consistently Pepsin (200 μ g/mL 0.2 M HCl) were used; this partially digested the section without appreciably altering its morphology. The incubation time is limited to ~25 min. To assist the proteolytic steps, sections were pre-treated for 20–30 min with 10 mM citrate buffer at pH 6.0 and 95 °C. After digestion, the sections were pre-hybridised in a buffer containing formamide and random DNA. This step ensured that non-specific DNA binding sites were saturated with unlabelled DNA. The probe (diluted in the same buffer) was applied to the sections, which were then incubated at 100 °C for precisely 10 min. Once removed, they were maintained at 42 °C for up to 48 h. The efficiency of probe binding is affected by salt concentration and temperature. These conditions are arrived at empirically after much careful pilot experimentation as each probe, target and environment combination has its own optimum balance between signal and background. All incubations were carried out in sealed, water vapour-saturated containers. Unbound labelled probe was removed

from the sections by high stringency washing (2 \times SSC containing 50% formamide) followed by (0.1 \times SSC with 2 mM MgCl₂ and 0.1% Triton X-100) at 42 °C.

2.3. Validation of probe

In order to confirm the specificity of the probe used, PCR primers 20 bases in length were identified using the published sequence [5] and synthesised. This yielded a Taq polymerase product approximately 0.22 kb in length. The product was then sequenced using the same primers in dideoxy-nucleotide sequencing reactions. Substantially overlapping sequence effective strand lengths of 150 (sense) and 142 bases (antisense) were obtained using the automated sequencing process (Applied Biosystems). Very high levels of identity (97% and 95% respectively) of the sequence of the PCR products with the published non-coding sequence were obtained so validating the probe.

2.4. Visualisation

To visualise the hybrids, an anti-DNP rabbit IgG coupled to horseradish peroxidase (HRP) was used. The sections were incubated for 1 h at room temperature with the antibody diluted 1:50 in 1% bovine albumen in Tris-buffered saline, pH 7.6 containing 0.1% Tween-20 (TBST). Sections were then washed in 5 changes of TBST, 3 min each. A coloured substrate, diaminobenzidine tetrahydrochloride (DAB), was oxidised by the HRP in the presence of H₂O₂ and nickel ions to produce an intense, insoluble black product at the hybridisation site. Sections were then counterstained with nuclear and/or other stains including Methyl green, Nuclear Fast Red and Kirkpatrick's carmalum. Sections were rinsed in water, blotted dry, dehydrated in 90% and 100% alcohol, cleared in xylene and coverslipped with DPX. For fluorescence signal the sections were incubated with a fluorescein isothiocyanate-labelled goat anti-rabbit IgG diluted 1:100 in TBST containing 1% BSA. This step replaced the DAB incubation in the immunohistochemical protocol. After 45 min, the sections were washed then coverslipped in Mowiol mountant. The sections were counterstained with propidium iodide (final concentration 0.1 μ g/ml) during the final rinsing process [10].

2.5. Microscopy

Sections were viewed and counts made by 3 independent observers using a Leitz Diaplan or a Zeiss Axioplan Imaging II fitted with a Zeiss Axiocam digital camera attachment. Fluorescence preparations were viewed using a Zeiss epifluorescence microscope and a Biorad MRC 600 CLSM attachment to a Zeiss Axiocam microscope. Images were recorded on Fujichrome Provia 400F film then scanned and digitised or recorded directly as digital image pic. files. Digital images were processed using Zeiss Axiocam software, exported to Adobe Photoshop for labelling and processing for publication. Stage mounted length standards were imaged under the same conditions as the specimen to calculate magnifications.

2.6. Statistical analysis

Counts of labelled versus unlabelled nuclei were made with $n = 500$ for each of six tissue samples from each placenta obtained from a pregnancy giving rise to male offspring using bright field and a Leica microscope. Counts were imported to an Excel spreadsheet and statistical and chart functions were applied for analysis and presentation of data. Tests of the 95% confidence intervals and p values for one proportion of these were estimated using MINITAB for each of the six proportions. The test of the 95% confidence intervals and p values for two proportions was applied to the villus and basal plate labelled endothelial nuclear proportions.

3. Results

3.1. Placentae of male babies

In situ hybridisations of the sampled areas are shown in Fig. 1a–d where both fluorescence and histochemical labelling of the Y-chromosome is evident as a discrete green dot (Fig. 1a) or a dark dot (Fig. 1b and d). Absence of labelling in the negative control 1c (see below) indicates the validity of the labelling. Further evidence is presented in Fig. 2 a–d. These regions include basal plate where a mixture of decidual and extravillous trophoblast cells label with intermediate frequency, chorionic villi where essentially all nucleated cells are highly labelled and junctional zones (Fig. 2d) where trophoblast (highly labelled) and endothelia (unlabelled) lining the basal plate can be compared. The specific groups of nuclei counted were fetal chorionic villus endothelium, fetal chorionic villus trophoblastic epithelium, fetal villus core stromal cells (mesenchymal, Hofbauer etc.), basal plate “other” cells (decidua

labelling. The same sections that include basal plate endothelium also contain endothelial cells lining fetal blood vessels in the core of chorionic villi. These we suggest form an excellent positive control for effective labelling of endothelial nuclei as in the placenta of male (δ) babies they are predicted to be strongly labelled as they lie deep within the fetal compartment and develop from the fetal side. We have carried out the necessary experiments to determine the genetic origin of the mosaic endothelial population.

2. Materials and methods

2.1. Tissue

Freshly delivered term placentae ($n = 22$, 19 from a male conceptus, 3 from a female) were obtained from Leicester Royal Infirmary maternity hospital following the birth of healthy babies after uncomplicated deliveries. The tissue was obtained with informed consent using procedures given approval by the Leicestershire Research Ethics Committee (Reference Nos. 6336 and 7144) and the University Hospitals of Leicester NHS Trust (Project Nos. 7180, 9161). From the maternal facing surface of the placenta the cobble pattern showing the cotyledons is clearly discernible. The tissue taken from this surface was examined. There were five distinct areas of the tissue studied from each placenta to ensure extensive sampling from central, peripheral and intermediate parts of the discoid placenta. The superficial layer, the basal plate (BP), was examined and smooth, undamaged areas chosen for dissection. These areas were initially injected at a low angle from one side with about 10 mL normal saline. This was slowly injected to lift the basal plate and to clear the blood from beneath it so that the basal plate swelled to form a transparent dome, like a blister. In this way, as it held the fluid, its continuity could be demonstrated and irrigation was said to be complete.

The site was injected with 10% unbuffered formal saline in tap water, allowed to stand for 5 min and the exposed surface was fixed. When the tissue became slightly firm, blocks were carefully excised using fine scissors (position indicated by the rectangles in Supplementary data, Diagram 1). These contained the intervillous space lining and were stored in fresh fixative in a universal bottle for 48 h prior to dehydration and embedding.

This was accomplished using an alcohol series (70, 90, 100%: 2–3 h) of either ethanol or isopropanol. Xylene (20 min) was used as clearing agent.

Tissues were impregnated with 60 °C melting temperature paraffin wax under vacuum before being orientated in plastic moulds so that the plane of the intervillous basal plate lining was orthogonal to the plane of sectioning and allowed to cool. For fluorescence *in situ* hybridisation (FISH) studies, 5 μ m frozen sections were cut from Tissue Tek embedding medium. Wax sections for enzyme labelling *in situ* hybridisation were cut at a thickness of 10 μ m. The thicker sections used for *in situ* hybridisation Y-chromosome signal scoring allowed greater efficiency of labelling. As section thickness increased from 5 to 10 μ m the proportion by volume of any nuclei included within a single section increased. As there is only 1 Y-chromosome which occupies a small fraction of each nucleus by volume it is more likely to be included within a given section and so detected as nuclear volume fraction within that section rises. Sections were floated out and attached to subbed slides. These were then dried overnight on a hotplate, dewaxed in two changes of xylene (10 min each), followed by rehydration through an alcohol series (5 min each) to water or citrate buffer (see below). The sections used for antibody-HRP conjugate histochemistry were pre-incubated for 15 min in 3% H₂O₂ in MeOH following the 100% EtOH step. These sections were also pre-digested for 25 min at 37 °C in 200 μ g/ml pepsin in 200 mM HCl to assist probe penetration [9].

2.2. Y-probe preparation and application

Labelled probe [7,8] pHY2.1 was synthesised by copying the template DNA carried on plasmid pBR328, in this case a human Y-chromosome DNA sequence, restricted with MspI, using Klenow fragment DNA polymerase in the presence of dinitrophenol (DNP)-labelled dUTP. The other nucleotides are not labelled. The reaction was carried out overnight at room temperature. To facilitate the penetration of the probe into the section, Pronase-E (< 150 μ g mL⁻¹) or more consistently Pepsin (200 μ g/mL 0.2 M HCl) were used; this partially digested the section without appreciably altering its morphology. The incubation time is limited to ~25 min. To assist the proteolytic steps, sections were pre-treated for 20–30 min with 10 mM citrate buffer at pH 6.0 and 95 °C. After digestion, the sections were pre-hybridised in a buffer containing formamide and random DNA. This step ensured that non-specific DNA binding sites were saturated with unlabelled DNA. The probe (diluted in the same buffer) was applied to the sections, which were then incubated at 100 °C for precisely 10 min. Once removed, they were maintained at 42 °C for up to 48 h. The efficiency of probe binding is affected by salt concentration and temperature. These conditions are arrived at empirically after much careful pilot experimentation as each probe, target and environment combination has its own optimum balance between signal and background. All incubations were carried out in sealed, water vapour-saturated containers. Unbound labelled probe was removed

from the sections by high stringency washing (2 \times SSC containing 50% formamide) followed by (0.1 \times SSC with 2 mM MgCl₂ and 0.1% Triton X-100) at 42 °C.

2.3. Validation of probe

In order to confirm the specificity of the probe used, PCR primers 20 bases in length were identified using the published sequence [5] and synthesised. This yielded a Taq polymerase product approximately 0.22 kb in length. The product was then sequenced using the same primers in dideoxy-nucleotide sequencing reactions. Substantially overlapping sequence effective strand lengths of 150 (sense) and 142 bases (antisense) were obtained using the automated sequencing process (Applied Biosystems). Very high levels of identity (97% and 95% respectively) of the sequence of the PCR products with the published non-coding sequence were obtained so validating the probe.

2.4. Visualisation

To visualise the hybrids, an anti-DNP rabbit IgG coupled to horseradish peroxidase (HRP) was used. The sections were incubated for 1 h at room temperature with the antibody diluted 1:50 in 1% bovine albumen in Tris-buffered saline, pH 7.6 containing 0.1% Tween-20 (TBST). Sections were then washed in 5 changes of TBST, 3 min each. A coloured substrate, diaminobenzidine tetrahydrochloride (DAB), was oxidised by the HRP in the presence of H₂O₂ and nickel ions to produce an intense, insoluble black product at the hybridisation site. Sections were then counterstained with nuclear and/or other stains including Methyl green, Nuclear Fast Red and Kirkpatrick's carmalum. Sections were rinsed in water, blotted dry, dehydrated in 90% and 100% alcohol, cleared in xylene and coverslipped with DPX. For fluorescence signal the sections were incubated with a fluorescein isothiocyanate-labelled goat anti-rabbit IgG diluted 1:100 in TBST containing 1% BSA. This step replaced the DAB incubation in the immunohistochemical protocol. After 45 min, the sections were washed then coverslipped in Mowiol mountant. The sections were counterstained with propidium iodide (final concentration 0.1 μ g/ml) during the final rinsing process [10].

2.5. Microscopy

Sections were viewed and counts made by 3 independent observers using a Leitz Diaplan or a Zeiss Axioplan Imaging II fitted with a Zeiss Axiocam digital camera attachment. Fluorescence preparations were viewed using a Zeiss epifluorescence microscope and a Biorad MRC 600 CLSM attachment to a Zeiss Axiometer microscope. Images were recorded on Fujichrome Provia 400F film then scanned and digitised or recorded directly as digital image pic. files. Digital images were processed using Zeiss Axiovision software, exported to Adobe Photoshop for labelling and processing for publication. Stage mounted length standards were imaged under the same conditions as the specimen to calculate magnifications.

2.6. Statistical analysis

Counts of labelled versus unlabelled nuclei were made with $n = 500$ for each of six tissue samples from each placenta obtained from a pregnancy giving rise to male offspring using bright field and a Leica microscope. Counts were imported to an Excel spreadsheet and statistical and chart functions were applied for analysis and presentation of data. Tests of the 95% confidence intervals and p values for one proportion of these were estimated using MINITAB for each of the six proportions. The test of the 95% confidence intervals and p values for two proportions was applied to the villus and basal plate labelled endothelial nuclear proportions.

3. Results

3.1. Placentae of male babies

In situ hybridisations of the sampled areas are shown in Fig. 1a–d where both fluorescence and histochemical labelling of the Y-chromosome is evident as a discrete green dot (Fig. 1a) or a dark dot (Fig. 1b and d). Absence of labelling in the negative control 1c (see below) indicates the validity of the labelling. Further evidence is presented in Fig. 2 a–d. These regions include basal plate where a mixture of decidual and extravillous trophoblast cells label with intermediate frequency, chorionic villi where essentially all nucleated cells are highly labelled and junctional zones (Fig. 2d) where trophoblast (highly labelled) and endothelia (unlabelled) lining the basal plate can be compared. The specific groups of nuclei counted were fetal chorionic villus endothelium, fetal chorionic villus trophoblastic epithelium, fetal villus core stromal cells (mesenchymal, Hofbauer etc.), basal plate “other” cells (decidua

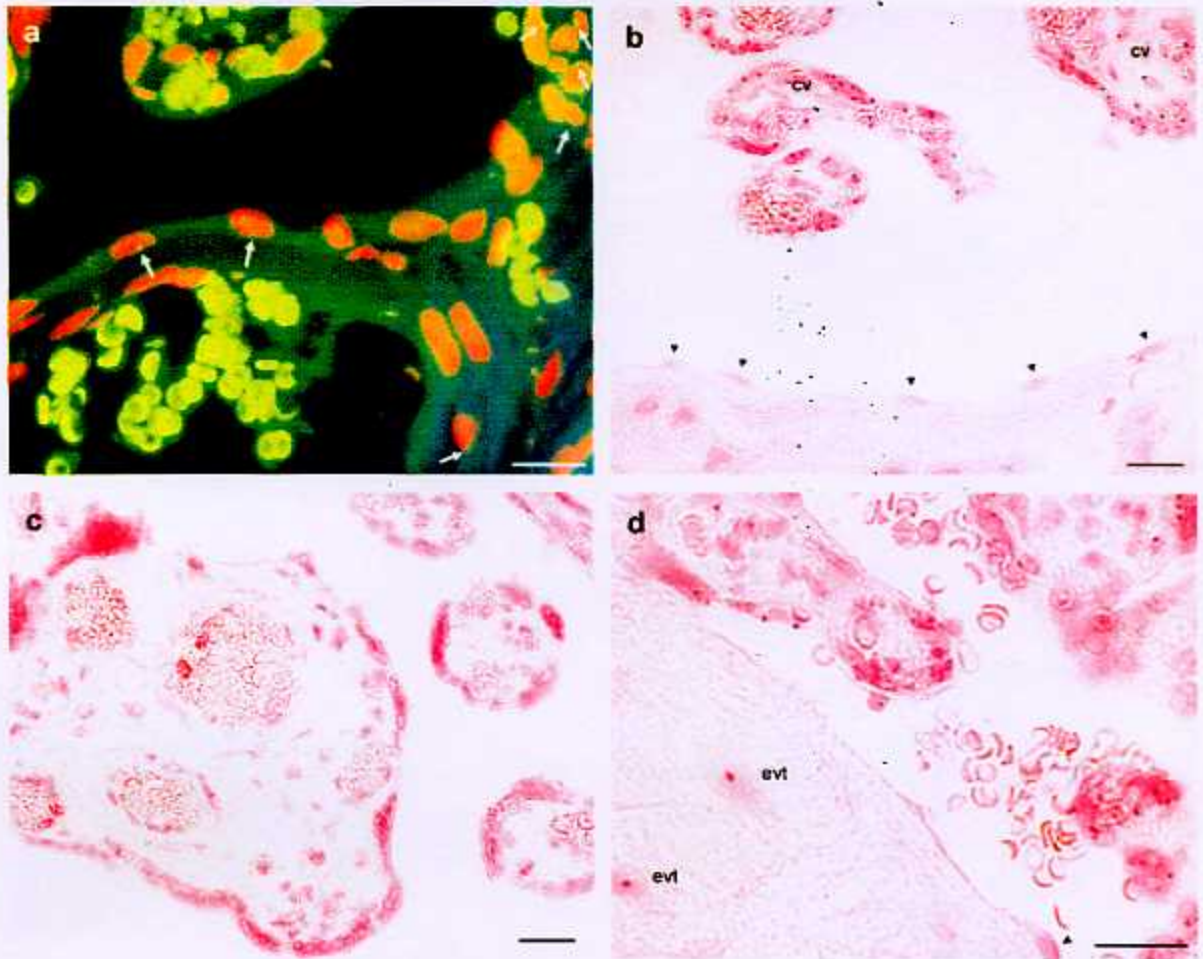


Fig. 1. a) This placenta is from a male child and chorionic villus nuclei containing Y-chromosomes are labelled with bright green dots (arrows). The labelling efficiency (40%) is lower than in the 10 μm sections of other male baby placentae (Fig. 1b and d, Fig. 2 a–d). Erythrocyte autofluorescence, yellow; nuclei, orange with propidium iodide [7]; Y-chromosomes label green with FITC conjugated Y-chromosome probe. The scale bar is 20 μm . b) In situ hybridisation (ISH) of the Y-specific probe to chromatin in the basal plate region is revealed by dark dots in male nuclei in tissue from a male baby's placenta. There is a high labelling efficiency of the trophoblastic and mesenchymal cells of the chorionic villi (cv). The endothelial cells lining the basal plate in this region are unlabelled (arrowheads) as are underlying basal plate nuclei. (Scale bar 20 μm ; δ baby). c) There is no ISH of the Y-specific probe to chromatin in the chorionic villi of this negative control female baby's placenta. The trophoblast, endothelial cells, mesenchymal cells, fetal erythrocytes, nucleated fetal blood cells in this region are all unlabelled. (Scale bar 20 μm ; ? baby). d) ISH of the Y-specific probe to chromatin in the basal plate region is revealed by the dark dots overlying the male nuclei in this male baby placenta. There is a high labelling efficiency of the trophoblastic and mesenchymal cells of the chorionic villi (upper-right part of the field). The endothelial cell nuclei lining the basal plate in this region are unlabelled (arrowhead) whereas the nuclei of the trophoblast continuous with this layer at the anchoring villus (top left) are labelled. Decidual nuclei, fetal and maternal erythrocytes are unlabelled. Note the labelling of two nuclei among the decidual cells. These are likely to be extravillous trophoblast (evt) but have been counted as basal plate other. (Scale bar 20 μm ; δ baby).

from the mother and extravillous trophoblast from the fetus) and the endothelial cells of basal plate monolayer lining the intervillus space. Labelling in the form of dots overlying nuclei in basal plate tissues of boy-child pregnancies were quantitated (Fig. 3). Labelling of basal plate trophoblast was similar to the labelling of chorionic villus trophoblast. Similar distributions were obtained by two independent observers and using different tissue samples (results not shown). The five distinct areas of the tissue: fetal chorionic villus endothelium, fetal chorionic villus trophoblastic epithelium, fetal villus core stromal cells (mesenchymal, Hofbauer etc.), basal plate "other" cells (decidua from the mother and extravillous trophoblast from the fetus) and the endothelial cells of basal plate monolayer lining the intervillus space were scored. As shown in Table 1 and Fig. 3 labelling of basal plate trophoblast was similar to the labelling of chorionic villus trophoblast. On the basis of these data from 10 μm sections the labelling efficiency is approaching 70% and the first three tissues are evidently male and therefore fetally genetic. There were no significant counts in endothelial

nuclei, reflecting a maternal genetic origin. The category "Basal plate other" is a mixture of cells of different gender and so expected to contain both maternally and fetally derived cells. The "other basal plate" cell counts were intermediate between the trophoblast and endothelial values reflecting the mixed population of fetally derived extravillous trophoblast and the maternal decidual cells. The higher standard deviations for this group of counts probably reflects the irregular clustering of the extravillous trophoblast in the basal plate previously noted in our immunofluorescence studies of extravillous trophoblast [11,12]. To summarise data from the 10 μm sections of male bearing pregnancies the labelling efficiency is approaching 70% and three tissues are evidently male and therefore probably fetally genetic.

3.2. Placentae of female babies

None of the tissues from female child bearing pregnancies had detectable labelling above background indicating the absence of Y-

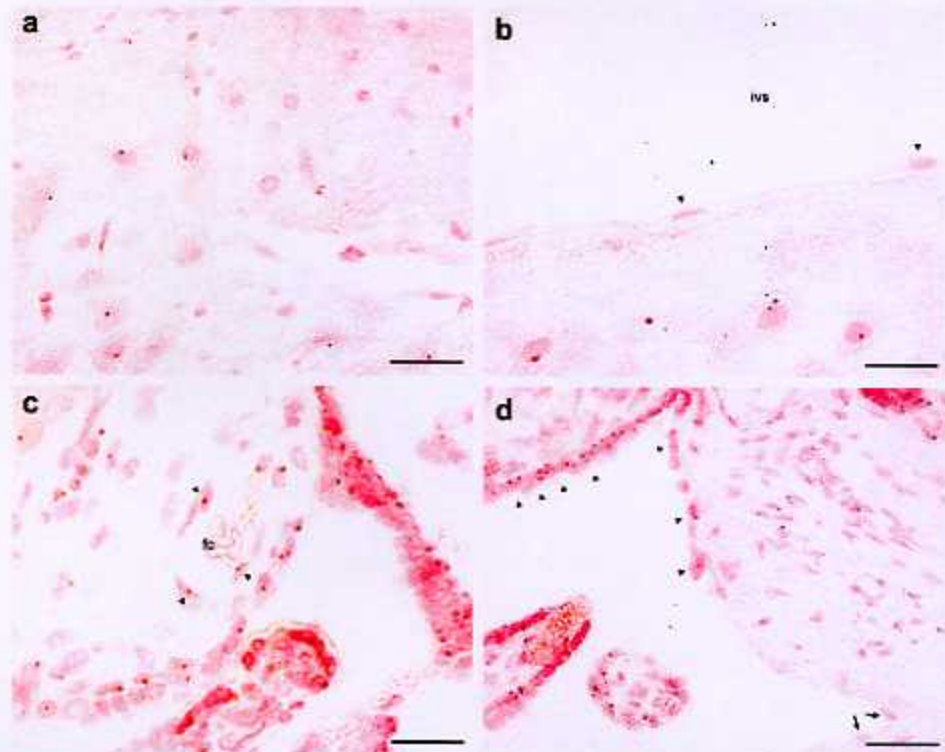


Fig. 2. a) ISH of endometrial decidual layer shows labelling of some but not all cells. (Scale bar 20 μ m; δ baby). b) ISH of endometrial decidual layer shows labelling of fetal cells that have penetrated this layer but not of the endothelial cells comprising the lining layer of the intervillous space (ivs). These (arrowheads) are genetically maternal. (Scale bar 20 μ m; δ baby). c) ISH of this villus region of a male baby associated placenta reveals a fetal capillary (fc) containing anucleate erythrocytes. Unlike the endothelial cells lining the intervillous space (Figs. 1b, d and 2b) these endothelial cells are labelled (arrowheads). (Scale bar 20 μ m; δ baby). d) This section shows a junctional region in the single-cell thick layer lining the intervillous space. The upper part of the lining is ISH labelled trophoblast of fetal genetic origin as it is heavily ISH labelled with the Y-chromosome probe (arrowheads). The nuclei of the endothelial part of the lining are unlabelled and therefore of maternal origin (arrows). (Scale bar 20 μ m; δ baby).

chromosomes in nuclei of all placental cells (Table 1; Fig. 1c). These negative controls also tell us that the stringency of the post-hybridisation washes was sufficient to remove non-specific hybrids.

3.3. Comparison

There were no significant counts in basal plate lining endothelial nuclei, in either male or female baby placentae. In contrast the endothelial cells lining fetal blood vessels within chorionic villi

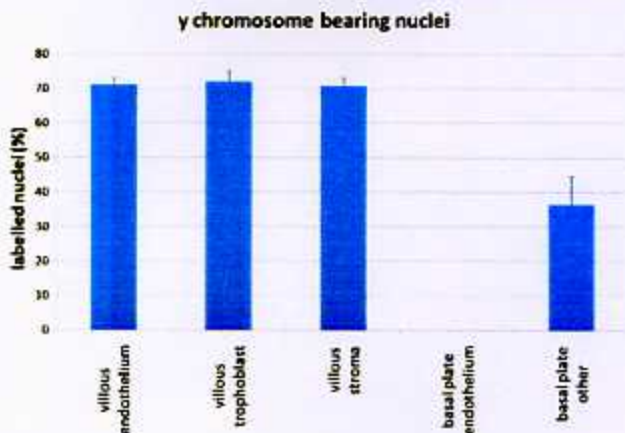


Fig. 3. This bar chart shows the mean Y-chromosome probe labelled nuclear counts from 10 healthy male baby placentae. The error bars show the standard deviations of the counts.

label strongly with male baby pregnancies but not with female baby pregnancies.

3.4. Statistical analysis

The analysis of the data presented in Tables 1, 2 and 3 is reassuring. The mean counts in Table 1 indicate great labelling differences between the cells expected to show differences, with absence of labelling in known female and presence of efficient labelling in known male cells. The basal plate lining cells fall into two genetically highly distinct groups indicating maternal endothelial origin and fetal trophoblastic origin. The probability of these results arising by chance are extremely low and in many cases effectively zero as shown in Tables 2 and 3. The last line comparison of Table 3 is a significant support to the view that the genetic origin of endothelial nuclei in the basal plate lining differs from that in the chorionic villi.

Table 1
Labelling of nuclei with Y-chromosome-probe.

Cell types	Y-probe labelled nuclei% male fetus (n = 10)	Y-probe labelled nuclei% female fetus (n = 3)
Villus trophoblast	72.12	0
Villus endothelium	71.29	0
Villus stroma	70.84	0
Basal plate endothelium	0.00	0
Basal plate other	36.44	0

Gives the mean labelling percentages of the nuclei of the different cell types represented in and close to the basal plate, n = number of placentae used.

Table 2
Test and Confidence intervals for One Proportion Test of $p = 0.5$ vs $p \text{ not} = 0.5$.

Sample	X	N	Sample p	95.0% CI	p value
Chorionic Villus endothelium	348	500	0.696000	(0.653607, 0.736057)	0.000
Chorionic Villus trophoblast	312	500	0.624000	(0.579910, 0.666614)	0.000
Basal plate "other cells"	350	500	0.700000	(0.657734, 0.739882)	0.000
Basal plate trophoblast	279	500	0.558000	(0.513235, 0.602075)	0.011
Basal plate "other cells"	133	500	0.266000	(0.227751, 0.307041)	0.000
Basal plate lining endothelium	7	500	0.014000	(0.005647, 0.028632)	0.000

Shows the test and confidence intervals for one proportion in tissue from male baby placentae. Where a p value is listed as 0.000 this is less than 0.0005. CI = confidence intervals. N is the number of nuclei scored, X the number of Y-chromosomes identified by ISH and Sample p the proportion of successes and the p value the probability of achieving the outcome by chance.

3.5. Phenotype

A variety of immunofluorescence microscopy data presented here and earlier clearly reveals the phenotypic mosaic nature of this layer. These are summarised in Table 4 [5,12] where we find the trophoblast labelling with anti-keratins reflecting its ectodermal origin and endothelial cells labelling with markers such as vimentin that are typical of cells of mesodermal origin.

4. Discussion

The short term survival of maternal blood borne apoptotic trophoblastic emboli from the placenta; the leakage of leukocytes from the fetal circulation into the maternal circulation and the migration of extravillous trophoblast into the basal plate and spiral arterioles are all events taking place in an immuno-modulated pregnant physiology that serve to make the materno-fetal interface one that is anatomically complex [12–16]. Cells originating from a male fetus and extracted from the mother's blood can be identified using the Y-chromosome with fluorescence microscopy and the high affinity of quinacrine dyes for the repetitive DNA on the Y-chromosomes long arm [16]. Trophoblast may play a major role in these processes as trophoblast secretions at the materno-fetal interface can be either immunosuppressive or immunostimulatory [14,15].

Up until 1998 [1] the consensus, evidenced by diagrams in the vast majority of embryology textbooks and reviews of placental

Table 4
Immunophenotype of basal plate intervillous space lining cells.

Marker Antibody (dilution)	Basal Plate Trophoblast Lining Immunoreactivity	Basal Plate Endothelial Lining Immunoreactivity
Pancytokeratin (1:800)	+	-
hCC (1:100)	+	-
hPL (1:800)	+	-
Vimentin (1:400)	-	+
Caveolin-1:NOS complex component (1:100)	-	+
Thrombomodulin:CD-141 (1:50)	-	+
Von Willebrand Factor (1:400)	-	+
PECAM-1:CD-31 (1:80)	-	+
ACE (1:25)	-	+
Endothelin:EN4 (1:100)	-	+

Summarises the target placental cells immunolabelled by a range of antibodies directed against characteristic marker antibodies used for cell lineage determination. The dilutions used are in brackets and the methods of their application published previously [1,3,5,11,12,20].

structure, was that at term the intervillous space was lined essentially by trophoblast. The latter is reflected from the sleeves of syncytiotrophoblast covering the villi onto the surface of the basal plate at the attachment point of anchoring villi. This idea has had to be modified as explained in the introduction. The consequences of this mosaic structure for a successful pregnancy are discussed in our other work. There we show how the mosaic varies its proportions in hypertensive pregnancies and how longer term cellular coverage that follows temporary repair of the basal plate lining layer with fibrin has to be accomplished by a different mechanism from that operating in chorionic villi [5,11–13]. It provides further evidence of a link between the trophoblastic origins of the pathology of pre-eclampsia and a consequent alteration in the maternal endothelial compartment that is implicated in the damaging later systemic hypertensive effects of the disease. This follows because the greater the damage to the trophoblast the more that is replaced by endothelium. It is not clear how this data may affect our understanding of the IUGR aspects of pathological pregnancies including pre-eclamptic ones, but one possibility is that the greater the area fraction of endothelium the greater the accumulated amount of trophoblast damage throughout the pregnancy. In chorionic villi this process is obscured by trophoblastic repair, but not in the basal plate lining.

Analysis of the statistical data presented here demonstrates the maternal genetic nature of the basal plate lining endothelia and the

Table 3
Test and Confidence intervals for Two Proportions Test for $p(1)-p(2) = 0$ (vs $\text{not} = 0$).

Sample	X	N	Sample p	Estimate for $p(1)-p(2)$	95% CI for $p(1)-(2)$	Z	p value
Chorionic villus endothelium	348	500	0.696000	0.072	(0.0134493, 0.130551)	2.41	0.016
Chorionic villus trophoblast	312	500	0.624000	-0.076	(-0.134447, -0.0175534)	-2.55	0.011
Basal plate "other cells"	350	500	0.700000	0.142	(0.0827691, 0.201231)	4.70	0.000
Basal plate trophoblast	279	500	0.558000	0.292	(0.233734, 0.350266)	9.82	0.000
Basal plate "other cells"	133	500	0.266000	0.252	(0.211924, 0.292076)	12.32	0.000
Basal plate lining endothelium	7	500	0.014000	-0.004	(-0.0609122, 0.0529122)	-0.14	0.890
Chorionic villus endothelium	348	500	0.696000	0.138	(0.0786665, 0.197334)	4.56	0.000
Basal plate trophoblast	279	500	0.558000	0.43	(0.374093, 0.485907)	15.07	0.000
Chorionic villus endothelium	348	500	0.696000	0.682	(0.640387, 0.723613)	32.12	0.000
Basal plate lining endothelium	7	500	0.014000				

Compares counts between pairs of cell types in tissue from male baby placentae. It shows the test and confidence intervals for two proportions. Abbreviations are as in the legend of Table 2. The Z statistic is $p(1)-p(2)/\text{standard error of the sampling distribution}$. The p value is the probability that the Z statistic is achieved by chance.

fetal genetic nature of the villus endothelium. Basal plate lining trophoblast exhibits labelled nuclear counts typical of fetal genetic origin. The data are consistent with all components of the villus tree being of fetal genetic origin and the basal plate cells as being of mixed maternal and fetal origin.

Definition of the endothelial component of the basal plate lining as maternal supports the view that they may derive from the adjacent linings of the maternal uterine blood vessels connected to the intervillous space. The intima of these vessels is continuous with the basal plate lining layer at the openings of the uterine veins and spiral arterioles. However there is evidence for circulating endothelia that is relevant [18].

Earlier published work [3,5,11–13,19,20] using an extensive array of immunofluorescence markers and summarised in Table 4 has clarified the position with respect to the germ layer origin of the basal plate lining. Our immunofluorescence results were consistent with those of others [21] regarding the identification of the related epithelial and endothelial cells in the chorionic villous tree and so we regard our techniques as independently validated.

We have quantitated the epithelial to endothelial ratio in the mosaic. We measured the endothelial compartment at 60.8% of the combined area [5,13]. This was very much greater than the proportion indicated by an earlier isolated observation of endothelial immunofluorescence labelling by Lang and colleagues [22] ascribed to "residual" endothelium. Possibly these authors did not appreciate the significance of this observation as they appear to have thought it related just to the bell shaped opening of uterine blood vessels which would be expected to have an endothelial lining.

On the basis of early and what are in our opinion highly equivocal sex chromatin studies Wanner [23] believed the basal plate lining to be entirely maternal. The results of our more definitive Y-chromosome probe based in situ hybridisation cytogenetic analysis presented here clearly show that the basal plate lining is a layer contributed to by both mother and fetus. Summarising the data we regard it as probable that the basal plate lining layer of the human placenta at term is a histologically unique *allo-epi-endo-thelium*.

The origin of the endothelial component of the mosaic comprising the basal plate lining layer is of interest. Our finding that these cells are genetically maternal in origin can be compared with the finding of Gussin et al. [17] who demonstrated that cultured peripheral blood mononuclear cells in pregnant women had greater endothelial progenitor cell proliferative capacity than peripheral blood mononuclear cells from non-pregnant women and that they were maternal in origin. A detailed review of the role of these endothelial progenitor cells in pregnancy [24] reveals a number of characteristics that would be consistent with them being a source of the endothelial component of the basal plate lining.

The existence of extravillous trophoblast and trophoblast deportation [11,15] has emphasised the distributed nature of the materno-fetal interface and its complexity. It is worth making clear that the endothelial mosaic cells described here are not bi/multi-nucleate neither do the endothelial cells contain a Y-chromosome in the boy-baby pregnancies. It is therefore highly unlikely that a process of cell fusion is occurring as in the ruminant placenta [25]. In addition the morphological phenotypes of mosaic cells are not intermediate between trophoblast and endothelium but typical of one or the other. The size of the cells is not unusually large for endothelial cells and the markers expressed are typical [26] and restricted to cells with the appropriate morphology (see Table 4). So, although unusual rare histological patterns do occur at the materno-fetal interface in other species, these situations are morphologically distinct. The accurate ruminant placenta

description does create a precedent that allows us to consider our conclusion more acceptable than embryonic stratification (ectoderm/mesoderm/endoderm are separate layers) theory would suggest.

The present investigation is based on an earlier less extensive and less well optimised *in situ* hybridisation study [4]. It is consistent with the findings from experiments using laser capture microdissection and PCR of amelogenin allelotype profiles published recently [6]. Both strongly indicate the maternal genetic origin of the endothelial component and the fetal origin of the trophoblastic component.

The area fraction of the mosaic is believed to be altered in pre-eclamptic gestation [5,13] and small for gestational age pregnancies [6].

With the unusual relationship identified here we add a new dimension to our understanding of the human materno-fetal interaction. Analogies of military or immunological type comparing the zone to one where invasion of aggressive trophoblast in interstitial implantation is suppressed by modulation of maternal immunity to an allograft are an oversimplification. Our data demonstrate a cooperative histological relationship where in the extra-embryonic membranes cells from two individuals and two germ layers form a monolayer lining a vascular sinus (the intervillous space) which is presumably at least functional as a sinus lining.

Acknowledgements

CDO thanks the Royal Society, the Chinese National Academy of Natural Sciences and the Anatomical Society of Great Britain and Ireland for support of his research. We thank John Beckett for statistical advice; Paul Bosio and Jason Waugh for clinical co-ordination, David Dinsdale and Chris Guerin for use of equipment, Chris d' Lacey and Nick Court for skilful assistance with presentation and Rebecca Smith for patient liaison. We thank Sharad Mistry for advice on sequencing analysis; Angie Gillies and Linda Potter for expert technical assistance. CO is a member of the EMBIC consortium funded under EU Project No. 512040: We thank Philip John Morgan for image rendering.

Appendix. Supplementary data

Supplementary data associated with this article can be found in the on-line version, at doi:10.1016/j.placenta.2010.02.005.

References

- [1] Byrne S, Cheent A, Dimond J, Fisher G, Ockleford CD. Immunocytochemical localisation of caveolin-1 in human term extra-embryonic membranes using confocal laser scanning microscopy. *J Anat* 1998;93:312–3.
- [2] Benirschke K, Kaufmann P. The pathology of the human placenta. 4th ed. Berlin: Springer; 2000. pp. 947.
- [3] Byrne S, Cheent A, Dimond J, Fisher G, Ockleford CD. Immunocytochemical localisation of caveolin-1 in human term extra-embryonic membranes: implications for the complexity of the materno-fetal junction. *Placenta* 2001;22:499–510.
- [4] Byrne S, Challis E, Williams JLR, Pringle JH, Hennessy JM, Ockleford CD. In-situ hybridisation using Y-chromosome specific probes to establish the origins of basal plate cells. In: Rhukavina D, Chaouat Gerard, editors. EMBIC handbook "embryo implantation: from basics to clinics". University of Rijeka Press; 2006. pp. 179–87.
- [5] Smith R, Ockleford CD, Byrne S, Bosio P, Sanders R. Healthy and pre-eclamptic placental basal plate lining cells: quantitative comparisons based on confocal laser scanning microscopy. *Microsc Res Tech* 2004;64:54–62.
- [6] Richani K, Romero R, Soto E, Nien JK, Cushenberry BS, Kim YM, et al. Genetic origin and proportion of basal plate surface-lining cells in normal and abnormal pregnancies. *Hum Pathol* 2007;38:269–75.
- [7] Cooke HJ, Schmidtkje J, Gosden JR. Characterisation of a human Y chromosome repeated sequence and related sequences in higher primates. *Chromosoma* 1982;87:491–502.

- [8] Frommer M, Prosser J, Vincent PC. Human satellite 1 sequences include a male specific 2.47 kb tandemly repeated unit containing one Alu family member per repeat. *Nucleic Acids Res* 1984;6:2887–900.
- [9] Evans MF, Allesky HA, Cooper K. Optimization of biotiny-tyramide-based in situ hybridization for sensitive background-free applications on formalin-fixed, paraffin-embedded tissue specimens. *BMC Clin Pathol*;2. <http://www.biomedcentral.com/1472-6890/3/2>, 2003;3.
- [10] Ockleford CD, Hsi B, Wakely J, Badley RA, Whyte A, Page Faulk W. Propidium iodide as a nuclear marker in immunofluorescence: I. Use with tissue and cytoskeleton studies. *J Immunol Methods* 1981;48:261–7.
- [11] Ahenkorah J, Hottor B, Byrne S, Bosio P, Ockleford CD. Immunofluorescence confocal laser scanning microscopy and immuno-electron microscopic identification of keratins in human maternofetal interaction zone. *Cellular and Molecular Medicine*, eprint ahead of publication. *J Cell Mol Med* 2009;13:735–48.
- [12] Ockleford CD, Smith R, Byrne S, Bosio P, Sanders R, Bosio PA. Confocal laser scanning microscope study of cytokeratin immunofluorescence differences between villous and extravillous trophoblast: cytokeratin downregulation in pre-eclampsia. *Microsc Res Tech* 2004;64:43–53.
- [13] Hottor BA, Bosio P, Waugh J, Diggle P, Byrne S, Ahenkorah J, Ockleford CD. Variation of the composition of the intervillous space in term placentas of mothers with pre-eclampsia. *Placenta*, submitted for publication, PL-10-00006R2.
- [14] Loke YW, King A. Human implantation: cell biology and immunology. England: Cambridge University Press; 1995. pp. 44–45.
- [15] Redman CW, Sargent IL. Placental debris, oxidative stress and pre-eclampsia. *Placenta* 2000;21:597–602.
- [16] Wooding FB. Current topic: the synepitheliochorial placenta of ruminants: binucleate cell fusions and hormone production. *Placenta* 1992;13:101–13.
- [17] Jackson L. Foetal cells and DNA in maternal blood. *Prenatal Diagn* 2003;23:837–46.
- [18] Gussin HA, Bischoff FZ, Hoffman R, Elias S. Endothelial precursor cells in the peripheral blood of pregnant women. *Journal Soc Gynaec Inves* 2002;9:357–61.
- [19] Ockleford CD, Smith R, Byrne S, Sanders R, Bosio P. Human placental basal plate lining cells: significant changes associated with pre-eclampsia. *Ann Anat* 2003;(Suppl. 185):166–7.
- [20] Byrne S, Barber H, Mercer N, D'Lacey C, Ockleford CD. ACE in the basal plate. *Placenta* 2003;24:A43.
- [21] Dye JF, Jablenska R, Donnelly JL, Lawrence L, Leach L, Clark P, et al. Phenotype of the endothelium in the human term placenta. *Placenta* 2001;22:32–43.
- [22] Lang I, Hartmann M, Blaschitz A, Dohr G, Skofitsch G, Desoye G. Immunohistochemical evidence for the heterogeneity of maternal and fetal vascular endothelial cells in human full-term placenta. *Cell and Tissue Res* 1993;274:211–8.
- [23] Wanner A. Wird bei der Geburtsplacenta des Menschen die Basalplatte von Trophoblastzellen oder Zellen mütterlicher herkunft überzogen. *Acta Anat* 1966;63:545–58.
- [24] Robb AO, Mills NL, Newby-DE, Denison FC. Endothelial progenitor cells in pregnancy. *Reproduction* 2007;133:1–9.
- [25] Wooding FB. Role of binucleate cells in fetomaternal cell fusion at implantation in the sheep. *Am J Anat* 1984;170:233–50.
- [26] Byrne S, Ahenkorah J, Hottor B, Lockwood C, Ockleford CD. Immuno-electron microscopic localisation of caveolin-1 in human placenta. *Immunobiology* 2007;212:39–46.
- [27] Cull P. The sourcebook of medical illustration. Lancs: Parthenon Publishing Group; 1990. pp. 1–481.

Healthy and Pre-Eclamptic Placental Basal Plate Lining Cells: Quantitative Comparisons Based on Confocal Laser Scanning Microscopy

R.K. SMITH,¹ C.D. OCKLEFORD,^{1*} S. BYRNE,¹ P. BOSIO,² AND R. SANDERS¹

¹Advanced Light Microscope Facility, Department of Infection Immunity and Inflammation, School of Medicine and Biological Sciences, University of Leicester and Warwick Medical Schools, Leicester, LE1 9HN, United Kingdom

²Pregnancy Hypertension Unit, Department of Obstetrics and Gynaecology, University of Leicester and Warwick Medical Schools, Leicester, LE2 7LX, United Kingdom

KEY WORDS pre-eclampsia; basal plate; intervillous space; caveolin-1; endothelial cells; trophoblast invasion; cytokeratin expression; placental development

ABSTRACT Immunocytochemical confocal laser scanning microscope images of the monolayer of cells lining the intervillous space at the basal plate of term placentae were analysed using stereology. Immunoreactively-distinct regions of this mosaic layer were measured. In basal plate from healthy pregnancies, trophoblast epithelium occupied 18.91% of the surface area and endothelium 60.81%. In pre-eclampsia the equivalent areas were 15.57% and 67.63%. Acellular fibrinoid covers the remaining area and this component decreases in area in pre-eclampsia. The statistically significant increase in the cellular endothelial compartment may be relevant to the hypertensive pathology of pre-eclampsia as endothelial signalling plays a major role in regulation of blood pressure. *Microsc. Res. Tech.* 64:54–62, 2004. © 2004 Wiley-Liss, Inc.

INTRODUCTION Interstitial Implantation

Humans develop in association with a haemo-chorial placenta. This type of maternofetal interaction exemplifies a strand of development that culminates in humans and related primates having a barrier layer between maternal- and fetal-blood. This contains fewer tissue layers than in most other mammals (Benirschke and Kaufmann, 2000). Mediating invasion is an ectodermal, extra-embryonic derivative of the blastocyst, the trophoblast. The trophoblast is the tissue of the conceptus that makes first contact with the uterine epithelium during the attachment phase. This epithelium and underlying endometrium is excavated by proteolysis and induced apoptosis and an intervillous space is thereby created. Although its vascular supply is initially plugged, it will, by approximately the 12th week of gestation, be irrigated by whole maternal blood (Burton et al., 2001). Some villous trophoblast cells detach from the others and become resident amongst decidual cells in the basal plate tissue underlying the implantation site. In advance of the primary villus invasion, a combined intra- and epi-vascular wave of trophoblast penetrates ahead of the remainder of the conceptus modifying the uterine spiral arterioles to supply the growing placenta adequately (Feng et al., 2001). A number of histological, cell and molecular pathological studies have revealed measurable quantitative differences between healthy and pre-eclamptic uteroplacental and specifically basal plate parameters. These include the following. The mean percentage of placental bed spiral arteries with failure of physiologic transformation in patients with pre-eclampsia is higher than in normal pregnant women at term ($P < 0.0001$) (Kim et al., 2003a,b). The basal plate of the normal decidua contains numerous CD14(+), HLA-DR(bright),

ManR(+) tissue macrophages but virtually none of these phagocytic cells can be found in the pre-eclamptic placenta (Burk et al., 2001). Placentae of pre-eclamptic pregnancies show villous cytotrophoblast proliferation, increased syncytial sprout formation, and impaired trophoblast invasion (Gratton et al., 2002). Cytotrophoblasts from fetal growth retarded (FGR) placentas differ from healthy placenta with respect to proliferation markers. These placentae were osteopontin (OPN)-positive until 30 weeks, unless pre-eclampsia accompanied the FGR. In this case, cytotrophoblasts were OPN-positive at 24–40 weeks. In pre-eclampsia, OPN immunoreactivity was detected at 24–40 weeks (Gabinskaya et al., 1998). Insulin-like growth factor binding protein 1 (IGFBP-1) expression was present only in the decidua of the basal plate and membranes, and this expression decreased significantly in pre-eclamptic placentae (Gratton et al., 2002). Endothelin-1 (ET-1) plays an important role as a modulator of vascular tone in the uteroplacental and fetoplacental units and may participate in the pathogenesis of pre-eclampsia (Barros et al., 2001). Women with pre-eclampsia exhibited an attenuated vasodilatory response to bradykinin, compared with normal pregnancy ($P < 0.0001$; Ong et al., 2003). Compared to placental tissues and membranes isolated from uncom-

*Correspondence to: C.D. Ockleford, Advanced Light Microscope Facility, Department of Infection Immunity and Inflammation, School of Medicine and Biological Sciences, University of Leicester and Warwick Medical Schools, University Road, Leicester, LE1 9HN, U.K. E-mail: cxo@le.ac.uk

Received 8 January 2004; accepted in revised form 30 March 2004

Contract grant sponsor: Pathological Society of Great Britain and Ireland; Contract grant sponsor: Royal Society; Contract grant sponsor: Chinese National Academy of Natural Sciences; Contract grant sponsor: Wellcome Trust.

DOI 10.1002/jemt.20047

Published online in Wiley InterScience (www.interscience.wiley.com).

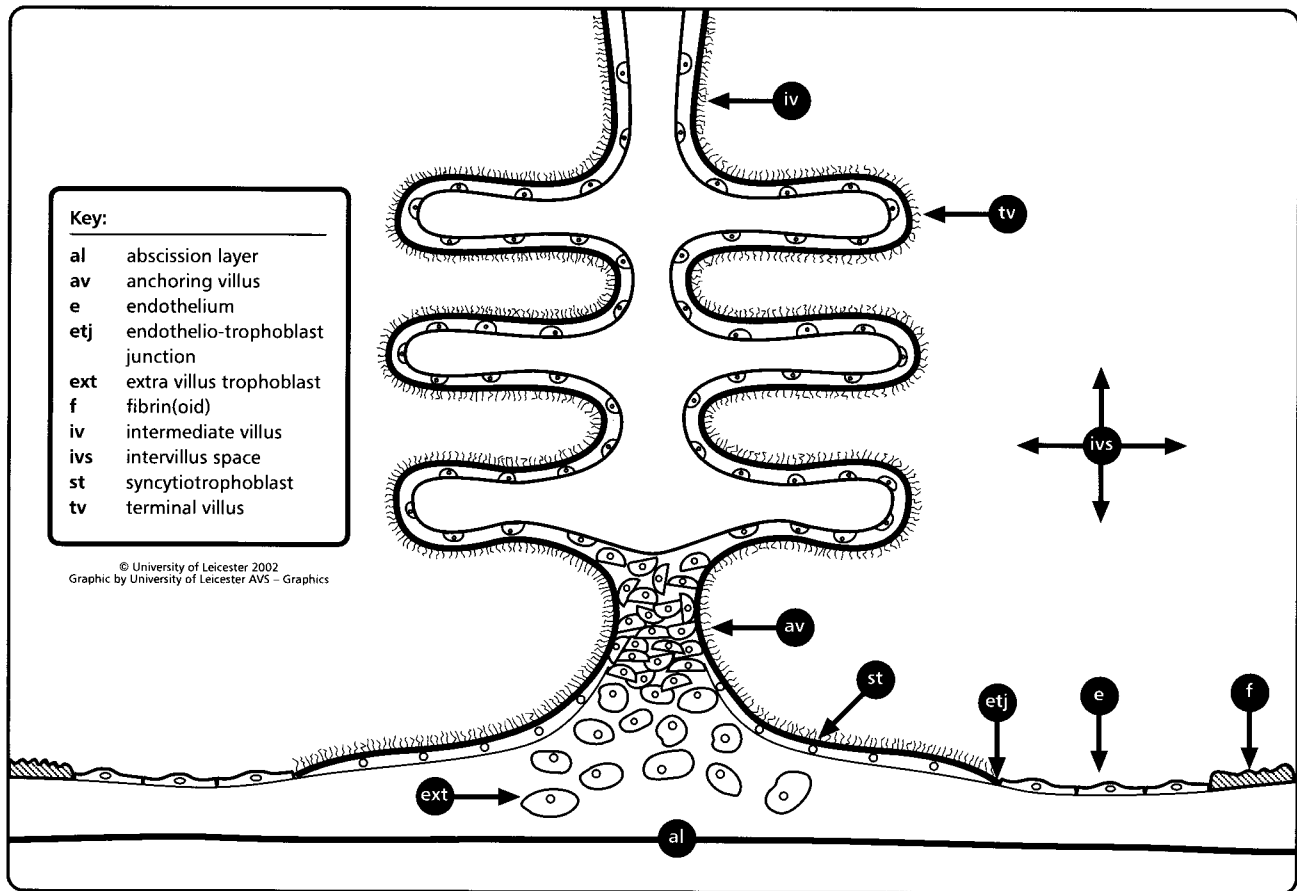


Fig. 1. Diagram that shows the basal plate lining cells and an anchoring villus attachment site.

plicated pregnancies, molecules induced by low oxygen tension, e.g., PROXY-1 expression, are elevated in tissues from pre-eclamptic pregnancies such as chorionic villi of peri-infarct regions, basal plate, and membrane decidua, as well as chorion (Graham et al., 2000). Immunofluorescence techniques revealed that the thickness of immunofluorescence of Nitabuch's membrane (a fibrinoid-rich layer of the basal plate extracellular matrix) was significantly greater in the study group vs. the control group (157.48 pixels vs. 63.80 pixels, $P = 0.006$, respectively; Balducci et al., 1997) and this is reminiscent of antibody precipitation in glomerulonephritis.

There is also one published study suggesting that in pre-eclampsia, hemosiderin depositions are not correlated quantitatively with impaired fetal growth (Sherer and Salafia, 2000). To hold the placenta to the uterus wall, some tertiary terminal villi bridge to the uterus. These are known as anchoring villi. At their junctions, the anchoring villi cores contain trophoblast cells similar to the extravillous trophoblast (Fig. 1). These are probably the source of the cells of the extravillous trophoblast lineage. Between the anchoring villi and lining the intervillous space is a thin unicellular layer that is the focus of this report. Its cells are the basal plate intervillous-space lining cells (Byrne et al., 1998, 2001).

Cytoskeletal and Other Markers

The use of antibodies to cytoskeletal proteins was first applied to extraembryonic tissues to define their structural importance to the architecture of the conceptus (Ockleford et al., 1981, 1984, 1990, 1993; Ockleford, 1990) but anti-cytokeratins were recognised as useful ectodermal lineage markers and have become widely used to assist identification of cell populations in the basal plate (Byrne et al., 1998, 2001) alongside markers directed against the products of placental endocrine glycoprotein secretion. Placental villus endothelial cells initially characterised by antibodies that recognised the presence of vimentin (Ockleford et al., 1990) have more recently been defined by the signalling platform membrane protein caveolin-1 (Byrne et al., 1998, 2001) and by a wide range of other markers (Dye et al., 2001).

The Intervillous Space

Our recent studies of proteolysis and apoptosis during implantation have thrown light on the development of blood spaces including vascular sinuses especially the intervillous space, its tributaries and its draining vessels. In particular, we have proposed modifications to currently orthodox views concerning the lining of the inter-villous space at term (Byrne et al., 1998, 2001).

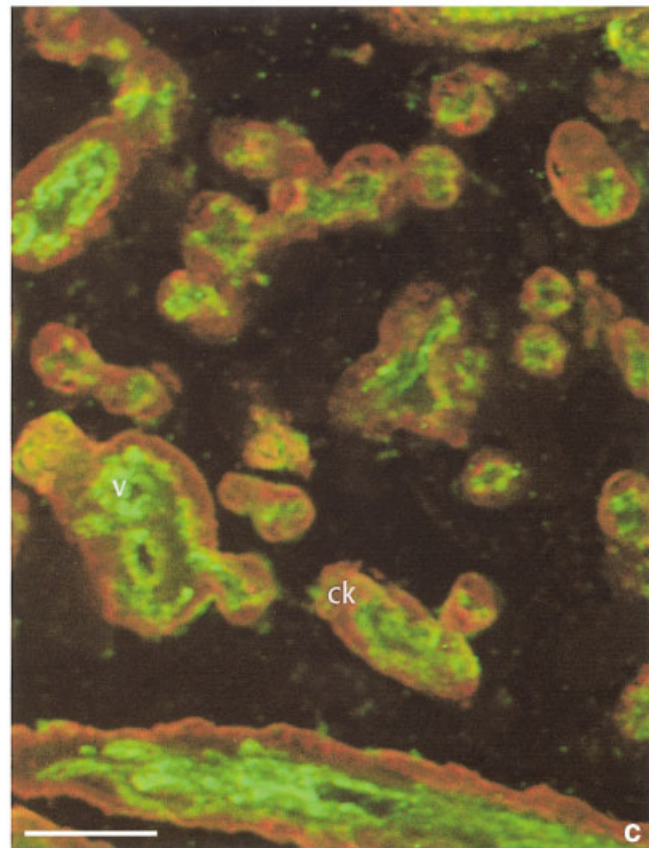
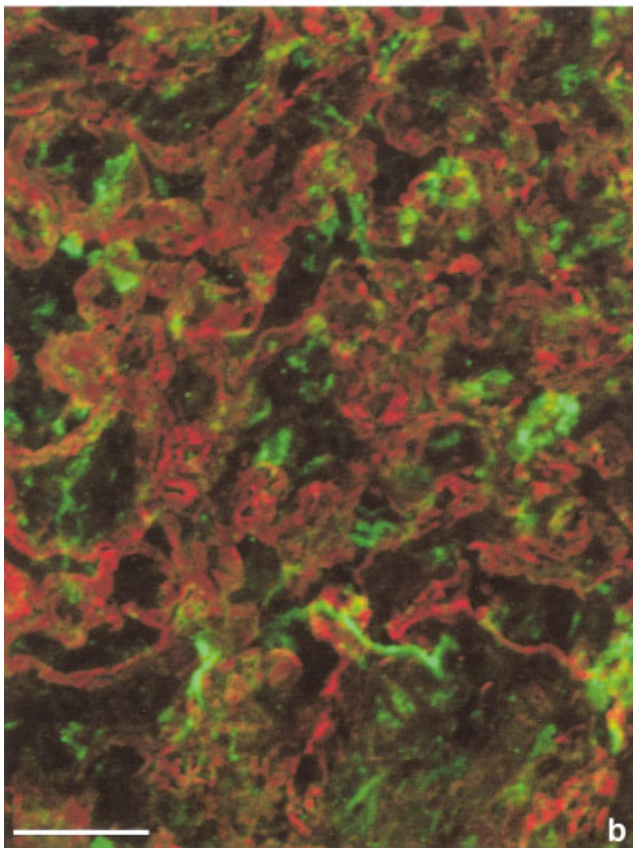
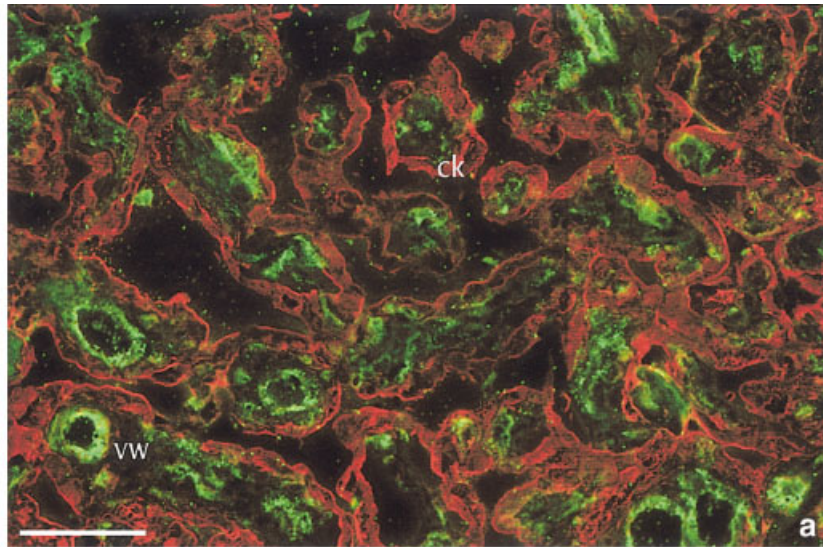


Fig. 2. **a:** Pancytokeratin (red) and von Willebrand factor (green) dual-channel indirect immunofluorescence detected using confocal laser scanning microscopy. The red labelling of the trophoblastic epithelium (ck) and the green of the fetal capillary endothelium (vW) distinguishes them. Scale bar = 100 μ m. **b,c:** Pancytokeratin (red)

and vimentin (green) dual-channel indirect immunofluorescence detected using confocal laser scanning microscopy. The red labelling of the trophoblastic epithelium (ck) and the green of the fetal capillary endothelium (v) distinguishes them. **b:** Healthy tissue. **c:** Pre-eclamptic tissue. Scale bar = 100 μ m.

We have challenged the conventional view that this is lined entirely by fibrin/fibrinoid and trophoblast (Boyd and Hamilton, 1970) and provided three independent lines of evidence that at least part of the surface is an endothelial cell sheet that abuts laterally to trophoblast reflected off the surface of anchoring villi (Byrne et al., 1998, 2001). Our view (Fig. 1) is supported by independent evidence (Lang et al., 1993; Wanner, 1966). This new insight presents opportunities to re-interpret the formation, function, and dysfunction of the blood-spaces supporting haematotrophic nutrition of the foetus.

Pre-Eclampsia and Maternal Vascular Remodelling

To appreciate the medical importance of pre-eclampsia (Cunningham and Lindheimer; 1992) it is worth considering the WHO statistics for 1996. In some developing countries, 1 in 12 women die as a result of a pregnancy-related problem (equivalent risk in an industrialised setting is 1:4,000). Approximately 12% of these deaths are a result of pre-eclampsia. Maternal mortality ratios (MMRs) are 27 per 100,000 live births worldwide and 480 up to 1,000 per 100,000 live births in the worst settings. The baby is also at mortal and morbid risk in the disease primarily from intra-uterine growth retardation (Davey and Macgillivray, 1998).

In this context, much attention has been given to the activity of the trophoblastic cells that enter and modify the uterine vasculature. In a healthy gestation, this "plugging" trophoblast appears to deny blood access to the fully formed intervillous space until about week 12 of gestation (Burton and Caniggia, 2001). By this time, the diameter of the vessels opening into the intervillous space has been widened. Such an adaptation is interpreted as allowing the presence of the Borelli jets of oxygenated blood that perfuse the intervillous space to be of reduced pressure, effectively slowing the flow rate of blood over the absorptive villi. One of the key histopathological features of pre-eclampsia is a *failure of the spiral arterioles to be opened up in this manner*.

In this report we estimate the area percent of the basal intervillous space lining epi/endothelium. We then compare this with that of pre-eclamptic tissue as this is expected to provide further evidence of the nature of implantation failure in pre-eclampsia.

MATERIALS AND METHODS

Patient Recruitment

Pre-eclamptic patients (n = 15) were from an antenatal hypertension clinic and a high-risk ward, at The Leicester Royal Infirmary. They met defined diagnostic criteria (Bosio et al., 1999; Davey and Macgillivray, 1988). Briefly, these were: a diastolic blood pressure of >90 mmHg on two or more separate occasions > 4 hours apart; one 24-hour urine collection with total protein excretion of >300 mg/24 hours or a random urine sample with >0.5 g/L protein. Recruitment was restricted to primigravidae meeting the above criteria after 20 weeks of gestation.

Exclusion criteria were previous cardiovascular disease (including underlying essential hypertension), diabetes, renal disease, hydatidiform mole, and multiple-pregnancy. Control (healthy) patients (n = 15) were recruited from the delivery suite. They were gravidity and gestational age matched to the pre-eclamptic pa-

tients recruited. Placentas from either pre-eclamptic or controls were taken following vaginal delivery or elective or emergency Caesarean section.

Informed written consent was granted before placental samples were taken. Protocols for both the research and the patient recruitment were given approval by the Leicestershire Research Ethics Committee (ref. no. 6336) and by the University Hospitals of Leicester NHS Trust (Project No. 7180).

Tissue Sampling

Tissue sampling was devised to generate isotropic uniform samples containing basal plate (Mayhew and Burton, 1997). Following delivery (<1 hour), the cord and membranes were trimmed off and the placenta was weighed. A radial 1-cm-thick strip was marked from centre to edge. Its length was recorded. Samples from the strip including the basal plate were placed in a mould and immersed in OCT cryo-embedding medium (Tissue-Tek, Bayer UK Ltd, Basingstoke, UK). This procedure was repeated for two further strips each cut at ~120° to the first strip. Tissue was freeze-fixed in a slush of liquid hexane and dry ice in a Dewar flask until solidified. Samples were stored at -80°C.

Histotechnique

Immunofluorescence labelling was carried out as previously described (Ockleford, 1990; Ockleford et al., 1997). Briefly, frozen sections were exposed for 18 hours at 4°C to the given dilutions of the following primary antibody in PBS containing 20% non-immune goat serum. Following 3 × 10-min PBS washes, the sections were then exposed to the fluorophore-conjugated second step antibodies in PBS containing 20% non-immune goat serum, for up to 2 hours at 20°C.

Trophoblast Markers: Primary Antibodies

Monoclonal mouse anti-Pan cytokeratin C2931 Sigma-Aldrich Inc. (St. Louis, MO) recognises human cytokeratins 4, 5, 6, 8, 10, 13, and 18. Concentration 1: 800.

Polyclonal rabbit anti-human chorionic gonadotrophin (hCG):(Alpha and beta chain) C8534 (Sigma-Aldrich). Concentration 1: 50.

Monoclonal mouse anti-human chorionic gonadotrophin (hCG):(beta sub-unit specific) C7659 (Sigma-Aldrich). Concentration 1:50 and 1:100.

Polyclonal rabbit anti-human placental lactogen NCL-PLp Novo Castra Laboratories (Newcastle-Upon-Tyne, UK). Concentration 1:800.

Trophoblast Localisation: 2nd Step Antibody

Cy3-conjugated sheep anti-mouse affinipure IgG Fab₂ fragment-specific (Jackson Immunoresearch Laboratories, West Grove, PA, 51787) Concentration 1:1,000.

Endothelial Markers: Primary Antibodies

Polyclonal rabbit anti-vimentin Ab7783 (Abcam, Cambridge, UK). Concentration 1:10–1:400.

Polyclonal rabbit anti-human von Willebrand factor, IgG fraction F3520 (Sigma-Aldrich). Concentration 1:400.

Monoclonal mouse anti-thrombomodulin Ab-1/

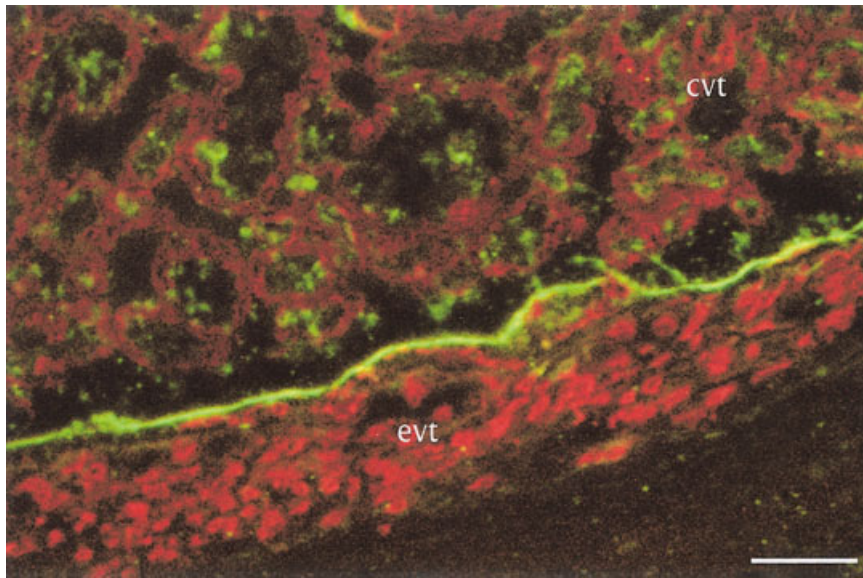


Fig. 3. Healthy human placental basal plate. The intervillous space lining is immunoreactive for endothelial cell markers (green). The layer divides the region containing chorionic villus trophoblast (cvt) from that containing extravillous trophoblast (evt). A substantial part of the layer is endothelial. The sheet of cells we have described, a combination of epithelium and endothelium (ectoderm and mesoderm), is probably a unique *allo-epi-endothelium*. The high intensity of the anti-pancytokeratin immunofluorescence of the extravillous trophoblast (evt) compared with that of chorionic villous trophoblast (cvt) is shown in this dual-channel micrograph (red channel, anti-pancytokeratin; green, PE-CAM-1). Scale bar = 100 μm .

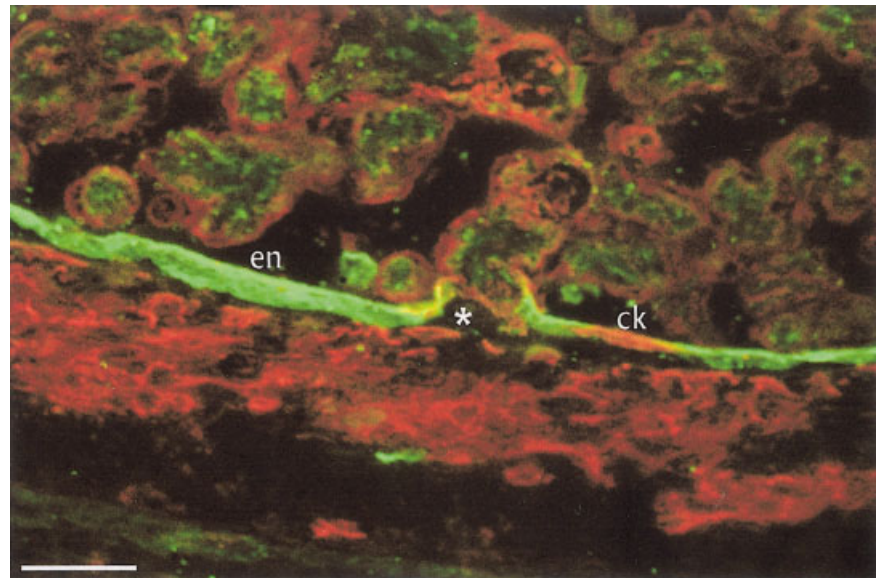


Fig. 4. This immunofluorescence confocal laser scanning image shows the anti-PE-CAM-1 (green) outlining the basal plate lining cells of the majority of the intervillous space (en). This layer is interrupted by a short section of pancytokeratin labelling (ck) lining layer and by the point of attachment of an anchoring villus (*). The endothelial layer appears thicker than usual owing to the sectional sectioning plane. The trophoblast and endothelium are continuous laterally and do not overlap. Together they constitute the ultimate basal-plate layer lining of the intervillous space. Scale bar = 100 μm .

CD141 (NeoMarkers, CA, MS-1102-R7). Concentration 1:30–1:50.

Monoclonal mouse anti-CD31/ PECAM- 1 Ab-1 (NeoMarkers, CA, MS-353-R7). Concentration 1:80.

Polyclonal rabbit anti-human caveolin-1 (BD Transduction Laboratories, Lexington, UK, 610059). Concentration 1:100.

Endothelial Localisation: 2nd Step Antibody

FITC-conjugated goat anti-rabbit whole molecule IgG (Sigma- Aldrich), F6005). Concentration: 1:500.

Finally 3 10-min washes in PBS were followed by mounting under a No. 0 coverslip in a photobleach retardant, glycerol-based mountant (Citifluor, Canterbury).

Confocal Laser Scanning Microscopy

Sections were studied using a confocal laser scanning attachment (Bio-Rad MRC 600) linked to a Zeiss Axiovert epifluorescence microscope as previously described (Ockelford, 1995; Mongan et al., 1998). This equipment utilised a reverse-light-path fibre-optic channelled Nomarski DIC signal to the second detector, to allow comparison of immunofluorescent and refractive index (RI) related images of the same specimen. The relationship between specimen RI and dry mass was a useful measure of the selectivity of the immuno-staining. Images were recorded using COMOS software (Bio-Rad) and exported to Adobe Photoshop for labelling and print production.

Measurement and Statistical Analysis

Digital merged images of contiguous basal-plate-containing microscope fields were measured using the

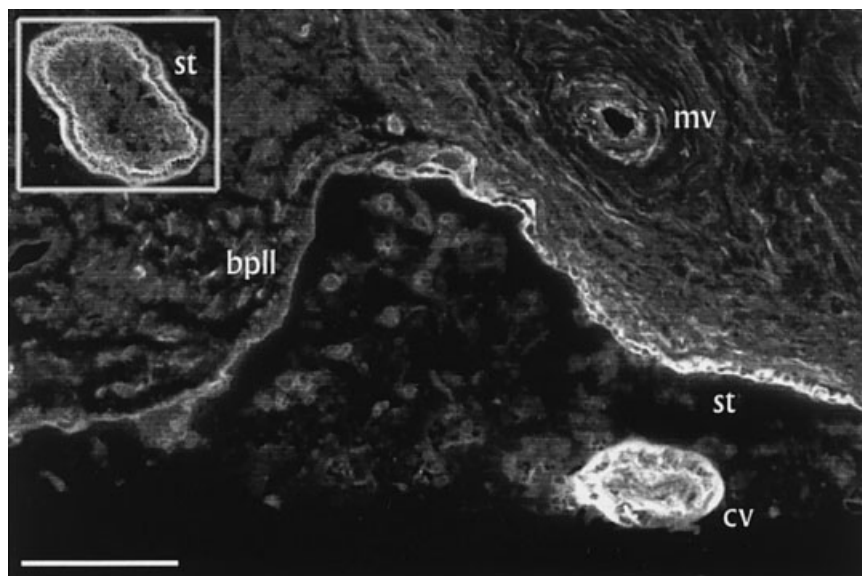


Fig. 5. The epithelial component of the basal plate lining cells exhibits strong immunoreactivity to trophoblast markers anti-hCG and also to anti-hPL (data not shown). The thinner cellular layer to the left (bpl), however, has a relatively thin and very faint labelling probably owing to hCG adsorbed from the blood. The obliquely sectioned villus (cv) and a trophoblast-lined maternal vessel (mv) are immunoreactive. **Inset:** Anti-hCG apical and basal epithelial localisation contrasting with the unreactive villus mesenchymal core. Scale bar = 100 μ m.

LENGTH/ PROFILE function in COMOS. The endothelium, trophoblast, and acellular components of the lining layer of the intervillous space were identified using immunofluorescent markers in dual channel studies where the two channels were encoded red and green. Their different coloured lengths were measured interactively and the length fraction of endothelium over trophoblast was assumed to be a measure of the area fraction (Mayhew and Burton, 1997). Results were recorded in an Excel spreadsheet and statistical analysis was carried out using SPSS (SPSS Inc., Chicago, IL).

RESULTS

The Basal Plate Lining

The immunofluorescence markers for endothelium and trophoblast confirmed that there was a thin cellular boundary layer overlying the basal plate and lining the intervillous space (Byrne et al., 1998, 2001). This extended over the surface between the attachment-points of anchoring villi. The single cell thick layer was divided into regions that labelled with cytoskeletal endothelial, trophoblast, or neither marker but not with both trophoblast and endothelial markers in the same location (Figs. 2–4).

The endothelial markers anti-caveolin-1, PECAM-1, vimentin, and thrombomodulin all labelled the thinner cellular aspects of the layer positively whereas the trophoblast markers anti-pancytokeratin, hCG, and hPL consistently labelled areas with greater thickness and more irregular surface. “Internal control” chorionic villus endothelium and trophoblast, associated with chorionic villi, were labelled with the appropriate markers and there was no significant cross-reactivity (Figs. 2–4). Dual channel images revealed continuity between the trophoblast and endothelial marker-labelled regions of the single cell layer. Where the layer was discontinuous, it appeared acellular. Unpublished experiments using anti-fibrin/ogen markers have indicated that these are fibrin-rich regions of the basal plate.

Markers Defining Heterogeneity

The endothelial markers with specificity for vimentin, caveolin-1, von Willebrand factor, thrombomodulin, and CD31/ PECAM-1 consistently bound to villous endothelium, uterine vessel endothelium, and to parts of the basal plate lining but did not label cytoplasm in villous or basal plate lining trophoblast (e.g., Figs. 2–4). The trophoblast markers hCG, hPL, and pancytokeratin invariably labelled the chorionic villus and basal plate trophoblast but not the chorionic villus core endothelium (e.g., Figs. 2–5).

Anchoring Villi

Chorionic villi are at term mainly tertiary villi with an epithelial trophoblast covering and an entirely mesenchymally derived core containing fibroblasts, capillary endothelial cells, and macrophages. This is reflected in the patterns of vimentin and cytokeratin antibody binding (Ockleford et al., 1981, 1984, 1990, 1993; Ockleford, 1990). This pattern is disturbed at the point of attachment that connects some villi to the basal plate. Such “anchoring villi” display trophoblastic immunofluorescence characteristics in a solid core of cyto-trophoblast cells close to the basal plate. These exhibit the bright immunofluorescent anti-cytokeratin characteristics of the extravillous trophoblast and differ from the relatively less intense chorionic villus covering syncytiotrophoblast (Ockleford et al., 2004).

Immunofluorescence in Pre-Eclamptic Tissue

The immunofluorescence patterns attributable to the specific antibodies used here fall into two groups, those that define endothelium and those that define trophoblast. The patterns are qualitatively similar in healthy and pre-eclamptic tissue samples. The fact that the basal plate lining is a heterogeneous mosaic of cells that may produce different secretions raises the possibility that the proportion of the cell type varies in the disease condition pre-eclampsia from that in healthy

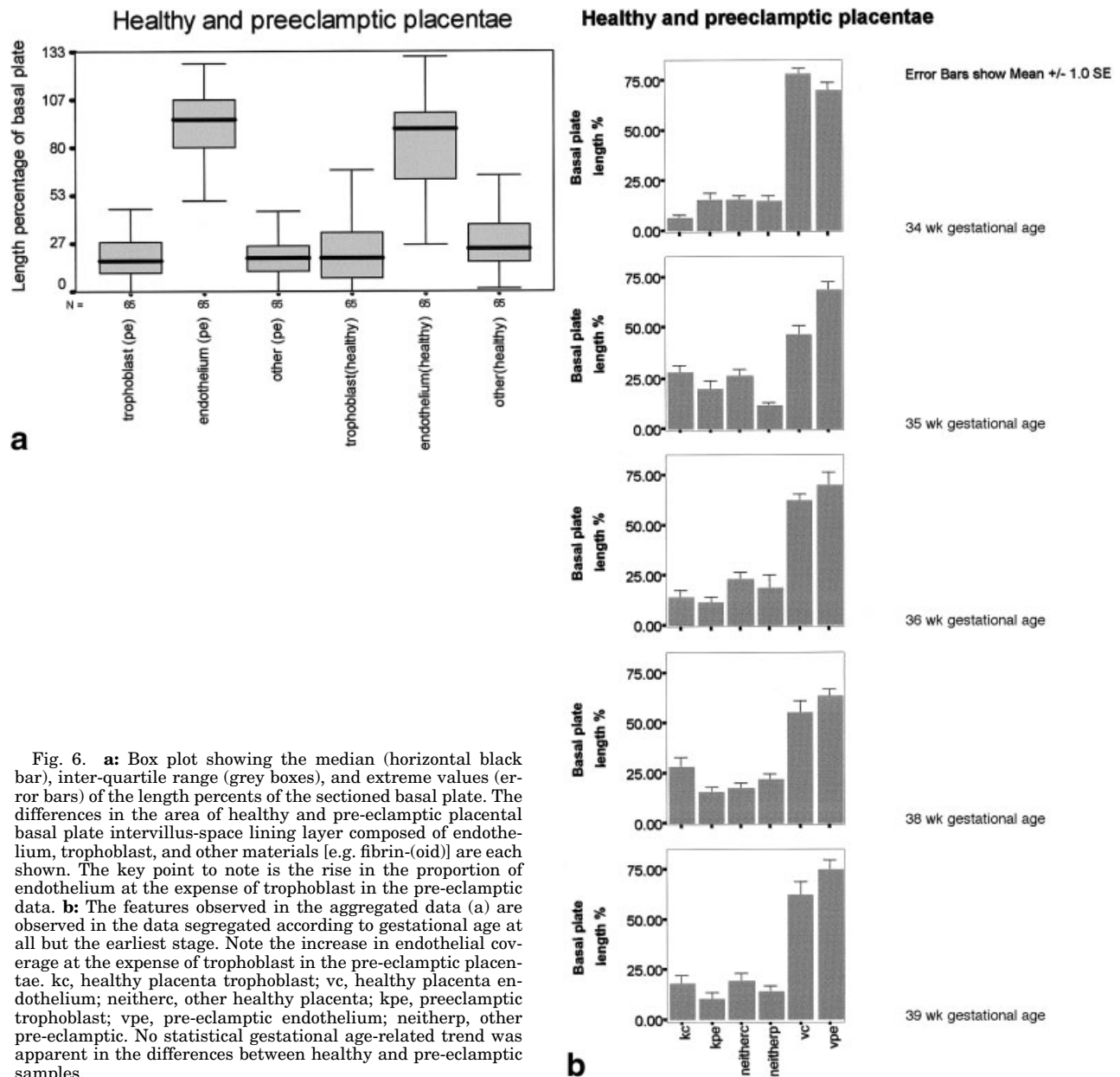


Fig. 6. **a:** Box plot showing the median (horizontal black bar), inter-quartile range (grey boxes), and extreme values (error bars) of the length percents of the sectioned basal plate. The differences in the area of healthy and pre-eclamptic placental basal plate intervillous-space lining layer composed of endothelium, trophoblast, and other materials [e.g. fibrin-(oid)] are each shown. The key point to note is the rise in the proportion of endothelium at the expense of trophoblast in the pre-eclamptic data. **b:** The features observed in the aggregated data (a) are observed in the data segregated according to gestational age at all but the earliest stage. Note the increase in endothelial coverage at the expense of trophoblast in the pre-eclamptic placentae. kc, healthy placenta trophoblast; vc, healthy placenta endothelium; neitherc, other healthy placenta; kpe, preeclamptic trophoblast; vpe, pre-eclamptic endothelium; neitherp, other pre-eclamptic. No statistical gestational age-related trend was apparent in the differences between healthy and pre-eclamptic samples.

cells. If so, the amount of local secretions affecting vascular tone may differ in pre-eclamptic pregnancies from normal pregnancy. With the exception of thrombomodulin, most of the antibodies applied here are simply endothelial cell markers and not secretions known to affect blood pressure. At this stage, our argument relies on the fact that endothelial cells are known to be important in producing secretions that control blood pressure and the fact that pre-eclampsia is seen as a general disease of endothelial cells. A further study is in progress. It is focussing on endothelial cell synthesis of molecules such as ACE and eNOS known to be important in the regulation of blood pressure and, thus far, data are supportive of our interpretation of endothelium at this location as being competent to regulate vessel tone.

Measurement of Basal Plate Area Fractions in Healthy and Pre-Eclamptic Placentae

Analysis of digital images of the basal plate lining (excluding anchoring villi) gave measured length ratios of endothelial:trophoblastic:other (60.81% endothelium, 18.91% trophoblast, 20.29% other) in sections of healthy placenta (Fig. 6a,b). The other component probably reflects regions of fibrin deposition. The mean (60.81%) percentage length of healthy basal plate occupied by endothelium rises to 67.63% in the pre-eclamptic group. A statistically significant difference was demonstrated between the medians (67.4% and 71.7% Man Whitney Rank Sum test, $P = 0.033$) in the endothelial compartment in pre-eclampsia. Although the most appropriate test for

significant difference between the two groups of measurements of this type, it applies only to medians and not to means.

Since the isotropic uniform random (IUR) sampling procedures adopted allow this, our stereological sample of basal plate lining-length-percentages can be used as an estimate of the area percentages.

DISCUSSION

Heterogeneity of Cell Types Contributing to the Basal Plate Lining

The finding of a mosaic unicellular layer lining the intervillous space comprising endothelium and trophoblast (Byrne et al., 1998, 2001) is confirmed here. This may be of mixed fetal and maternal origin (Byrne et al., 1998, 2001) and reacts with the marker antibodies used in this study as expected of a layer of mixed mesenchymal and ectodermal embryonic origin. The present study presents quantitative data revealing the extent of endothelium and trophoblast. This excludes the possibility that endothelium is a rare component or one found immediately adjacent to vessel entry and exit points only. To be leak-proof, the fetal trophoblast must meet side by side with maternal endothelium at some point and this report shows where this occurs and what the mean relative contributions are (60.81 % endothelium, 18.91 % trophoblast, 20.29% other) in healthy placentas. Our interpretation of the basal-plate/intervillous-space lining structure is thus intermediate between the "all trophoblast" view portrayed in current embryology textbooks and the alternative extreme view of Wanner (1966), that apart from anchoring villus attachment sites, this is "all endothelial." Our view is based on length quantitation of endothelial/trophoblast marker studies described here as well as semi-thin section histology, scanning, and transmission electron microscopy and observations not fully interpreted from an earlier marker study (Byrne et al., 1998, 2001; Lang et al., 1993).

The origin of the basal plate lining endothelial cells described here requires consideration. Endothelium in this location is probably of maternal origin and this is currently being tested using cytogenetic probes. Should this prove to be the case, then the proliferation and/or relocation of cells lining the maternal vessels linked to the intervillous space is an obvious possibility. As the endothelium lining the uterine spiral arterioles is replaced early in pregnancy by the wave of endovascular trophoblast invasion, these endothelial cells may be the progenitors. This is provided they are displaced as opposed to destroyed by this process, or replaced, a matter that is unclear at present. Alternatively the endothelium may derive from the lining of the venous/lymphatic vessels that drain the intervillous space throughout pregnancy. Further study is required to define their origin precisely.

Basal Plate Composition Changes in Pre-Eclampsia

Our most important conclusion with regard to pre-eclampsia is that there is an increase in the endothelium component of the intervillous space basal-plate lining layer (60.81% rises to 67.63%) at the expense of trophoblast (18.91% drops to 15.57%). The residual acellular fibrin/oid covered areas constitute a further proportion of the total in both healthy and pre-eclamptic gestations (20.29% and 16.81%).

A number of compounds synthesised by endothelial cells affect vascular physiology and this has been seen as a major feature of pre-eclamptic pathophysiology (Bosio et al., 1999; Carter and Charnock-Jones, 2001; Dekker and Sibai, 1998; Lyall and Myatt, 2002; Roberts et al., 1995; Walker, 2000). These include prostacyclin (a vasodilator and inhibitor of platelet aggregation); eNOS and its product nitric oxide (a vasodilator and inhibitor of platelet adhesion and aggregation); haemoxygenase and its product carbon monoxide (a vasodilator and inhibitor of platelet aggregation); tissue plasminogen activator (activator of fibrinolysis in blood vessels and amniotic fluid); thrombomodulin (an anticoagulant); thromboplastin (a promoter of blood coagulation); platelet activating factor (activation of platelets and neutrophils); and von Willebrand factor (promoter of platelet adhesion and activator of blood coagulation).

In the light of this information, we propose that an increase in the quantity of non-proliferative endothelium at the materno-fetal interface observed here causes hypertensive changes in vascular physiology mediated by endothelial signalling. Signalling interactions subtended by caveolin platforms may prove to be an important aspect of the development of our understanding of the placental pathology of this condition.

Developmental Aspects of Pre-Eclampsia

Identification of the cause of pre-eclampsia will require further data. There are genetic and immunological dimensions to the disease indicating paternal imprinting and partner change effects, respectively, on incidence (Moffett-King, 2002). These are as yet unlinked to the present findings. As an informed first guess, there are likely to be genetic aspects to the predisposition to pre-eclampsia and environmental triggers such as paternal antigenicity that release these. To reproductive endocrinologists, the influence of the steroid hormones oestrogen and progesterone on the signalling systems operative is of great interest. The nuclear translocation processes of receptor-bound oestrogen and the control and activation of caveolar platforms indicate that this is a disease with many potential levels of control and signalling pathways to be explored.

An interesting feature of the disease is its progressive nature with symptoms worsening as pregnancy progresses through the second and third trimester and, ultimately, with more severe cases presenting earlier than the mild cases. In this respect, the role of endothelial caveolin-1 may be relevant (Lala and Desoye, 2001; Liu et al., 1999; Ramirez et al., 2002). This protein is available to meet its caveolar cell-signalling role in the non-proliferative endothelial cell but sequestered in the cleavage furrow zone of the dividing (proliferative) cells. The greater area percent at term in pre-eclamptic patients indicates a greater population of endothelial cells. Whilst this population is expanding, its effect on blood pressure will be held in check as signalling platforms will be disassembled. Only later, once quiescent, will the down-regulation of, e.g., NOS, feed through to affect blood pressure. The improvement in maternal health following parturition is understandable given the model presented here as the basal plate is expelled during the third stage of labour.

Any complete explanation of the cause of the disease will need to include a reason for the cyokeratin-based

cytoskeletal aspects described recently (Ockleford et al., 2004). These observations are a useful step in understanding how alterations in the developmental programme of transcription (Beck et al., 1995; Knöfler et al., 2001) lead to the implantation deficits typical of pre-eclampsia. Structural, anchorage failure or motility deficits could all explain features of the pathology such as shallow implantation, and the change in the endothelium:trophoblast area ratio in the basal plate lining-layer described here.

ACKNOWLEDGMENTS

We thank the Pathological Society of Great Britain and Ireland for an Open scheme grant to support R.K.S. C.D.O. thanks the Royal Society, the Chinese National Academy of Natural Sciences, and the Wellcome Trust for support of his research. We thank John Beckett for statistical advice; Aidan Halligan and Jason Waugh for their support, encouragement, and clinical co-ordination; and Chris d' Lacey, Nick Court, Chris Ward, and Angela Chorley for skillful assistance with presentation.

REFERENCES

- Balducci J, Weiss PM, Atlas RO, Pajarillo MF, Dupree WB, Klasko SK. 1997. Preeclampsia: immunologic alteration of Nitabuch's membrane? Clinical sequelae. *J Maternal-Fetal Med* 6:324–328.
- Barros JS, Bairos VA, Baptista MG, Fagulha JO. 2001. Immunocytochemical localization of endothelin-1 in human placenta from normal and pre-eclamptic pregnancies. *Hypertens Preg* 20:125–137.
- Beck F, Erler T, Russell A, James R. 1995. Expression of Cdx-2 in the mouse embryo and placenta: possible role in patterning of the extra-embryonic membranes. *Dev Dyn* 204:219–227.
- Benirschke K, Kaufmann P. 2000. Pathology of the human placenta. Early development of the human placenta, 4th ed. New York: Springer Verlag. p 1–968.
- Bosio PM, McKenna PJ, Conroy R, O'Herlihy C. 1999. Maternal central hemodynamics in hypertensive disorders of pregnancy. *Obstet Gynecol* 94:978–984.
- Boyd JD, Hamilton WJ. 1970. The human placenta. Cambridge: Heffer.
- Burk MR, Troeger C, Brinkhaus R, Holzgreve W, Hahn S. 2001. Severely reduced presence of tissue macrophages in the basal plate of pre-eclamptic placentae. *Placenta* 22:309–316.
- Burton GJ, Cannigia I. 2001. Hypoxia implications for implantation to delivery—a workshop report. *Placenta* 22:S83–S92.
- Burton GJ, Hempstock J, Jauniaux E. 2001. Nutrition of the human fetus during the first trimester: a review. *Placenta* 22:S70–S76.
- Byrne S, Cheent A, Dimond J, Fisher G, Ockleford CD. 1998. Immunocytochemical localisation of Caveolin-1 in human term extra-embryonic membranes using confocal laser scanning microscopy. *J Anat* 193:312–313.
- Byrne S, Cheent A, Dimond J, Fisher G, Ockleford CD. 2001. Immunocytochemical Localisation of Caveolin-1 in human term extra-embryonic membranes: implications for the complexity of the maternal-fetal junction. *Placenta* 22:499–510.
- Carter AM, Charnock-Jones DS. 2001. Angiogenesis and blood flow: implications for pathobiology: a workshop report. *Placenta* 22:S66–S68.
- Cunningham FG, Lindheimer M. 1992. Hypertension in pregnancy. *N Engl J Med* 326:927–932.
- Davey DA, Macgillivray I. 1988. The classification and definition of the hypertensive disorders of pregnancy. *Am J Obstet Gynecol* 158:892–898.
- Dekker GA, Sibai BM. 1998. Etiology and pathogenesis of preeclampsia. workshop report. *Trophoblast Res* 16:S142–S145.
- Dye JF, Jablenska R, Donnelly JL, Lawrence L, Leach L, Clark P, Firth JA. 2001. Phenotype of the endothelium in the human term placenta. *Placenta* 22:32–43.
- Feng Q, Liu K, Liu Y-X, Byrne S, Ockleford C. 2001. Plasminogen activators and inhibitors are transcribed during early macaque implantation. *Placenta* 22:186–199.
- Gabinskaya T, Salafia CM, Gulle VE, Holzman IR, Weintraub AS. 1998. Gestational age-dependent extravillous cytotrophoblast osteopontin immunolocalization differentiates between normal and preeclamptic pregnancies. *Am J Reprod Immunol* 40:339–346.
- Graham CH, Postovit LM, Park H, Canning MT, Fitzpatrick TE. 2000. Adriana and Luisa Castellucci award lecture 1999: role of oxygen in the regulation of trophoblast gene expression and invasion. *Placenta* 21:443–450.
- Gratton RJ, Asano H, Han VK. 2002. The regional expression of insulin-like growth factor II (IGF-II) and insulin-like growth factor binding protein-1 (IGFBP-1) in the placentae of women with pre-eclampsia. *Placenta* 23:303–310.
- Kim YM, Bujold E, Chaiworapongsa T, Gomez R, Yoon BH, Thaler HT, Rotmensch S, Romero R. 2003a. Failure of physiologic transformation of the spiral arteries in patients with preterm labor and intact membranes. *Am J Obstet Gynecol* 189:1063–1069.
- Kim YM, Chaiworapongsa T, Gomez R, Bujold E, Yoon BH, Rotmensch S, Thaler HT, Romero R. 2003b. Failure of physiologic transformation of the spiral arteries in the placental bed in preterm premature rupture of membranes. *Am J Obstet Gynecol* 187:1137–1142.
- Knöfler M, Vasicek R, Schrieber M. 2001. Key regulatory factors involved in placental development: a review. *Placenta* 22:S83–S92.
- Lala P, Desoye G. 2001. Signal transductions: variants on developmental control from implantation to delivery. *Placenta* 22:S98–S100.
- Lang I, Hartmann M, Blaschitz A, Dohr G, Skofitsch G, Desoye G. 1993. Immunohistochemical evidence for the heterogeneity of maternal and fetal vascular endothelial cells in human full-term placenta. *Cell Tissue Res* 274:211–218.
- Liu J, Razani B, Tang S, Terman BI, Ware JA, Lisanti MP. 1999. Angiogenesis activators and inhibitors differentially regulate caveolin-1 expression and caveolae formation in vascular endothelial cells. Angiogenesis inhibitors block vascular endothelial growth factor-induced down-regulation of caveolin-1. *J Biol Chem* 274:15781–15785.
- Lyll F, Myatt L. 2002. The role of the placenta in pre-eclampsia. *Am J Obstet Gynecol* 179:1359–1375.
- Mayhew TM, Burton GJ. 1997. Sterology and its impact on our understanding of human placental functional morphology. *Microsc Res Tech* 38:195–205.
- Moffett-King A. 2002. Natural killer cells and pregnancy. *Nature Rev Immunol* 2:656–663.
- Mongan LC, Gormally J, Hubbard ARD, d'Lacey C, Ockleford CD. 1998. Confocal microscopy: theory and applications. In: Lambert D, editor. Calcium signalling protocols. Totowa, NJ: Humana Press New Jersey. p 1–39.
- Ockleford CD. 1990. A quantitative interference light microscope study of human first trimester chorionic villi. *J Microsc* 157:225–237.
- Ockleford CD. 1995. Editorial: The confocal laser scanning microscope (CLSM). *J Pathol* 176:1–2.
- Ockleford CD, Wakely J, Badley RA. 1981. Morphogenesis of human placental chorionic villi: cytoskeletal, syncytioskeletal and extracellular matrix proteins. *Proc R Soc B* 212:305–316.
- Ockleford CD, Dearden L, Badley RA. 1984. Syncytioskeletons in choriocarcinoma in culture. *J Cell Sci* 66:1–20.
- Ockleford CD, Bradbury FM, Indans I. 1990. Localisation of cytoskeletal proteins in chorionic villi. In: Cedard L, Alsat E, Challier J-C, Chaouat G, Malassine A, editors. Placental communications: biochemical, morphological and cellular aspects. Paris: Colloque INSERM/John Libbey Eurotext Ltd. 199:239–250.
- Ockleford CD, Malak T, Hubbard A, Bracken K, Burton S-A, Bright N, Blakey G, Goodliffe J, Garrod D, d'Lacey C. 1993. Confocal and conventional immunofluorescence and ultrastructural localisation of intracellular strength giving components of human fetal membranes. *J Anat* 183:483–505.
- Ockleford CD, Mongan L, Hubbard ARD. 1997. Techniques of advanced light microscopy and their applications to morphological analysis of human extra-embryonic membranes. In: Danzer V, Leiser R, editors. Placenta, comparative and functional morphology by different methodological approaches. *Microsc Res Tech* 38:153–164.
- Ockleford CD, Smith RK, Byrne S, Sanders R, Bosio P. 2004. A confocal laser scanning microscope study of cytokeratin immunofluorescence dimming indicates a mechanism of trophoblast deportation and its upregulation in pre-eclampsia. *Microsc Res Tech* 64:43–53.
- Ong SS, Moore RJ, Warren AY, Crocker IP, Fulford J, Tyler DJ, Gowland PA, Baker PN. 2003. Myometrial and placental artery reactivity alone cannot explain reduced placental perfusion in pre-eclampsia and intrauterine growth restriction. *BJOG* 110:909–915.
- Ramirez M, Pollack L, Millien G, Yu X-C, Hinds A, Williams MC. 2002. The α isoform of caveolin-1 is a marker of vasculogenesis in early lung development. *Journal of Histochemistry and Cytochemistry* 50:33–42.
- Roberts JM, Hubel CA, Taylor RN. 1995. Endothelial dysfunction yes, cytotoxicity no! *Am J Obstet Gynaecol* 173:978–979.
- Sherer DM, Salafia CM. 2000. Chronic intrauterine bleeding and fetal growth at less than 32 weeks of gestation. *Gynecol Obstet Invest* 50:92–95.
- Walker J. 2000. Pre-eclampsia. *Lancet* 356:1260–1265.
- Wanner A. 1966. Wird bei der Geburtspacenta des Menschen die Basalplatte von Trophoblastzellen oder Zellen mütterlicher herkunft überzogen. *Acta Anat* 63:545–558.